1990

An introduction to truss models and their application in the design of precast and prestressed concrete connections

John Pensiero
Lehigh University

AN INTRODUCTION TO TRUSS MODELS AND THEIR APPLICATION IN THE DESIGN OF PRECAST AND PRESTRESSED CONCRETE CONNECTIONS

by

John Pensiero

A Thesis
Presented to the Graduate Committee
of Lehigh University
in Candidacy for the Degree of
Master in Science
in
Civil Engineering

Lehigh University
Bethlehem, Pennsylvania

December 1989

Certificate of Approval

This thesis is accepted and approved in partial fulfillment of the requirements for the degree of Master of Science in Civil Engineering.

12-17-89

Date

Dr. Peter Mueller
Professor in Charge

Irwin J. Kugelman
Department Chairman

Acknowledgement

This work has been conducted and completed in the Fritz Engineering Laboratory, Department of Civil Engineering, Lehigh University under the observation and guidance of the Center for Advanced Technology for Large Structural Systems (ATLSS), an NSF Sponsored Engineering Research Center. Dr. Irwin J. Kugelman is Chairman of the Department of Civil Engineering and Director of Fritz Engineering Laboratory. Dr. John W. Fisher is Director of the ATLSS Center.

Funding for the study on Precast and Prestressed Concrete Using Truss Modeling Concepts was provided by the NSF, Grant No. ECD-8943455 under the ATLSS program.

For their dedicated assistance in the typing of the manuscript, I sincerely thank Joann Frey, Cheryl Hendricks, and Ruth Grimes. Their patience carried me through. I also thank the entire ATLSS staff for their efforts in making this work possible.

Without his insight and reasoning capabilities, this work could not have been completed without the guidance of Dr. Peter Mueller, professor at Lehigh University and ATLSS Principle Investigator in the Advancement of Connection Technology and Design Concepts. From his persevering assistance, a great deal has been accomplished and I am grateful to have had him as my advisor.

Table of Contents

LIST OF FIGURES

Abstract

This thesis presents a consistent and unified design methodology for precast and prestressed concrete connections based on rational models -- namely, truss models. The basic concepts and principles are first presented for readers who are unfamiliar with truss models, yet would like to apply these concepts to the analysis and design of reinforced concrete and precast concrete connections. In essence, rational design of connections requires design of both the interface between the connected elements as well as the design of the disturbed regions immediately adjacent to the interface. Truss models represent a tool for the latter. Both quantitative and qualitative analyses are presented which provide insight into the characteristic behavior of these disturbed regions. Treatment includes the nibs and ends of dap-ended beams, monolithic corbels, monolithic opening and closing knee joints of both large and small concrete dimensions, monolithic interior and exterior joints, precast simple connections, precast wall panel connections, and precast beam-to-column moment connections. The effects of prestressing (in a truss modeling context) is also treated.

The presented truss analyses demonstrate that the crucial issue in connection design is full anchorage of all internal elements in the correct location. Truss models represent a rational tool which assists the engineer in both the design of the structural component itself, and just as importantly, the design of the details. Proper truss modeling of the details ensures full anchorage and development

of all primary and secondary internal structural elements such as the reinforcement.

This work paves a path to a first step toward a rational design methodology for connections. Presented within this study are rules and guidelines to be used for the design of any structural component. In addition, first draft code provisions for the design of concrete connections are outlined. It is hoped that these rules and provisions will contribute to structurally safe and sound connections.

AN INTRODUCTION TO TRUSS MODELS AND THEIR APPLICATION IN THE DESIGN OF PRECAST AND PRESTRESSED CONCRETE CONNECTIONS

1. INTRODUCTION

At present, the U.S. construction industry is faced with an increasing threat of loosing its competitiveness in the global construction marketplace. It is lagging behind in productivity, innovative technology, computer-integrated design/construction, and automated fabrication/construction, and is steadily losing market share. In response, the National Science Foundation has established the ATLSS Center (Advanced Technology for Large Structural Systems) with the goal to assist the U.S. construction industry, through research on advanced technologies and education of engineers, in maintaining its competitive edge in the global construction market.

1.1 OPPORTUNITIES FOR PRECAST CONCRETE

One long-term objective of ATLSS' research plan is improved construction productivity. In concrete construction, precast concrete offers significant opportunities in this respect. Already today, precast elements allow not only for uncompromising and varied designs, but also for efficient, high quality factory fabrication and speedy erection on site. Precast concrete lends itself therefore particularly well to innovative automation and computer integrated manufacturing technologies.

1.2 PROBLEMS OF PRECAST CONCRETE

However, precast concrete is not without its problems. There is a general perception that precast concrete structures do not have the required ductility and general structural integrity required in seismic regions. But also in regions of low seismicity precast concrete has problems. It is well known that volumetric changes due to creep, shrinkage, and temperature changes are a constant source of problems. The ultimate cause of these problems is again a lack of continuity and ductility. Brittle behavior of precast concrete is usually observed in the vicinity of connections. This comes as no surprise, since the regions adjacent to the connection interfaces often exhibit complex stress paths and severe stress concentrations which are not easily predictable. Furthermore, there is no general and consistent design methodology. Design procedures differ for different types of connections. Many of these procedures are based on very limited experimental data and are often purely empirical. Some of these experimental results are derived from test setups which do not truthfully model the actual service conditions. It is questionable, for instance, whether test results from studs in uncracked, unreinforced concrete blocks apply to studs in reinforced members that are cracked due to seismic action or volumetric changes at the time the stud is loaded. Current connection design typically comprises, first, design of the interface between the connected elements based on shear friction or cone pullout strength of studs and, second, design of the connected element using beam theory. However, beam theory is not valid until about a distance equal to the

member depth away from the connection interface. The region adjacent to the connection interface within which the stress paths deviate from beam theory, is often not explicitly designed due to the lack of an adequate model. As will become clear in this report, it is within this region that connections are often inadequately detailed. Many reinforcement details exhibit anchorage deficiencies and unexamined eccentricities, which are not immediately obvious without a rational model. Due to such inadequacies these regions often rely on the concrete tensile strength resulting in inadequate strength and/or brittle behavior.

In addition to these design deficiencies, weld deficiencies too often seem to be the cause for poor performance (23). Unless weldable steel, such as A706 rebars or preheated GR60 rebars are used, an undesirable weld rupture in the heat affected zone (HAZ) may develop.

As an example for a questionable detail, Fig. 1.1(a) illustrates a typical steel bracket connection detail adapted from the PCI Design Handbook[1] and the PCI Connections Handbook[2]. This detail shows studs welded to the embedded vertical plate but no other reinforcement details in the column. This implies that the column longitudinal and transverse reinforcement will be dimensioned on the basis of the column moment, shear, and axial force without any further consideration of the connection. Design of the connection itself is based on the stud strength in cone pullout failure mode and, therefore, explicitly relies on the tensile strength of concrete. However, if the column cracks due to primary flexure,

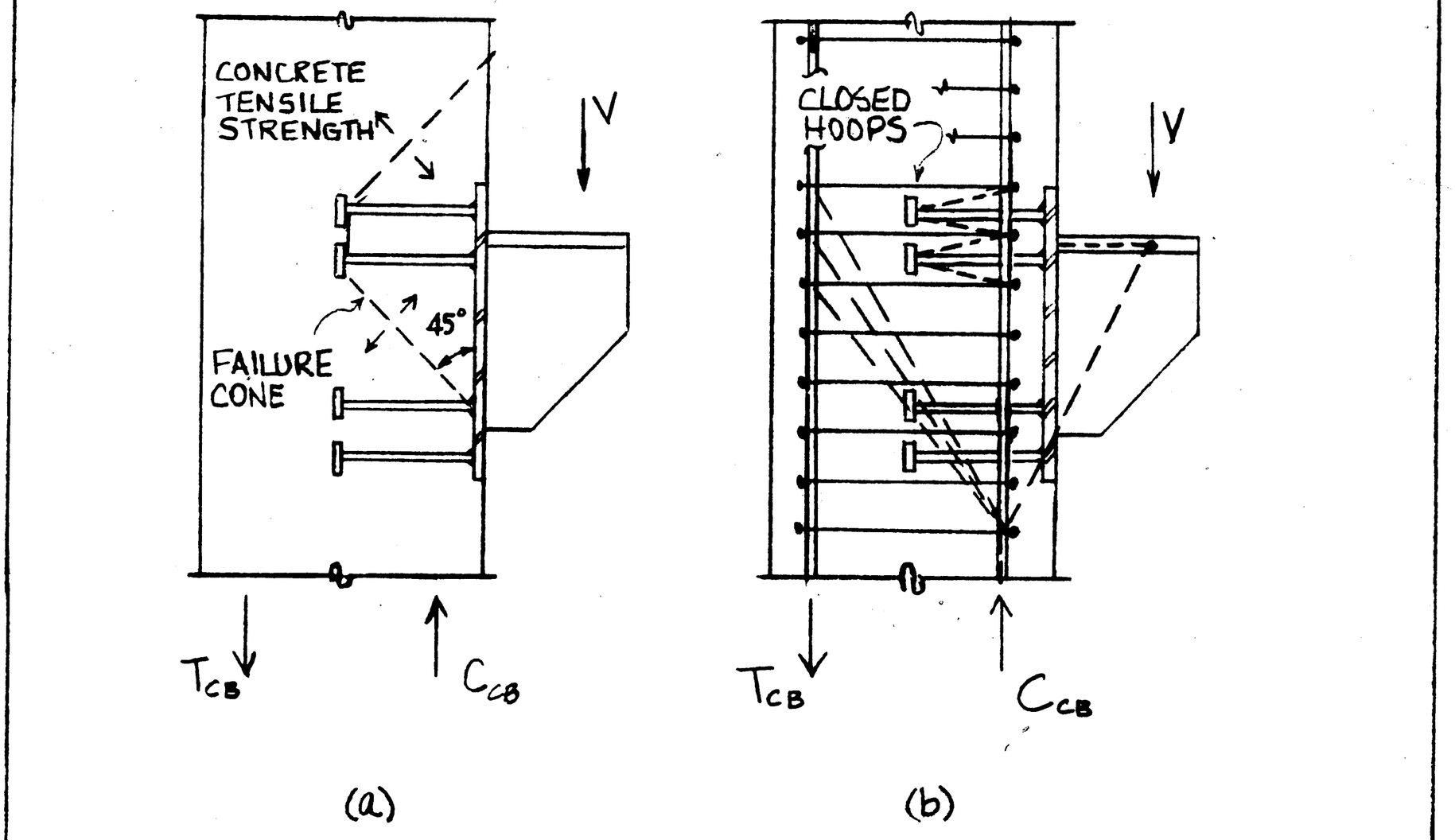

FIGURE 1.1: Steel corbel details using welded headed studs

shear, and axial loads, or if it is precracked due to creep, shrinkage, and other volumetric changes, then it is at least questionable whether the full stud strength measured in tests with uncracked concrete blocks can be reached. Even if it can be reached, a cone pullout failure is brittle. Indeed, test results by Roeder and Hawkins[4], [5] indicate that failure of such connections is brittle if there is a significant moment at the connection interface.

However, the problem goes beyond that. The task at hand is not merely to anchor the studs in the column concrete. Rather it is to turn the moment (force couple) from the bracket around the corner

into the column. The ACI code does not allow us to rely on the concrete tensile strength for flexural strength. There is thus no reason to permit it, if a moment turns a corner. Therefore the question is how to reinforce the column concrete "behind" the connection interface such that the moment turns the corner without relying on the concrete tensile strength. Obviously, the detail of Fig. 1.1(a) does not address this question at all.

1.3 TRUSS MODELS

Truss models represent a simple tool to address such questions. Because of its consistency and rationality, truss modeling provides for a methodological and unifying alternate design procedure. It offers help in determining load paths and finding anchorage locations and provides insight into the structural behavior. The function and purpose of all internal elements are clearly identified. Thus the appropriate reinforcement detailing becomes visible. For example (as will be shown later), anchorage and development of a rebar versus a splice of that bar, or, whether a stirrup acts as shear reinforcement or rather as "hanger reinforcement" (see section 2.4.3), can be clearly differentiated.

Since truss models assume the concrete to be cracked, the resulting designs do not rely on the concrete tensile strength for global behavior; rather only possibly for local behavior such as development.

As an example a truss model has been constructed for the monolithically cast concrete corbel detail shown in Fig. 1.2, also

adapted from the PCI Design Handbook[1]. The dashed lines represent

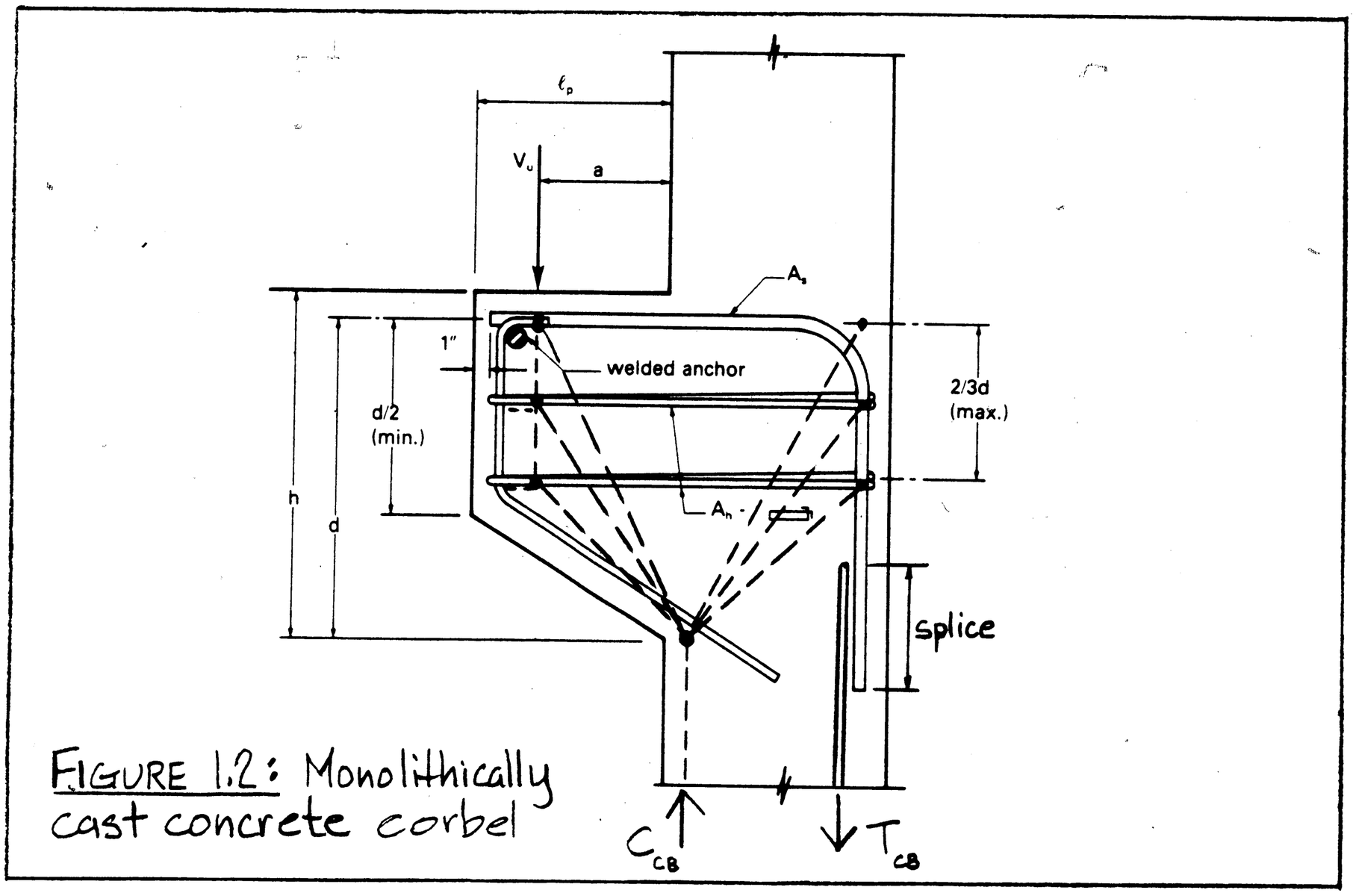

FIGURE 1.2: Monolithically cast concrete corbel

the lines of action of the resultants of concrete compression fields. The concrete compression fields interlock with and engage the tensile steel reinforcement. The tension in the top horizontal rebar is carried back through the column to the opposite face and anchored there by the equal and opposite horizontal component of a diagonal compression strut. The vertical component of this strut anchors the tension in the vertical leg of the bent rebar which is spliced to the column longitudinal reinforcement. At the lower end this diagonal compression strut is anchored by the column compressive resultant and the horizontal component of the diagonal compression strut transferring the corbel load into the column. The horizontal

stirrups "deconcentrate" the diagonal compression both in the corbel and in the column. In essence, all tension reinforcement is anchored by the compression struts and, conversely, all compression struts are anchored by the tensile reinforcement. This reinforcement detail allows the moment (force couple) from the corbel to turn the corner into the column without relying on the concrete tensile strength.

The detail shown in Fig. 1.1(a) can be modified so that it too allows for a truss-like behavior similar to that shown for the monolithic corbel of Fig. 1.2. The stud lengths need to be extended far enough out so that they can interlock with the column longitudinal reinforcement at the opposite face. Just as the bent rebars in Fig. 1.2 allow for a "pocket" to "catch" the diagonal compression struts, so does the interlocking of the stud heads behind the longitudinal reinforcement. The studs are in uniform tension along their lengths and transfer the tension from the plate of the steel bracket at the interface through the column to the column longitudinal reinforcement at the opposite face where this tension is anchored by diagonal struts.

Alternatively, if short studs are more economical, their tensile forces can be transferred and anchored through "hanger" reinforcement (closed hoop stirrups), which assume the task of carrying the uniform tensile force back and behind the longitudinal column reinforcement. This detail is illustrated in Fig. 1.1(b) in which the compression field resultants are shown as dashed lines. In the PCI Handbooks[1], [2] this hanger reinforcement which is required in addition to the longitudinal and transverse reinforcement for flexure, shear, and

axial force in the column, is obviously missing. Without it, transfer of the moment around the corner relies on the concrete tensile strength.

Truss models are most useful as a *design tool*: (1) select a truss which satisfies both the geometric and static boundary conditions of the structural component, (2) determine where reinforcement is necessary based on the locations of the truss members, (3) proportion the reinforcement so that the component can develop its ultimate strength, (the steel should yield before the concrete crushes), and (4) detail the reinforcement so that all the truss members are fully anchored, thus allowing the truss to indeed develop at the ultimate state. Since a designer is relatively free in selecting a truss, design is straightforward. He selects the geometric variables, in particular the location of the reinforcement. On the other hand, analysis requires more effort, since he must try to fit trusses to already given reinforcement and select among the possible trusses the one with maximum resistance. This analysis task becomes complex particularly if the reinforcement in the structure is not designed using a truss. The resulting truss models are often complex, or do not even exist, because the details rely on the concrete tensile strength. Thus a finite element procedure is a much more suitable *analysis tool*.

While finite element models provide a tool for this analysis task, they do not assist in the design task of deciding where reinforcement is to be placed and where it is to be anchored, (unless it is used iteratively).

Truss models have put design of beams and deep beams for shear and torsion on a rational and theoretically sound structural mechanics foundation (theory of plasticity, compression field theory). They have unified the design of beams, deep beams, brackets, corbels, and slabs [ref. (6) - (18)]. They also provide for a consistent transition from slender to deep beams, and from beams subjected to torsion to slabs under twist. It is only natural to therefore extend the truss model design methodology to connections. This will not only eliminate empiricism and put connection design on a theoretically sound structural mechanics foundation, but will unify the design procedure through general principles and rules, which would apply to all connections.

1.4 OBJECTIVES AND ORGANIZATION OF REPORT

The objective of this report is to present an introductory overview on a design methodology based on truss models for connections. This design methodology is placed in the context of the truss model based design methodology for beams, deep beams, brackets, corbels, and knee joints subjected to shear, flexure, and axial loads.

Accordingly, chapter 2 introduces the basic background knowledge accumulated over the past few decades on truss modeling and the behavioral insights and design rules gained from it. The first three sections, 2.1 to 2.3, introduce the basic concepts: Shear transfer through diagonal compression fields; the basic elements of truss models; and the distinction between B and D regions based on whether

or not beam theory is applicable. They lead to the hard core of this chapter: Truss models for B regions such as beams in shear and flexure (section 2.4); truss models for D regions such as deep beams, corbels, and joints (section 2.5); and the boundary conditions that must be observed between B and D regions (section 2.6). Two levels of truss modeling are presented for beams in shear and flexure: truss models for beam sections (section 2.4.1) and truss models for the complete member (section 2.4.2). Special emphasis is placed on the proper treatment of suspended loads and indirect supports (section 2.4.3) and of inflection points (section 2.4.4). Section 2.7 addresses the treatment of prestress. Sections 2.8 and 2.9 present a treatment of anchorage and development from a truss modeling perspective and illustrate it through qualitative analyses of tested nib details of beams with dapped ends. A summary of general rules for truss modeling is offered in section 2.10. Section 2.11 concludes chapter 2 with a treatment of interface shear transfer which is compatible with the use of truss models in the regions adjoining the interface.

Chapter 3 presents, from a truss modeling perspective, a treatment of monolithic concrete joints such as corbels, knee-joints, and beam-column joints, and of other disturbed regions such as dapped ends. Truss models are used to investigate anchorage and development requirements and to interpret test results. While most of the treatment is qualitative, section 3.5 presents results of a quantitative truss model analysis for the dapped end of a

pretensioned T-beam verifying the experimentally observed failure mode.

The behavioral insight gained and design guidelines identified are of direct relevance to precast concrete connections, since the behavioral characteristics and problems of the regions adjacent to the connection interface are very similar to those of monolithic joints.

Chapter 4, finally, applies the basic concepts developed in Chapter 2 and 3 to precast concrete connections, both "simple" connections and moment-resisting connections. As examples for simple connections various angle seat bearing connections are treated (Sections 4.1 to 4.4). The treatment emphasizes that connection design comprises not only design of the interface but also of the adjacent disturbed regions and that simple connections are not really simple in that they transfer moments around a corner in a manner very similar to monolithic joints. To provide an understanding over the full range of behavior of such connections, truss models and failure modes are associated with the various regions that they control in the connection interaction diagram in terms of moment, shear, (and axial) force at the interface. Section 4.5 puts the design of a simple connection such as an angle seat bearing connection into the context of the design of a member such as a wall panel, thus pulling together and illustrating the principles derived in chapters 2, 3, and 4. The inter-relation between connection and structural member design is demonstrated thus illustrating that both should be the responsibility of the same engineer.

Sections 4.6 and 4.7 treat behavior and design of moment resisting connections both qualitatively and quantitatively. The treatment shows that the behavior of the disturbed regions adjacent to moment-resisting connection interfaces is, in principle, very similar to that of monolithic joints. However, the complex behavior of these regions is further complicated in precast concrete by the need to connect or splice reinforcement in the same location. Design of precast connections requires therefore a deeper understanding than that provided by the current empirical or semi-rational design approaches for monolithic joints, and this is the reason for the extensive presentation of rational joint models in Chapter 3. The presented examples show, though, that once the behavior of monolithic joints is fully understood, the design of precast concrete moment connections, including adjacent disturbed regions, is relatively straightforward and follows similar principles. Specifically, anchorage and development play a similarly crucial role. If the connection hardware also solves the anchorage problems inherent in monolithic joints, precast concrete connections could perform even better than monolithic joints. Special attention is called to the eccentricities which are often present when rebars are welded to insert plates. These can lead to unsatisfactory performance if left unattended. It is shown that connection truss models allow for a rational and natural treatment of such eccentricities.

Finally, chapter 5, summarizes the conclusions and findings of this report. It offers preliminary design guidelines for precast

concrete connections in code language. Needs for future research are also identified.

2. TRUSS MODELING CONCEPTS

Experimental and analytical research over the past two decades has shown that reinforced concrete beams, deep beams, corbels and slabs assume a truss-like behavior under combined flexure, shear, and torsion when fully cracked at the ultimate state [ref. (6) - (14)]. Such observations gave rise to the utilization of truss models in the design of such elements in practice. In fact, the design of these elements by truss models is already incorporated in the Swiss Code[15], the Canadian Code[16], and the European Model Code[17]. The PCI Design Handbook[1] contains the code provisions for combined torsion and shear of the Canadian Code[16]. The truss model approach is also planned to be introduced in chapter 11 of the ACI 318-92 Building Code for structural member design.

The following sections introduce some of the basic, but necessary concepts needed to utilize and understand truss models, whether it be for primary structural members or for connections. Also, anchorage phenomena are described from a truss modeling perspective. In line with the scope of the introduction, only two-dimensional truss models are treated. In particular space truss models for beams and slabs in torsion are not treated. Extension to three-dimensional or space truss models is relatively straightforward, once the basic concepts are understood in two dimensions.

2.1 SHEAR IN CONCRETE

Consider an uncracked, linearly elastic, simply supported concrete beam with uniform loading, as shown in Fig. 2.1(a). Mohr's circle can be drawn for the elements A, B, and C of the concrete beam to indicate the principle stress directions as shown in Fig. 2.1(b). If the principle stress directions were plotted for an infinite number of elements over the entire area of the beam, a stress trajectory pattern as shown in Fig. 2.1(c) would result. Along the neutral axis of the beam, normal stresses are zero and the element is in pure shear as shown by element B. Pure shear in uncracked concrete is transferred by diagonal (45^o inclination) compressive and tensile stresses. With the addition of normal flexural stresses to the element, the diagonal will deviate from 45^o as shown for elements A and C. Since cracks develop normal to the principle tensile stresses, when the concrete tensile strength is exceeded, they will roughly follow the compression stress trajectories. In particular, they will be inclined by 45^o at the neutral axis if there is no axial load or prestress.

Now let us consider a cracked reinforced concrete element under pure shear which, as shown in Fig. 2.2(a), may be viewed as a composite consisting of a plain concrete element and a steel mesh element. Since the concrete is diagonally cracked, it can resist the applied shear, τ_A, only by diagonal compression. Hence, normal compressive stresses, σ_c, must be acting, too. However, since no externally applied normal stresses exist, σ_c must be balanced internally by steel tensile stresses. Thus, in cracked reinforced

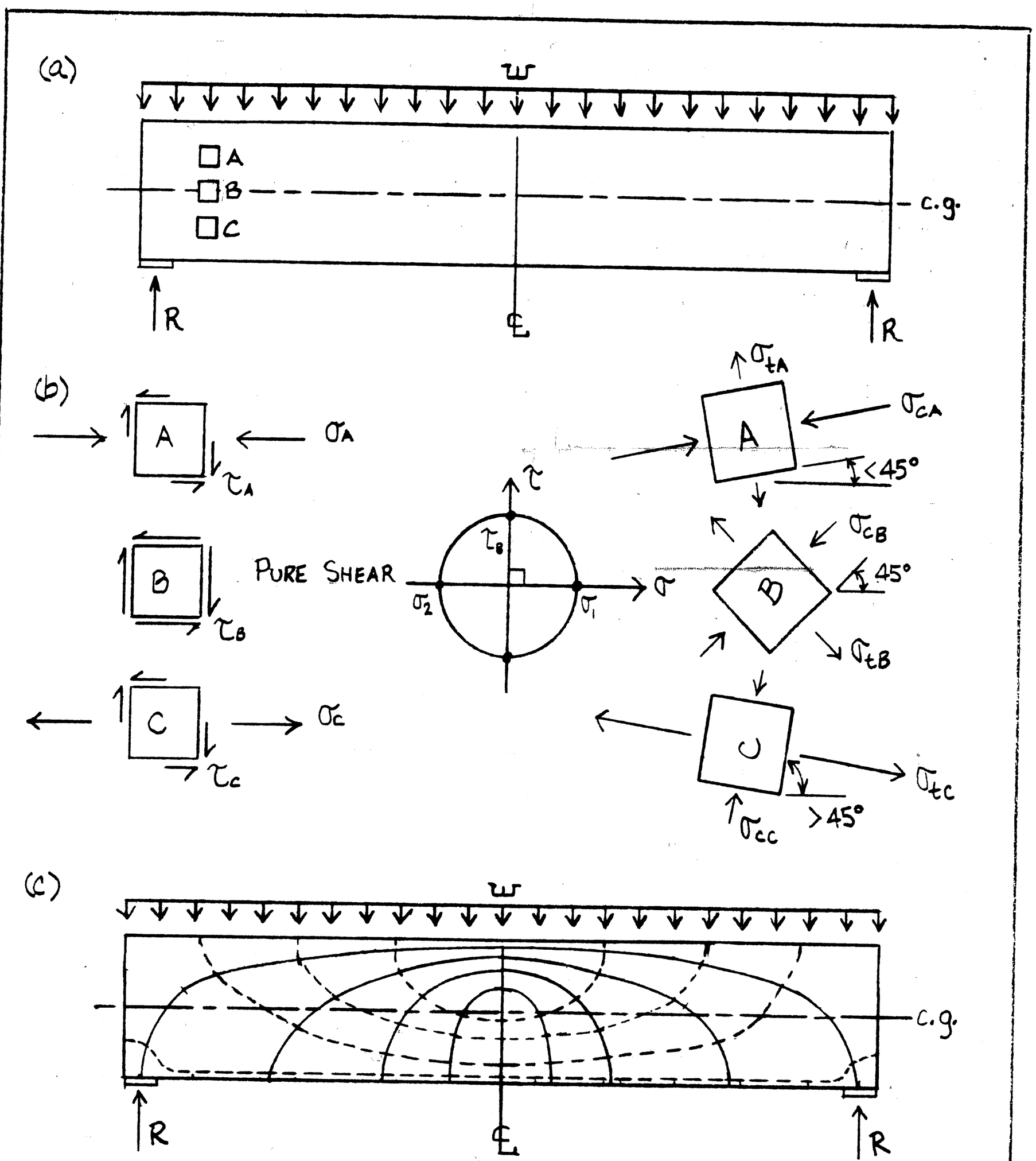

FIGURE 2.1: Principle stress trajectories in a linear elastic concrete beam

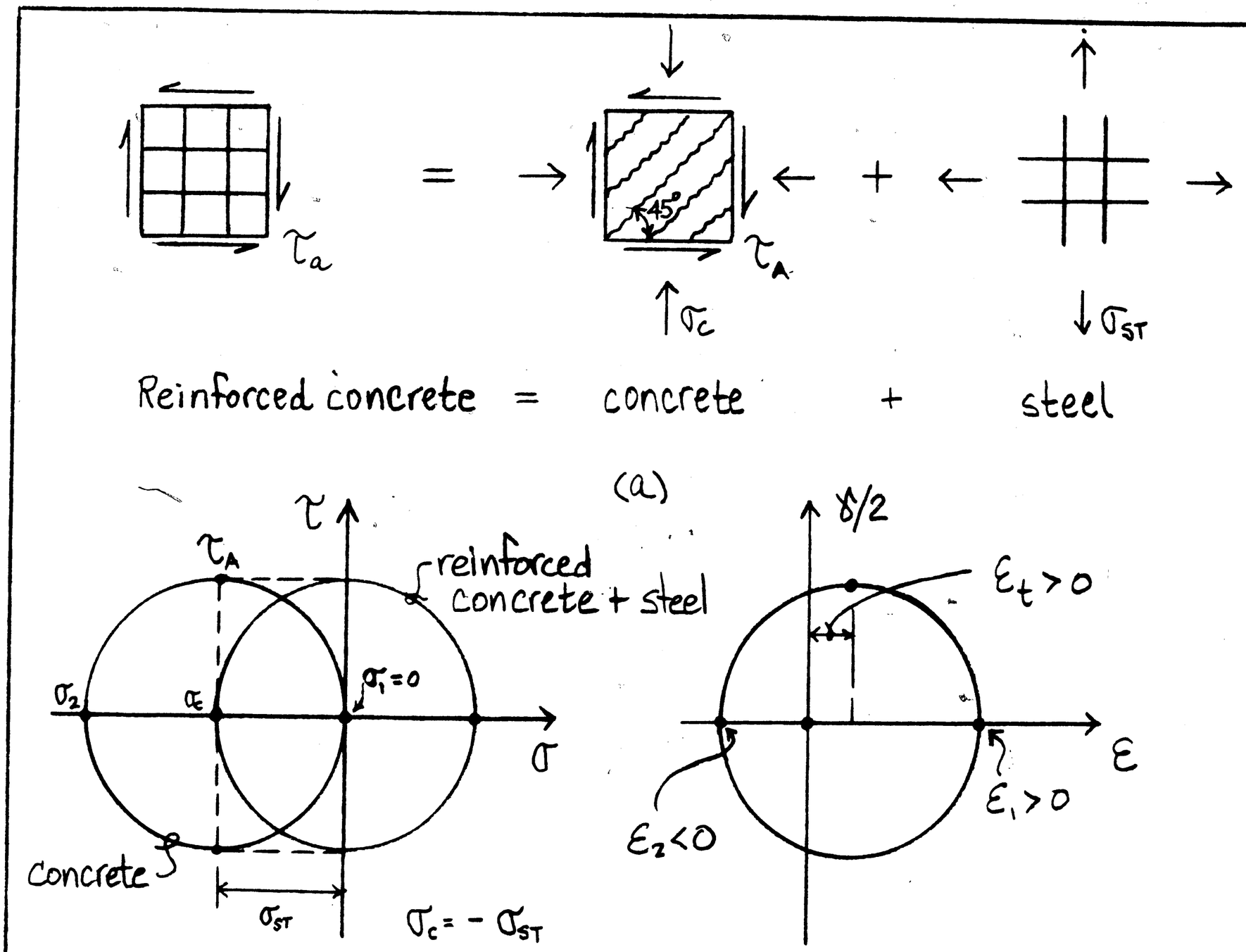

FIGURE 2.2: Pure shear in cracked reinforced concrete

concrete, shear is resisted by diagonal concrete compression and steel tension. Figure 2.2(b) shows the corresponding Mohr's circles of stress. In general, shear transfer in cracked concrete requires reinforcement in two directions (usually orthogonal). In slender beams, the longitudinal reinforcement required for shear is usually combined with the primary flexural longitudinal reinforcement.

Mohr's strain circle, Fig. 2.2(c), illustrates that it is indeed possible for the steel to be in tension, while the concrete is in diagonal compression.

If the steel volumes in the two directions are different, stress redistributions develop as the loading increases. The diagonal compressive stresses may become flatter or steeper than the original cracks. The crack pattern at ultimate will not, in general, coincide with the initial cracks. Indeed, it is often observed in tests that a second, differently inclined crack pattern overlays the first. Therefore, for design, the inclination angle θ of the compression diagonals (Fig. 2.3) can be selected within certain limits, typically $25^{o} < \theta < 65^{o}$. However, since diagonal compression struts at

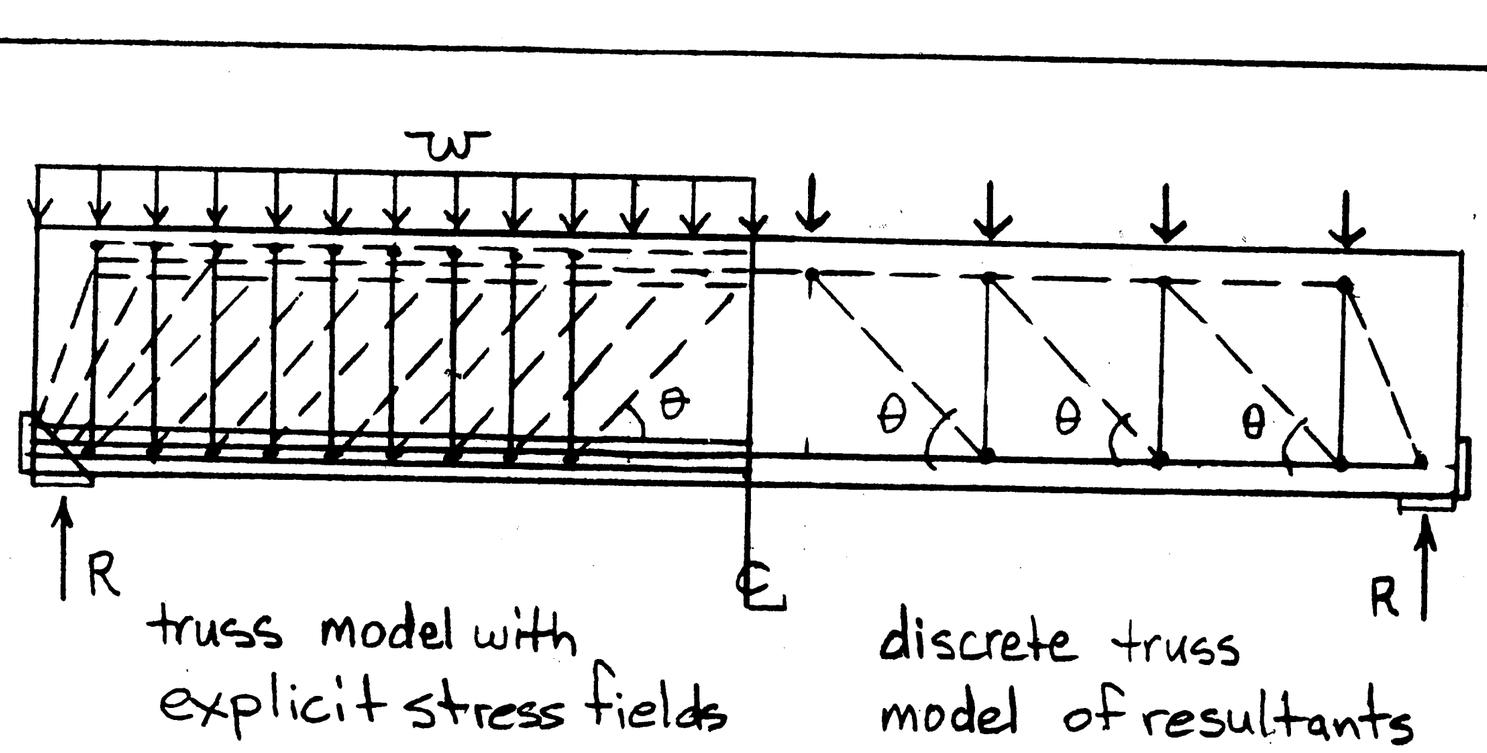

FIGURE 2.3: Truss action for uniformly loaded simple beam

ultimate usually cross cracks, the diagonal compressive strength is lower than the flexural compressive strength. The more θ deviates from 45^{o} for pure shear, the lower becomes the diagonal compressive

strength. Experimental research by Vecchio and Collins[19] has shown that large transverse tensile strains acting on the diagonal compressive strut tend to lower f'_d. According to the Vecchio-Collins softening law, the compressive strength of diagonally cracked concrete is given by:

$$f'_d = \frac{f'_c}{(.8 + 170\,\epsilon_1)} \leq 0.85f'_c \qquad (2\text{-}1)$$

where

$$\epsilon_1 = \epsilon_x + \frac{\epsilon_x - \epsilon_2}{\tan^2\theta} \quad ; \quad \theta \leq 45° \qquad (2\text{-}2)$$

and where f'_d and ϵ_x represent the adjusted concrete compressive strength and the longitudinal strain, respectively. The strain ϵ_x may be taken as the strain at mid-depth for beams and can be determined from a strain compatibility analysis. Alternatively, it may be taken as the yield strain of steel, 0.002 in/in. The principal compressive strain, ϵ_2, at which concrete crushes diagonally may be taken as .002 in/in.

From Eq. (2-2), (Mohr's circle), it is observed that for given longitudinal strain, ϵ_x, the principal tensile strain transverse to the struts, ϵ_1, increases with decreasing inclination, θ, of the diagonal compression struts. Therefore, according to Eq. (2-1), the flatter the inclination θ selected in design, the lower is the diagonal compressive strength. For given θ, on the other hand, a reduced longitudinal strain, ϵ_x, and, hence reduced ϵ_1, as may be the case in regions away from the maximum moment section or in axially loaded members, results in increased diagonal compressive strength.

A good approximation for f'_d has been suggested by Mueller[31]:

$$f_d' = \kappa f_c' \tan\theta \not> .5 f_c'/\tan\theta \qquad (2\text{-}3)$$

where k = 0.5 for ϵ_x = 0.002 (flexure)

k = 0.85 for ϵ_x = 0 (flexure and axial at balanced failure)

and linear interpolation may be used for $0 < \epsilon_x < .002$. This approximation results in simple analytical expressions for the shear force at diagonal crushing.

Figure 2.3 shows a typical truss model for a uniformly loaded, simply supported concrete beam with compression diagonals inclined at a selected angle of $\theta = 45^o$. The left half illustrates a truss model with explicit compression and tension fields, while the right half shows only their resultants, forming a discrete truss model.

2.2 B AND D REGIONS

Stress paths developed as a result of shear, flexure, torsion, and/or axial loads in regions where beam theory applies, differ significantly from those developed in regions where beam theory does not apply.

In regions where beam theory applies, it can be assumed that the longitudinal strains are linearly distributed over the cross-section and that the total, resultant transverse normal stress in concrete and steel is negligible. The diagonal compressive stresses can be assumed to be approximately uniformly distributed over the depth of the member. Such regions are called B regions.

Regions where beam theory is not valid are called D regions.

Beam theory is not valid where stress concentrations develop as a result of some kind of disturbance or discontinuity. Geometric discontinuities such as dapped ends and openings, static discontinuities such as application of concentrated loads or reactions, transfer of prestress through anchor plates or over the transfer length of strands, or any combination of these -- they all give rise to the existence of a D region. The extension of a D region may be estimated by the principle of St. Venant as illustrated in Fig. 2.4. Any regions remaining between the D regions are B regions. Note that some structures, such as deep beams, consist entirely of D regions.

2.3 TRUSS MODEL ELEMENTS

Truss models consist of three basic kinds of elements. *Compression elements* join with *tension elements* at *nodal zones*.

2.3.1 TENSION ELEMENTS

Tension elements are called *ties* or *chords*. The theoretical ties of truss models are realized in design by steel reinforcement. Flexural reinforcement, stirrups, studs, prestressing tendons, and any other axially stressed tension elements act as ties.

Since truss models are intended to represent fully cracked reinforced concrete at the ultimate state, concrete tensile stresses are neglected. Although they may exist in local regions of concrete, the concrete tensile stresses should never be modeled as ties because doing so often results in premature brittle failures.

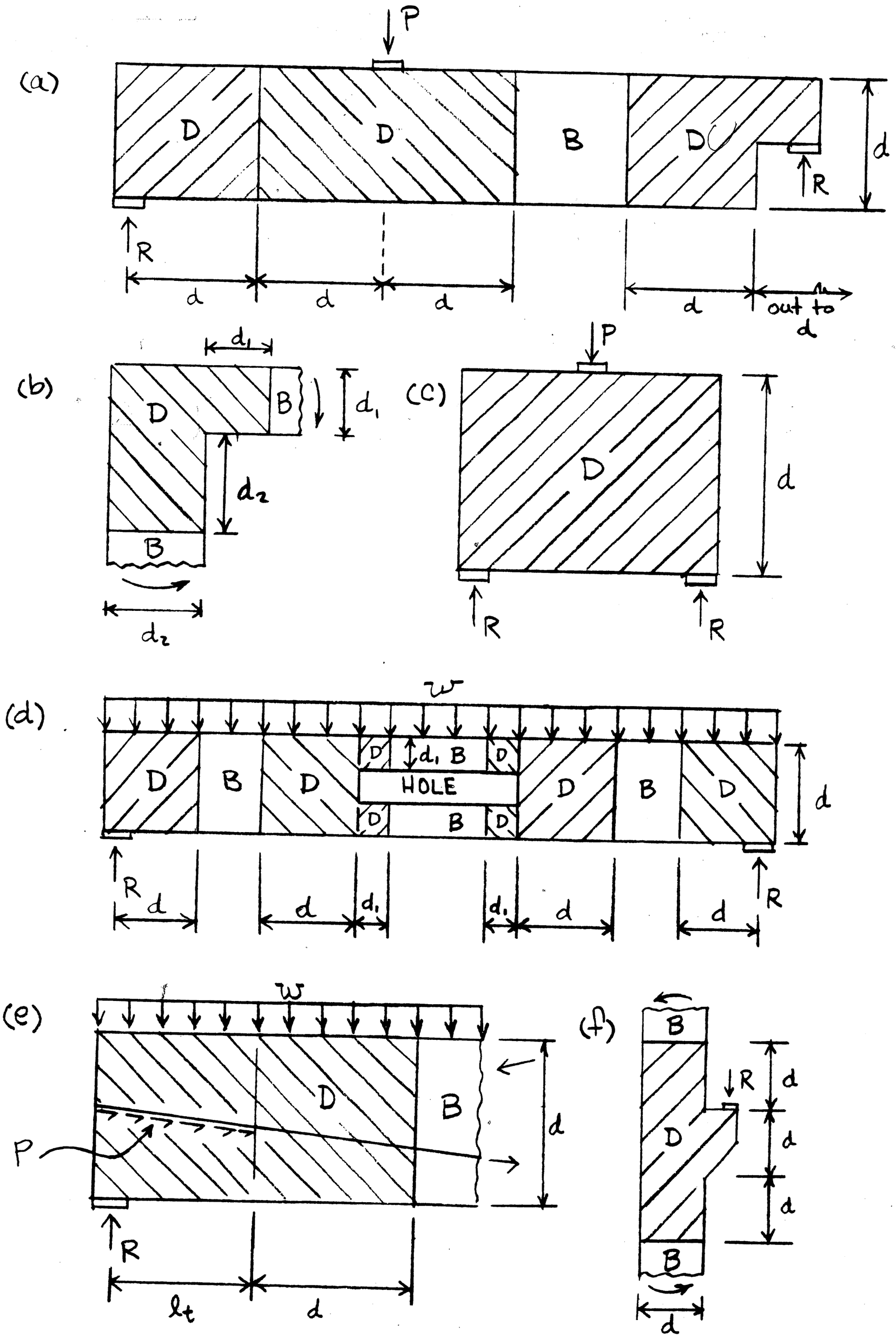

FIGURE 2.4: B and D regions

To assure a ductile behavior at the ultimate state, the ties should yield before the diagonal compression elements crush.

2.3.2 COMPRESSION ELEMENTS

The compression elements of a truss model represent concrete compression fields and therefore always have a finite dimension. As loading is increased from zero to ultimate, the compression elements tend to contract thus occupying narrower and narrower dimensions about their resultant's line of action. At ultimate state, the elements' final dimensions would be given by:

$$C = \nu f_c' b a \qquad (2\text{-}4)$$

where

ν = reduction factor considering reduced diagonal compressive strength

C = resultant compression force in element

f'_c = concrete compressive strength

b = compression element width

a = compression element depth

The geometry of a compression element can be approximated with compression struts, Fig. 2.5(a), compression fans, Fig. 2.5(b), and arches, Fig. 2.5(c). The compression strut has parallel compression trajectories and the stresses are uniformly distributed. The trajectories of a fan radiate out from the "center" of the disturbance and the stresses vary inversely proportionally to the distance from the center of the fan. Eq. (2-4) is meant to apply at the center of the fan adjacent to the nodal zone. Finally, the

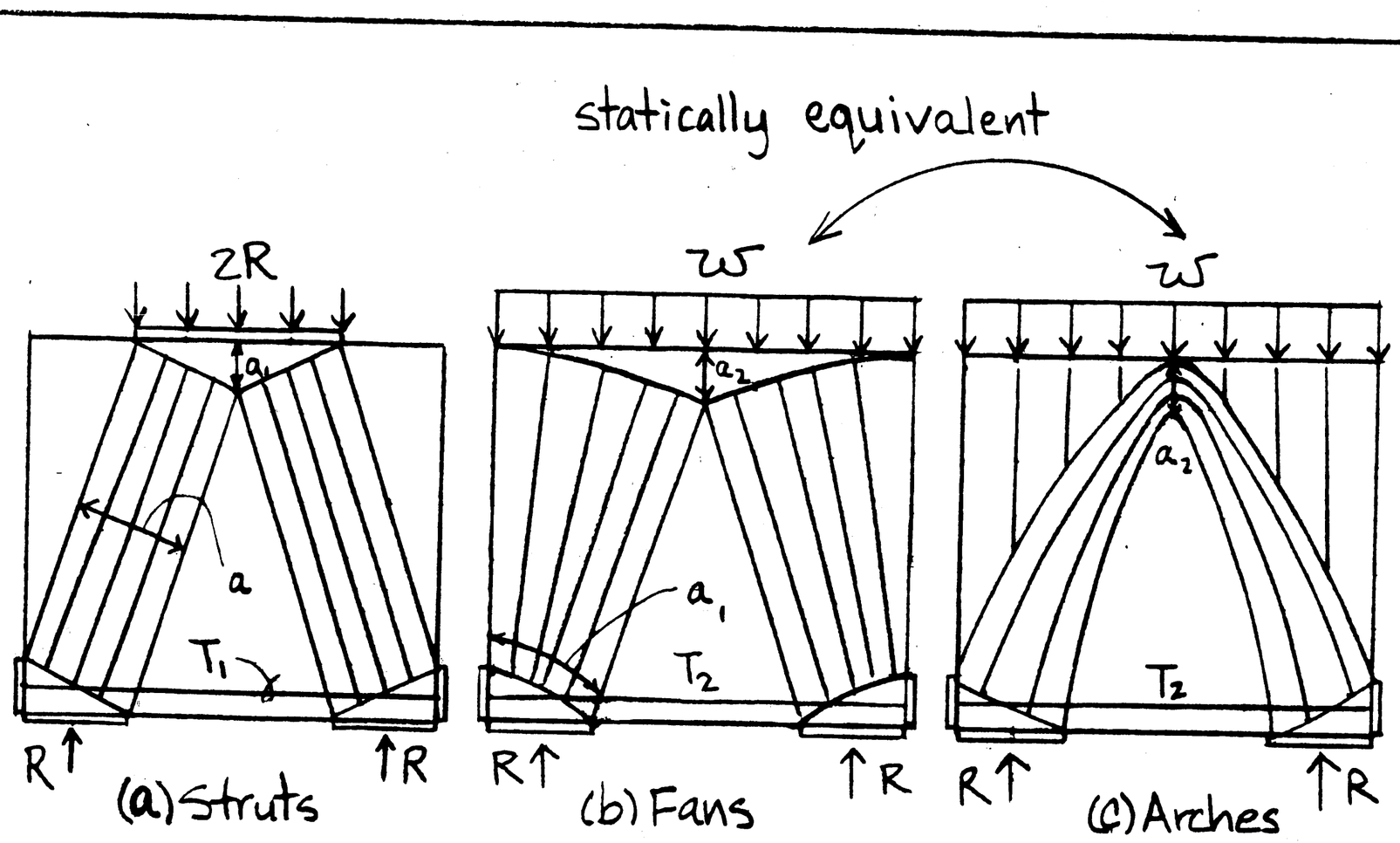

FIGURE 2.5: Compression Elements

compression trajectories of the arch are changing direction due to the applied transverse loads.

In general, the finite dimensions of concrete compression elements affect the geometry of the truss and, hence, the forces they must resist. In Fig. 2.5(a), for instance, the inclination of the struts depend on the depth, a, of the struts.

While the struts, fans, and arches of Fig. 2.5 model quite realistically the stress fields at ultimate, they form only after significant inelastic stress redistributions. To provide the concrete with this inelastic redistribution capacity (ductility), it must be reinforced with distributed reinforcement in two directions. Although all of the following figures will show only the primary ties

for clarity, this minimum distributed reinforcement is always implied.

Although the same deep beam is modeled using fans in Fig. 2.5(b) and using arches in Fig. 2.5(c), the two models are actually statically equivalent and would each yield identical results for the required tensile reinforcement. Note that a_1 and a_2 in Fig. 2.5 represent the flexural compression block depth at ultimate according to normal beam theory.

2.3.3 NODAL ZONES

Compression elements and tension elements join in biaxially compressed regions called nodal zones. Nodal zones must be in vertical, horizontal, and moment equilibrium. A nodal zone is equivalent to a pin in an ordinary truss, thus the lines of action of the resultants of the truss elements must intersect in one point. Eccentricities at a node are therefore unacceptable.

All nodal zones must be detailed such that they are in a state of biaxial compression, i.e., each face of the node being in compression. A CCT node, (compression-compression-tension), as shown in Fig. 2.6(b), is compressed by two struts on two of its three faces. By bringing the tension tie through the nodal zone and fixing it to a anchor plate, its tension is introduced as compression on the third face of the node. Figures 2.6(a), (c), and (d) respectively illustrate CCC, CTT, and TTT nodes. The anchor plates shown may be replaced by other means of bar anchorage as discussed in section 2.8. In this case they are called fictitious anchor plates and indicate

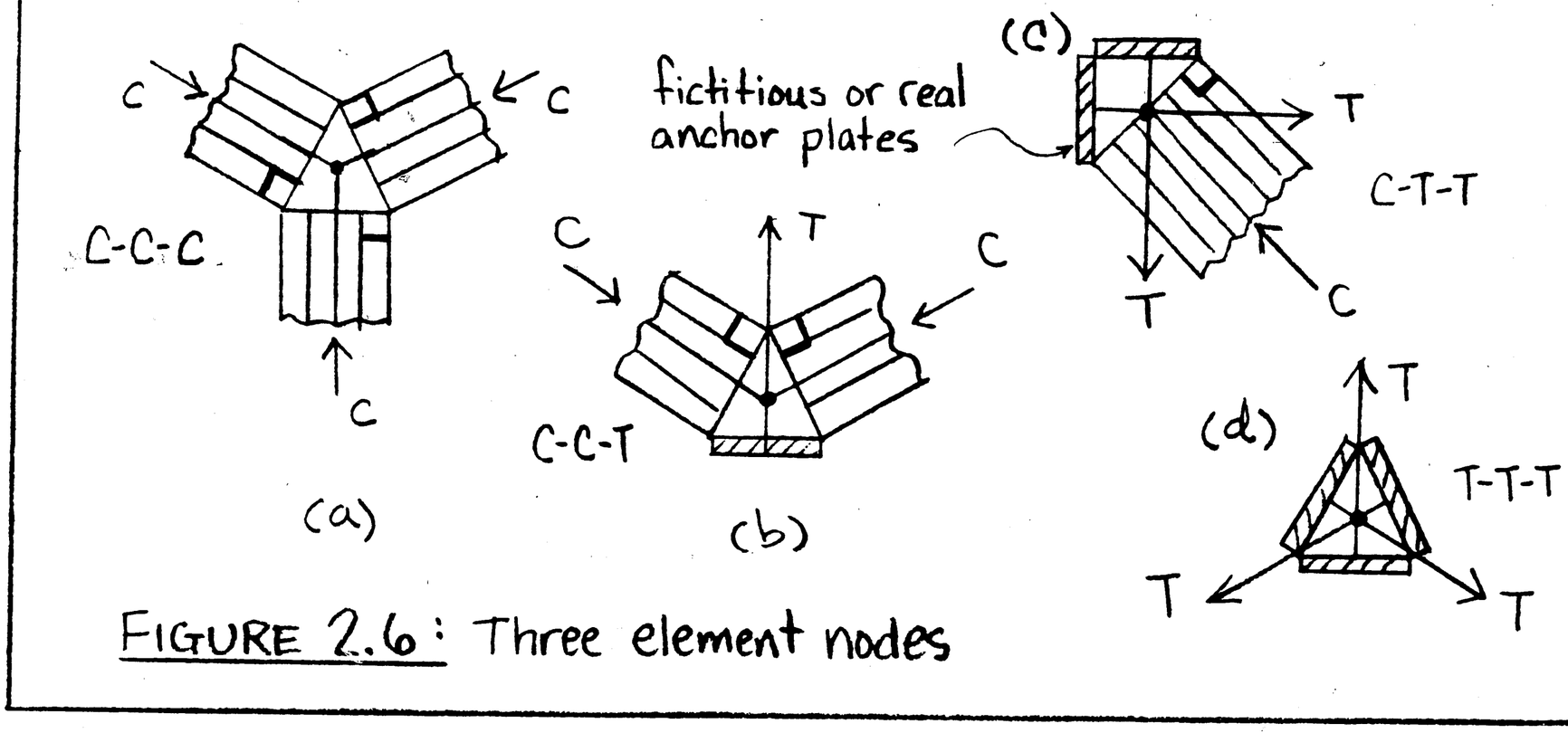

FIGURE 2.6: Three element nodes

the location where a bar must be fully developed or anchored.

When more than three elements are entering a node, they can be broken down into the simpler "three element nodes" just described, as shown in Fig. 2.7.

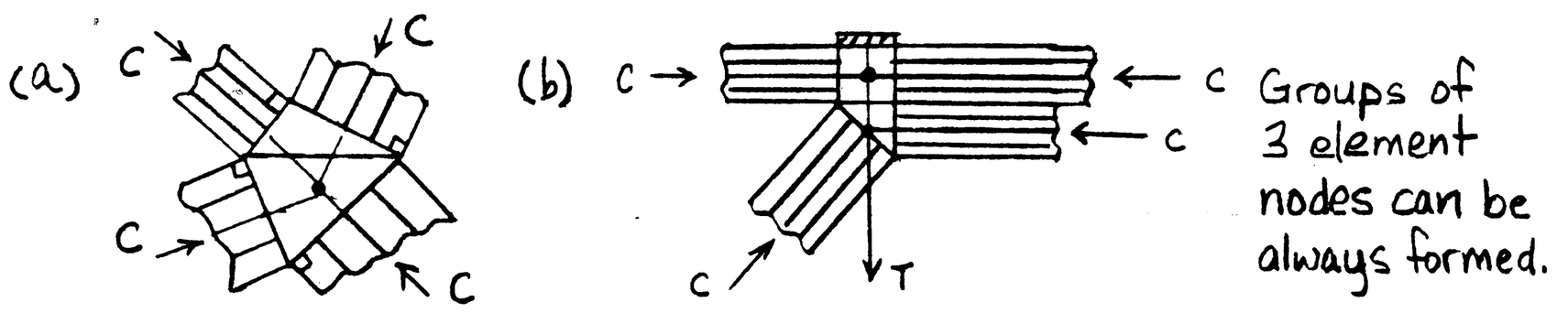

FIGURE 2.7: More than three element nodes

If the compressive stresses exerted on each face of the nodal zone are the same, the nodal zone is in a "hydrostatic" stress state and the struts or ties entering the node are normal to the nodal faces as illustrated in Fig. 2.6. If, on the other hand, the strut

dimensions are chosen beforehand, as in design, the struts will be subjected to different compressive stresses, in general, and will no longer be normal to the nodal faces (Fig. 2.8(a)). This situation is discussed further by Marti[12] who uses Mohr's circle (Fig. 2.8(b)) to determine the stress state in the nodal zone.

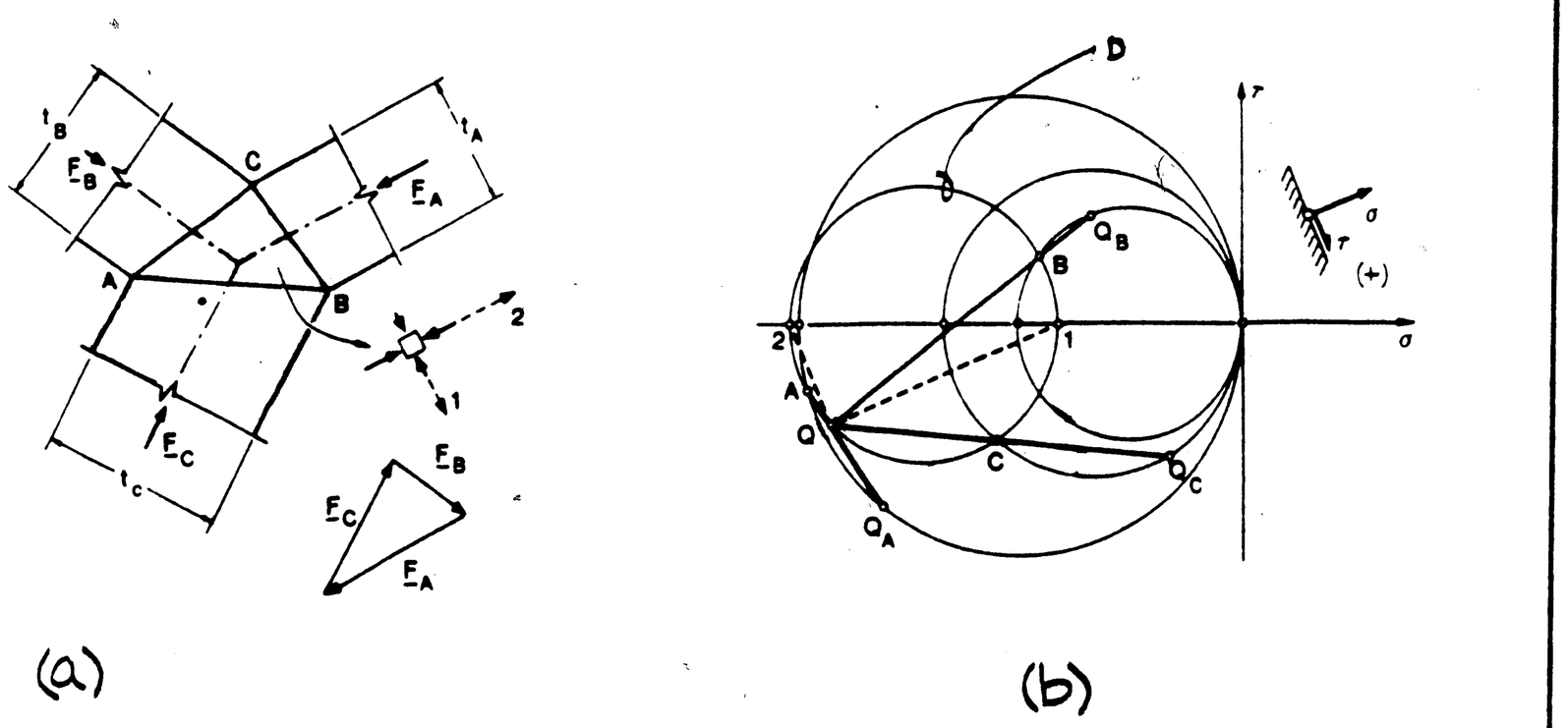

FIGURE 2.8: Nodal zone for intersecting struts with different stresses

The general nodal zones ABC of Fig. 2.8(a) is in a biaxially stressed state defined by Mohr's circle D in Fig. 2.8(b). "This stress state is found by drawing parallel lines to the sides BC, CA, and AB of the triangle through points Q_A, Q_B, and Q_C of the individual struts' Mohr's circles in Fig. 2.8(b). The intersection points A, B, and C of these lines with the corresponding Mohr's circles define the Mohr's circle for the biaxial compressive stress state in the triangle ABC of Fig. 2.8(a). The center of this circle

must lie on the σ-axis and the straight lines $Q_A A$, $Q_B B$, and $Q_C C$ must all intersect at its pole Q''[12].

The general node described above and in Fig. 2.8 is rarely needed in practice. In practice nodes have typically two orthogonal faces subjected to normal stresses only, such as the node in Fig. 2.6(c), or can be resolved into such nodes. However, typically the normal stresses exerted on the orthogonal faces are different, because the tension in the two ties is different or because the plates have a different size. While the compression strut bearing onto the hypotenuse face of the node is no longer normal to that face, its direction can be readily found from the force triangle for the stress-resultants of the truss members. The state of stress of the nodal zone is fully defined by the normal stresses on the orthogonal faces, since they are principal stresses. In the top node in Fig. 2.5(a) and the node in Fig. 2.6(b) only normal stresses are acting across the line of symmetry for reasons of symmetry. Thus each half of these nodes represents a node of the type just described, if the bearing stresses under the plate are different from the compressive stresses in the struts.

For compression fans entering a node, the nodal faces are curved; namely, "convex out" at the "pinch" of the fan and "concave in" at the "spread" of the fan. Such nodal zones are illustrated in Fig. 2.5(b). A mathematical treatment for "curved" nodal zones can also be found in Marti[12].

The hoop forces exerted by a bent or looped rebar "wrapping" around the strut of a CTT node, give rise to a biaxially compressed

nodal zone which could be termed a "hydrostatic" node. The uniform change in direction of the bar tensile force creates a uniform biaxial compression field inside the perimeter of the loop. The stresses are of constant magnitude anywhere and in any direction inside and in the plane of the loop, (analogous to hydrostatic pressure at some depth in a liquid). Figure 2.9 illustrates such nodes.

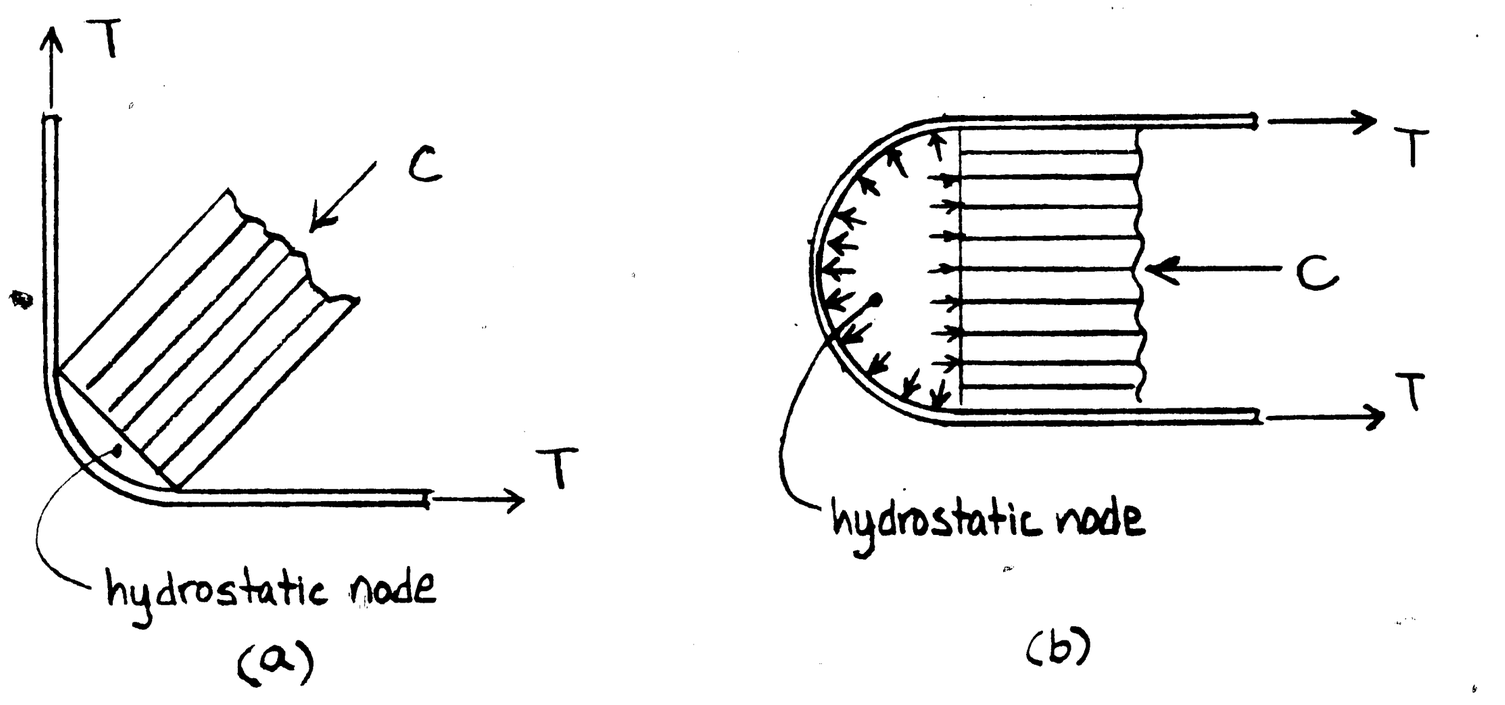

FIGURE 2.9: Hydrostatic nodes

2.4 TRUSS MODELS FOR B REGIONS

Within B regions, the usual assumptions of beam theory are valid: 1. plane distribution of longitudinal strains, 2. sections are free to warp, 3. cross sectional shapes are preserved, and 4. total transverse normal stresses are negligible. In reinforced concrete the additional assumption is usually made that transverse reinforcement such as stirrups is closely enough spaced that it can be treated as uniformly "smeared" reinforcement. With these

assumptions it can be shown on the basis of the theory of plasticity, that a uniform diagonal compression field exists over the depth of the web of a cross-section, as illustrated on the left of Fig. 2.3[11].

For B-regions, two levels of truss modeling or two types of truss models can be distinguished:

(1) truss models which describe the behavior in the vicinity of a cross-section and which have their theoretical foundation in the aforementioned assumptions of beam theory; they are treated in section 2.4.1.

(2) truss models which describe explicitly the behavior of the whole beam at the level of a plane stress problem; they are treated in section 2.4.2. While the second type of truss model provides better insight into the force flow, the first readily provides simple expressions for the usual section-by-section proportioning of reinforcement and concrete dimensions. Sections 2.4.3 and 2.4.4, finally, conclude the truss modeling for B-regions with discussions of the proper treatment of suspended loads, indirect supports, and inflection points.

2.4.1 SECTION BY SECTION APPROACH

In a simple section by section approach, internal actions are determined by considering various cross-sections along the axis of the member. Truss models describe the behavior in the vicinity of such a cross-section. Consider a beam with constant shear as shown in Fig. 2.10(a). The section x-x can be free-bodied as illustrated

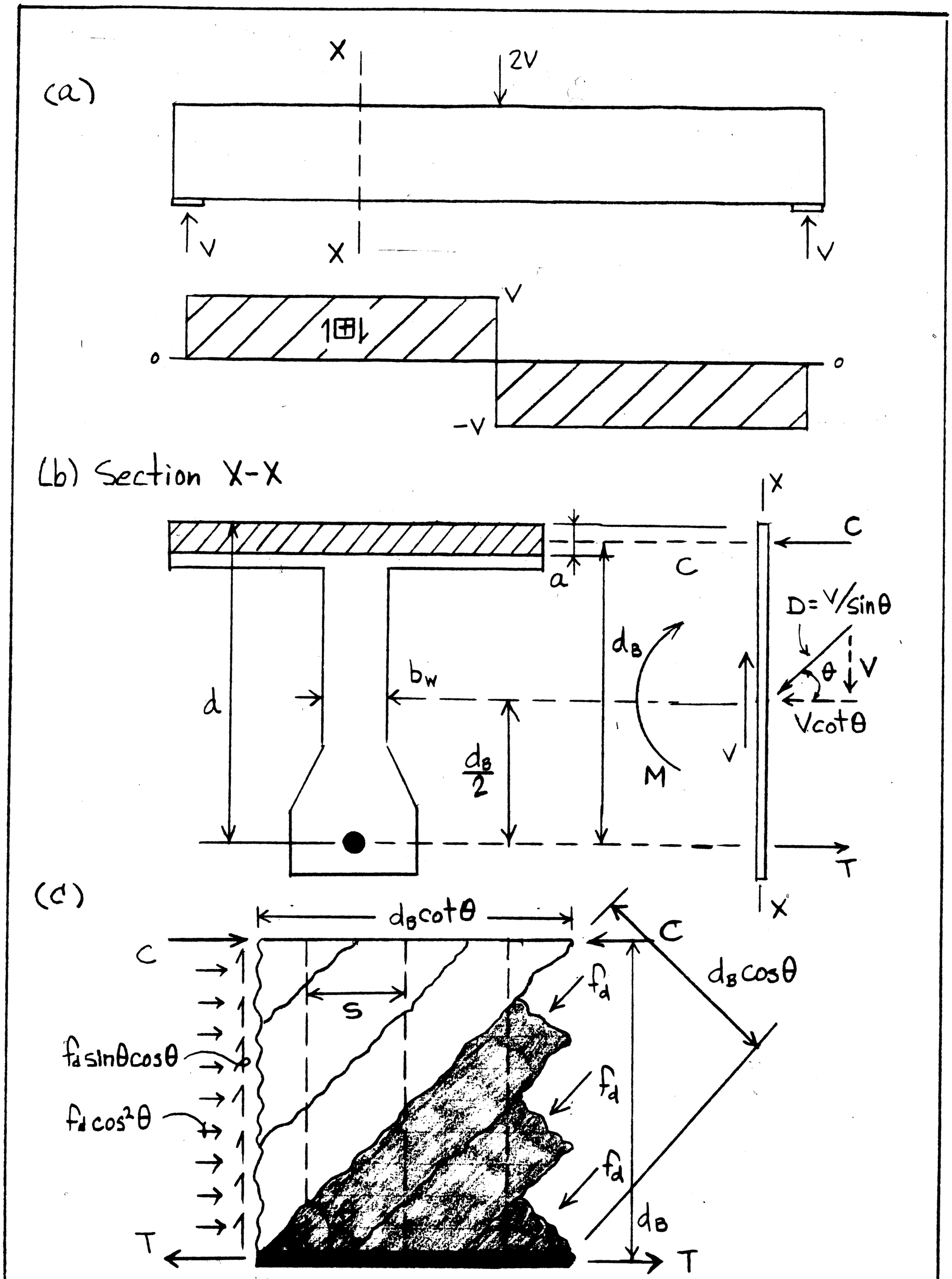

FIGURE 2.10: Section by Section approach

in Fig. 2.10(b) in which the external load actions are shown on the left face of the section and the internal actions on the right face. In addition to the tensile and compressive resultants, T and C, in the flanges resisting flexure, there is an internal diagonal compressive resultant, D, in the web resisting shear. Vertical equilibrium requires that the vertical component of D equals the shear force, V, as shown in Fig. 2.10(b). Hence its magnitude is $D = V/\sin\theta$ and its horizontal component is $N_v = V\cot\theta = D\cos\theta$. The design equations for section x-x become simple, if a uniform diagonal compression field exists over the depth d_B as illustrated in Fig. 2.10(c). Indeed, as mentioned above, this can be deduced from the usual assumptions of beam theory. As shown in Fig. 2.10(c) the diagonal compressive force, D, acts over a width of $d_B\cos\theta$ with a diagonal compressive stress, f_d; hence, $D = f_d\cos\theta b_w d_B$, where b_w is the web thickness. Combining this expression with the two expressions above and solving for V yields

$$V = f_d\, b_w\, d_B \sin\theta \cos\theta \tag{2-5}$$

and

$$N_v = V\cot\theta = f_d\, b_w\, d_B \cos^2\theta \tag{2-6}$$

Obviously, Eqs. (2-5) and (2-6) simply represent the integral over the web area of the shear and normal stresses shown on the left of Fig. 2.10(c).

As shown in Fig. 2.10(c) the compression diagonal of width $d_B\cos\theta$ is supported at the level of the flexural steel by stirrups over a horizontal extension of $d_B\cot\theta$. Over this horizontal distance there are $d_B\cot\theta/s$ stirrups, where s is the stirrup spacing. At

their yield capacity, $A_v f_y$, these stirrups must be capable of supporting the vertical component, V, of the diagonal compressive resultant, thus

$$A_v f_y = \frac{V\, s}{d \cot \theta} \tag{2-7a}$$

or rearranging,

$$V = \frac{A_v f_y}{s}\, d \cot \theta \tag{2-7b}$$

Inserting Eq. (2-5) into Eq. (2-7a) yields $A_v f_y/(b_w s) = f_d \sin^2\theta$: The tension in the transverse reinforcement, expressed as a nominal stress acting over the web thickness, equals in magnitude the transverse compressive normal stress in the concrete. Thus the resultant transverse normal stress is zero as postulated by the 4th assumption of beam theory and similarly to the pure shear element of Fig. 2.2.

Moment equilibrium about both the tension and compression resultants of section x-x in Fig. 2.10(b) yields

$$C = \frac{M}{d_B} - \frac{N_v}{2} \tag{2-8}$$

$$T = \frac{M}{d_B} + \frac{N_v}{2} \tag{2-9}$$

where N_v is defined by equation (2-6). Equations (2-5) through (2-9) can directly be used in design. Equation (2-9) is used to proportion the longitudinal reinforcement, while the stirrups are proportioned with Eq. (2-7). Equations (2-5) and (2-8) serve to proportion the

concrete dimensions such as the web and flange widths. They should be chosen so that the concrete does not crush prior to steel yielding. The diagonal concrete compressive strength f'_d is given by the Vecchio-Collins softening law[19] or Mueller's approximation[31] (see equations (2-1) through (2-3) in section 2.1). To provide good support for the diagonal struts, stirrups should be closely spaced, must enclose the longitudinal reinforcement, and must be anchored within the flexural compression zone with 135° hooks around longitudinal bars. For high diagonal compressive stresses, closed stirrups are preferable. An enlarged tension flange, as shown in Fig. 2.10(b), also considerably improves the support and anchorage conditions for the diagonal struts. While these detailing parameters do not appear in Eqs. (1) to (3), they do affect the diagonal crushing strength. In the Swiss[15] and European[17] codes, f'_d depends on stirrup spacing similarly as in the ACI Code the maximum stirrup spacing depends on the level of shear.

Note that equations (2-8) and (2-9) reveal that additional longitudinal reinforcement for shear is needed everywhere, over and beyond that for pure flexure (M/d_B). Specifically, reinforcement to cover $1/2\ N_v = 1/2\ V\cot\theta$ is also needed where the moment is zero, i.e. at inflection points, (which are covered in more detail in section 2.4.4), and at the ends of beams. Since the longitudinal steel is terminated in these locations, careful anchorage of this steel for these shear induced forces is crucial. As pointed out in the discussion of the pure shear element, Fig. 2.2, shear transfer requires reinforcement in two directions. In slender beams the

longitudinal reinforcement of Fig. 2.2 is combined with the primary flexural reinforcement in the top and bottom flanges as indicated in Eqs. (2-8) and (2-9). These equations also show that these shear induced forces can be readily incorporated in an analysis for flexure and axial loads by simply introducing a fictitious additional axial tensile load of magnitude N_v at mid-depth of the web.

Reducing in design the inclination, θ, of the diagonal compression field reduces the required stirrup reinforcement, Eq. (2-7), but increases the longitudinal reinforcement requirements, Eqs. (2-8) and (2-9). The smallest possible inclination θ is governed either by Eqs. (2-8) and (2-9) or by the diagonal crushing strength, Eq. (2-5). Reducing θ below 45^o reduces both f'_d (Eqs. (2-1) through (2-3)) and the trigonometric expression in Eq. (2-5).

Note that there is no "shear transferred by concrete" or "shear transferred by stirrups", and Eqs. (2-5) and (2-7) should certainly not be misinterpreted in this way. Neither stirrups nor diagonally cracked concrete can transfer shear alone. Rather concrete and steel are working together in a truss-like manner. During loading, the inclination, θ, of the diagonal compression field and, hence, the geometry of the truss, adjust until failure occurs in the more critical of two failure modes: (1) diagonal crushing of the web concrete combined with, in general, stirrup yielding or (2) yielding of both the stirrups and the longitudinal reinforcement (diagonal tension failure). Inserting f'_d from Eq. (2-3) and θ from Eq. (2-7) into Eq. (2-5) gives the shear resistance in the diagonal crushing failure mode as a function of the stirrup reinforcement. Inserting

the yield strength of the longitudinal steel and θ from Eq. (2-7) into Eqs. (2-9) or (2-8) gives the flexure-shear interaction relationship in the diagonal tension failure mode.

Equations (2-5) through (2-9) are strictly valid for any section within the B region of a structural member, if the shear force is constant. If, on the other hand, the shear force is varying, then equations (2-5) through (2-9) are strictly valid (in the B region) only at selected sections x-x for which a uniform diagonal compression field exists over the entire depth as more fully discussed in section 2.4.2.

2.4.2 EXPLICIT TRUSS MODELS FOR B REGIONS

While the section by section method is strictly limited to the design of B regions, explicit truss models may be used to design or analyze both B and D regions of any reinforced concrete structure. Consider the simply supported beam with a concentrated load at midspan as shown in Fig. 2.11(a). How does the beam transfer the concentrated load to the reaction? As shown in Fig. 2.11(a), the load applied at point F is transferred down to the tension chord through fan F-K-L. The vertical component of the fan, V, is equilibrated by the vertical tension field E-F-K-L provided by transverse reinforcement (dashed lines) along boundary K-L ("spread" of the fan). The vertical tension field E-F-K-L is then exactly equilibrated by the vertical component of the diagonal compression field E-F-J-K along boundary E-F. From this boundary, the diagonal compression field transfers its vertical component, V, down and to

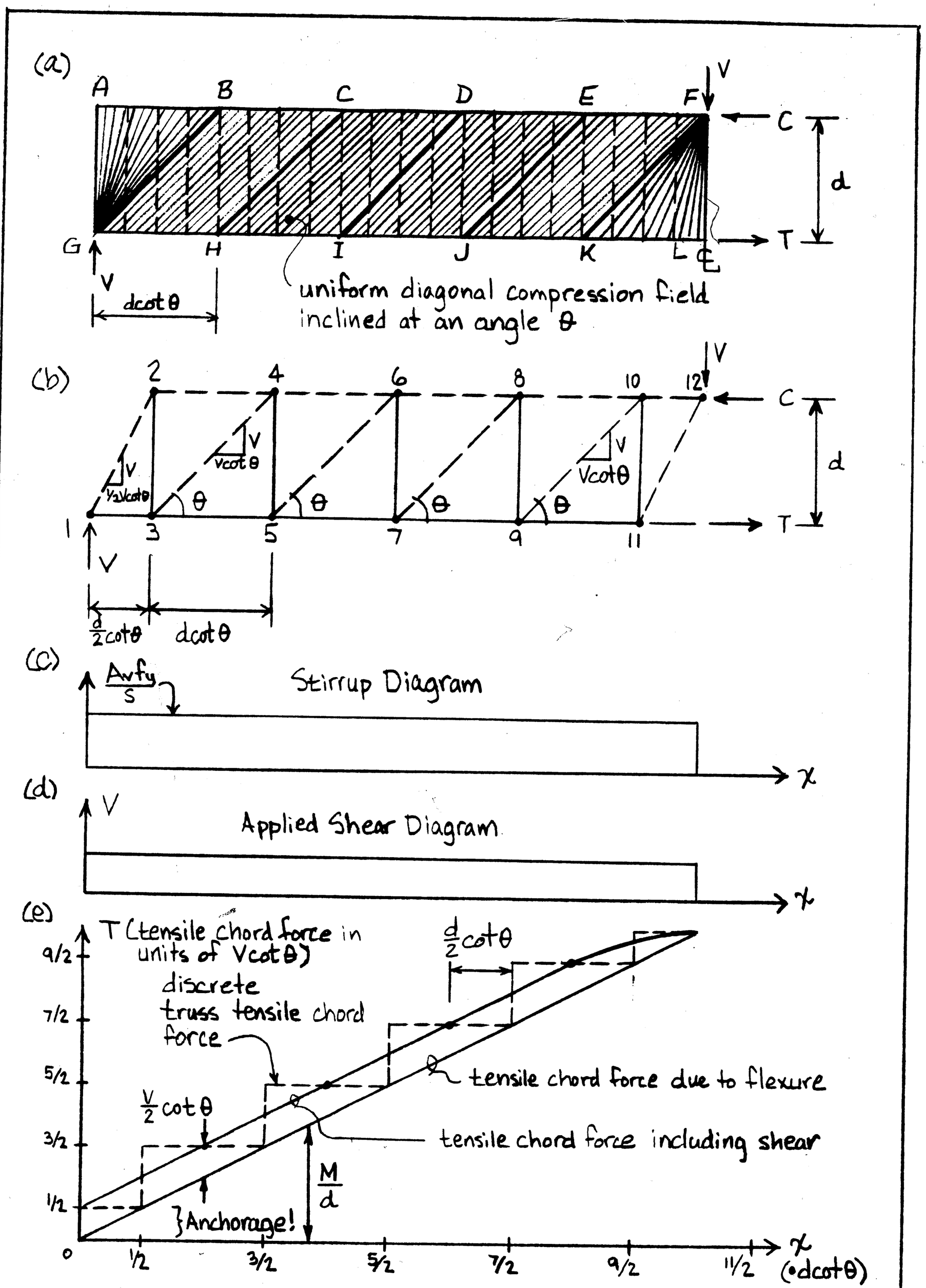

FIGURE 2.11: Simply supported beam with concentrated load @ ℄

the left to boundary J-K where the shear, V, is again equilibrated by the vertical tension field D-E-J-K (dashed lines). Completing the description of the force flow in the beam, the vertical shear, V, is transferred up through the vertical tension field D-E-J-K, down through the diagonal compression field D-E-I-J, up through the tension field C-D-I-J, down through diagonal compression field C-D-H-I, etc., until end fan G-A-B equilibrates the shear, V, of the vertical tension field A-B-G-H. The vertical component of fan G-A-B, V, is finally equilibrated at point G ("pinch" of fan) by the vertical support reaction. The horizontal component of fan G-A-B at point G, on the other hand, must be anchored by longitudinal reinforcement as discussed below. If the vertical tension fields are assumed to be uniform within each segment $d\cot\theta$, then the required transverse reinforcement capacity is uniform over the length of the beam (Fig. 2.11(c)) and proportional to the applied shear (Fig. 2.11(d)). Furthermore the diagonal compression field is then uniform within the region B-F-G-K. For any vertical section lying fully within this region (i.e. between the fan end points B and K) the diagonal compression field is uniform over the depth of the beam and, hence, equations (2-5) through (2-9) derived from beam theory hold exactly. The B region thus extends between sections B-H and E-K through the end points of the compression fans radiating from the concentrated load or support reaction.

The force flow described in the previous paragraph can only be realized if the diagonal compression fields are fully anchored to the vertical tension fields at the tension and compression chord levels

and vice versa. The vertical tension fields may be realized in practice through closely spaced stirrups which are anchored by "wrapping" them around the flexural compression and tension zones. Closed stirrups provide more effective anchorage than open stirrups, since the transverse loops allow for transverse truss action (see section 2.8, Fig. 2.20(d)). However, as important as anchoring the stirrups to the diagonal compression field is anchoring the diagonal compression fields to the stirrups and longitudinal chords, and this includes adequate support for the diagonal compression fields between stirrups. Closely spaced stirrups with heavy longitudinal corner bars and heavy flanges allow for better support and higher average diagonal compressive strength (shear strength) than widely spaced stirrups with light longitudinal bars and no flanges as discussed in the previous section.

The flexural tension chord is realized through longitudinal reinforcement along the bottom of the beam. The tension chord, (which includes the flexural reinforcement and any surrounding concrete and steel), must resist not only the longitudinal tensile force due to pure flexure, $T=M/d$, but also an additional force due to shear as shown in Fig. 2.11(e). Since the longitudinal component of the diagonal compression field, $V\cot\theta$, must be equilibrated by the tension and compression chords, the chord forces are respectively increased and decreased by 1/2 $V\cot\theta$ over that for pure flexure within the B-region as found in section 2.4.1, equations (2-8) and (2-9).

In the D-regions containing the fans, the explicit truss model

provides new insights. Since the bond stresses decrease linearly along the spread of the fan K-L near midspan, the shear term of the tensile chord force decreases parabolically to zero at the center line. Thus only the reinforcement required by pure flexure is needed at sections of maximum moment. Near the support, on the other hand, the diagonal compressive stresses along tension chord H-G remain constant up to the support and the bond stresses are therefore also constant and equal to those in the B-region H-K. The slope of the tension chord force remains constant to the support and, hence, the shear contribution to the tension chord force remains at its B-region value of 1/2 $V\cot\theta$ up to the support, where it balances the longitudinal thrust of compression fan A-B-G as previously noted. Thus at simple supports flexural reinforcement must be provided and fully anchored for a capacity of 1/2 $V\cot\theta$. Similarly, it can be concluded that the reduction of the compression chord force due to shear increases parabolically from zero at point A to 1/2 $V\cot\theta$ at point B and then remains constant at this B-region magnitude up to point F, where it is equilibrated by the longitudinal thrust of fan K-L-F such that the compression chord force reaches its full flexural magnitude, $C=M/d$, at the section of maximum moment. It is worthwhile to note from Fig. 2.11(e) that designing for the tensile chord force including shear effects is equivalent to pure flexural design for a moment diagram which is horizontally shifted by a distance 1/2 $d\cot\theta$.

The ACI code[3] does not cover these longitudinal reinforcement requirements for shear explicitly, but rather implicitly through a detailing rule: flexural reinforcement shall be extended by a

distance d beyond the location where it is no longer required to resist flexure except at simple supports; i.e. the moment diagram is shifted by a distance d, which is sufficient for cotΘ < 2. However, this additional reinforcement is particularly important at simple supports, where no reinforcement is required to resist flexure. While the ACI code[3] contains the detailing rule that one third of the longitudinal reinforcement shall extend 6 in. into the support, full anchorage is only required, if the flexural member is part of a primary lateral load resisting system. But when shear effects become larger relative to flexure such as in deep beams, this rule may no longer be sufficient. Truss models, on the other hand, allow for a consistent transition between beams and deep beams (see section 2.5).

The force flow for this beam has been modeled using compression and tension fields. This force flow becomes particularly clear, if only the discrete truss of the resultants of these compression and tension fields is shown as in Fig. 2.11(b). For example elements 1-2 and 3-4 represent fan A-B-G and compression field B-C-G-H, respectively, while elements 2-3 and 4-5 represent tension fields A-B-G-H and B-C-H-I, respectively. If the tensile chord force is plotted for the discrete truss of resultants, the dashed stepped curve in Fig. 2.11(e) results. It can be observed that the tensile (or compression) chord force calculated for the discrete truss of resultants is exactly correct at sections A-G, B-H, C-I, etc., i.e. at the sections between segments of equal length dcotΘ. Thus for these sections the tensile chord force may conveniently also be determined from the discrete truss of resultants in design. Between

these sections the chord force varies linearly except in the segment K-L, where linear interpolation is a good approximation. Similarly, the stirrups required within each segment of length $d\cot\theta$ may be calculated from the forces in the vertical posts of the discrete truss of resultants.

Let us now consider the truss model for a simply supported uniformly loaded reinforced concrete beam, (Fig. 2.12(a)). Since a uniformly distributed load, w, is applied along the top of the beam, the diagonal compression field E-F-J-K equilibrating w along E-F must be uniform, if the inclination, θ, of the diagonal compression trajectories are assumed to be uniform within the region B-F-G-K. The vertical tension field D-E-J-K equilibrating the uniform diagonal compression field along J-K must therefore also be uniform and of magnitude w. Since the diagonal compression field D-E-I-J must equilibrate along D-E not only the uniform tension field D-E-J-K but also the uniform external load, it has a larger magnitude than the compression field to the right. Repeating this reasoning, it follows that the diagonal compression and vertical tension fields are piece-wise uniform in "bands" of horizontal width $d\cot\theta$.

The flow of forces for this beam may now be described as follows: Along boundary E-F, the uniform load with resultant $W=wd\cot\theta$ is equilibrated by the vertical component, W, of the uniform diagonal compression field E-F-J-K. The vertical component of E-F-J-K is then equilibrated along boundary J-K by the uniform vertical tension field D-E-J-K. The force W is carried up through the tension field to boundary D-E, where an additional, external load W is

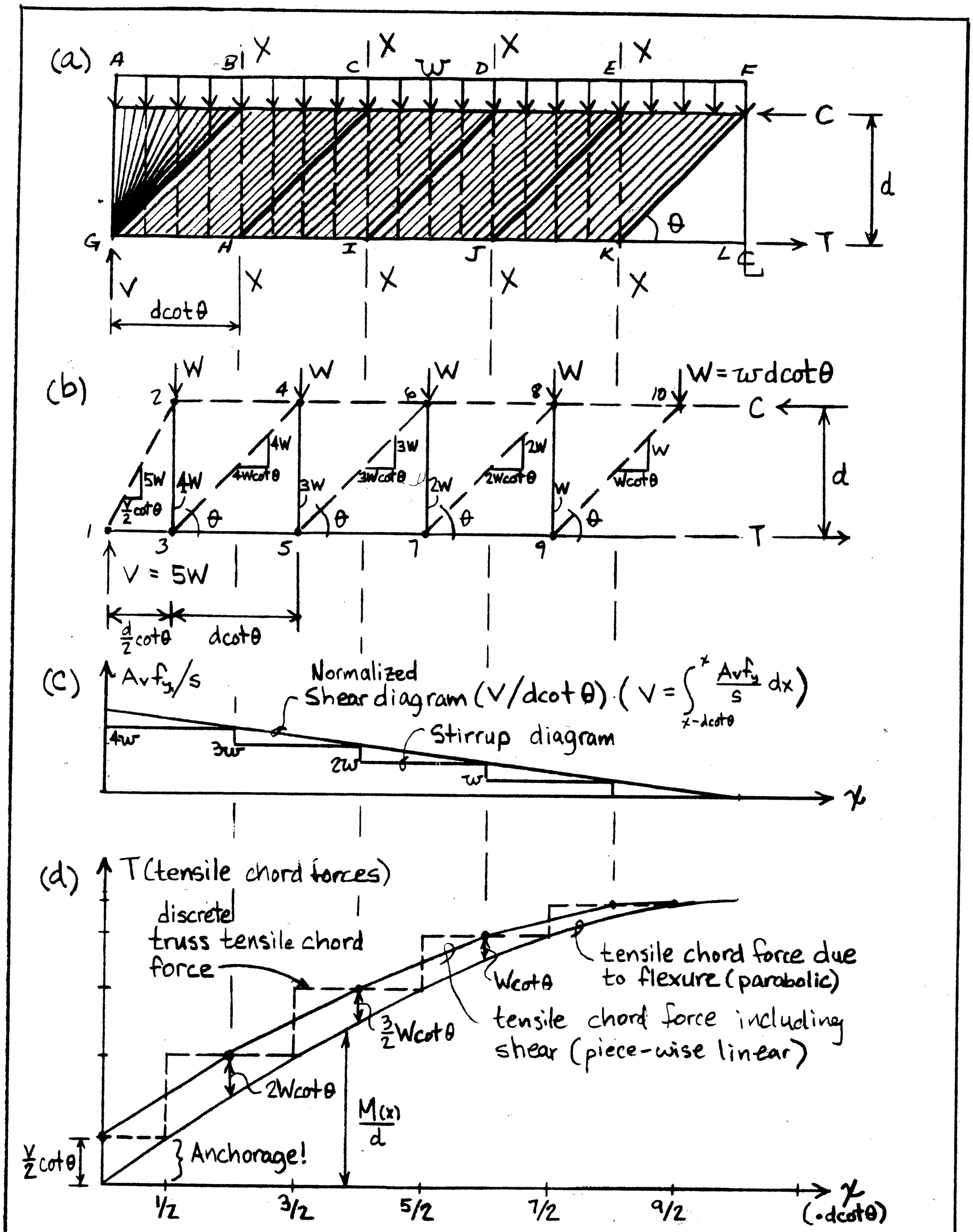

FIGURE 2.12: Simply supported beam with a distributed load

introduced. Thus, the uniform diagonal compression field D-E-I-J must equilibrate a total vertical force of 2W along boundary D-E. The force 2W flows down through the diagonal compression field D-E-I-J to boundary I-J, where it is picked up by the uniform vertical tension field C-D-I-J and transferred up to boundary C-D where, again, an additional external load W is picked up. Thus, the uniform diagonal compression field C-D-H-I must equilibrate a total vertical force of 3W along boundary C-D.

Completing the description of the force flow from boundary C-D, the vertical force 3W flows down through C-D-H-I to boundary H-I and up through B-C-H-I to boundary B-C, where an additional, external load W is introduced. Thus, a vertical force of magnitude 4W flows down through B-C-G-H and up through A-B-G-H. Along boundary A-B, the last external load W is introduced and therefore fan A-B-G is required to transfer a vertical force 5W down to the support, where it is equilibrated by the vertical reaction V at point G. The horizontal thrust of fan A-B-G, on the other hand, must be anchored by longitudinal reinforcement as discussed below.

The explicit truss model described above provides significant new insights. Since the diagonal compression and vertical tension fields are only piece-wise uniform in "bands" of horizontal width $d\cot\theta$, the assumptions of the section-by-section approach of a uniform diagonal compression field over the depth of a section, and of uniform stirrup forces over a distance $d\cot\theta$ from a section, are only satisfied in the sections labeled X-X in Fig. 2.12(a). Hence, equations (2-5) through (2-9) hold exactly only in the sections X-X

separating longitudinal segments dcotθ. Equation (2-7) relates then the shear force in a section X-X with the stirrup forces on the side of increasing shear.

The stirrup forces per unit length, represented by the vertical tension fields, are piece-wise uniform over longitudinal segments dcotθ, and their magnitude increases from segment to segment by an amount equal to the distributed load, i.e. w, such that the stirrup diagram in Fig. 2.12(c) "staggers" below the normalized shear diagram. This does not imply, however, that the shear strength between sections X-X is deficient; rather it means that equation (2-7) is not valid in these sections as previously noted. Vertical equilibrium for a diagonal cut along a diagonal compression trajectory passing through two segments with differing stirrups yields

$$V_n(x) = \int_{x\text{-}d\cot\theta}^{x} \frac{A_v f_y}{s}\, dx \qquad (2\text{-}10)$$

which replaces equation (2-7) for nonuniform stirrups. It is easy to verify that the shear strength calculated with equation (2-10) for the stirrup diagram of Fig. 2.12(c) yields exactly the shear diagram plotted in the same figure for all sections.

The realization in practice of the "banded" tension fields through stirrups, whose capacity and spacing is constant over segments dcotθ, should follow the same anchorage principles as outlined in the previous sections.

The flexural tension chord, realized through longitudinal reinforcement along the bottom of the beam, must resist not only the

parabolically varying tensile force due to pure flexure, $T=M(x)/d$, but also an additional force due to shear as shown in Fig. 2.12(d). At the sections labeled X-X in Fig. 2.12, the shear contribution to the tensile chord force is exactly equal to $1/2\ V(x)\cot\theta$ as previously observed. While this is not exactly true for sections in between, it is known that the total tension chord force including shear effects must vary linearly within longitudinal segments $d\cot\theta$, since the diagonal compressive stresses and, hence, bond stresses are constant within segments $d\cot\theta$ along the chord G-L. Similarly as for beams with constant shear, the tension chord force is equal to $1/2\ V\cot\theta$ at the simple support G, where it is required to balance the longitudinal thrust of fan A-B-G. It must again be emphasized that at simple supports "flexural" reinforcement must be provided and fully anchored for a capacity of $1/2\ V\cot\theta$.

The flow of forces in the truss model using tension and compression fields becomes particularly clear, if only the discrete truss of the resultants of the tension and compression fields is shown as in Fig. 2.12(b). Elements 1-2 and 3-4, for example, represent fan A-B-G and compression field B-C-G-H, respectively, while elements 2-3 and 4-5 model the resultants of tension fields A-B-G-H and B-C-H-I respectively. If the tensile chord force for the discrete truss of resultants is plotted, the (dashed) stepped curve in Fig. 2.12(d) results. The discrete truss gives exactly the correct tensile chord force at sections X-X. Furthermore, as illustrated by Figs. 2.12(b) and (c), the uniformly distributed stirrup forces in each longitudinal segment $d\cot\theta$ can also be

conveniently calculated from the forces in the vertical posts of the discrete truss.

The conclusions from the study of explicit truss models for beams can be summarized as follows. Each shear span (point of zero shear to support) should be divided into longitudinal segments of equal length $d\cot\theta$. Concentrated loads should preferably lie at segment boundaries. The principle of St. Venant, refined for the ultimate state of concrete, says then that D regions extend a segment length (or longitudinal fan length) $d\cot\theta$ from the disturbance. In sections X-X separating segments, the longitudinal chord forces can be determined from equations (2-8) and (2-9) or, alternatively from the chord forces in the discrete truss panel containing section X-X. Between sections X-X, the chord forces vary linearly. At simple supports, the tension chord force is $1/2\ V\cot\theta$, where V is the support reaction. At sections of maximum moment, the tension chord force is equal to the tensile force due to pure flexure. The uniformly distributed stirrup forces per unit length in each segment can be calculated from equation (2-7), applied to the adjacent sections X-X with the lower shear, or, alternatively from the force in the discrete truss vertical tie within that segment. Between sections X-X the diagonal tension shear strength varies linearly according to equation (2-10). Within each diagonal compression band, the diagonal compressive stress can be checked using equation (2-5) applied to the section X-X within that band. In sections X-X the chord forces can also be calculated using a strain compatibility analysis in which shear effects are approximately considered by an

additional fictitious tensile force N_v according to equation (2-6). These conclusions may not hold if suspended loads and indirect loads are treated differently than indicated in section 2.4.3.

2.4.3 SUSPENDED LOADS AND INDIRECT SUPPORTS

Some structural members may be subjected to loads hung along the bottom of the member. To allow for a truss model that is equally safe as the truss model for the same structural member with top compression loads, the suspended tensile loads must be transferred by additional suspender bars to the top face of the member, where they are introduced as compressive loads. Figure 2.13(a) illustrates this. The suspender bars must be fully anchored at the top similarly to stirrups. For the simply supported, uniformly loaded beam of Fig. 2.13(a), the shear diagram and the stirrup diagram are plotted in Fig. 2.13(b). Note that for top compression loads the stirrup diagram would stagger below the shear diagram. As discussed in section 2.4.2, this does not mean that the shear reinforcement is deficient, since the integration of the stirrup diagram according to equation (2-10) gives exactly the shear diagram. However, since the distributed load is hung from the bottom, additional stirrups serving as suspender bars must be added. Thus the stirrup diagram including both shear reinforcement and suspender bars now staggers above the shear diagram, as shown in Fig. 2.13(b). If the loads are hung at mid depth as shown in Fig. 2.13(c), the suspender bars need only be half as long, but they must still be proportioned and spaced identically as would be required if the loads were hung from the

(a)

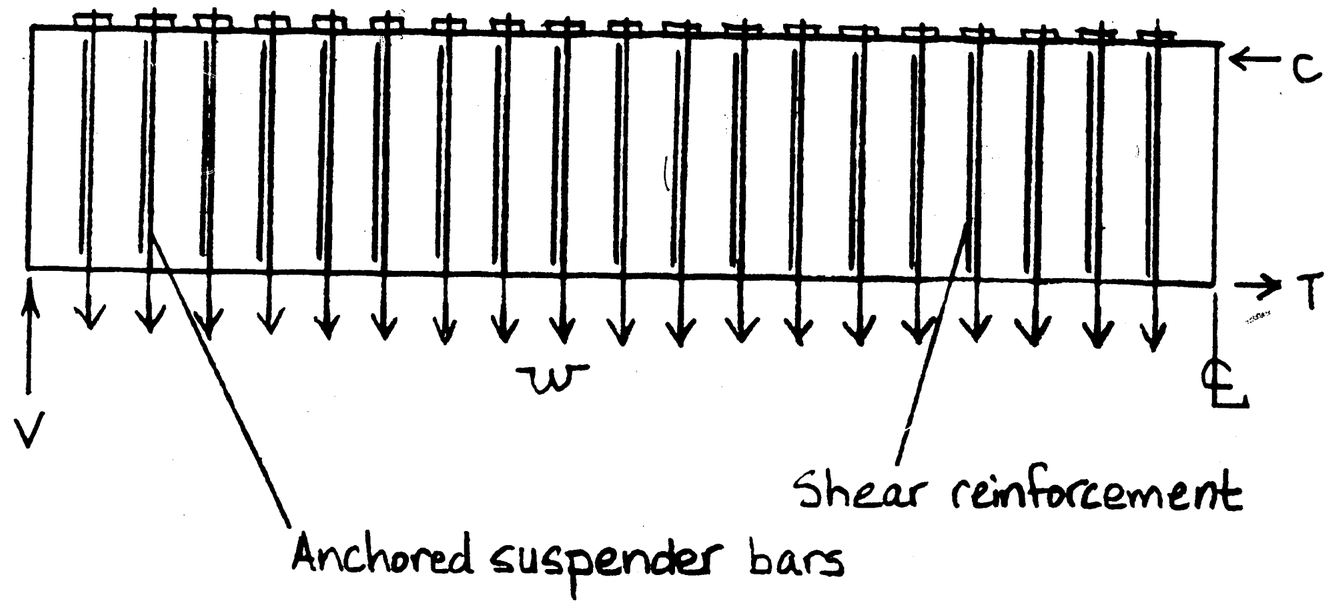

(b)

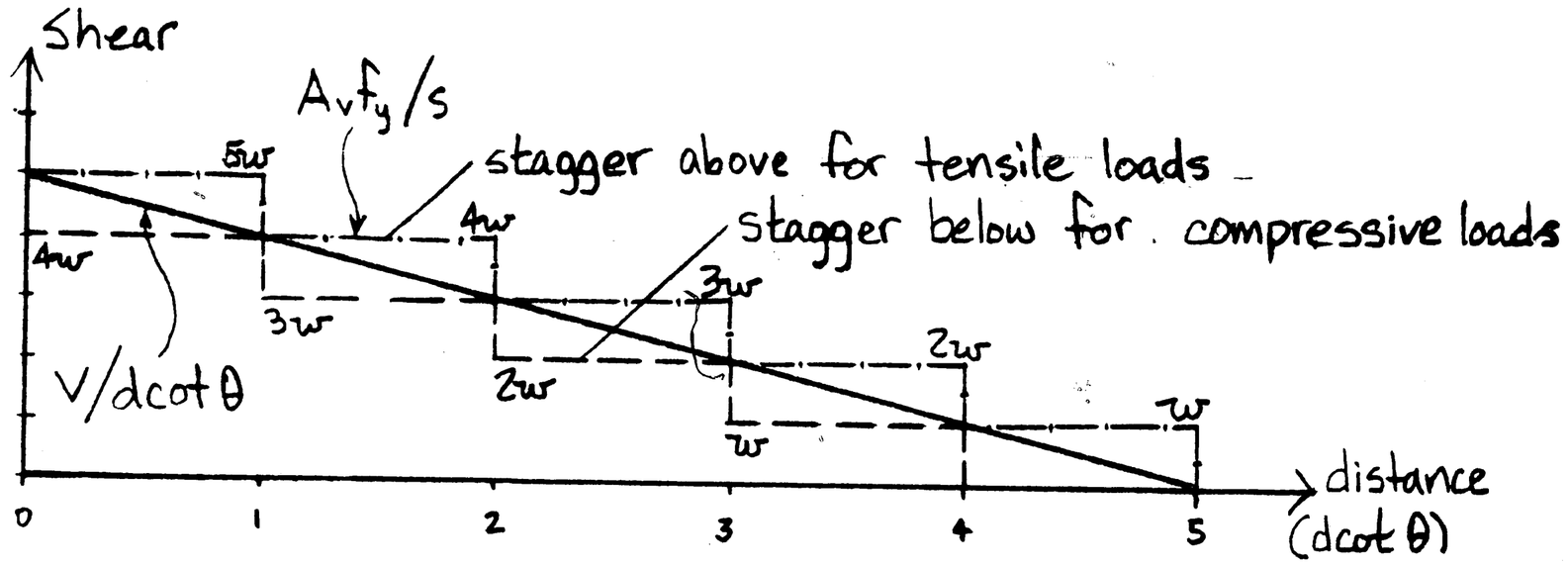

$W = wd\cot\theta$

(c)

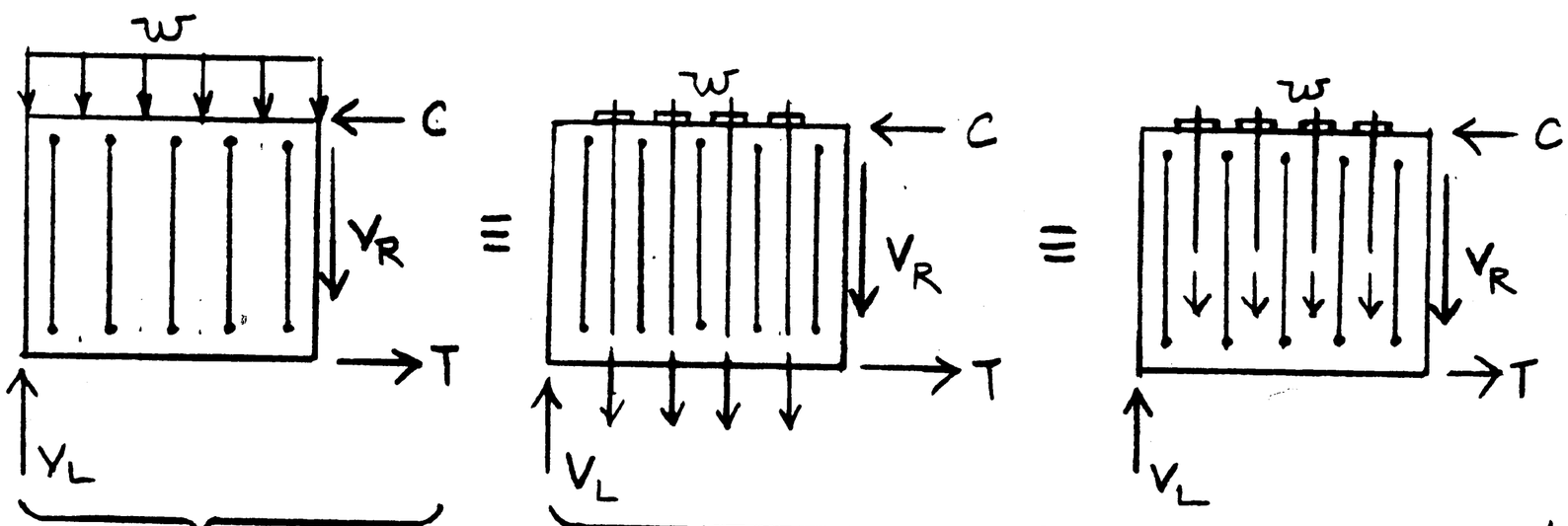

stirrup diagram staggers below shear diagram

stirrup diagram staggers above shear diagram.

Truss models in all ~~three~~ cases are the same as in Fig.'s 2.12(a) & (b).

FIGURE 2.13: Suspender bars for tensile loads

bottom.

In both of the just stated cases, the suspender bars were assumed to be fully anchored at the top. To realize the anchor plates shown in Fig. 2.13, the suspender bars must be anchored as close as possible to the opposite face, similarly to stirrup anchorage. They must be fully anchored within the flexural compression zone if the opposite face is in compression, and they must also enclose the longitudinal reinforcement if the opposite face is in tension. If, on the other hand, the suspender bars are anchored by development over the member depth, then the longitudinal reinforcement requirements along the bottom of the beam increase. Consider a beam with a concentrated load hung from the bottom at midspan, (Fig. 2.14). If the suspender bars are fully anchored at the top, Fig. 2.14(a), then a fan can develop near the section of maximum moment and the maximum tensile force in the longitudinal reinforcement is given by

$$T_{max} = \frac{M_{max}}{d} \qquad (2\text{-}11a)$$

i.e. there is no shear contribution at the section of maximum moment as shown by the tensile chord force diagram. Note that the situation is completely analogous to that shown in Fig. 2.11. If the suspender bar is developed over $\ell_d = d$, Fig. 2.14(b), then no fan develops and there is also a shear contribution at the section of maximum moment.

$$T_{max} = \frac{M_{max}}{d} + \frac{1}{2} V\cot\theta \qquad (2\text{-}11b)$$

The 1/2 Vcotθ term is due to the fact that the compressive diagonals cannot fan out from the upper tip of the suspender bar as in Fig.

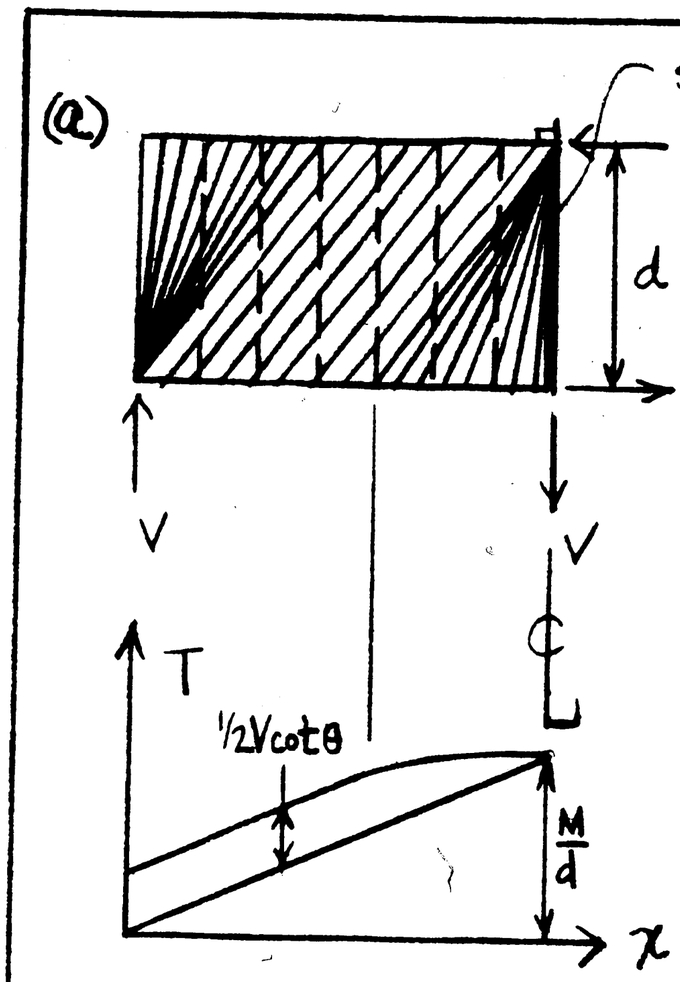

$$T_{max} = \frac{M_{max}}{d}$$

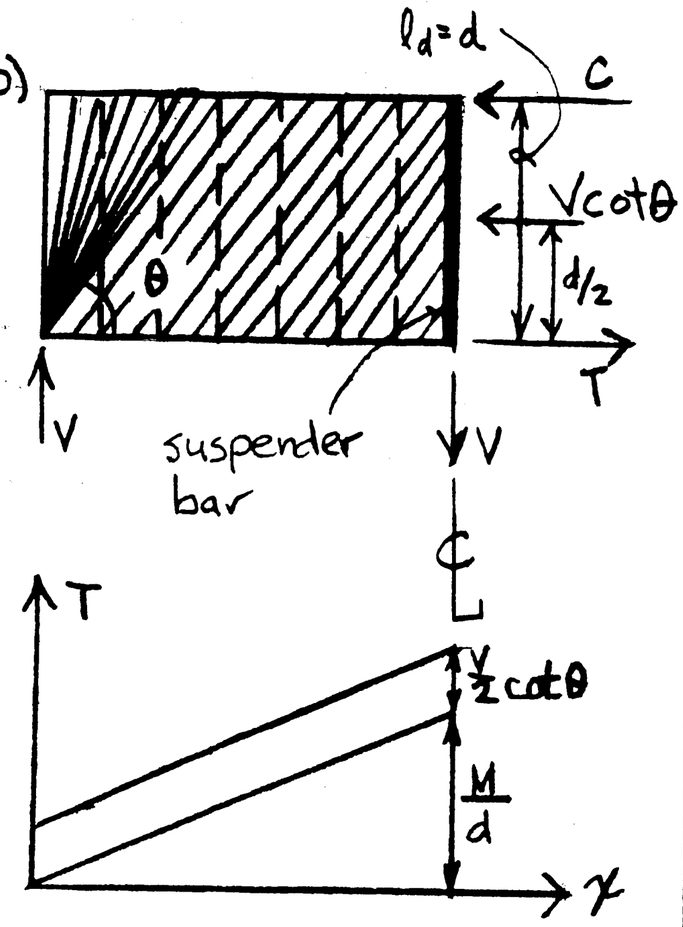

$$T_{max} = \frac{M_{max}}{d} + \frac{V}{2}\cot\theta$$

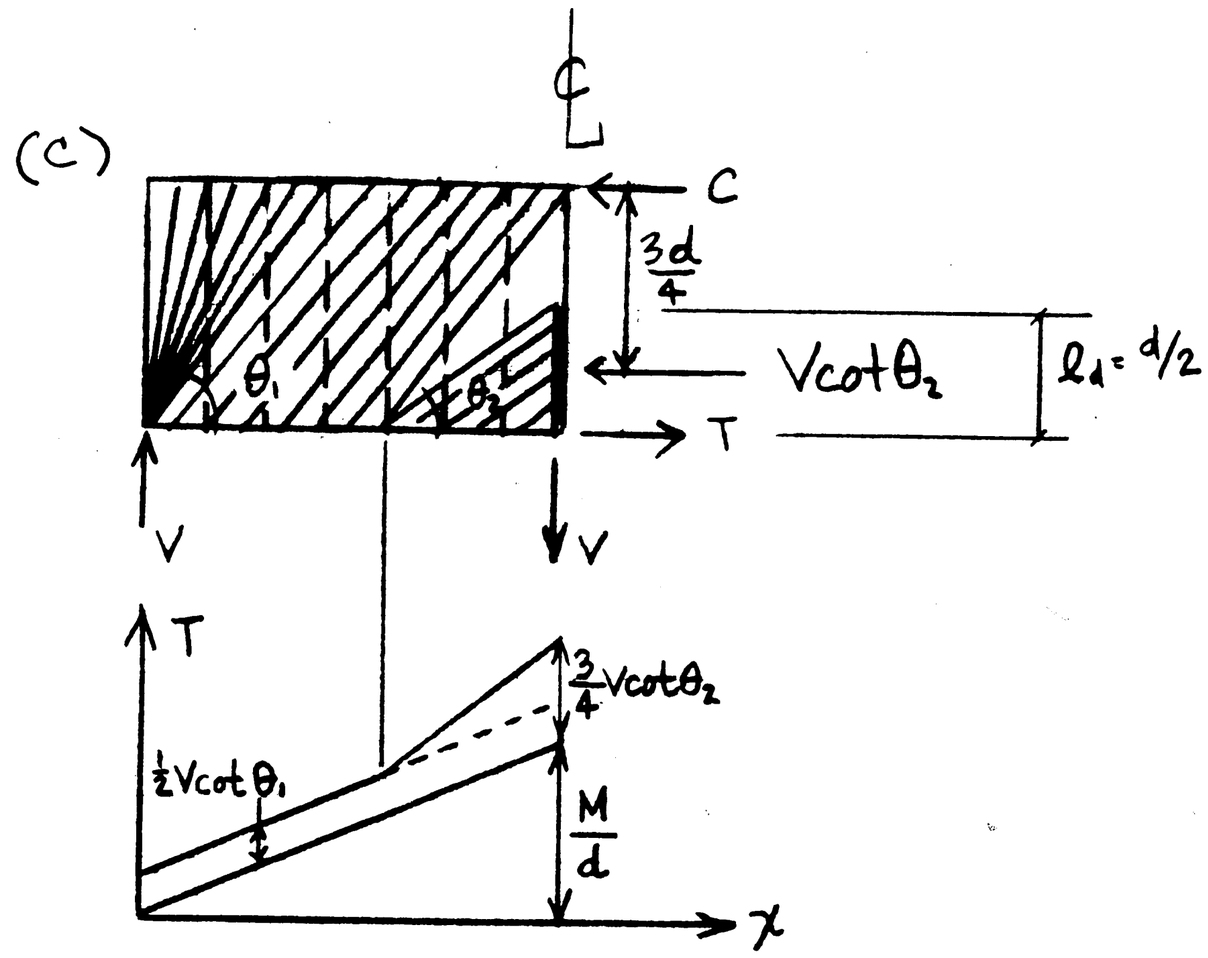

$$T_{max} = \frac{M_{max}}{d} + \frac{3}{4}V\cot\theta_2$$

FIGURE 2.14: Effect of suspender bar anchorage on tensile chord

2.14(a) but form a uniform diagonal compression field whose horizontal resultant is located at mid depth. Thus Eq. (2-9) applies also to the section of maximum moment. If the suspender bars are only inserted to mid depth, and $\ell_d = d/2$ for example, Fig. 2.14(c), then the maximum tensile force in the longitudinal reinforcement is further increased to

$$T_{max} = \frac{M_{max}}{d} + \frac{3}{4} V\cot\theta_2 \qquad (2\text{-}11c)$$

Since the suspender bar extends only to mid-depth, so does the diagonal compression field which transfers the suspended load to the left. Its longitudinal results, $V\cot\theta_2$, is therefore located deeper than in case (b), at a distance 3d/4 rather than d/2 from the flexural compression resultant. As importantly, its inclination, θ_2, is flatter than the inclination, θ, used for the design of the shear reinforcement; specifically, $\cot\theta_2 = 2\cot\theta_1$. Thus the magnitude of $V\cot\theta_2$ is double that of case (b) and the shear contribution in Eq. (2-11c) is three times that in Eq. (2-11b). It should be noted that Eqs. (2-11) follow directly from moment equilibrium about the compressive resultant at the section considered, similarly as Eq. (2-9). The reduced depth and the flatter angle, θ_2, of the diagonal compression field also imply a significantly larger diagonal compressive stress than for cases (a) or (b). The suspender bar effects on the longitudinal reinforcement requirements predicted by truss models have indeed been observed in tests[20].

For design it is desirable to select truss models which yield similar longitudinal reinforcement requirements and similar diagonal

compressive stresses for top and bottom loads. This section has shown that, in order to achieve this, hanger reinforcement or suspender bars in addition to the normal shear reinforcement are needed in the case of suspended loads and that these suspender bars must be fully anchored at the opposite face.

If the supports are indirect, such as in the suspended wall panel, shown in Fig. 2.15, then the support reactions must be transferred to the bottom and introduced as compression where the direct supports would be located. The suspender bars, which carry

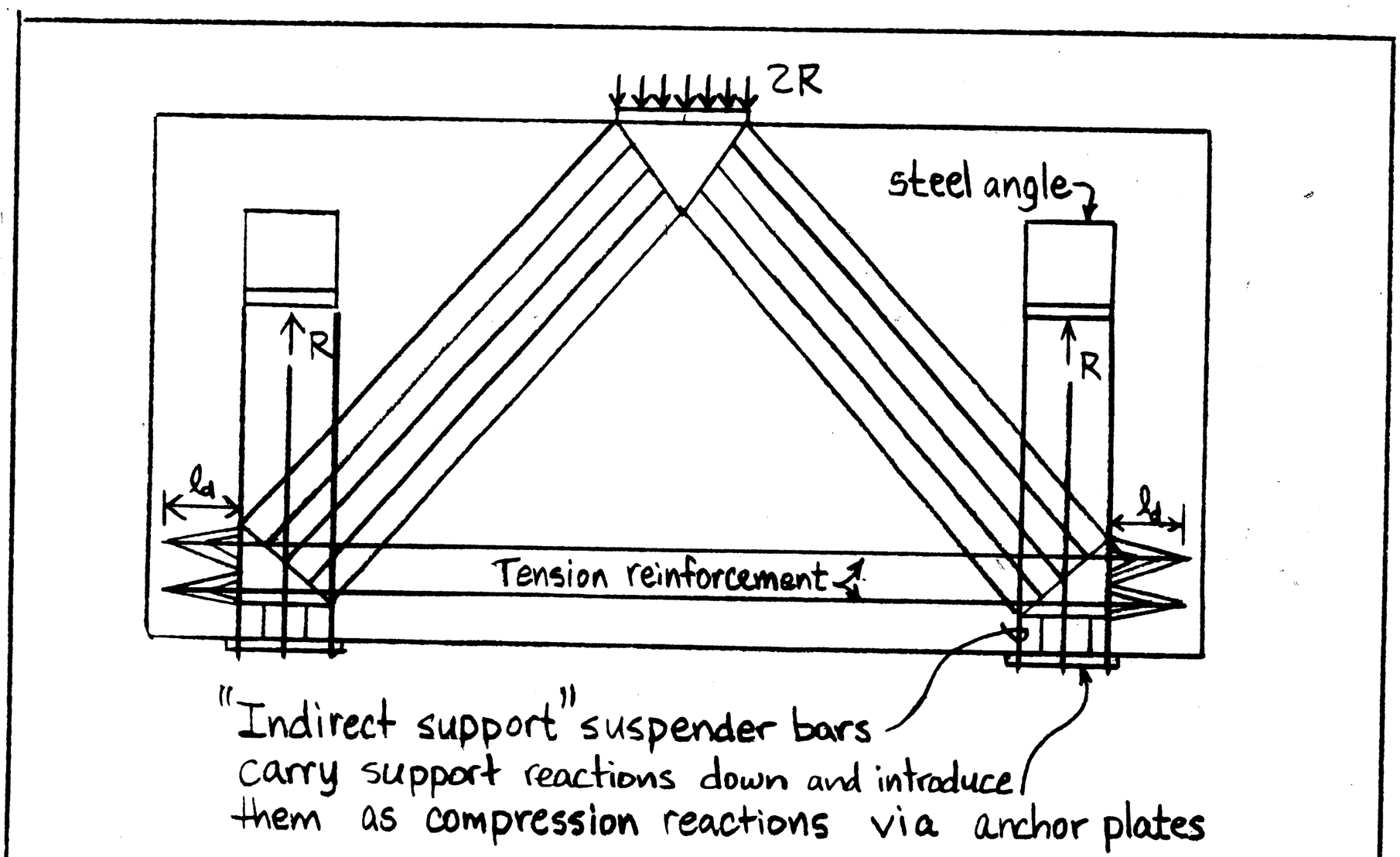

FIGURE 2.15: Indirectly supported wall panel

the indirect support reaction down, must be anchored *below* the longitudinal reinforcement, such that their anchor plates introduce

compression below the longitudinal reinforcement as indirect compression supports. Only then can truss models such as those in Figs. 2.5, 2.11 and 2.12 be used for both direct and indirect supports. If the suspender bars in Fig. 2.15 are not fully anchored below the longitudinal reinforcement, then diagonal cracks extending from the lower corners are not prevented from opening resulting in premature diagonal tension failure. Note that the bottom nodes of the truss model in Fig. 2.15 are CTT nodes and that their detailing follows exactly the principles outlined in section 2.3.β and Fig. 2.6. As indicated there and in more detail in section 2.8, the anchor plates could in practice be replaced by stirrups or looped bars enclosing the longitudinal reinforcement.

A three step process can be followed in design:

(1) Assume all loads and supports are compressive and use normal procedures in choosing the longitudinal and shear reinforcement (stagger below the V diagram).

(2) If the loads are suspended from the bottom or mid-depth, add suspender bars to fully transfer the loads to the top of the beam and anchor them fully there so that they introduce the loads as compression at the top, (equivalent to staggering above the V diagram).

(3) If supports are indirect, provide suspender bars for the full reaction, fully anchored below the longitudinal reinforcement, so that they introduce this reaction as compression below the longitudinal reinforcement.

These rules are valid for both slender beams and deep beams

which consist entirely of D-regions. Truss modeling for D-regions is addressed in more depth in section 2.5.

2.4.4. INFLECTION POINTS

While points of inflection denote points of contraflexure or zero moment, the longitudinal reinforcement requirements are not zero. Similar to the simply supported beams of section 2.4.2, the diagonal compression fields increase the top and bottom tensile chord forces over and beyond the flexural requirements at the inflection point. These additional tensile forces beyond the inflection point, must be covered by reinforcement while observing bond strength requirements. To illustrate, let us consider the continuous beam with constant shear in Fig. 2.16(a). Fig. 2.16(b) shows the top and bottom chord forces due to both flexural and shear effects. Line B represents the tensile steel forces due to pure flexure. Lines A and C represent the total tensile chord forces including shear effect in the top and bottom chords, respectively. As described in section 2.4.2, lines A and C plot parallel to line B a vertical distance of 1/2 $V\cot\theta$ apart. Alternatively, lines A and C can be viewed as the line for pure flexure (line B) shifted horizontally by a distance 1/2 $d\cot\theta$. Accordingly, the total tensile chord forces become zero not at the inflection point, but at distances 1/2 $d\cot\theta$ away from the inflection point. Thus, it becomes apparent that longitudinal reinforcement must at least extend beyond the inflection point by 1/2 $d\cot\theta$. This geometric requirement, evident from Fig. 2.16(b), can be stated as

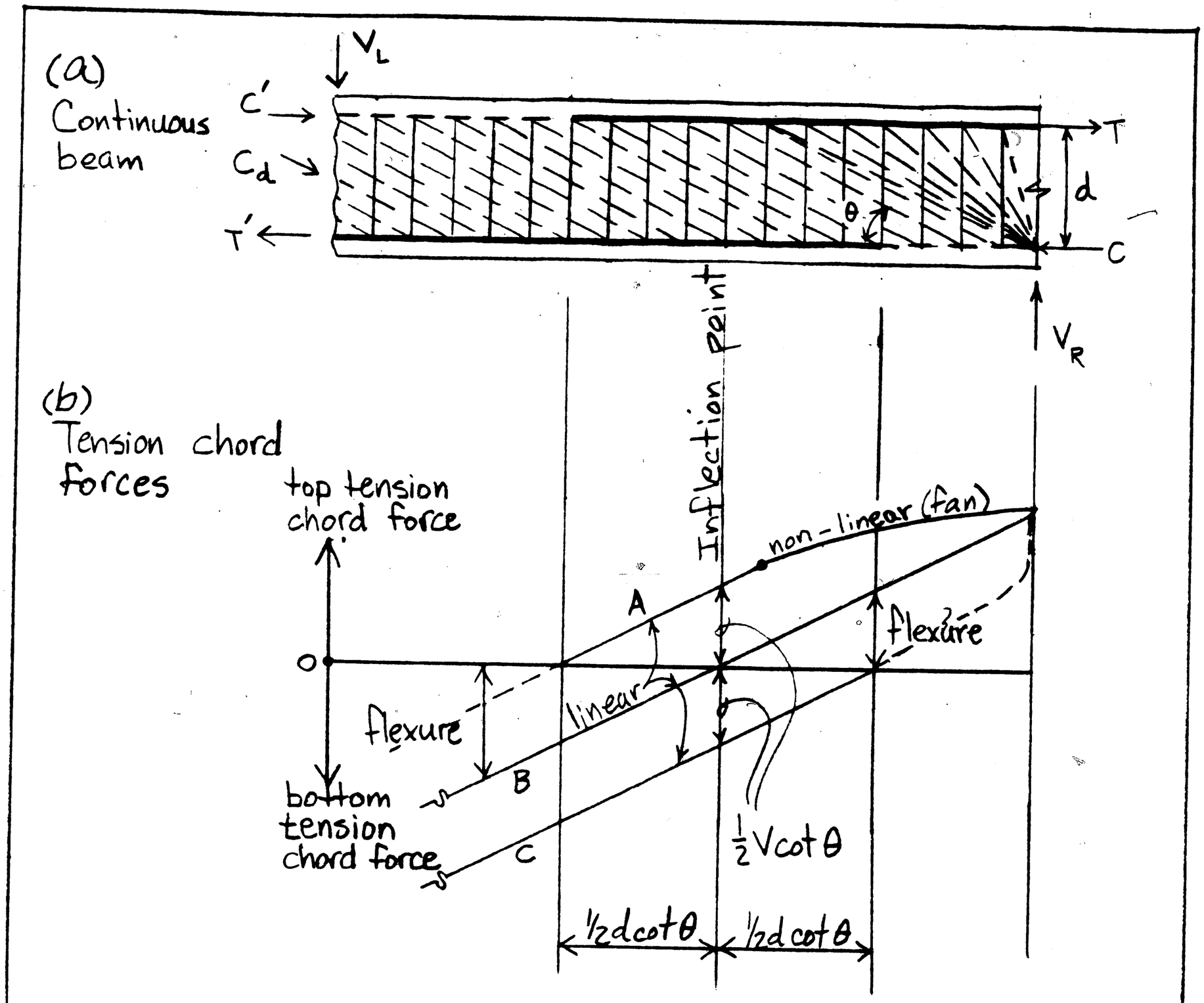

FIGURE 2.16: Inflection points

$$\ell_e \geq \tfrac{1}{2}\, d\cot\theta \qquad (2\text{-}12)$$

where ℓ_e is the bar embedment length measured from the inflection point. But as previously stated, if the longitudinal reinforcement is to be fully anchored, it must also independently satisfy the "bond" strength requirements. Specifically, the rate at which the tensile force 1/2 Vcotθ in the bars is applied per unit length, must

be less than or equal to the rate at which the bar can be developed,

$$\frac{\frac{1}{2}\,V\cot\theta}{\frac{1}{2}\,d\cot\theta} \leq \frac{A_s f_y}{\ell_d} \qquad (2\text{-}13a)$$

Simplifying equation (2-13a) yields

$$\ell_d \leq \frac{A_s f_y d}{V} \qquad (2\text{-}13b)$$

Equation (2-13b) partially explains ACI 318 equation 12-1 (section 12.11)[3] which is reproduced as equation (2-14) below.

$$\ell_d \leq \frac{A_s f_y d}{V} + \ell_e \qquad (2\text{-}14)$$

Equation (2-14) incorrectly (from a truss model point of view) gives credit for bar embedment beyond the inflection point, similarly as for bar embedment beyond the center of simple supports. However, at a simple support the shear force and, hence, the bond stresses beyond the support are theoretically zero. Thus this unstressed bar extension may be used to make up for any deficiencies in the span. At the inflection point, on the other hand, the shear force and, hence, the bond stresses are exactly the same on either side of the inflection point until the tensile resultant become zero. Thus credit should only be given for the embedment length exceeding 1/2 $d\cot\theta$.

In summary, equations (2-12) and (2-13) must be satisfied independently, equation (2-12) has nothing to do with development and

simply reflects the fact that reinforcement is needed until the tension become zero. Equation (2-13) checks bar development.

2.5 TRUSS MODELS FOR D REGIONS

While truss models have put the design of B-regions for shear and torsion on a rational basis and have been instrumental in the correct treatment of combined torsion, shear, flexure, and axial force[6-18], the true power and usefulness of truss models becomes only evident for D-regions. The most striking experimental evidence for the truss-like behavior of reinforced concrete stems from D-regions. And truss models are most useful as a design tool for D-regions because present codes have little to offer for these.

The best understood D-regions are those of deep beams: simple and continuous deep beams, deep coupling beams, and deep cantilever beams (brackets, corbels). Referring back to the simple beam with concentrated load of Fig. 2.11(a), the flattest possible, experimentally verified inclination of the diagonal compression field corresponds to $\cot\theta = 2$ to 2.5. Thus for a span to depth ratio of 5 or less, the uniform diagonal compression field BFGK disappears and only the fans remain. The beam consists entirely of D-regions and the tension in the longitudinal reinforcement at the simple support due to shear, Fig. 2.11(e), amounts to 50% of that at the section of maximum moment. Indeed, the ACI-Code[3] defines deep beams as beams with span to depth ratio less than 5 and its detailing provision for beams that 30% of the reinforcement required at the section of maximum moment be continued to the support and anchored there, is no

longer sufficient. The ACI code warns about this situation but provides little further guidance. If the span to depth ratio is reduced further, so that the fans would start to overlap, a direct strut forms between load and support which transfers part of the shear. In a short deep beam, such as the one shown in Fig. 2.17(a), actually all the shear can be transferred from the load to the support by a direct strut (without any stirrups). The tension tie force is now constant throughout its length. Rogowsky and MacGregor[7], [18] give experimental results for both simple and continuous deep beams in which the tensile tie force measured is nearly constant along the length, indicating that the direct struts indeed formed. Results for a simple deep beam are reproduced in Fig. 2.17(b). The most important point to note is that the deep beam can develop its flexural strength only if the longitudinal reinforcement is fully anchored for the indicated tensile force at the supports. Assuming that this is possible, the addition of stirrups, Fig. 2.17(b), does not increase the strength of deep beams, rather it makes the failure mode desirably more ductile and reduces the tensile force that must be anchored at the support as shown in Fig. 2.17(b). If the flexural strength of a deep beam cannot be developed, it is

(a)

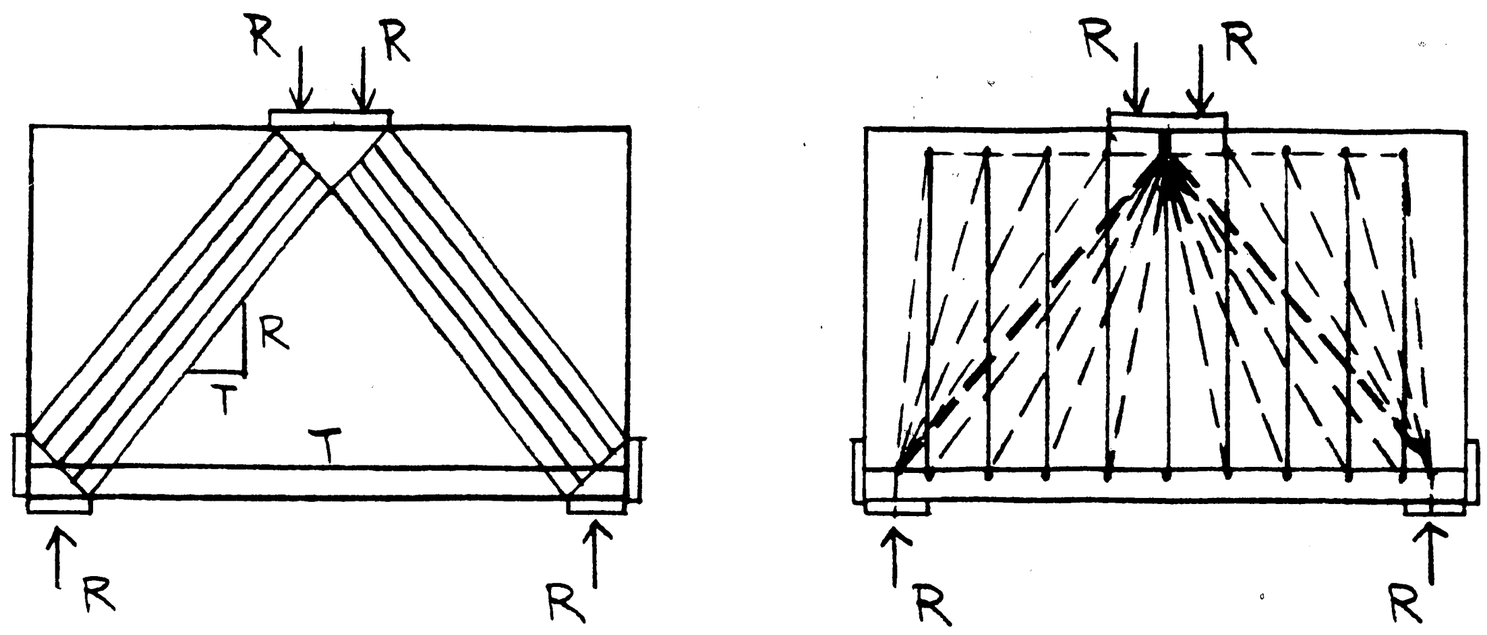

Truss model for a simple beam with web reinforcement

(b)

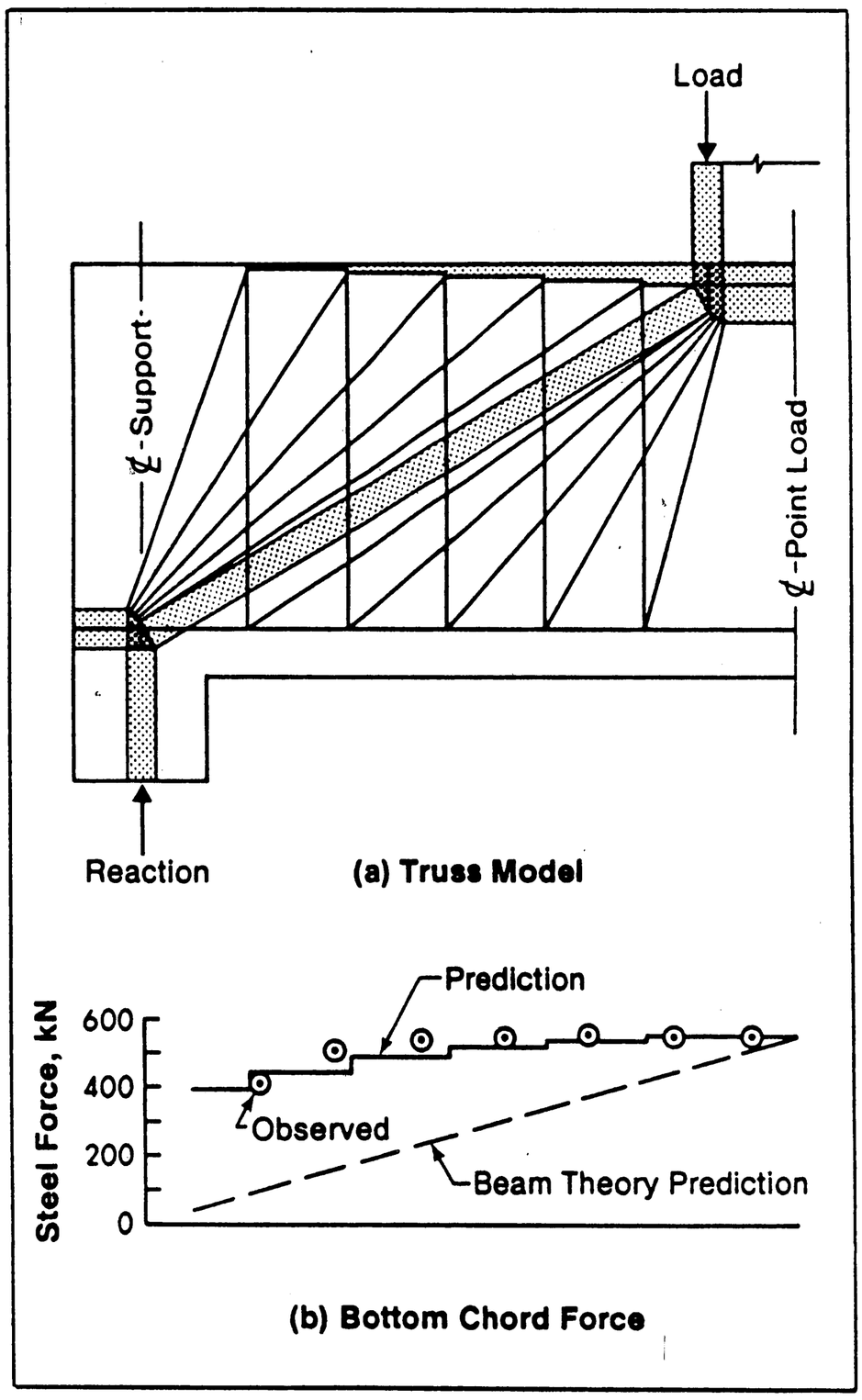

Observed results agree quite well with the predicted Chord force computations.

FIGURE 2.17: Deep beam behavior [18]

usually due to a loss of anchorage at the supports. Thus the amount of stirrups required becomes mainly a question of how large a tensile force can be anchored at the supports. Since significant internal stress redistributions are required for the struts to form, a minimum amount of distributed reinforcement should always be placed to provide the necessary inelastic deformation capacity.

In essence, Rogowsky and MacGregor's tests[7], [18] verify the truss-like behavior of D regions at the ultimate state. Specifically, they verify direct strut action. The significance of deep beam D-regions for connection D regions becomes clear, if it is noted that, in essence, each half of the deep beam in Fig. 2.17(a) "turns a moment around a corner": The (external) vertical force couple, R-R, is converted into a (internal) horizontal force couple, C-T, at the midspan section. However, the function of each of the connections or joints shown in Fig. 2.18 is precisely to turn a moment (or a force couple) around a corner. Thus the "shaded" struts in Fig. 2.18(a)-(e) are analogous in behavior and function to the direct struts observed in deep beams, Fig. 2.17.

Design of the connections in Fig. 2.18 requires choosing a reinforcement scheme which permits the compression struts to fully anchor the tension ties and vice versa. The opening and closing knee joints, the beam-column joint, and the corbel of Fig. 2.18(a), (b), (d), and (e) -- they all require that the tension reinforcement be anchored "behind" the node as indicated by the anchor plates, so that its tension is introduced as compression on the node, thus balancing the outward thrust of the compression struts. Similarly as in deep

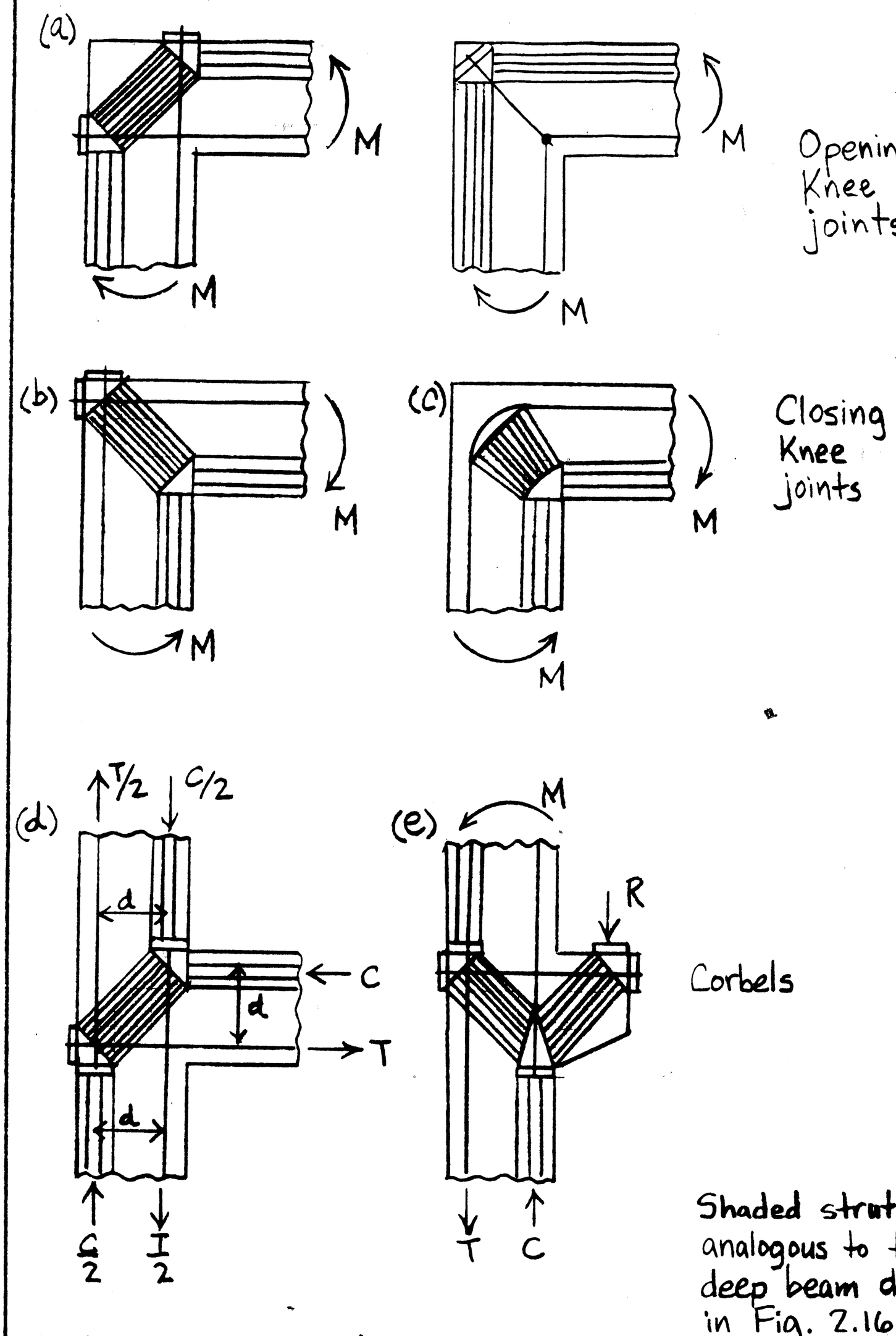

FIGURE 2.18: D region connections

beams, providing stirrups within the joint core reduces the forces that must be anchored at the location of the anchor plates.

D regions analogous in function and behavior to those shown in Fig. 2.18, also form adjacent to the interface of precast concrete connections. D regions for reinforced concrete joints and precast concrete connections are treated in detail in chapters 3 and 4, respectively.

2.6 BOUNDARY CONDITIONS BETWEEN B AND D REGIONS

In an analysis or design by truss modeling, equilibrium, strength conditions, and geometric constraints must be satisfied everywhere in the structure. This also includes the boundaries between the B and D regions (as described in section 2.2). Specifically, the truss model used for the design of the D-region and the model used for the design of the B-region must be compatible at the B/D region boundary. This is particularly important, if beam theory and a section-by-section approach (section 2.4.1) are used for the B-region, while an explicit truss model is used for the D-region. Therefore analysis or design of D regions by truss modeling first requires that all B/D region boundary forces and their locations be determined. These include magnitude, direction, and location of the flexural compressive and tensile resultants and of the diagonal compressive resultant transferring shear. The flexural compressive and tensile resultants may be obtained from any standard method of beam theory such as strain compatibility analysis or cracked section analysis provided the effect of shear is incorporated by considering

an additional, fictitious axial tensile force, N_v, as described in section 2.4.1 in the section-by-section approach. If the B/D region boundary is significantly below ultimate, an elastic cracked section analysis may be performed to obtain realistic results.

Once the strut and tie forces and locations according to beam theory are obtained, they can then be used as the boundary conditions for the D regions, from which an initial assumption on the truss geometry within the D region (which approximates the load path) can be made. If this assumed truss does not violate equilibrium, strength conditions, geometric constraints, or boundary conditions, then a solution has been reached. Otherwise, an adjustment on the assumed truss within the D region is made, and the new truss is reanalyzed. This iterative process is repeated until a solution is obtained. If no valid truss model can be found, then the D-region controls strength and is not capable of transferring the forces imposed by the B-regions.

2.7 TREATMENT OF PRESTRESS

In principle treatment of prestress is straightforward. Following the suggestions by Schlaich, Schafer, and Jennewein[6], the effects of the prestressing force can be considered in the form of "equivalent loads"[21] acting from the tendon and its anchorages on the concrete. The prestressing steel not yet "used up" by the prestressing force, $(f_{pu} - f_{pe}) A_p$, is treated as "passive" reinforcement similarly as any other nonprestressed reinforcement.

The equivalent loads include the anchor forces the "bond" forces along the transfer length of pretensioned strands (Fig. 2.19), the concentrated or distributed transverse forces due to the "hoop effect" of bent strands or tendons, and the friction forces along post-tensioned tendons.

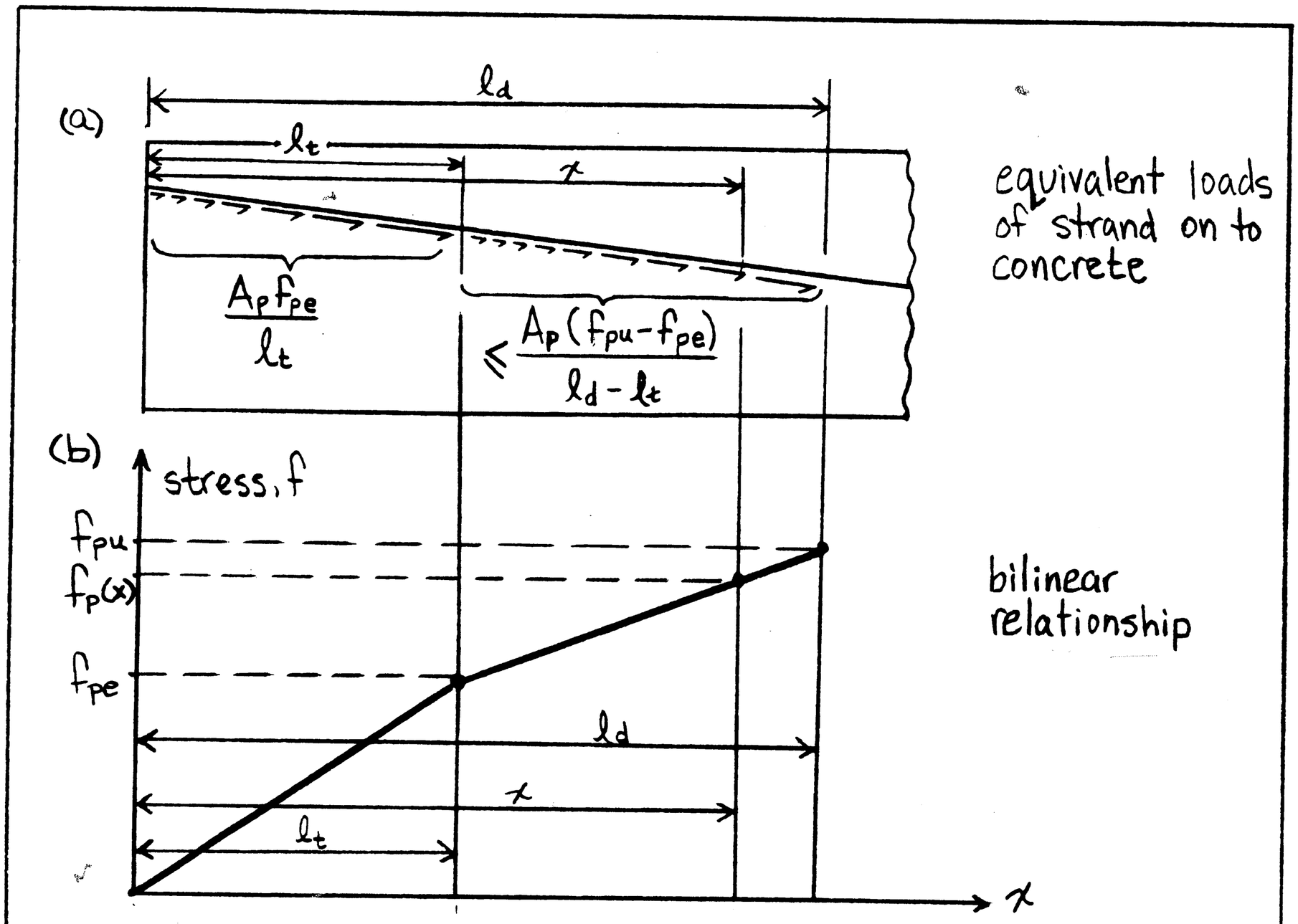

FIGURE 2.19: Treatment of prestress

These equivalent loads are treated equivalently as any other actually external loads. The concept of equivalent loads is treated by most standard textbooks on prestressed concrete[21].

Unless also transversely prestressed, the web of prestressed beams must be considered cracked at the ultimate state, if the concrete tensile strength is not relied upon, whether the precompressed tension flange is cracked (flexure-shear cracking) or not cracked (web shear cracking). As evidenced by the experimentally observed crack patterns, the inclination of the diagonal compression fields transferring shear is still fairly uniform in the B-regions of members with both compression and tension flanges, i.e. outside the vicinity of concentrated loads, reactions, and prestressing anchorage zones.

Thus, prestressing can be readily included in the section-by-section approach for B-regions presented in section 2.4.1. Simply, an equivalent external axial force, P, and shear force, V_p, due to prestressing acting at the eccentricity of the tendon, are included among the external load actions in Fig. 2.10, and the equilibrium equations (2-5) through (2-9) are accordingly modified. Initially, the tension chord may be assumed to coincide with the centroid of the precompressed tension flange. If the tension chord force turns out to be tension, then the tension flange is cracked and the tension chord is located at the combined centroid of the non-prestressed reinforcement and the "passive part" of the prestressing steel. Thus, the depth of the section , d_B, depends on whether or not the initially precompressed tension flange is cracked. It is worthwhile noting that if the tension flange remains precompressed at the ultimate state, the diagonal compressive strength, equations (2-1) to (2-3), is significantly higher and permits the inclination, θ , of the

diagonal compression field, to be selected much flatter than in non-prestressed beams. Thus, prestressing "saves" stirrups.

The stress distributions according to beam theory for the B regions are, of course, no longer valid in D regions, i.e. near supports and prestress anchorages. As demonstrated in section 3.5 for a dapped end beam, explicit truss models for such D regions permit the designer to consider in a rational and actually quite simple manner the interaction of prestress transfer and shear transfer. Since beam theory is not valid, it is not, in general, possible to work only with the resultant of the prestressing force. Rather the equivalent loads for each strand should be treated explicitly at the location where they arise. These equivalent loads follow directly from the transfer lengths specified in codes, as illustrated in Fig. 2.19. The variation of the strand force and, hence, bond forces beyond the transfer length may be determined by cracked section analysis, but must not exceed the slope of the strand development diagram, as shown in Fig. 2.19(b) and (a).

Particular attention must be paid in pretensioned beams to the fact that the tension chord force is not zero at the end of simply supported beams, as shown in Fig. 2.12(d). This tension chord force due to shear becomes, of course, quite large if only minimal stirrup reinforcement is provided, i.e. if $\cot\theta$ is large. However, in pretensioned beams with little or no overhang beyond the support, virtually no prestressing force is transferred up to the support. Therefore, the outward thrust of fan A-B-G in Fig. 2.12 must be

anchored with supplemental reinforcement which must be properly spliced to the strands. Otherwise a combined diagonal tension/bond/splice failure mode may control. The experimental evidence on 15 pretensioned double tees with minimal stirrup reinforcement which all failed in an undesirable diagonal tension failure mode[22] attests to the problem. As demonstrated in section 3.5, an explicit truss model for this D region allows analyzing this problem in more depth in a rational manner.

2.8 ANCHORAGE AND DEVELOPMENT OF STRUTS AND TIES AND SPLICES

The transition from the idealized truss model to the actual structural member raises a significant question: Having properly proportioned the concrete and reinforcement dimensions, how should the structural member be detailed so that both the compressive struts and the tensile reinforcement are properly anchored at the nodes? If the anchorage details are not properly chosen, the truss-designed structure is likely to perform poorly. In essence, good detailing of a node requires that all the elements entering a node be fully anchored at or "behind" that node so that the intended truss will indeed develop at ultimate state. Anchorage and development determines not only the strength but, even more importantly, the location of the nodes, and, hence, the geometry of the very truss on which design is based. Therefore, it must be the engineers' responsibility to detail the structural member -- including the connections and their anchorage details.

In a truss model, all the elements must be anchored and/or

developed, i.e., it is equally important to anchor the compression elements (struts, fans, and/or arches) as it is to anchor the tension elements. In fact, at a node, the compression elements supply the forces which anchor the tension ties, and conversely the tension ties supply the forces which anchor the compression elements, (an action-reaction relationship). While in standard design practice the flow of the forces which an anchored bar introduces into the concrete, is not investigated, it is in truss modeling, at least at a global level: the bar anchorage forces flow into the explicitly modeled compression elements of the truss model, thus in truss modeling anchorage and development of bars amounts to design and detailing of the "local connections" at the truss.

The single most important basic principle for proper anchorage of compression elements and tension ties at a node can be stated as follows: the tension tie forces must be carried through and brought "behind" the node where those tensile forces on the node face. Those compressive forces exactly equilibrate any compression element forces bearing on the remaining nodal faces, thus placing the node in a state of biaxial compression.

If tension ties and compression elements interlock in this manner, only the concrete compressive strength is relied upon, the various mechanisms at anchorage and development discussed in the next section

(direct bearing, development, and friction) differ in the manner in which the tension ties convert their tensile forces into compression at a node.

2.8.1 MECHANISMS OF ANCHORAGE AND DEVELOPMENT

When three struts bear against each other in a C-C-C node such that a biaxially compressed nodal zone forms, Fig. 2.20(a), or when a strut bears into a rigid angle such that a biaxially compressed nodal zone forms within the angle, Fig. 2.20(b), the struts are anchored in

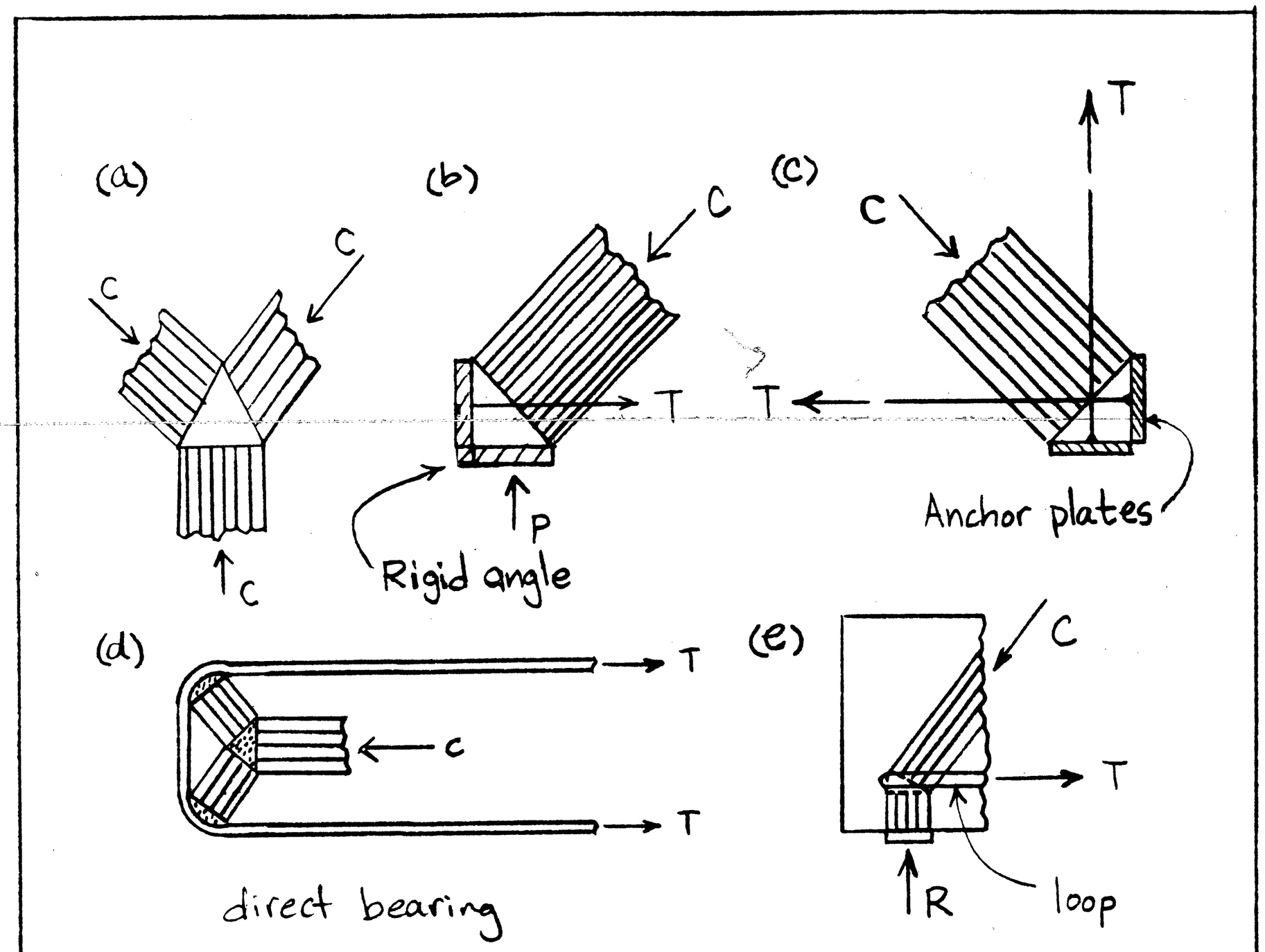

FIGURE 2.20: Direct bearing and interlocking

direct bearing. When the anchor plates of two reinforcement ties are *interlocked* at a C-T-T node such that a biaxially compressed nodal zone can form against which the strut can bear, Fig. 2.20(c), the ties and the strut are anchored in *direct bearing*.

When a strut is bearing in a C-T-T node against the "hydrostatic" nodal zone that forms within the bend of a rebar, Fig. 2.20(d), or when two struts are bearing in a C-C-T node against the triaxially compressed nodal zone that forms within the loop of looped rebars, Fig. 2.20(e), the struts and ties are also anchored in *direct bearing*. However, since very high bearing stresses exist under the minimal bearing surface provided by bends and loops, bend and loop anchorages can only anchor large forces, if transverse compression is present such as in the C-C-T node configuration at the simple support of a beam shown in Fig. 2.20(e). In such a C-C-T node the nodal zone is in triaxial compression and can sustain stresses up to several times the uniaxial compressive strength. Using closely spaced loops or bends and effectively creating a bent "sheet" of steel increases the effective bearing surface.

Note how *interlocking, in essence, converts tension into compression* at C-C-T and C-T-T nodes. In order to ensure that the struts of the truss which develops upon cracking, can indeed interlock with the anchorages of the reinforcement ties, the location of the anchorages must be carefully chosen as discussed in Section 2.8.2.

Development length is the length over which a rebar must be embedded in concrete to fully develop its yield capacity in axial tension or compression. From a truss modeling point of view, *development* itself is nothing more than local truss action and anchorage through bearing. As shown in Fig. 2.21(a), an increase in

"granularity" makes visible this refined, local truss action in the vicinity of the rebar.

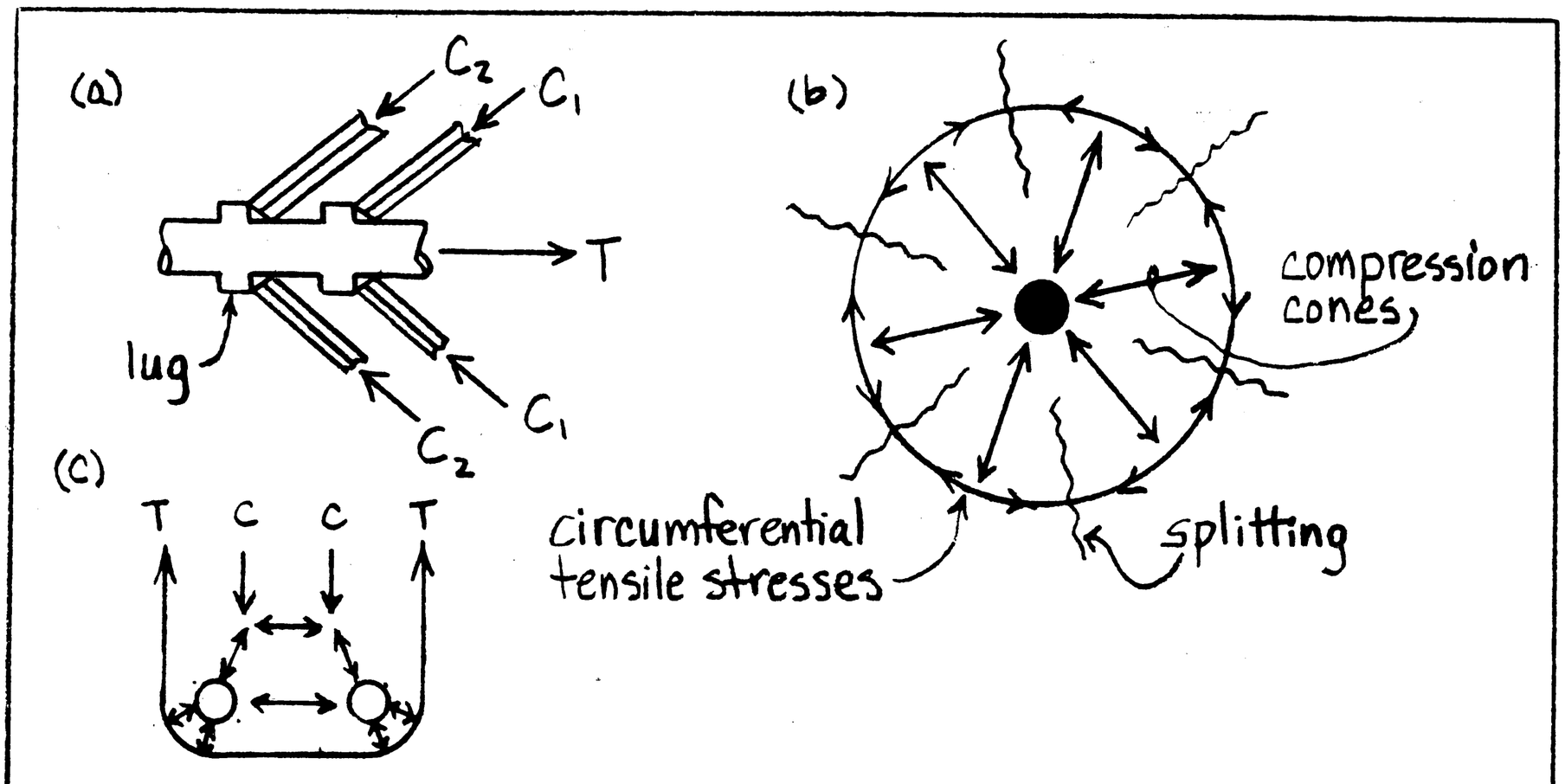

FIGURE 2.21: Truss action in development lengths

Narrow compressive cones interlock with, bear against the lugs of the rebar. These compressive cones cause circumferential tensile stresses around the bar as shown in Fig. 2.21(b). If the tensile stresses exceed the tensile strength of the concrete, longitudinal splitting occurs. This truss action in bar development has indeed been experimentally observed. If flexural rebars are "encased" in the bends of closed stirrups as shown in Fig. 2.21(c), then the transverse compression from the diagonal shear struts bearing into the bends of the stirrups can postpone this longitudinal splitting. Upon longitudinal splitting "bond" is essentially lost, since the diagonal compression cones loose their anchorage at the opposite

end. In diagonally cracked beams bar development is therefore only effective, if the bars are enclosed in stirrups as required by the ACI Code.[3]

If a rebar is pulled through a node and extended by a development length beyond the location where an anchor plate would be located, the diagonal compression cones can bear against the nodal zone as visualized in Fig. 2.22. Thus, in the sense shown in Fig.

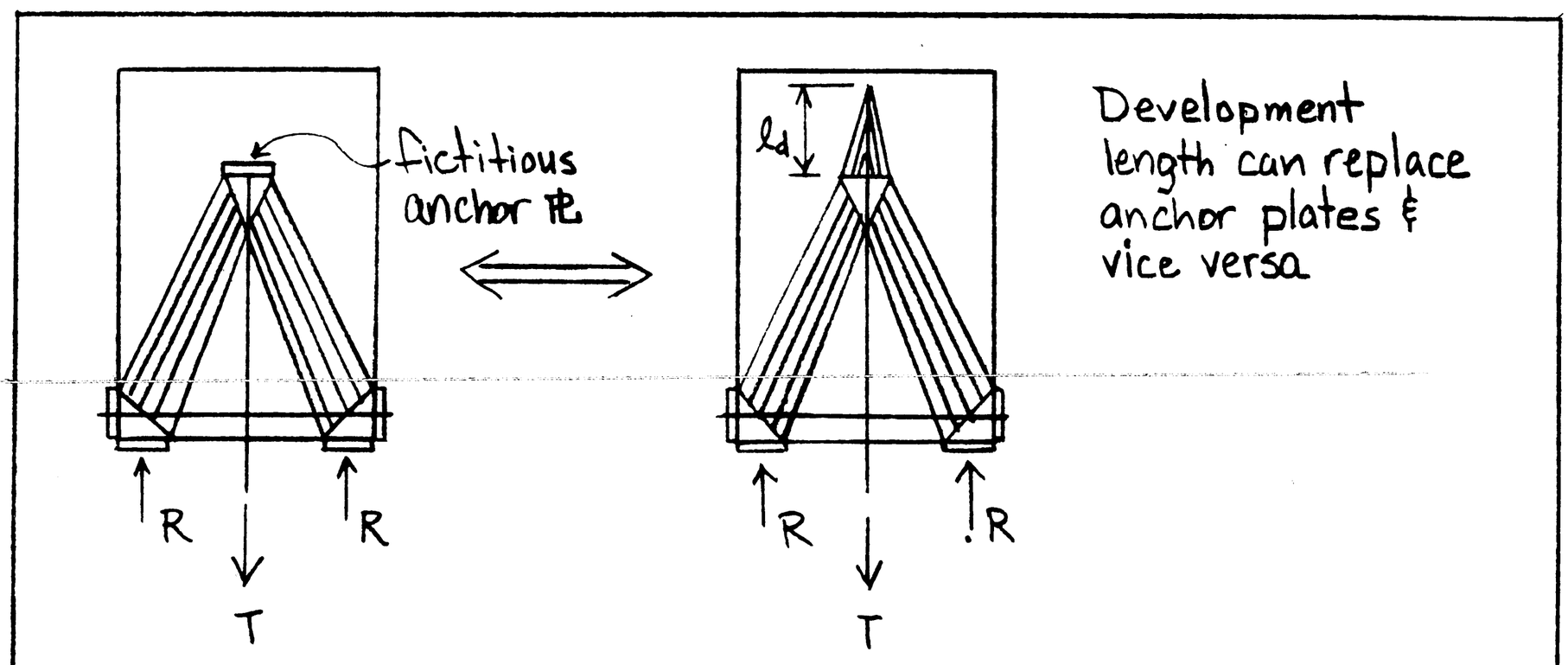

FIGURE 2.22: Development length vs. anchor plate

2.22, anchor plates and development lengths can replace each other. In truss modeling it is convenient to indicate with an anchor plate where a bar must be anchored or fully developed. If the bar is anchored through a development length, the anchor plate is called a *fictitious anchor plate*. In design the truss model is constructed first and the fictitious anchor plate indicates from where the bar must extend a development length. In analysis, when the reinforcement is already given, the fictitious anchor plate must be

placed a development length from the end of the bar and indicates where a truss node can form. Figure 2.23 illustrates a T-T-T node in which the (fictitious) anchor plates at the T-T-T node of Fig. 2.6(d) are replaced by their equivalent development lengths. Note

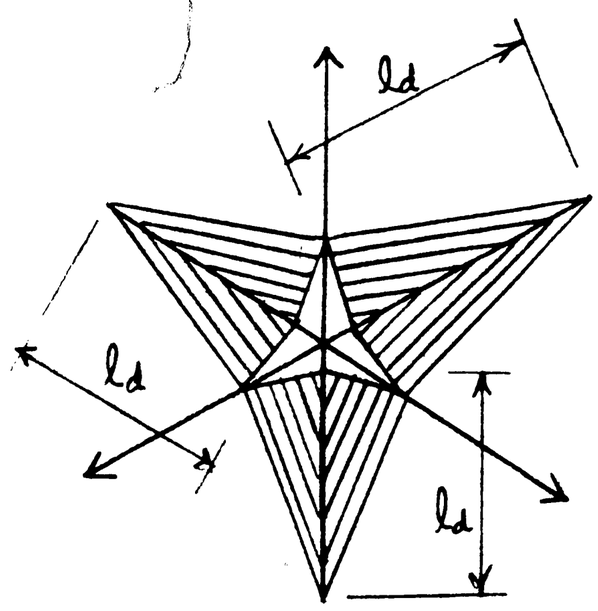

The anchor plates of the T-T-T node of Figure 2.6(d) may be replaced by development lengths

FIGURE 2.23: T-T-T node utilizing development lengths

again how *interlocking* in essence converts tension into compression at a node.

In contrast to the T-T-T node of Fig. 2.23, the T-T node shown in Fig. 2.25 - a lap splice - cannot be in equilibrium by itself and needs transverse compression supplied by other reinforcement. A part of the bar force can be transferred directly from bar to bar through a diagonal compression field between the bars as shown in Fig. 2.25(a). Another and larger part must be transferred through the surrounding concrete. If the two bars are lapped two development lengths, the compression cones extending from each bar's individual "development length" can bear against each other as shown in Fig.

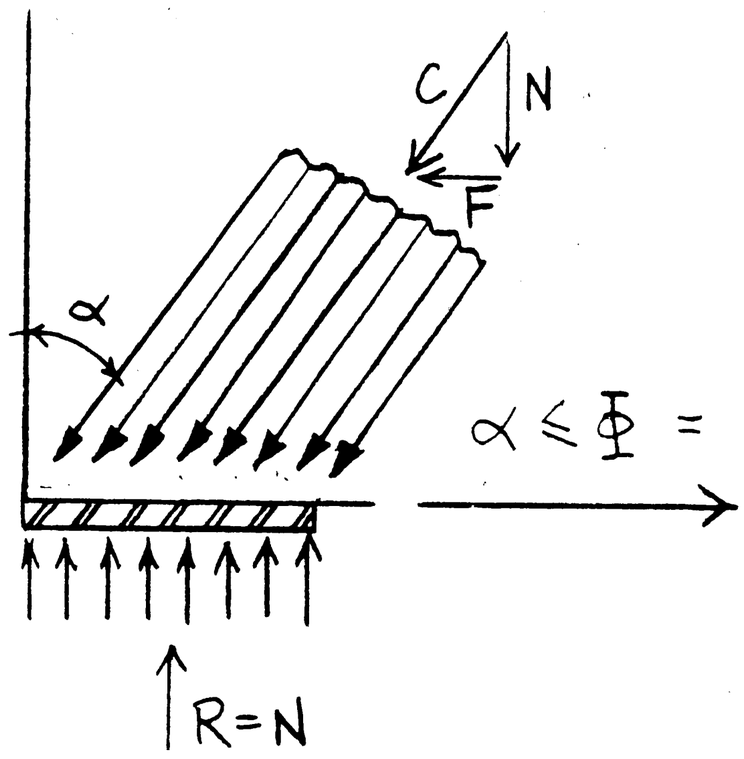

$F_{MAX} = \mu N$ where $\mu = \tan \Phi$

FIGURE 2.24: Frictional resistance

2.25(b). While the interlocking of the compression cones at section X-X is analogous to that of the T-T-T node of Fig. 2.23, the lap splice needs for either transfer mechanism transverse compression to balance the transverse component of the diagonal compression fields or cones. Placing the lap splice within the bends of stirrups [Fig. 2.21(c)] or spiral reinforcement ensures that such transverse compression is present. For a 100% lap splice the ACI code requires a lap length of 1.7 development lengths. This would imply that at least 15% of the bar force must be transferred by the mechanism of Fig. 2.25(a).

As in direct bearing and development, a purely mechanical resistance can be developed parallel to the fraying surface of two materials in contact if a normal force is acting on the surface.

This friction resistance can be explained using a highly refined local truss model in which compression fibers interlock with the irregularities of the rough contact surfaced. Globally, the horizontal component of the inclined compression strut in Fig. 2.24 is said to be resisted by friction, given by

$$F = \mu_s N \qquad (2\text{-}15)$$

where μ_s = coefficient of friction

= .6 (concrete to hardened unroughened concrete)

= .7 (concrete to rolled steel)

= 1.0 (concrete to hardened roughened concrete)

= 1.4 (monolithic concrete)

The angle between the inclined compressive strut and the normal to the surface is α. Should α reach the friction angle ϕ, the strut will be in impending slip motion. The conservative designer usually avoids relying on friction for anchorage. If the surface in Fig. 2.24 is a steel plate, a cross bar can be welded to it which changes the mechanism of anchorage to direct bearing.

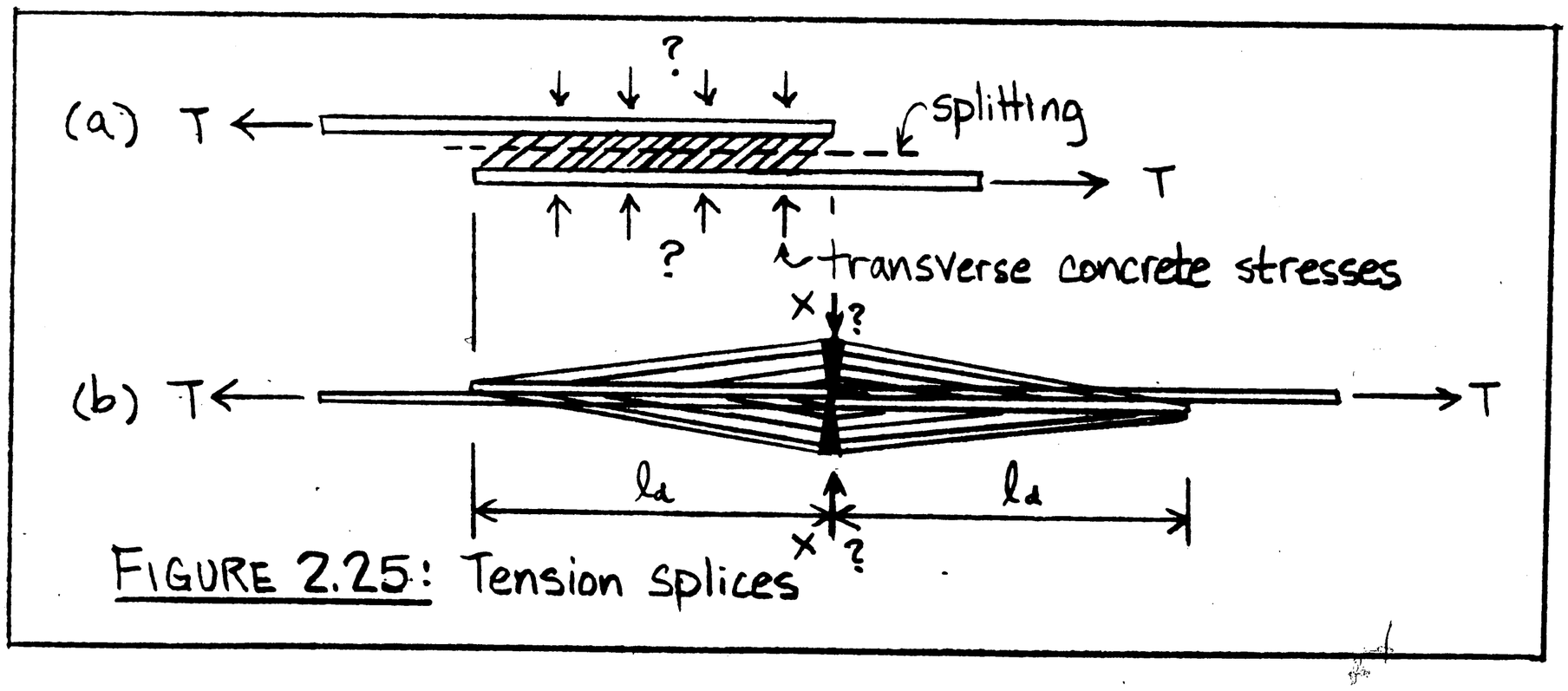

FIGURE 2.25: Tension splices

2.8.2 ANCHORAGE AND DEVELOPMENT REQUIREMENTS

As described in the previous section, anchoring a rebar requires that it be "locked" behind the node through an anchor plate, loop, or alternatively, a development length. While it is obvious that an anchor plate and the weld to the rebar must be proportioned to develop the rebar, it is often overlooked that the anchor plate must be situated at a location so that it indeed provides a bearing surface against which the full width of the incoming compression strut can bear. Figure 2.26(a) illustrates a C-C-T node in which the anchor plate is incorrectly located. Although the anchor plate is capable of anchoring the reinforcement the incoming compression strut is only partially anchored.

To fully anchor strut C in Fig. 2.26(a) without relying on the concrete tensile strength, one of three changes must be made: (1) shift the resultant line of action of C so that the full width of the incoming diagonal compressive strut can in fact bear against the anchor plate. This does not require a change in the reinforcing detail, but rather a change in the geometry of the truss, which changes the forces in the truss elements and can therefore not simply be neglected, (2) increase the size of the anchor plate so that the compressive strut can be intercepted by it, Fig. 2.26(b), or rather than increasing the anchor plate size, (3) shift it by a distance, ℓ', Fig. 2.26(c), so that the incoming strut can be equilibrated. The just stated changes are purely geometric in that the anchor plate's dimensions or location is adjusted so as to develop the full compressive strut and tensile tie capacities. Thus

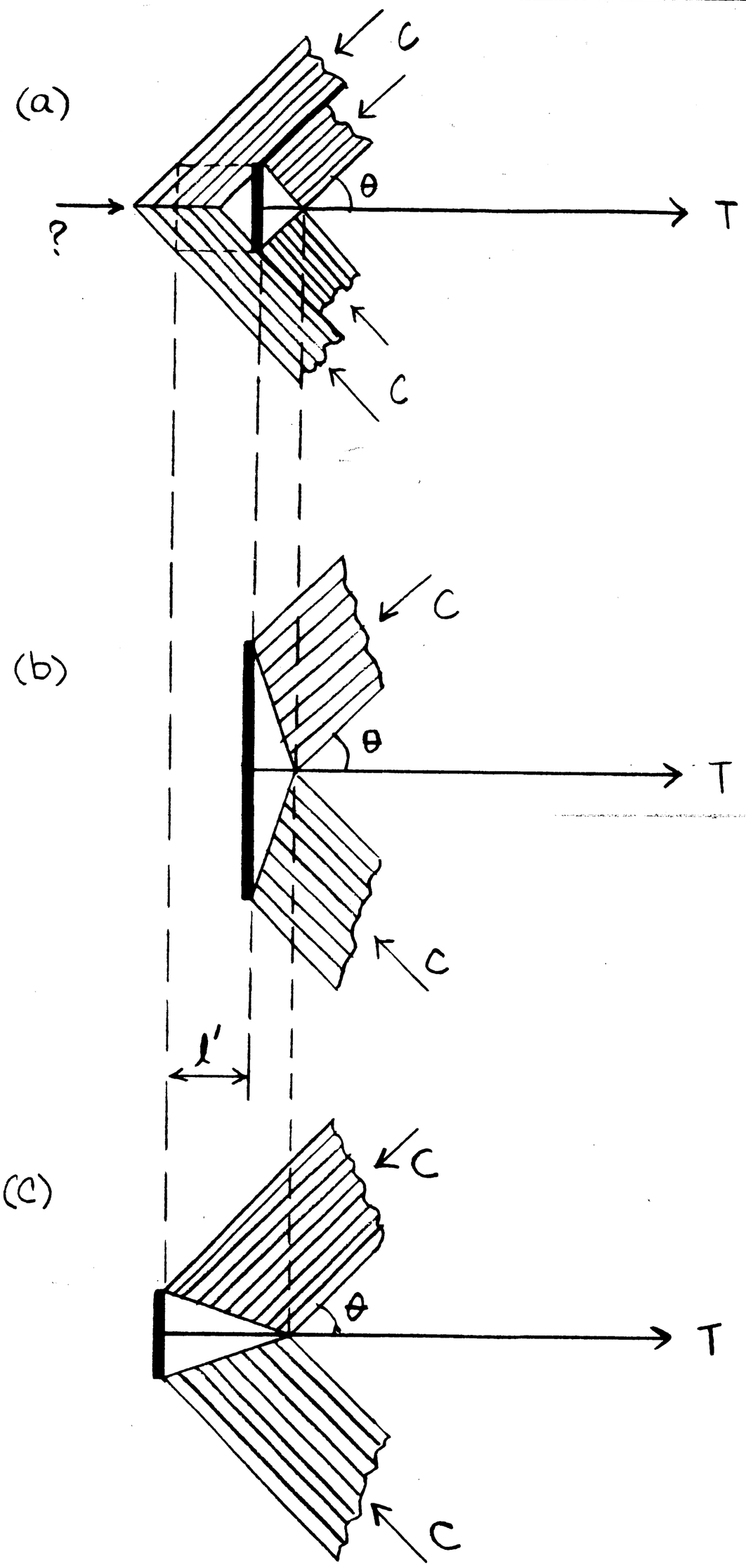

Strut is not fully anchored

∴

Increase anchor ℄ size to fully anchor C

or

Relocate anchor ℄ by moving it back a distance l'

FIGURE 2.26: Anchor plate requirements of a CCT node

it becomes clear that anchorages must meet two requirements: (1) the location and site of the anchor plate must be geometrically compatible with the geometry of the truss model, i.e. with the location and size of the nodal zone or struts, and (2) the anchor plate must have sufficient strength.

Similarly, a bar anchored through development must meet both geometric and strength requirements. Since (bond) strength, too, is geometrically expressed by development length, the geometric requirement is often overlooked. Figure 2.27 illustrates this for a C-C-T node over a support. If the (fictitious) anchor plate in Fig.

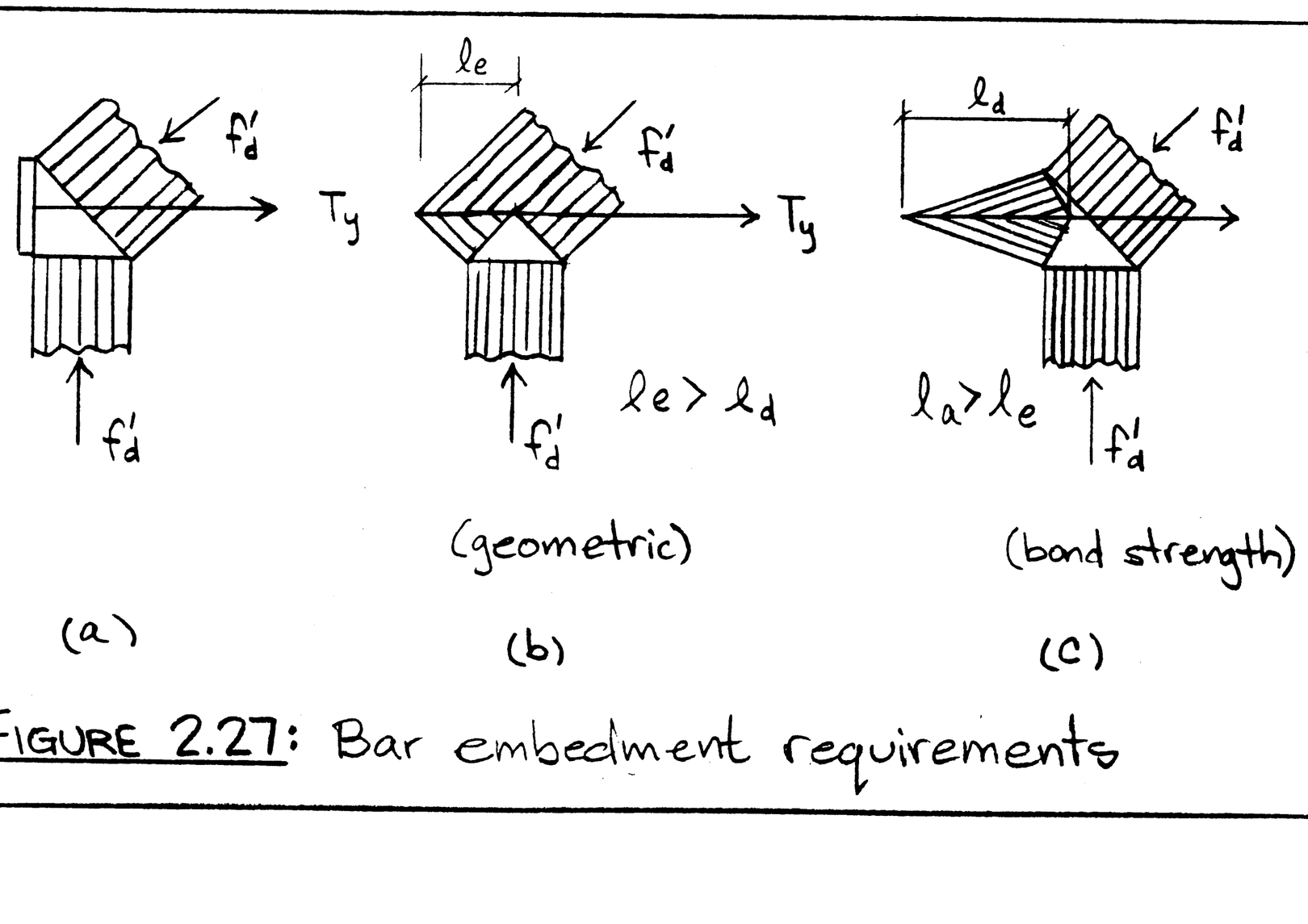

FIGURE 2.27: Bar embedment requirements

2.27(a) is replaced by bar embedment length, the bar must at least extend to the point of intersection of the outermost compression fiber of the inclined strut with the line of action of the bar in

order to intercept the full width of the strut, as shown in Fig. 2.27(b). If the development length is shorter than the distance between this point and the center of the support strut, this geometrically required embedment length controls. If the development length is larger, as shown in Fig. 2.27(c), the development length is theoretically to be measured from a point somewhere between the center of the support strut and the location of the fictitious anchor plate. To simplify, and since development lengths are not that accurate and conservatism is in place for anchorages, the development length is measured from the location of the fictitious anchor plate in Fig. 2.27(a). The geometrically required embedment length is likely to control if the bar diameter and, hence, development length is small and if the inclined strut is flat and due to the reduced diagonal compressive strength wide.

Both geometric and strength requirements must be met at a C-T-T node, whether anchorage is achieved through anchor plates, development lengths, or (bent) reinforcement (Fig. 2.28). If anchor plates are used, they must be sized and located so as to geometrically intercept the full width of the compression strut [Fig. 2.28(a)]. Similarly for the detail of Fig. 2.28(b), the rebars need to be extended at least to the second point of intersection of the outermost compression fibers of the strut with the lines of action of the two reinforcement ties (geometric requirement) or a development length beyond the location of the fictitious anchor plate ("bond" strength requirement), whichever controls. Finally, the number and

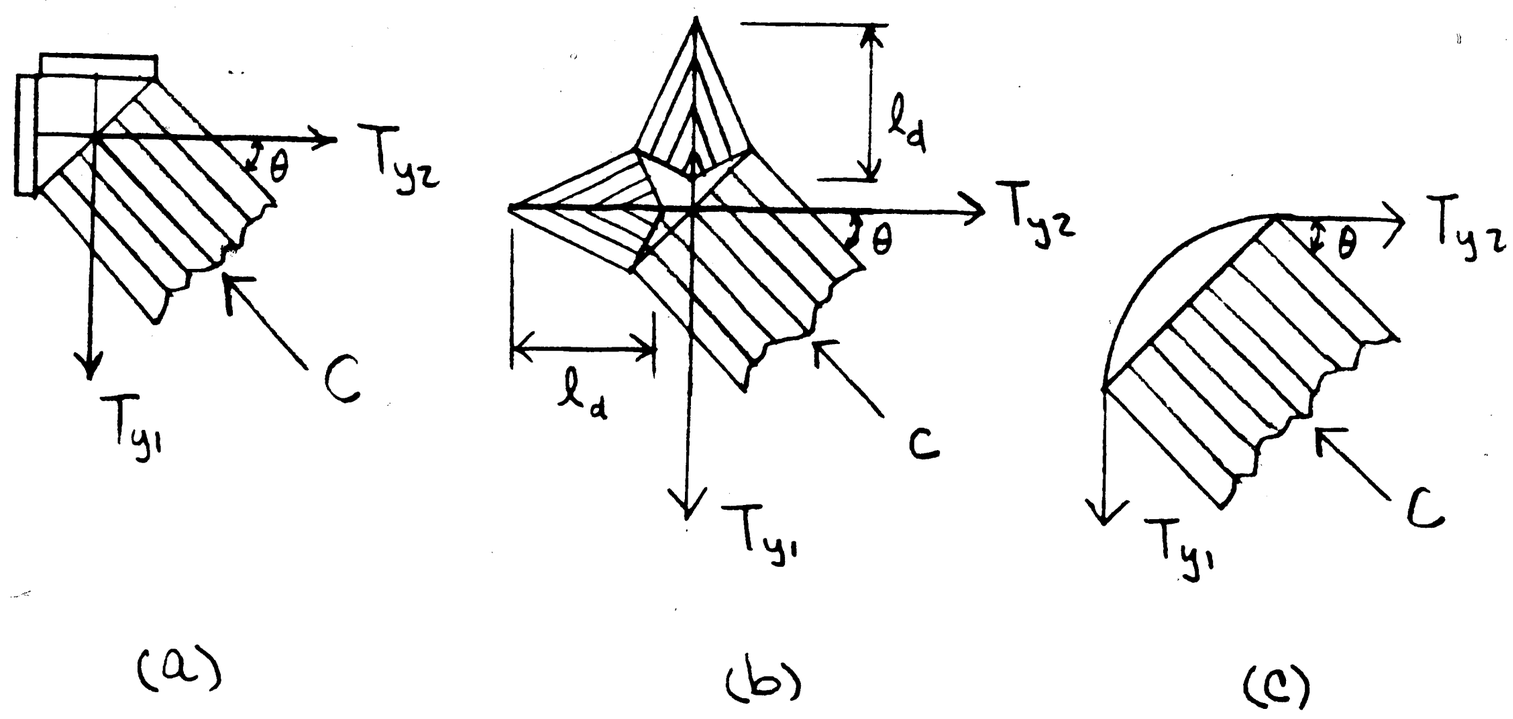

FIGURE 2.28: Anchoring of a CTT node

radius of the bent bars in Fig. 2.28(c) must not only be large enough that the concrete does not crush under the bend (strength), but the bend must also be large enough that it can intercept the full width of the incoming strut (geometry), since the strut must be contained within the bend where the hoop forces originate.

Figure 2.29 illustrates the anchorage problems at the end of a simply supported beam, where a straight development length beyond the support is often not available. Care is needed if the longitudinal reinforcement is bent upward or anchored with a hook as shown in Fig. 2.29(a). In the detail shown, the diagonal compression struts, which should develop the vertical bar extension beyond the bend, have no horizontal support. Therefore, horizontal ties enclosing the vertical bar extension must be provided. Experience shows that without such ties the vertical leg tends to "pop off" the cover as it

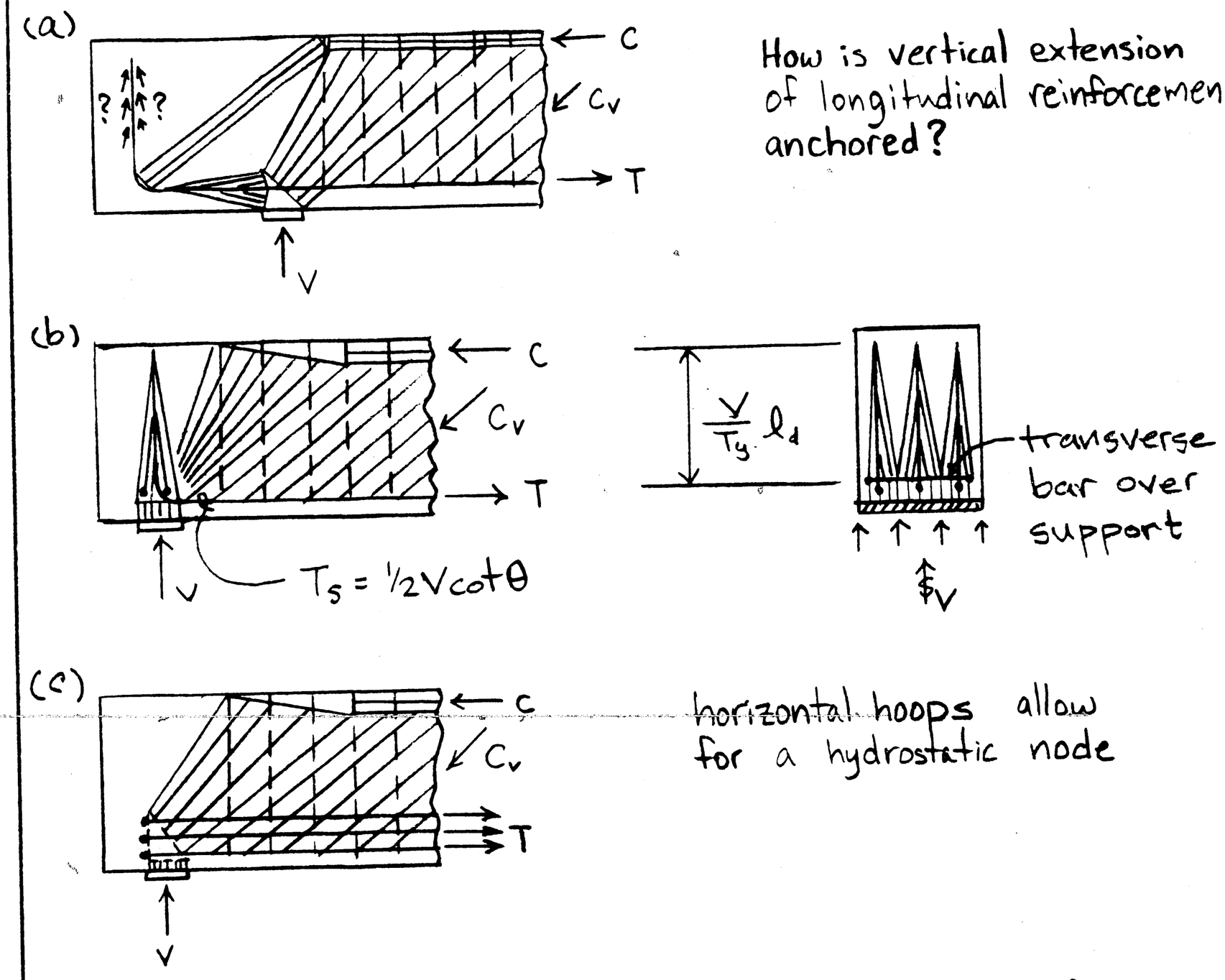

FIGURE 2.29: Anchorage of flexural reinforcement of a simple beam

tries to straighten when the bar is pulled out. If the vertical legs are located directly over the support, the compressive support reaction struts could develop the vertical extension of the flexural reinforcement, as shown in Fig. 2.29(b). If the vertical extension can develop the vertical component of the beam end fan, the bend can now serve as a "pocket" to "catch" the diagonal compression fan. Also this detail should have horizontal ties over the depth of the

beam. A good beam end anchorage is provided by horizontally looped reinforcement as shown in Fig. 2.29(c).

2.9 QUALITATIVE ANALYSIS OF NIB DETAILS OF PRETENSIONED DAP-ENDED BEAMS

The following sections serve to illustrate the just described anchorage principles through qualitative analyses of several nib details of a pretensioned dap-ended beam. Specifically, the best and the worst nib details are looked at in some detail, namely specimens 1B and 2C for which test results are reported in a PCI report.[22] These details are also listed in the PCI Connection Design Handbook.[2] A quantitative analysis of the complete dapped end beam specimen 1B can be found in section 3.5.

This section demonstrates that a purely qualitative truss analysis (except for the graphic statics inherently contained in truss models) allows a designer to "catch" many anchorage deficiencies without ever performing any tests. The test results for these nibs confirm the conclusions from these qualitative analyses.

2.9.1 NIB OF SPECIMEN 1B

The nib detailing of specimen 1B, Fig. 2.30, allows for all compression struts and reinforcing ties to be fully anchored by direct bearing on the anchor plates. The tensile strength and/or chemical bond strength of concrete are never relied upon. Thus, the full capacity of this nib can be realized and is only limited by the global properties of the nib such as geometry and material strengths.

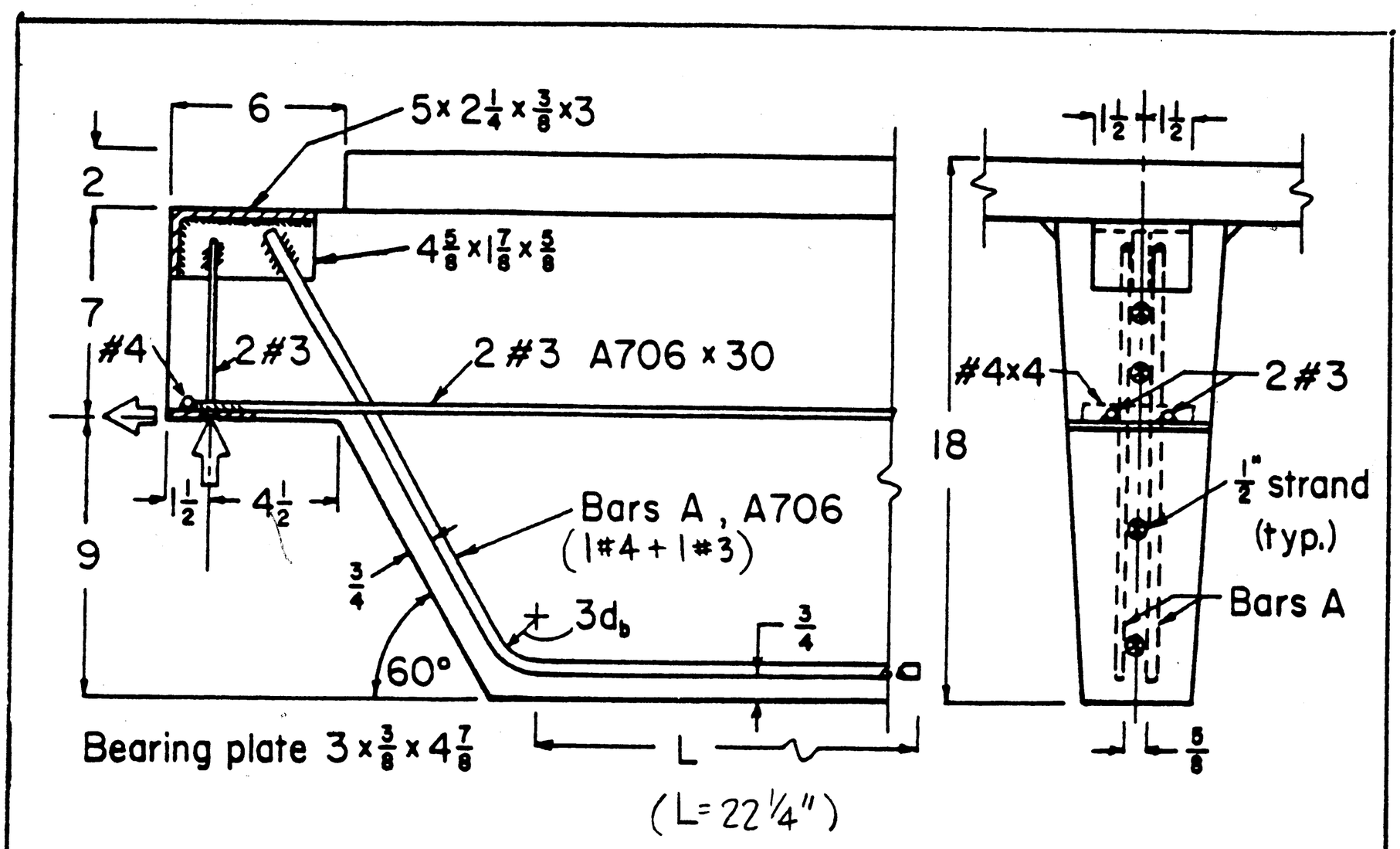

FIGURE 2.30: Details of specimen 1B [22]

Usually, such an anchorage detail can be relied upon without verification tests.

Figure 2.31 shows the truss model for nib 1B. The continuation of this truss model in the beam can be found in Fig. 3.23. Eighteen kips of the total shear force of 23 kips are transferred by the inclined hanger bar into the beam, while the rest is transferred by the inclined compression chord strut C2 [Fig. 2.31(a)]. In a nib at its own capacity, the compression chord strut C2 would touch the upper re-entrant corner. In this case, the capacity of the beam is controlled by the D region to the right (see section 3.5); specifically, there are not enough "hanger bar" stirrups immediately

(a)

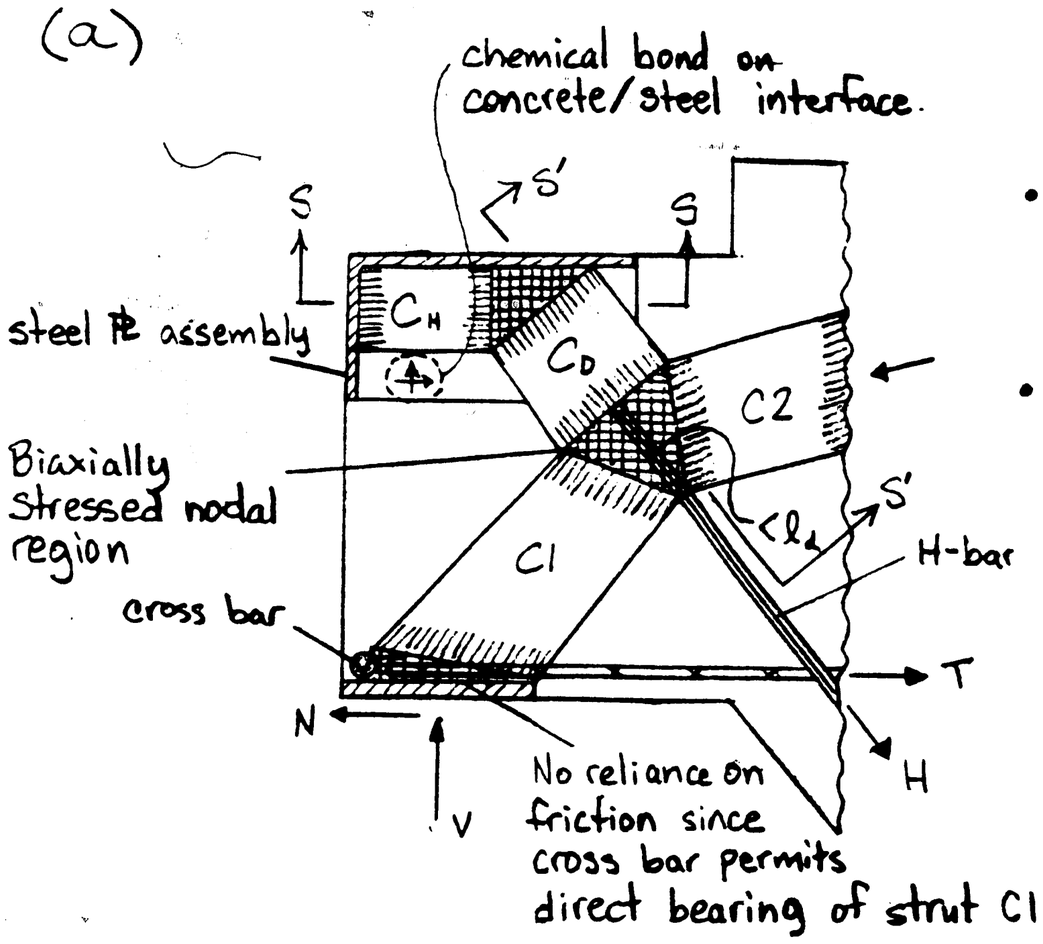

- Strut C_D is along line of action of H-bar, and is the resultant of outward thrust of C1-C2
- C_H forms if friction/bond of plate and concrete is not large enough to resist the horiz. component of C_D.

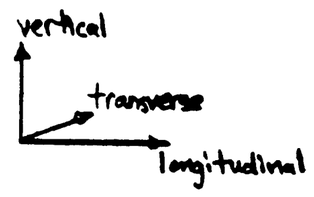

(b) Section S-S or S'-S':

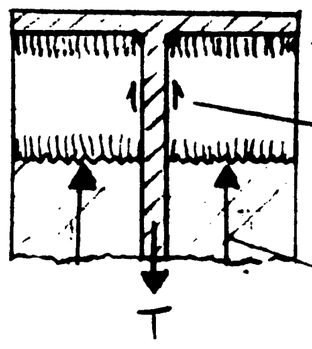

Direct bearing of strut

no reliance on chemical bond

Outward thrust of C_H (S-S) or C1-C2 (S'-S')

(c)

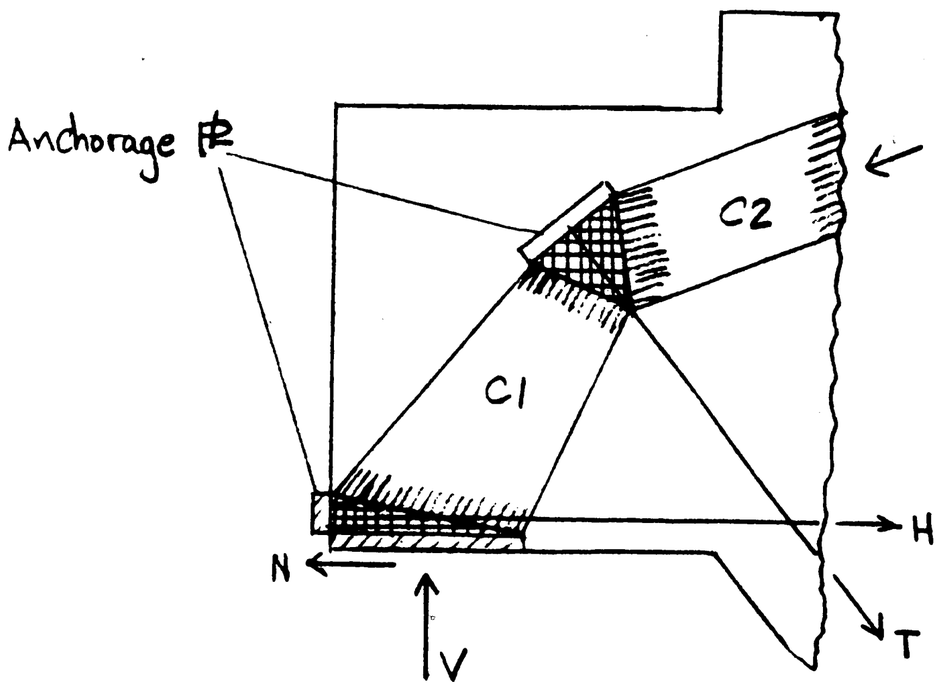

- This model is statically equivalent to (a)

FIGURE 2.31: Truss action for specimen 1B

to the right which forces strut C2 into the deeper position shown. Compression struts C_H and C_D in Fig. 2.31 are "anchor struts" formed in order to fully anchor (balance) the outward thrusts of struts C1-C2. The inclined hanger bar (H-bar) is anchored by welding it to the anchorage assembly, the transverse plates of which, in turn, anchor the outward thrust of C1-C2 over the struts C_H and C_D. Note how the "anchor plates" of the H-bar "interlock" with struts C1-C2 and how the forces anchoring the struts and the bar are related by the action-reaction principle. Nowhere is the concrete/steel interface bond or the concrete tensile strength used, since direct bearing of the sub struts is possible, as shown in Fig. 2.31(b). Direct bearing allows the concrete to develop its full compressive strength, provided that the longitudinal and vertical transverse plates are relatively rigid in shear and flexure. Finally, the existence of a vertical transverse plate ensures that the nib capacity is not controlled by friction between concrete and the horizontal transverse plate. Similarly, the transverse cross-bar welded to the support plate ensures that the nib capacity is not controlled by friction between strut C1 and the support plate, and acts in effect as an anchor plate for the longitudinal nib bar which is also welded to the support plate.

Since the steel assembly allows for direct bearing against biaxially stressed regions and/or transverse (anchor) plates, it is structurally equivalent to the fictitious anchor plate shown in Fig. 2.31(c). In fact, the steel assembly as detailed is actually better than the anchorage plate of Fig. 2.31(c), since the transverse steel

plates are at the geometric boundaries of the nib. This anchorage scheme is, therefore, not sensitive to the exact location of node C1-C2 or the exact width of struts C1-C2. Since exact node location and strut width vary between service and ultimate load, this is an important quality which ensures adequate performance at any load stage. Clearly, this is an excellently detailed nib and, quite probably, its designer had a truss model in mind.

2.9.2 NIB OF SPECIMEN 2C

The detailing and dimensions for this specimen are shown in Fig. 2.32. Its associated truss model which may, or rather, may not form, is shown in Fig. 2.33 and explained below. To anticipate the conclusions below, this scheme relies for anchorage soley on the tensile (shear) strength of plain concrete and the minimal "chemical bond" which may may not exist between a steel plate and concrete in the absence of transverse compression. Such anchorage details are to be discourage, even in the presence of test results, since they are extremely sensitive to the local details of the actual loading conditions which include the effects of creep, shrinkage, temperature changes, and building frame movement.

As illustrated in Figure 2.32 a 6" x 3/8" x 6" vertical steel plate is embedded within the nib such that its left vertical side extends only 1/2" to the left of the vertical support reaction. Due to the insufficient bearing area of the base of the vertical steel plate, which is limited to 2x1/2" = 1" by equilibrium, the full

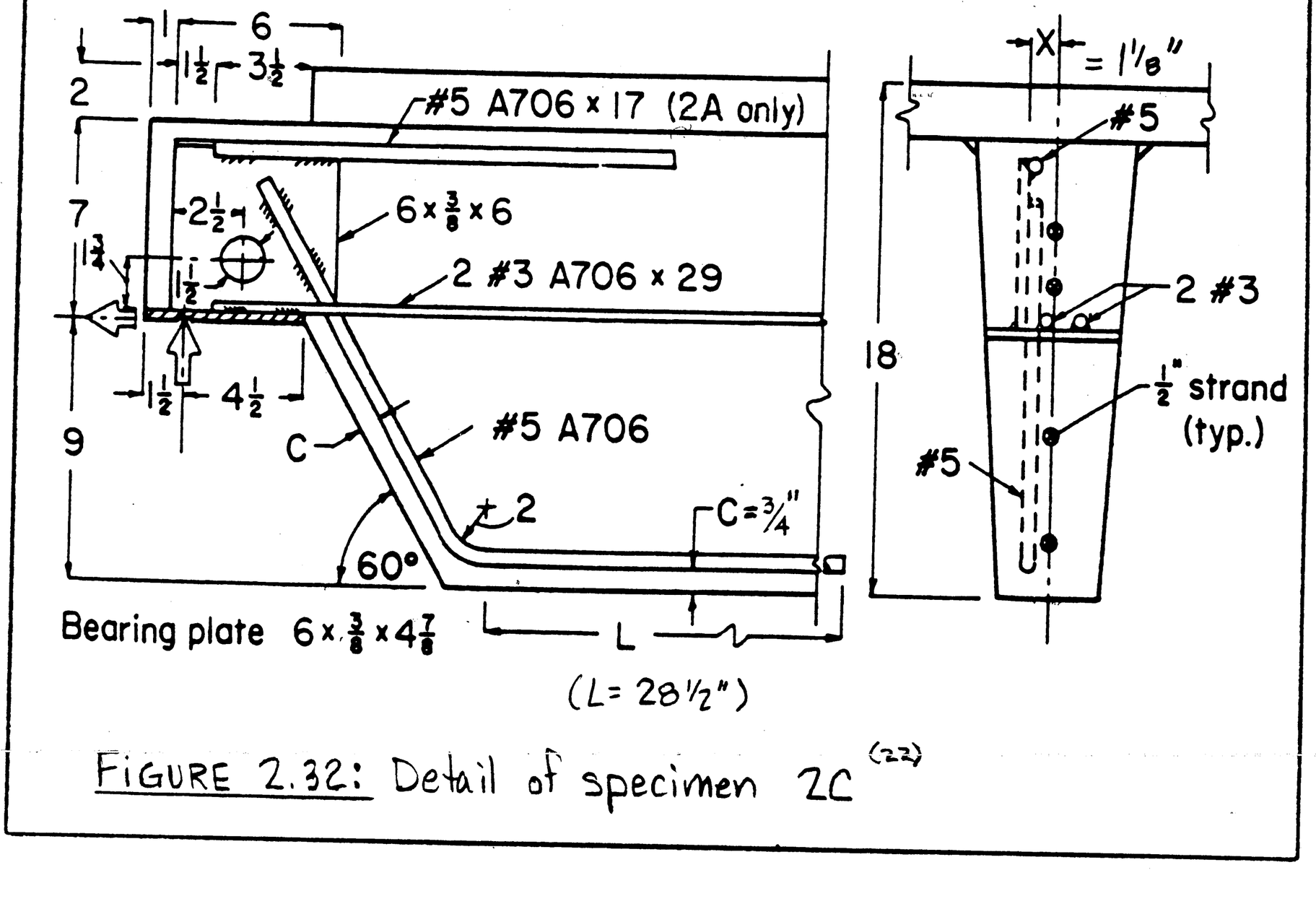

FIGURE 2.32: Detail of specimen 2C (22)

design shear of 23 kips cannot be introduced into the steel plate, rather only:

$$V_{PL} = 1" \times 3/8" \times 36 \text{ ksi} = 13.5 \text{ kips} \; (< V_{DES} \sim 23 \text{ K})$$

Any additional shear must be transferred by formation of struts C1-C2 [Fig. 2.33(a)]. Since the H-bar is welded to the vertical plate (the vertical plate itself bearing against the concrete) it is conceivable that the H-bar could be developed in a section through the re-entrant corner, although the plate thickness of 3/8" is awfully small for the plate to act as an anchor plate as conceptually illustrated in Fig. 2.33(c). However, the issue is not simply developing the H-bar, but as importantly, anchoring the outward thrust of struts C1-C2. More

(a)

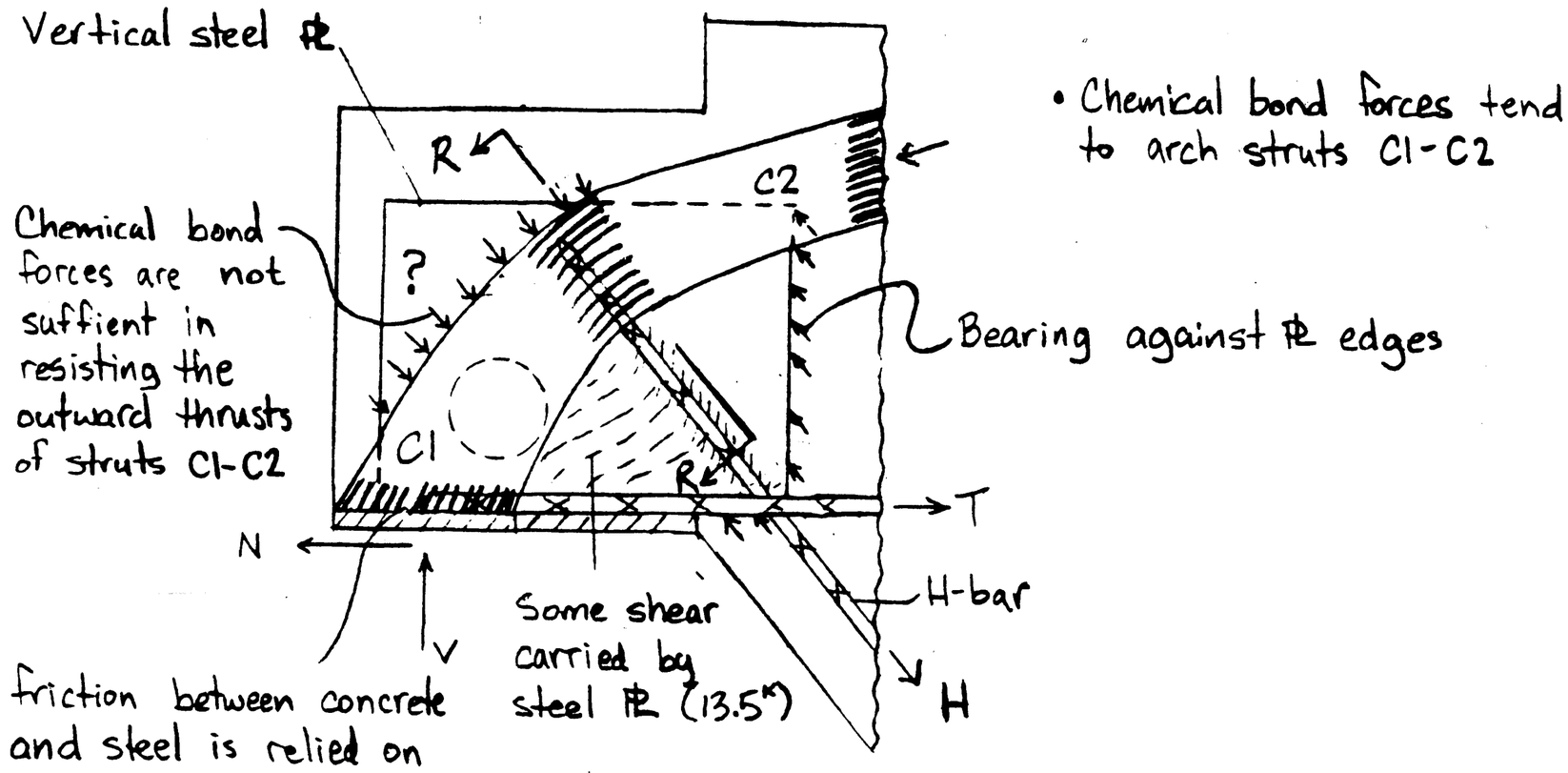

- Chemical bond forces tend to arch struts C1-C2

(b)

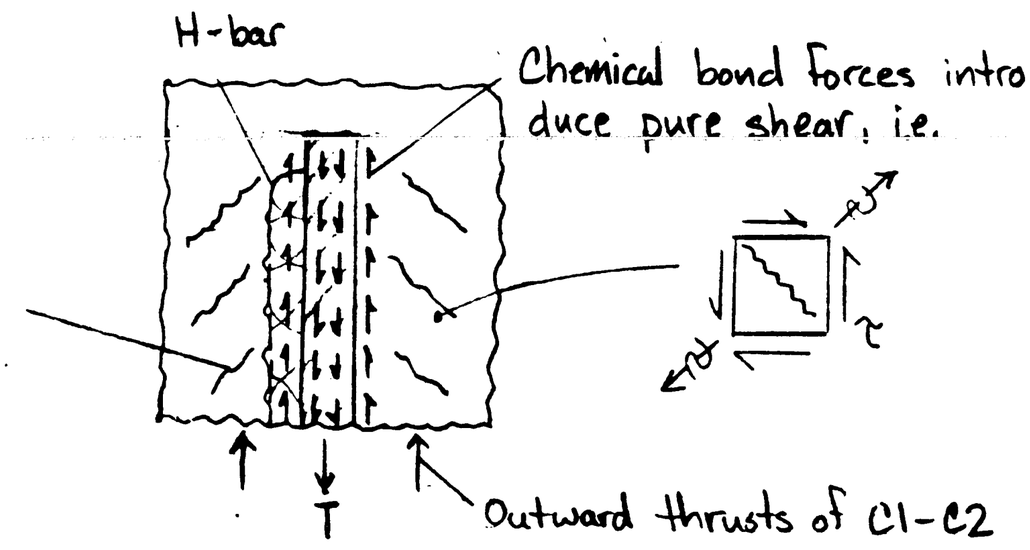

Section R-R:

tensile cracks from pure shear in unreinforced concrete

(c)

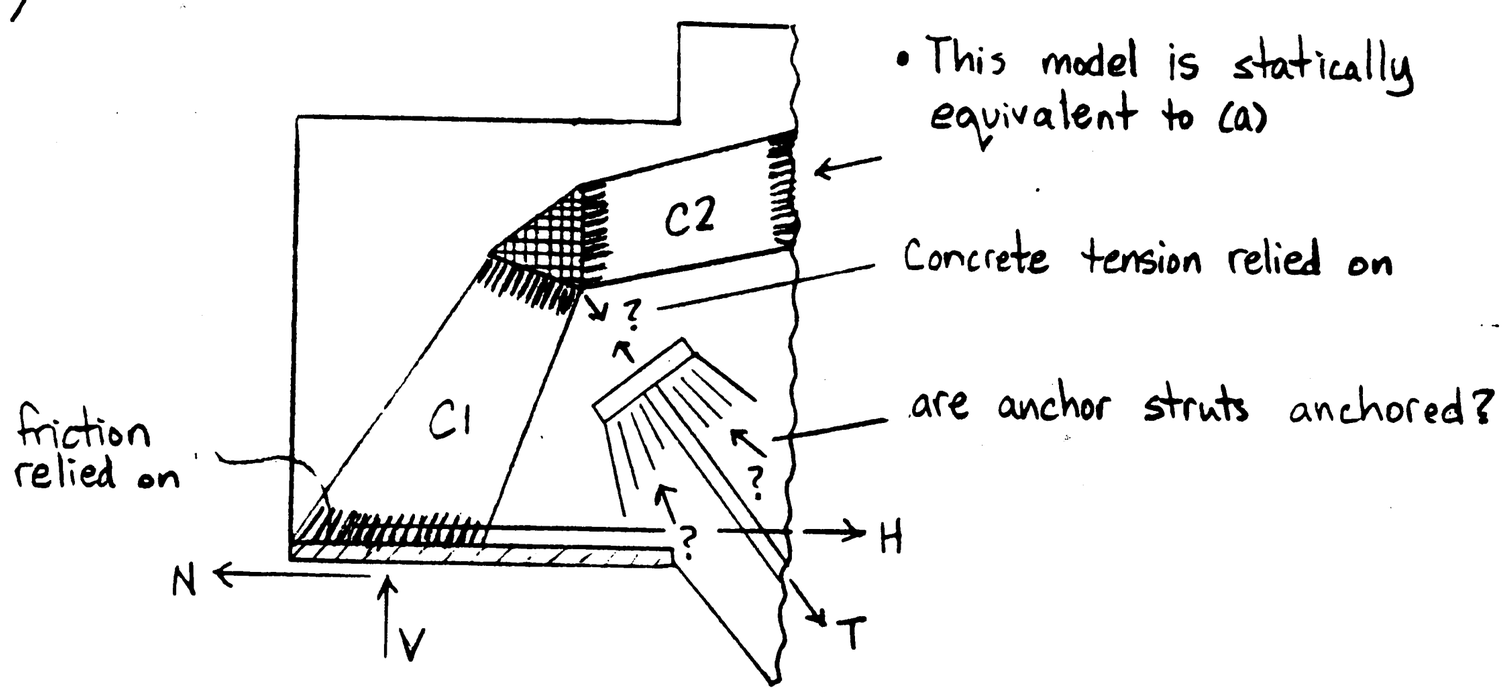

- This model is statically equivalent to (a)

FIGURE 2.33: Truss action of specimen 2C

specifically, the reactions to the force developing the bar must anchor the outward thrust of C1-C2. Hence, only if struts C1-C2 are fully anchored to the vertical steel plate, can the capacity of the nib as determined by the truss model, be realized. This is the weak link of this nib detail. Due to the lack of transverse compression, the anchorage of struts C1-C2 to the vertical plate relies on the minimal chemical bond that may exist between steel plate and concrete, and also on concrete tensile strength, as shown in Fig. 2.33(b). Note, however, that neither the ACI Code[3] nor the PCI handbooks[1,2] permit interface shear transfer in the absence of transverse compression or transverse reinforcement. The behavior of this nib is structurally equivalent to that in Fig. 2.33(c). Node C1-C2 forms outside the location where the H-bar introduces compression by "anchor plate action." "Anchor plate" and struts *do not interlock* and concrete tension and chemical bond is needed to transfer shear and anchor the struts. Also, strut C1 at the support reaction is only anchored to the extent that friction between the concrete and steel is not exceeded. A cross-bar, as in specimen 1B, would eliminate this problem since it would provide for direct bearing of strut C1.

In summary, no interlocking of struts with rebars or plates is provided and anchorage of struts C1-C2 relies on the tensile (shear) strength of plain concrete and on chemical bond which is not permitted by codes. Whether or not this detail works can only be determined by tests. Usually, such details do not work as exemplified by this test. This nib was only able to carry

approximately 12 kips in shear before the nib failed by diagonal tension failure in the lower re-entrant corner of the nib. Note that this 12 kips is not much different from the maximum force that can be introduced into the plate as calculated above, V_{PL} = 13.5 kips.

Clearly, this nib is poorly "detailed" and violates codes on closer inspection. It exemplifies detailing that is not guided by a rational model such as truss models. Even the hole in the plate is in the wrong location; it would be more effective "outside" node C1-C2. It clearly demonstrates that "detailing" is not a detail but a crucial and essential part of design which must not be left to "detailers". It cannot be left to detailers because the "details" determine the possible node locations of the very truss model on which analysis and design is based. The importance of anchorage through interlocking of struts and other reinforcement casts doubt on the common practice of showing "supplemental" reinforcement for connections on drawings without the primary reinforcement.

2.10 RULES FOR TRUSS MODELING

In the design of structures by use of truss models, several rules should be followed. Since many different truss models can be created for the same structure under the same loading, the choice would be one that uses the simplest and shortest internal force paths and maximizes the stiffness. Elements with the least amount of deformation such as diagonal concrete struts should be frequently used and preferred over, for instance, diagonal reinforcement ties,

since this minimizes the energy. Schlaich, Schafer, and Jennewein[6] derived an expression from the principle of minimum strain energy,

$$\sum_{o}^{i} F_i \ell_i \epsilon_{mi} = \text{minimum} \qquad (2\text{-}15^*)$$

where F_i = force in strut or tie i

ℓ_i = length of element i

ϵ_{mi} = mean strain of element i

It can be seen from equation (2-15*) that minimizing the member lengths and using as few ties as possible (since they have large strains compared to struts), will minimize the strain energy.

Generally, there are two types of trusses, those which transfer shear with diagonal compression struts and those that transfer shear with diagonal tension ties. Clearly, equation (2-15*) prefers the first type over the second. Primary reinforcement ties should generally follow the geometric boundaries of the component and maximize the internal flexural lever arm. They should never be bent around concave corners, since this leads to T-T-T nodes which should be avoided. It is extremely difficult to make a T-T-T node in a concave corner stiff and tight enough that the bent bar doesn't "pop-out" before the third tie is activated. Rather, primary B-region reinforcement entering a D region such as a joint should be extended straight and anchored at the far geometric boundary of the D-region, where its anchorage can introduce compression. This rule is evident in most of the truss models described in chapters 3 and 4. Generally, anchorages should be located as close to the opposite geometric boundaries of a component as possible, since this provides maximum freedom to the truss which develops upon cracking, to choose

its optimal node locations at different stages of loading.

The truss models described in this report operate at the ultimate state, in full accordance with the design philosophy of the ACI Code[3], and require significant inelastic stress redistributions. In order to permit the truss to indeed develop, the concrete must be given minimum ductility with well distributed, caging type, minimum reinforcement in two or at least one direction.

Once a general geometry for the design truss model is chosen, additional rules and considerations should be followed so that the structural component will behave as modeled.

1. Since the structural component is fully cracked at the ultimate state, the concrete tensile strength should never be relied on (except for shear in slabs).
2. Make certain that the same chunk of concrete is not used more than once as a structural element. Concrete compression struts must never intersect nor overlap. If they intersect, a node must be introduced explicitly. Intersecting struts are not compatible with open cracks, since it signifies biaxial compression.
3. Once the required depths of the struts are known, make sure they do not exceed the geometric limits of the structural component nor overlap.
4. Reinforcement ties should pass through the truss nodes and be anchored "behind" the node so that the tension in the reinforcement can introduce compression on the node.

Compression struts should bear or interlock with the supports or the reinforcement.

5. Provide whenever possible a well distributed caging type of reinforcement. A ductile component more readily accepts the design truss model.

6. All hardware such as plates and angles should be sized so that they do not govern the truss model's behavior, i.e., they should be relatively rigid.

7. Welding should be kept to an absolute minimum since brittle weld failures are not uncommon. Many of the failures observed in the tested connections of the PCI project 1/4[23] were due to brittle weld,ruptures.

2.10.1 SUMMARY ON ANCHORAGE AND DEVELOPMENT

The significance of anchoring and developing the truss elements cannot be overemphasized, since full anchorage and development of the members determine the behavior and performance of the structural component. Proper anchorage is the key to a successful truss model. It is just as, if not more, important as the concrete strength. Therefore, the *designer* should detail his structural component and be conservative with anchorage and development.

This means that he should not except possibly locally for development, rel y on the concrete tensile strength. Reliance on the concrete tensile strength will result in poor performance if the concrete is precracked due to volumetric changes or building frame movement.

Sections 2.8 and 2.9 clearly show that both tension ties and compression struts need to be anchored. Tension elements should be brought through a node and anchored behind it with an anchor plate or its equivalent. Anchorage of compression elements requires that the compressive thrust component be fully equilibrated by anchor plates (or their equivalent) and that the anchor plates be located so as to intercept all of the fibers of the compression elements (section 2.8.2). The details of section 2.9 exactly demonstrate the need to anchor both the compression and tension elements.

Since loops wrap around biaxially stressed nodes, they allow the tension to be brought behind the node and introduce compression through the node, thus allowing interlock. Hence, loops are recommended for anchoring rebars. But loop location is crucial if compressive struts are to be anchored at locations predetermined from the truss. As demonstrated in section 2.9.2, incorrect location of the anchor plate (or a loop) may result in reliance on the concrete tensile strength for compressive strut anchorage. Of course, loops should be oriented, so that the plane of the loop is transverse to the compression strut it interlocks. The beneficial effects of transverse compression can then be used. Horizontal loops over supports in beams, for example, would use this transverse compression. Compressive strut anchorage achieved through frictional resistance should be avoided.

2.11 INTERFACE SHEAR TRANSFER WITH MOMENT

The shear friction procedure, as described by the ACI code[3],

provides a design method for conditions in which shear transfer should be considered, such as at an interface between concrete and steel, at an interface between concretes cast at different times, in design of reinforcing details for precast concrete structures, and in other instances where shear transfer must be considered across a plane in structural concrete.

According to the ACI code[3] the shear friction resistance is given by

$$V_n = (A_{vf} f_y - N)\,\mu_s \qquad (2\text{-}16)$$

but

$$V_n \leq 0.2\, f_c' A_c$$

$$\leq (800 \text{ psi})(A_c) \qquad (2\text{-}17)$$

where A_{vf} = area of shear friction reinforcement

N = positive tensile loads on the interface

μ_s = coefficient of friction

In this form it is not immediately clear how shear friction relates to truss models and how combined moment and shear at the interface should be treated. In particular, the question is often asked whether reinforcement located in the flexural compression zone may be included in the shear friction reinforcement. The purpose of this section is to present shear friction in a form that is compatible with truss modeling and to address some of these questions.

The shear friction concept can be understood through the local truss model for an infinitesimal element of unit length shown in Fig.

2.34(a).

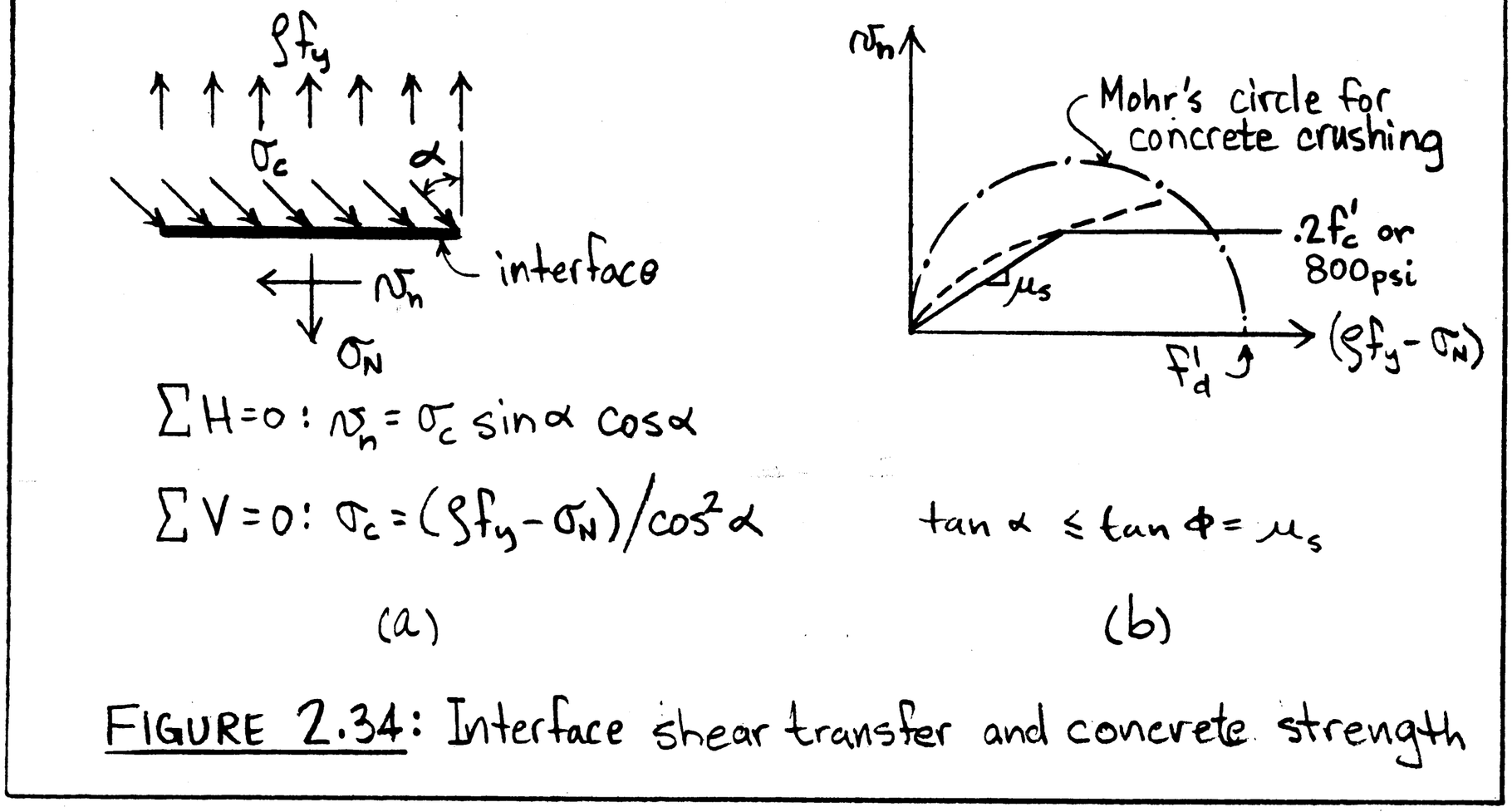

FIGURE 2.34: Interface shear transfer and concrete strength

Of course, it is not the reinforcement, but diagonal compressive stresses in the concrete which resist shear along the interface. Combining the equilibrium equations in both the horizontal and vertical directions and considering that the diagonal compressive stresses cannot exceed the diagonal compressive strength and their inclination cannot exceed the angle of friction, gives

$$\sum H = 0: \qquad \nu_n = \sigma_c \sin\alpha \cos\alpha \tag{2-18}$$

$$\sum V = 0: \qquad \sigma_c = \frac{(\rho f_y - \sigma_N)}{\cos^2\alpha} \leq f'_d \tag{2-19}$$

$$\nu_n = (\rho f_y - \sigma_N) \tan\alpha \tag{2-20}$$

$$\tan\alpha \leq \tan\phi = \mu_s \tag{2-21}$$

where α = angle of inclination of the diagonal compressive stresses

ϕ = friction angle

ϱ = reinforcement ratio

The maximum shear stress that can be transferred over the interface according to equations (2-18) to (2-21) is plotted in Fig. 2.34(b). The dashed line corresponds to equation (2-20) at its upper limit, equation (2-21), and also considers that the shear friction coefficient, μ_s, depends on the concrete normal stress. The dash-dotted Mohr's circle represents the diagonal concrete crushing criterion. The solid line represents a safe approximation of the dashed line using a constant friction coefficient and the limit specified by equation (2-17).

The diagonal compressive strength depends according to equations (2-1) and (2-2) on the strain conditions. If the steel across the interface is, as assumed above, at the yield strain, the diagonal compressive strength is 0.33 f_c' and 0.4 f_c' for $\tan\theta = \tan\phi = 0.6$ and 0.7, respectively. Inserting these values into equation (2-18) gives a shear stress at diagonal crushing of 0.15 f_c' and 0.19 f_c' for $\mu_s = \tan\phi = 0.6$ and 0.7, respectively. Thus, if the steel is yielding in tension, Mohr's circle for diagonally crushing concrete intersects the shear friction line at a shear stress approximately equal to the limit specified by equation (2-17).

Thus, the ACI Code equations (2-16) and (2-17) in essence represent the local interface failure surface for transverse steel yielding in tension multiplied by the interface area, except that the failure condition is not closed to the right. However, shear occurs

rarely without moment. If a moment is acting across the interface, the (diagonal) compressive stresses must be concentrated in the flexural compression zone, as shown in Fig. 2.35(a), and a shear force can be resisted by the inclined flexural compressive resultant.

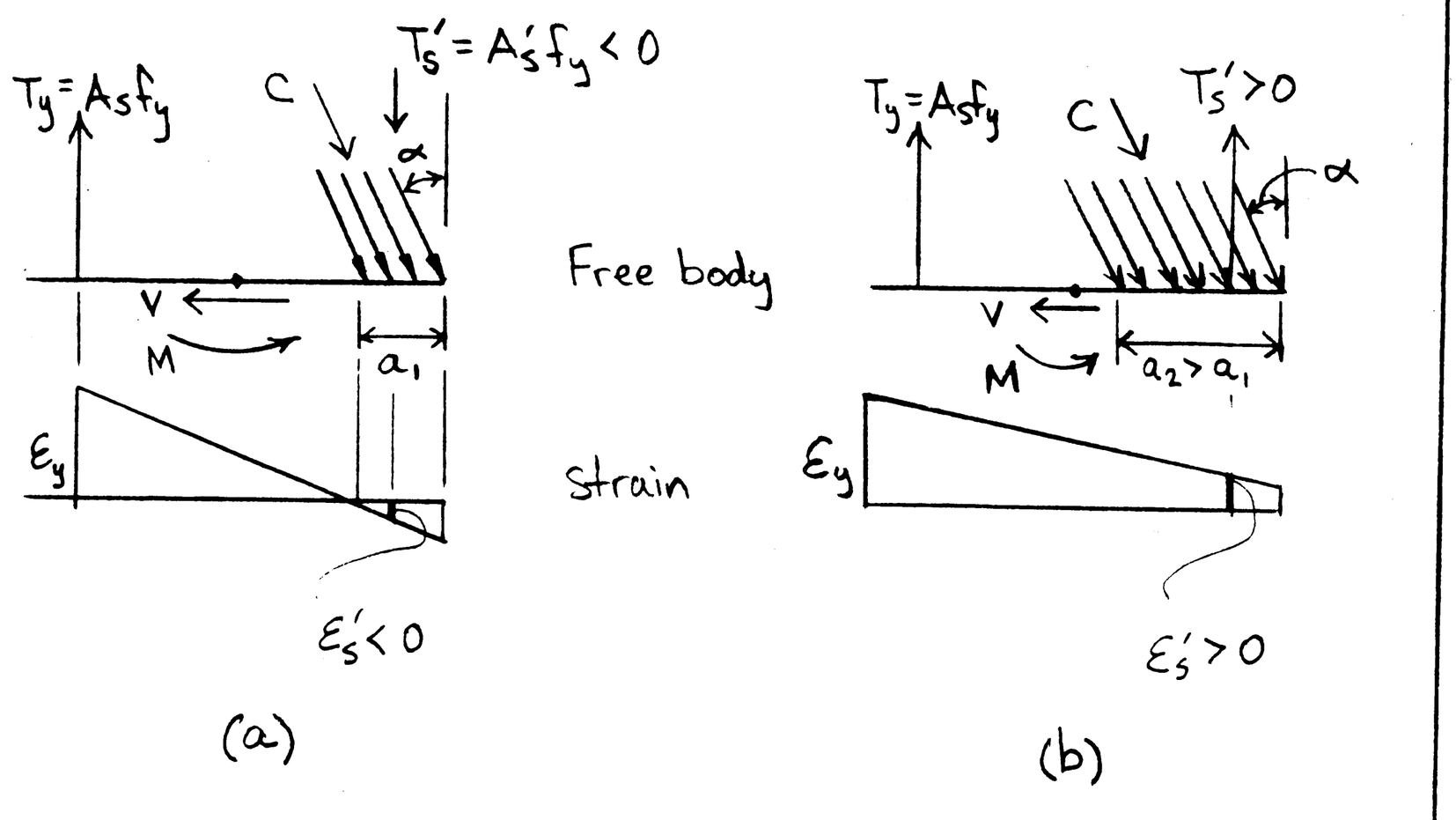

FIGURE 2.35: Various interface stress - strain distributions

If the compression steel is in compression, the diagonal compressive strength, equations (2-1) and (2-2) is close or equal to its flexural value of 0.85 f_c' and the maximum transferable shear force is close to the product of flexural compressive resultant times friction coefficient. However, the friction coefficient to be used must be that associated with concrete normal stresses close to 0.85 f_c'. If this value were used, the limit specified by equation (2-17) would not apply, since this limit simply defines the point beyond which the

code-specified constant friction coefficients become unconservative, as illustrated in Fig. 2.34(b). Unfortunately, there is practically no experimental data on friction coefficients for such high concrete normal stresses.

In Fig. 2.35(a) it has been assumed that the compression steel is acting in compression. However, a larger shear force could be transferred over the interface, if the (inclined) flexural compressive resultant were increased, i.e. if the "compression" steel were acting in tension, as shown in Fig. 2.35(b). Specifically, the shear force defined by equation (2-16), if the compression steel is included in the shear friction steel, could be reached, if the "compression" steel were yielding in tension. Naturally, the question arises whether steel yielding in tension in the flexural compression zone does not violate strain compatibility. It is precisely this strain compatibility which is expressed by equation (2-2) where $\theta = \alpha$ in Fig. 2.34 . Tensile strains in the steel imply transverse strains across the inclined compressive resultant and reduce according to equation (2-1) the (diagonal) compressive strength. Therefore, the depth of the inclined flexural compression block must become significantly larger, and the lever arm and, hence, flexural strength is reduced in comparison with the condition when the compression steel is in compression. In other words, a moment-shear interaction must exist for the interface. In the next section the equations for this interface interaction diagram are derived.

2.11.1 INTERFACE MOMENT SHEAR INTERACTION EQUATIONS

The derivation of the equations governing the interface interaction diagram is based on the assumption of under reinforced behavior, i.e. on the assumption that the flexural tension steel is yielding at the interface. Figure 2.36 shows the free body diagram for the interface and also the notation and sign conventions. All forces are plotted in the positive direction. Figure 2.37 shows qualitatively the interface interaction diagram and will be explained as the governing equations are derived. Formulating the three equilibrium equations for the interface yield:

$$\sum H = 0: \qquad C \sin \alpha = V \tag{2-22}$$

$$\sum V = 0: \qquad C \cos \alpha = T_y - N + T_s' \tag{2-23}$$

$$\sum M_B = 0: \qquad M = T_y\, d - N\, \frac{h}{2} + T_s'\, d_H' - C\, \frac{t}{2} \tag{2-24}$$

Combining the first two equations and calculating the depth at the inclined compression strut (compression block) gives:

$$C^2 = V^2 + (T_y - N + T_s')^2 \tag{2-25}$$

$$t = \frac{C}{b\, f_d'} \tag{2-26}$$

Substituting equations (2-25) and (2-26) into equation (2-24) gives

$$M = T_y\, d - N\, \frac{h}{2} + T_s'\, d_H' - \frac{V^2 + (T_y - N + T_s')^2}{2\, b\, f_d'} \tag{2-27}$$

Dividing equation (2-22) by (2-23) and observing that the inclination of the compressive resultant cannot exceed the friction angle yields

$$\tan \alpha = \frac{V}{(T_y - N + T_s')} \qquad (\leq \mu_s) \qquad (2\text{-}28)$$

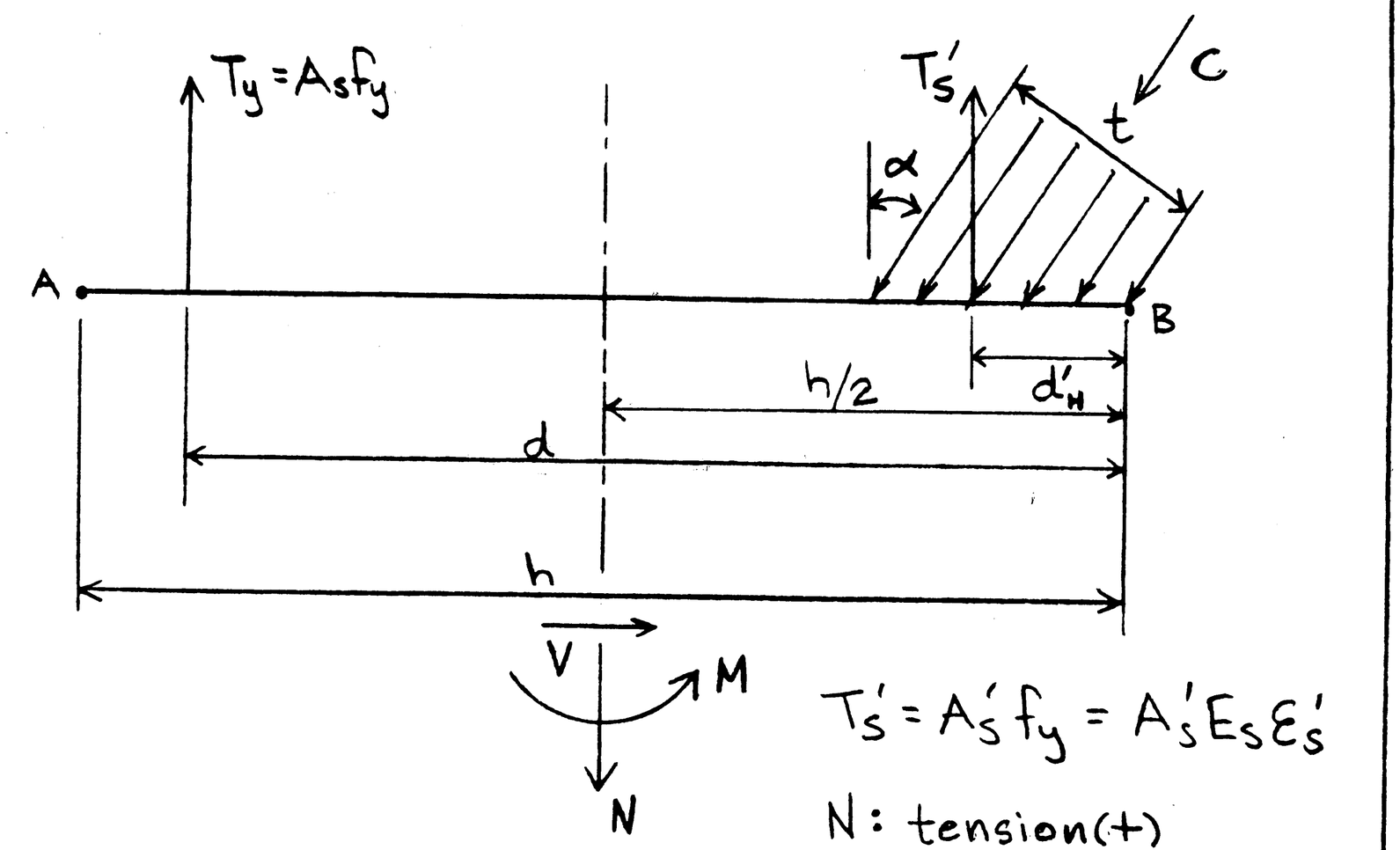

$T_s' = A_s' f_y = A_s' E_s \varepsilon_s'$

N: tension(+)

$\Sigma H = 0$: $C \sin\alpha = V$

$\Sigma V = 0$: $C \cos\alpha = T_y - N + T_s'$

$\Sigma M_B = 0$: $M = T_y d - N\frac{h}{2} + T_s' d_H' - C\frac{t}{2}$

where $t = \frac{C}{b F_d'}$

FIGURE 2.36: Equilibrium of the interface

Equation (2-27) describes curve A-B in the interaction diagram of Fig. 2.37 and the limit in equation (2-28) defines point B on this curve. The magnitude of the compression steel force, T_s', may be assumed to remain constant at its value for pure flexure,

T_{sm}', as determined from a strain compatibility analysis for pure

flexure. Thus, along A-B the compressive resultant simply becomes more inclined without changing its normal component as the shear

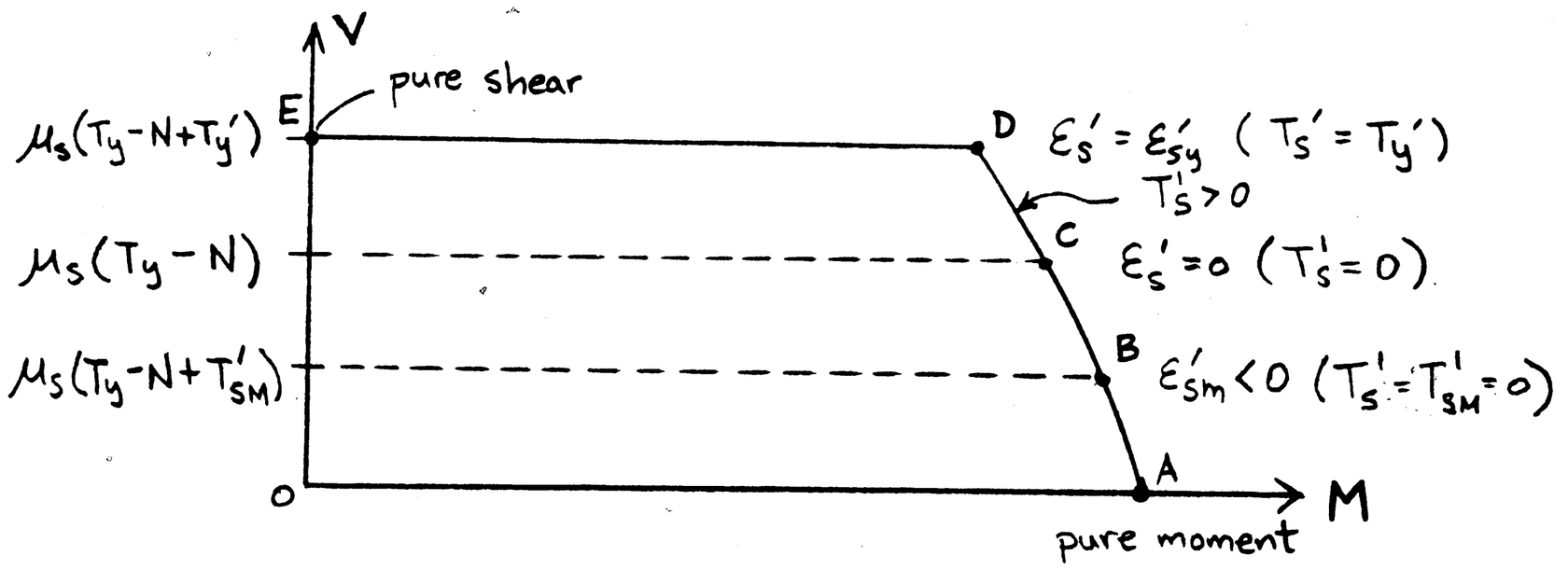

FIGURE 2.37: Interface shear-moment interaction diagram

force increases. At point B its inclination, equation (2-28), equals the angle of friction. As discussed previously, the value of the friction angle or coefficient must be that for concrete normal stresses close to the uniaxial compressive strength. The force in the compression steel, T_{sm}' may be compression or tension depending on the geometry and loading of the interface. If T_{sm}' is compression, the diagonal compressive strength in equation (2-27) may be assumed to remain at its value for pure flexure, 0.85 f_c'. The same is true if T_{sm}' is tension, but the compression face steel lies outside the inclined compression zone.

Since the compressive resultant is inclined at the friction angle at point B, any further increase in shear force is only possible, if its normal component increases, i.e. if the force in the

compression face steel, T_s', algebraically increases above the value T_{sm}'. Since for shear forces equal to or higher than that of point B

$$\tan \alpha = \mu_s \tag{2-29}$$

$$V = \mu_s (T_y - N + T_s') \tag{2-30}$$

the required value of T_s' for a given shear force can be determined by solving equation (2-30) for T_s'

$$T_s' = \frac{V}{\mu_s} - (T_y - N) \leq T_y' \tag{2-31}$$

while equation (2-27) can be rewritten as

$$M = T_y d - N \frac{h}{2} + T_s' d_H' - \frac{V^2 (1 + \frac{1}{\mu_s^2})}{2 b f_d'} \tag{2-32}$$

Equations (2-31) and (2-32) describe curve B-C-D. At point D the compression force steel yields in tension, $T_s' = T_y'$, and the maximum possible shear force

$$V = \mu_s (T_y - N + T_y') \tag{2-33}$$

is reached. As before the friction coefficient associated with the actual concrete normal stresses in the compression zone must be used. Since the compression face steel is in tension, the softening of the diagonal compressive strength with increasing transverse strain must be considered, as discussed above. In an iterative procedure diagonal compressive strength, compression zone depth, strain distribution over the interface, and moment can be calculated for a given shear force.

The "plateau" D-E in Fig. 2.37 reflects the fact that the resultant of the diagonal compressive stresses can simply shift its location in accordance with the applied moment, as shown in Fig. 2.38, without affecting the shear capacity, if the friction angle is assumed constant. The stress distributions in Fig. 2.38(a) and (b)

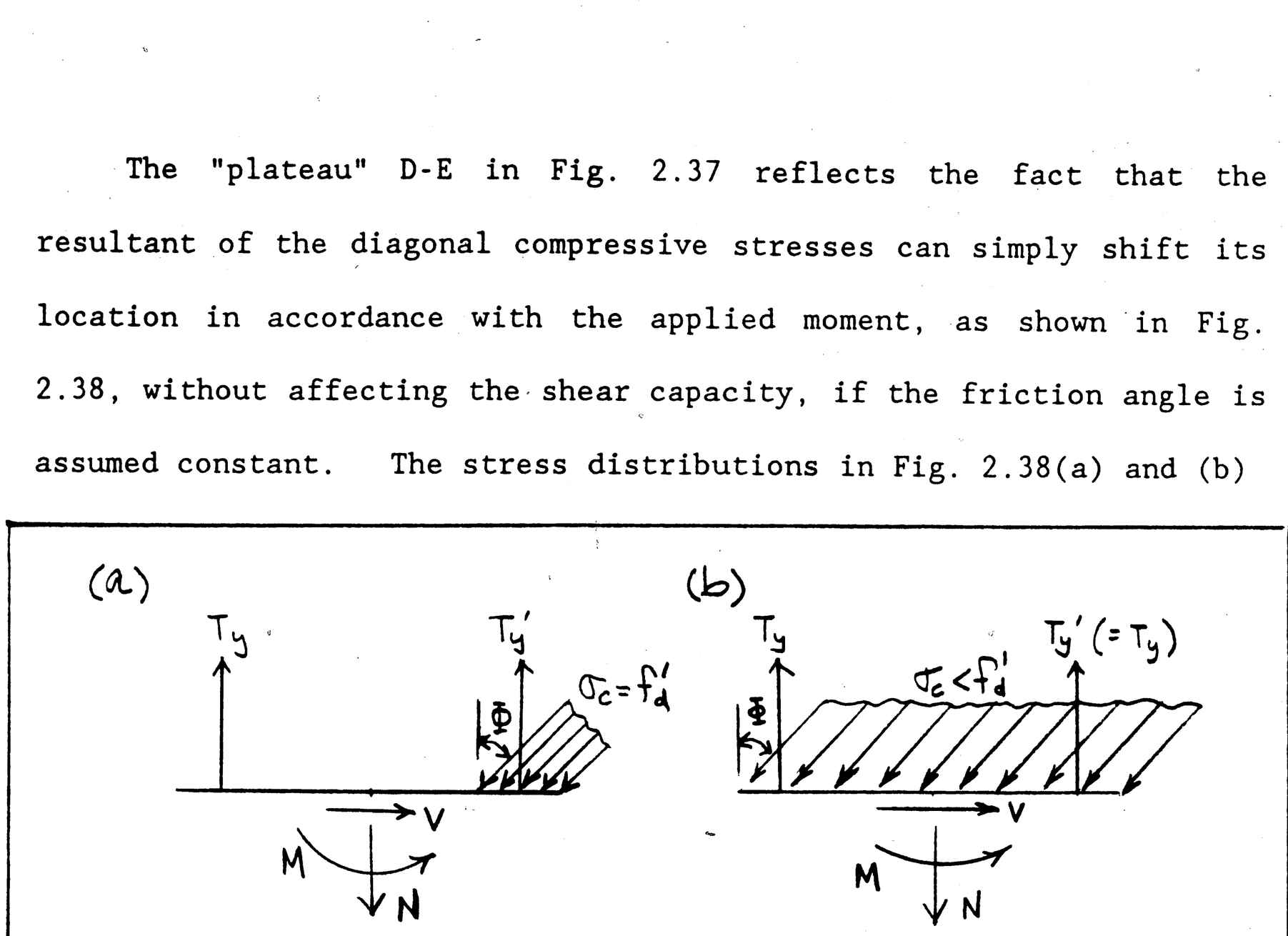

FIGURE 2.38: Maximum shear stress redistributions on interface

corresponds to points D and E, respectively. If the dependency of the friction angle or coefficient on the normal stress is considered line D-E becomes curved, too, with a maximum at point E for pure shear.

The question whether or not softening of the diagonal compressive strength according to equations (2-1) and (2-2) occurs at an interface, and, if it does, whether these equations are directly applicable is further discussed in chapter 4. As noted there, experimental data is needed on the diagonal compressive strength for certain interface types and, as observed above, on the friction coefficient for high concrete normal stresses. Finally, it must be noted that this treatment of interface shear transfer neglects dowel action for reasons further discussed in chapter 4.

3. AN UNDERSTANDING OF REINFORCED AND PRESTRESSED CONCRETE CONNECTIONS AND JOINTS

This chapter presents, from a truss modeling perspective, a treatment of monolithic concrete joints such as corbels, knee-joints, and beam-column joints, and of other D regions such as dapped ends of beams. Understanding the behavior and potential problems of monolithic joints provides a key to the understanding of precast concrete connections, since the D-regions adjacent to the connection interface play rather similar roles. Truss models are used to investigate anchorage and development requirements and to interpret test results. Emphasis is on anchorage, because it is the primary cause of unsatisfactory performance. While most of the treatment is qualitative, the dapped end analysis is quantitative and also illustrates the treatment of prestressing.

Many of the experimental test results presented here are adapted from MacGregor[18] and Park and Paulay[24].

3.1 CHARACTERISTIC BEHAVIOR OF CORBELS

Monolithically cast concrete corbels are widely used to support a beam or girder and transfer its reaction to a column. Corbels usually have a span-to-depth ratio of less than or equal to unity and are thus expected to behave similarly to deep beams in which shear is primarily transferred by direct struts from load to support resulting in truss-like behavior. The idealized truss model shown in Fig. 3.1(a) is for a corbel located at the top of a column. The direct struts bear onto the anchor plates which anchor the horizontal and

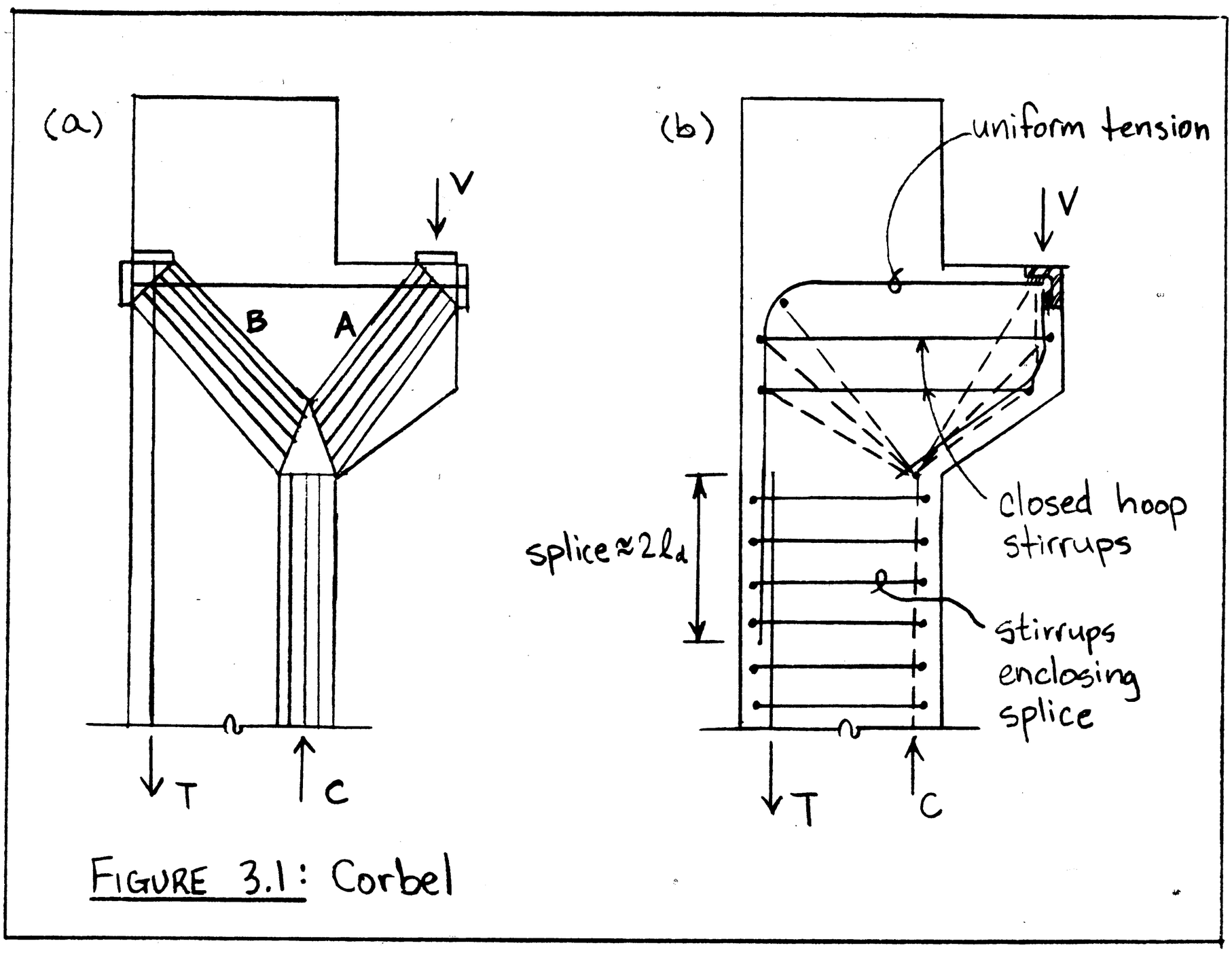

FIGURE 3.1: Corbel

vertical reinforcement. Note how the reinforcement interlocks such that the anchor plates form a pocket into which the strut can bear.

Many tests have been conducted on corbels, most recently by Cook/Mitchell[10]. The observed test results seem to agree quite well with the predictions of the simple truss model of Fig. 3.1(a). It was further shown[10] that the detailing substantially affects the strength and performance.

The function of the internal elements becomes clearer upon closer inspection of the truss of Fig. 3.1(a). For instance, the top

horizontal rebar is not developed from the corbel-column interface. Rather it is over its full length in uniform tension which must be anchored behind the node at the opposite exterior face and, in effect, transferred around a 90^{o} "turn" into the column longitudinal reinforcement through the anchor plate assembly. The diagonal strut in the column provides the equilibrating thrust for the orthogonal tensile forces "exiting" that node. Similarly the diagonal strut in the corbel bears into the plates and equilibrates the forces at the load application point of the corbel. The two diagonal struts are anchored at their opposite end by bearing against each other and the flexural compression block resultant in the column.

As described in chapter 2, though, such a truss model can only develop, if the elements are fully anchored at or behind the nodes and if the necessary ductility requirements are met by providing a minimum amount of distributed reinforcement in at least one direction.

Figure 3.1(b) shows a detailing scheme which allows the realization of the truss in Fig. 3.1(a). In this detail, closed hoop stirrups are provided in addition to the primary bent rebar along the top face. A steel angle is used at the corbel corner to which all steel entering that corner is welded. If the angle is relatively rigid, it provides for interlocking of the compression strut with the tensile reinforcement at that node.

The closed hoop stirrups in this detail play a significant role in that they

(1) provide for the necessary minimum ductility by confining the concrete,

(2) provide for transverse reinforcement necessary for 3-D behavior as well as alleviating column splitting (which may result from the transverse strains under the in-plane bend of the primary horizontal corbel reinforcement),

(3) "deconcentrate" the diagonal compressive struts by spreading or fanning them over the height of the stirrups. This "deconcentration" not only reduces the diagonal compressive stresses, but also allows the exterior face vertical reinforcement to be developed over the height of the stirrups, as shown by the dashed lines of Fig. 3.1(b).

The bearing stresses on the inside perimeter of the bend and the tendency of the concrete to split in the plane of the bend can be reduced by increasing the bend diameter beyond the permissible minimum and by using closely spaced small bars so that the bends form a "sheet". Rigid transverse bars welded to the inside of the bend are very effective: they provide additional bearing area; help in bar development, if the tension in the horizontal and vertical legs is different; alleviate splitting; and provide for 3-D truss action.

The force developed in the vertical legs of the bent rebars must be spliced with the column's longitudinal exterior face reinforcement, as discussed in section 2.8.1. The splice should be located far enough away from the corbel so that its development does not interact with and affect the actions of the column diagonal strut and the hydrostatic node in the bend. Continuing the bent rebar

approximately $2\ell_d$ beyond the bottom of the corbel, and extending the lapped rebar up to the bottom of the corbel would be safe. The splice should also be enclosed with hoops.

For corbels located at intermediate floor levels, anchorage becomes more complex since boundary forces exist above and below the corbel. This situation is analogously treated in section 3.4 for exterior beam-column joints.

3.2 CHARACTERISTIC BEHAVIOR OF KNEE JOINTS

In framed concrete structures, continuity must be maintained between adjoining members. Corner or knee joints fall in this category. Knee joints must effectively turn moments (or tension/compression force couples) "around a corner" as well as transfer shear forces through the joint and introduce them as axial forces to the adjacent member.

The efficiency of knee joints not only depends on the relative and absolute member sizes, but also on the reinforcement ratio and, most importantly, detailing of the reinforcement. Efficiency is here defined as the ratio (expressed as a percentage) of the failure moment of the joint to the moment capacity of the members entering the joint. The sense of loading significantly affects the internal behavior and efficiency of the joint. Thus, knee joints can be treated in two categories -- opening and closing.

The following sections describe the characteristic behavior as well as the efficiency of such joints from a truss modeling point of view. For the sake of simplicity joints subjected to moments only

will be shown, since consideration of shear and axial forces does not change the fundamental behavior.

3.2.1 OPENING KNEE JOINTS

In opening knee joints, the loads tend to rotate the adjoining members away from each other. Figure 3.2(a) shows an idealized truss model for a joint under pure opening moment for which the flexural compression zone of the members are located at the exterior faces. The interior face longitudinal bars extend completely through the joint core and are anchored by anchor plates on the opposite exterior faces. The diagonal compression strut anchors the flexural steel through bearing into the anchor plates. In an opening joint, the flexural compressive resultant turns around the exterior, convex corner, while the tensile resultant turns around the interior, concave corner. Therefore both corners have a tendency to "pop out" unless they are very carefully tied back.

The truss model of Fig. 3.2(a) can be easily realized in prestressed concrete (post-tensioning). In a non-prestressed opening knee joint, though, anchorage of the tension ties, T_1 and T_2, is usually not achieved through the use of the anchor plates shown in Fig. 3.2(a). The effect of an anchor plate can be reproduced by providing closely spaced, transversely looped tension ties as shown in Fig. 3.2(b). The use of loops, though, is restricted to the extent that the minimum loop diameters must fit within the width of the joint. Furthermore, since the loops are not located at the geometric boundaries of the joint core, due to cover requirements,

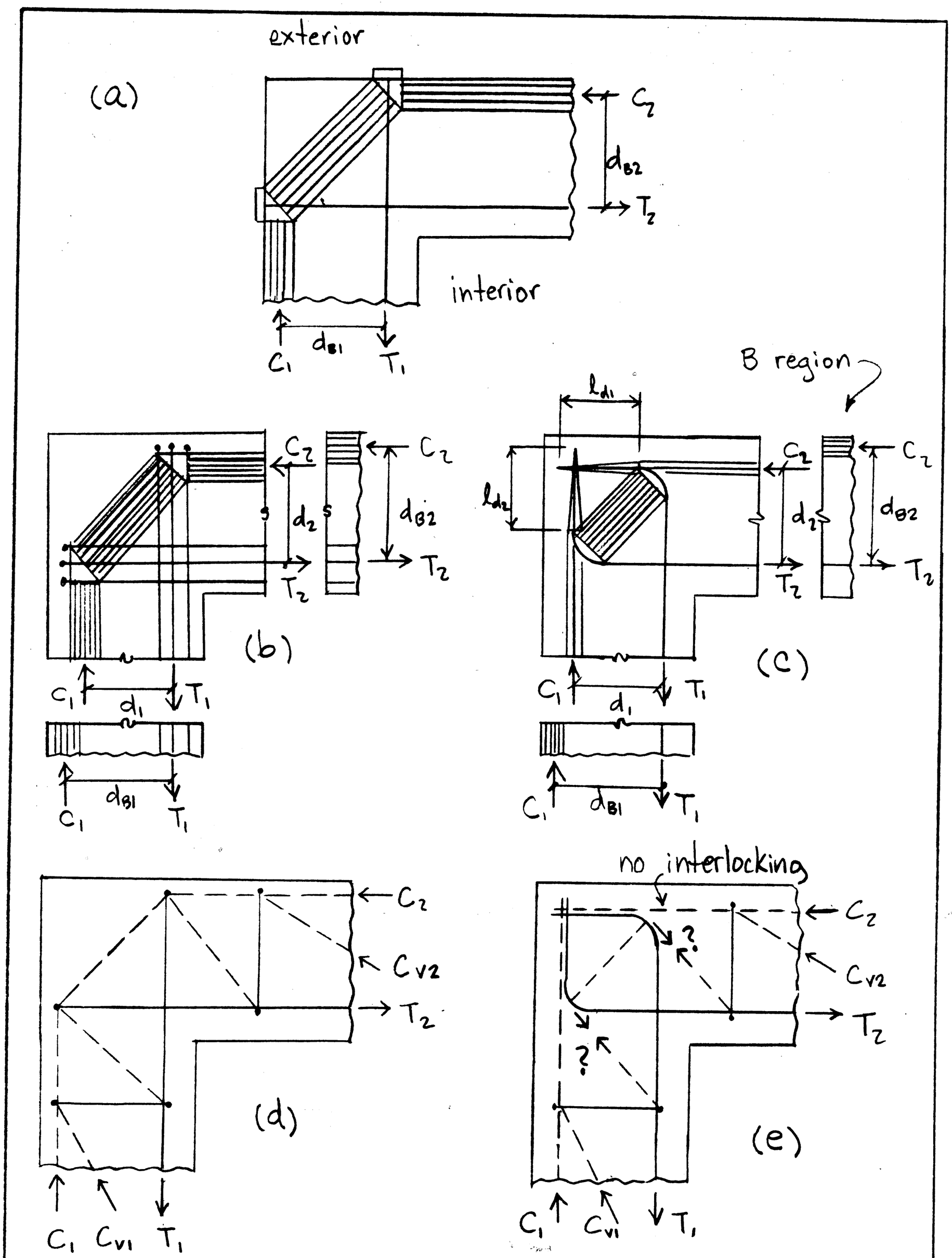

FIGURE 3.2 : Opening knee joints with various loadings

the full flexural capacity of the adjoining members can never be realized (without relying on concrete tensile strength). As shown in Fig. 3.2(b) the lever arms d_1 and d_2 are less than the flexural lever arms of the B regions, d_{B1} and d_{B2}, in the adjoining members.

Figure 3.2(c) shows another detail which anchors the diagonal strut using bends in the plane of the joint. The bends must point away from the adjoining members and the extension beyond the bends must be long enough to develop the rebar. Even if this is the case, the full flexural capacity of the connected members cannot be achieved unless the extensions beyond the bends are as close to the exterior face as the flexural compressive resultants in the B-regions which develop the rebars.

If the members are subjected to shear and axial forces in addition to flexure as shown in Figs. 3.2(d) and (e), it is easily found from equilibrium that the shear force in the horizontal member, for instance, flows directly into the interior face longitudinal reinforcement of the vertical member (and vice versa) without further affecting the force flow in the joint. While the transverse loops in the detail of Fig. 3.2(d) also provide an effective support (anchorage) for diagonal struts due to shear, the bends pointing to the joint core in the detail of Fig. 3.2(e) are not very effective in supporting (anchoring) "incoming" shear struts.

The effectiveness of these details strongly depends on proper anchorage which has two aspects:

(1) correct *location* of the anchorage plate, loops, or bends, at the ends of T_1 and T_2, and

(2) sufficient *strength* of these anchorage details.

As was shown in Fig. 3.2(b), choosing the correct location of the loops directly determines the magnitudes of the flexural lever arms d_1 and d_2, which in turn determines the largest possible moment resistance of the joint core. As long as d_1 or d_2 are less than d_{B1} or d_{B2}, the flexural capacity of the adjoining members can never be reached, unless supplementary flexural reinforcement in the joint is provided. Thus the anchor plates should be located so as to maximize these lever arms, i.e. make the ratios d_1/d_{B1}, d_2/d_{B2} as large as possible.

If the strength of an anchorage detail is a problem because of too high bearing stresses under the loops or bends or insufficient development length, the end anchorage requirements for T_1 and T_2 can be reduced by providing closed hoop stirrups in two directions within the joint core as illustrated in Fig. 3.3. As in the corbel of section 3.1, the stirrups not only confine the concrete and give the joint core the necessary ductility to develop the truss in three dimensions, but also, most importantly, "deconcentrate" the diagonal strut, thus allowing the tensile reinforcement to be developed completely or partially within the joint core. The larger the volume of the stirrups, the more the tensile forces T_1 and T_2 decrease within the joint core. Figures 3.3(a) and (b) show how the forces T_1 and T_2 that must be anchored at the bar ends, and the direct strut force can be reduced or even eliminated by increasing the hoop capacity. In the case of Fig. 3.3(b) the joint core is in a state of pure uniform shear as discussed in section 2.1, Fig. 2.2.

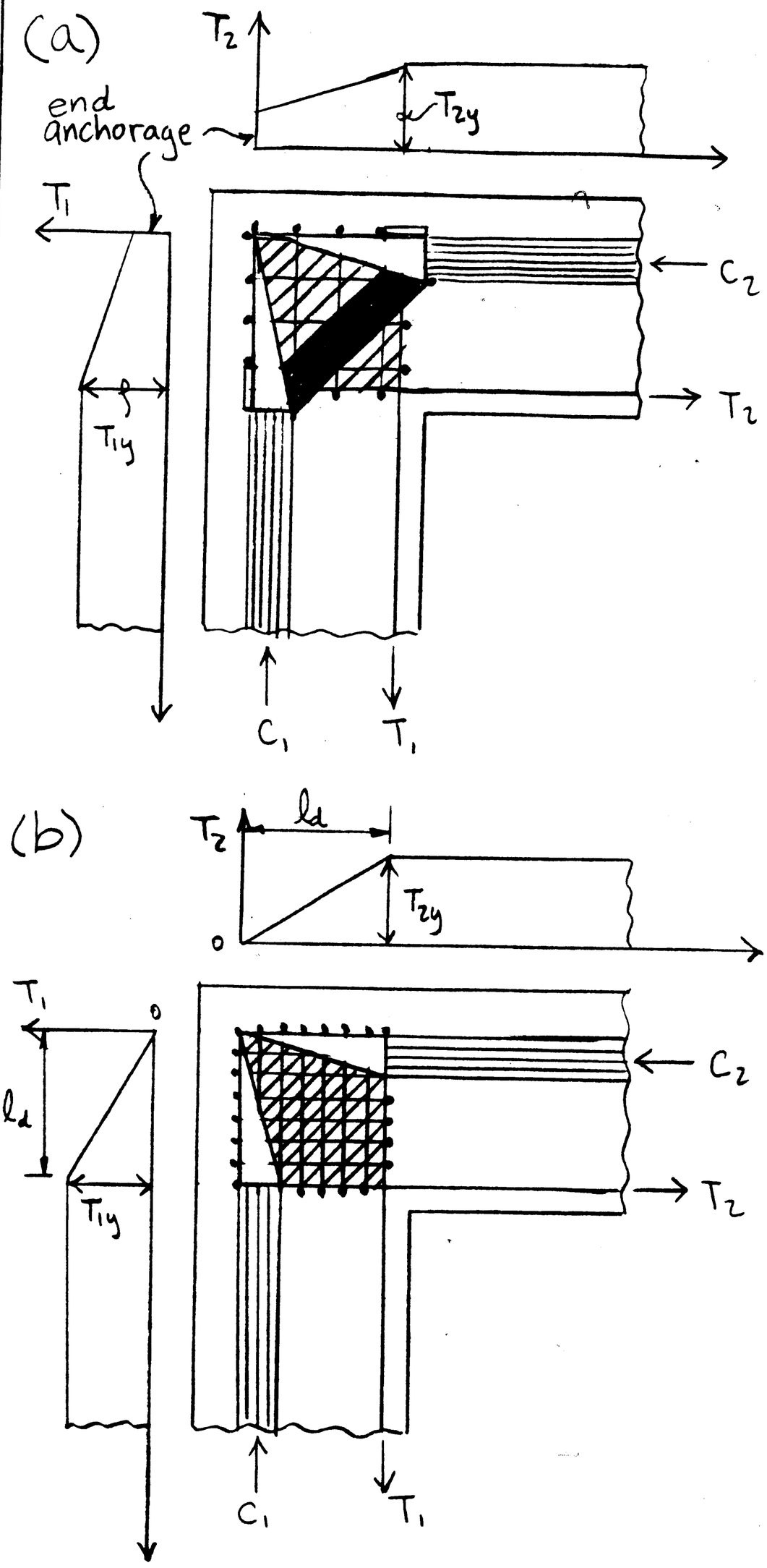

End anchorage requirements for flexural steel

No fictitious anchor plate requirements for flexural steel

FIGURE 3.3: Opening knees with stirrups in 2 directions

While the best detailing scheme calls for closed stirrups in two directions in the joint core, this is not very practical. Rather it is more common to provide stirrups in only one direction as shown in Fig. 3.4. For this scheme, only the tensile force, T_2, can be developed partially within the joint core as previously described. Since the stirrups are in only one direction, fans must always originate from the effective anchor plates, and therefore the end anchorage requirement for T_2 can never be fully eliminated. Although the stirrups reduce the anchorage requirements at the end of bar T_2, the full capacity of T_1 must still be anchored at its end by an effective anchorage plate as shown by Fig. 3.4(a).

The behavior of the joint in Fig. 3.4(a) is analogous to that of the left shear span of a deep beam with stirrups, in which the left support and the (suspended) center load are located at the locations of the compressive and tensile resultants, respectively of the vertical member. The end anchorage and development requirements of T_2 correspond to those of the flexural reinforcement of the deep beam, while T_1 plays the role of hanger or suspender bars.

If the full capacity of T_1 cannot be anchored at the top face and part or all of T_1 is developed over the depth of the joint core, then hanger or suspender bars in the form of additional closed stirrups on either side of T_1 are required. These hanger bars must be capable of transferring T_1 (or that part of T_1 which is not anchored at the top face) back up to the top face as shown in Fig. 3.4(b).

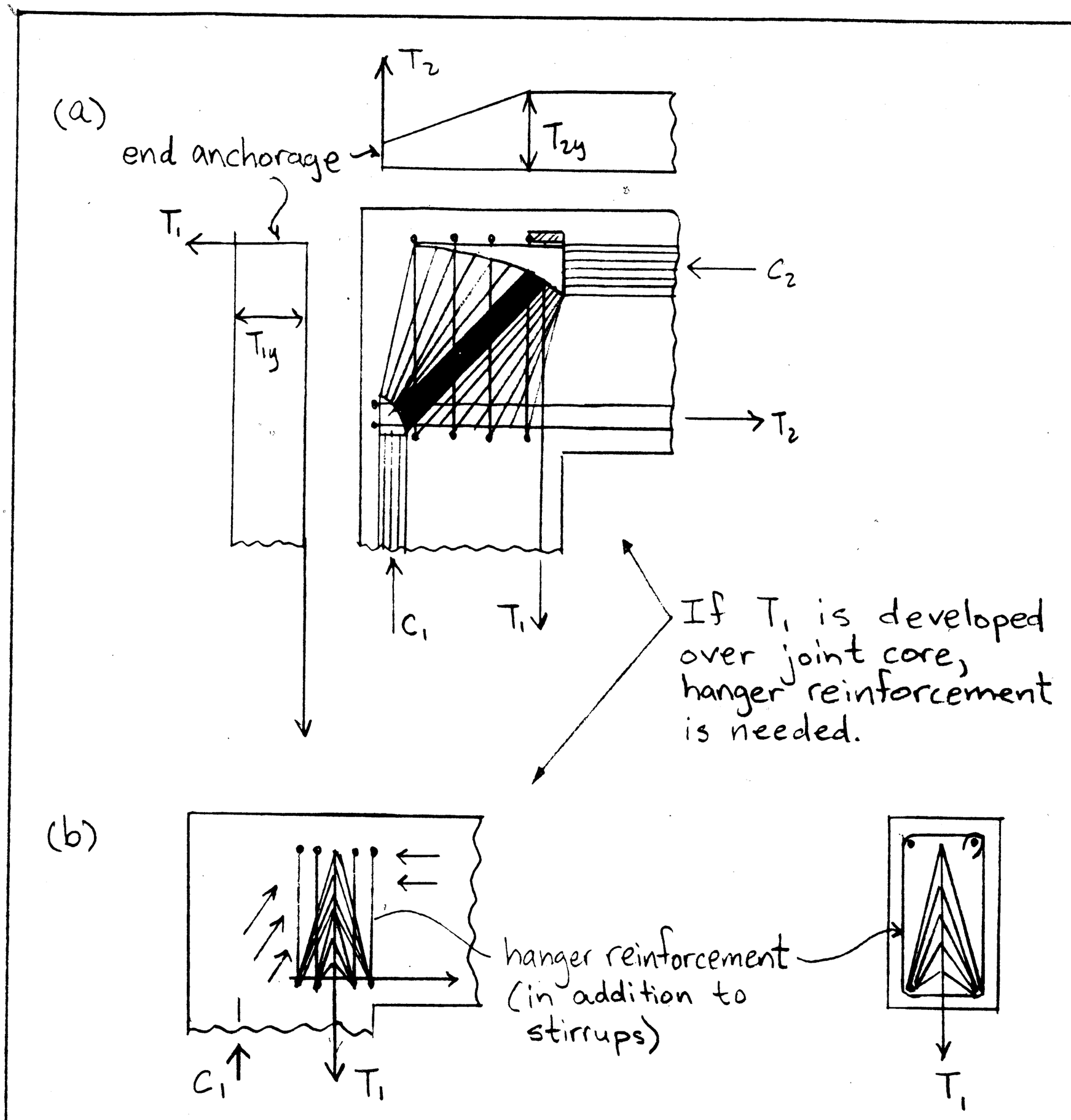

FIGURE 3.4: Opening knee with stirrups in 1 direction

If the concrete dimensions become small, as would be the case for floors framing into walls, minimum bend radii and cover requirements become large relative to the depth of the adjoining members thus making the ratio of $d_{1,2}/d_B$ small (Fig. 3.2(b)).

Furthermore stirrups become impractical or ineffective and the anchorage of the ties T_1 and T_2 becomes more dependent on the local bond strength of those ties. For these reasons opening knee joints with small dimensions can show very poor performance (efficiency) for rather common reinforcement details. Section 3.3 will investigate in more detail opening knee joints with small concrete dimensions and discuss test results.

3.2.2 CLOSING KNEE JOINTS

In closing knee joints, the loads tend to rotate the adjoining members toward each other. Figure 3.5(a) shows an idealized truss model for a joint under pure closing moment for which the flexural compression zone of the members are always located at the interior faces. The exterior face longitudinal bars extend through the joint core and are anchored by anchor plates on the opposite exterior faces. The diagonal compression strut bears into these anchor plates at the far exterior corner of the joint, thus anchoring the tension ties. Note how the reinforcing bars/anchor plates interlock to create a "pocket" for the diagonal strut.

The truss model of Fig. 3.5(a) can be easily realized in prestressed concrete (post-tensioning). In a non-prestressed closing knee joint, though, anchorage of the tension ties, T_1 and T_2, is usually not achieved through the use of the anchor plates shown in Fig. 3.5(a). Instead, the effect of the anchor plates can be reproduced by providing closely spaced looped tension ties as shown in Fig. 3.5(b) or, alternatively, by continuous bent rebars "around

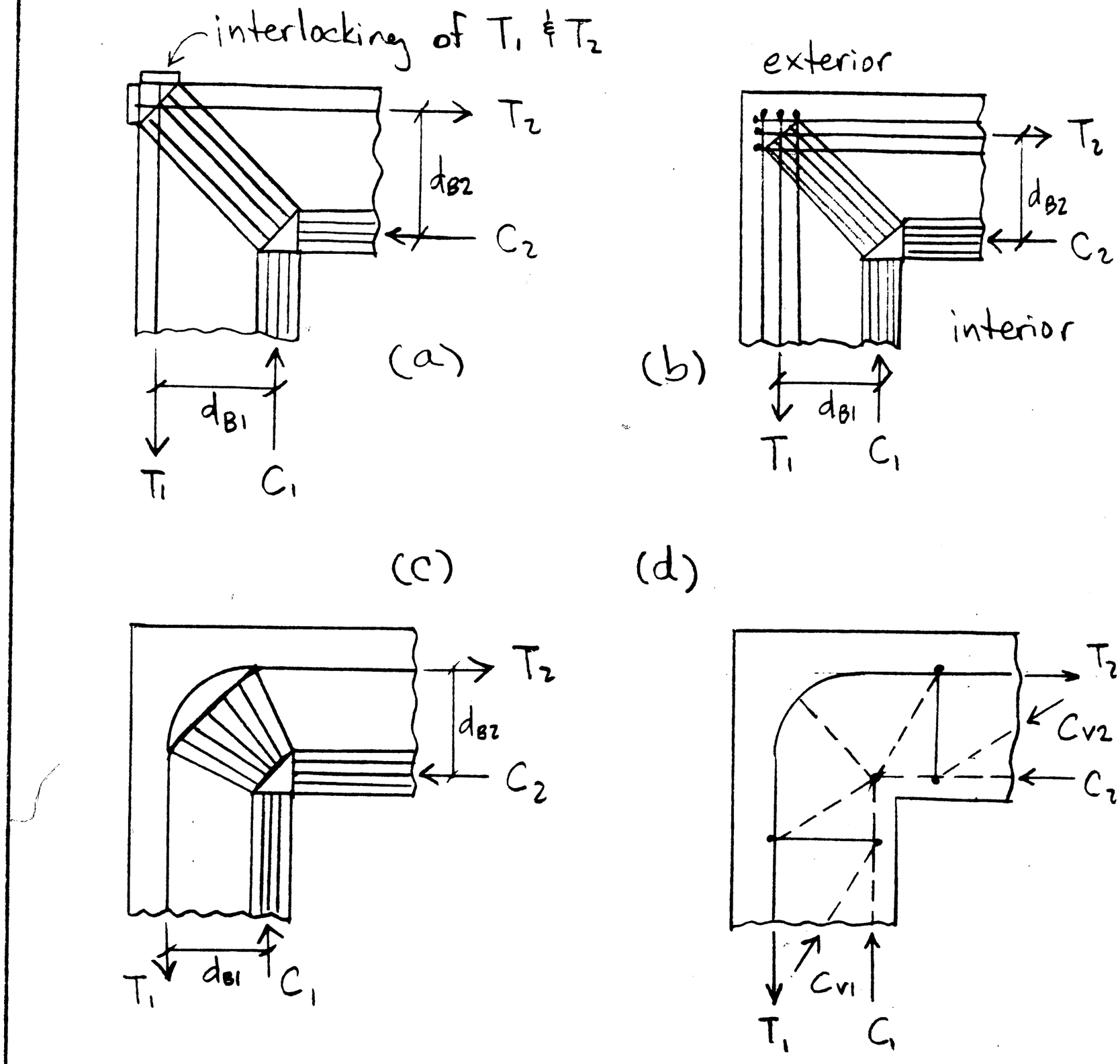

FIGURE 3.5: Closing knee joints with various loadings

the corner" as shown in Fig. 3.5(c). Since the use of loops is restricted to the extent that minimum loop diameters must fit within the width of the joint, and since the bent rebars are much easier to place in construction, the scheme shown in Fig. 3.5(c) is more practical. The bend provides for a pocket to anchor the diagonal

compressive strut. If the members are subjected to shear and axial forces in addition to moments, Fig. 3.5(d), it is easily found from equilibrium that the shear force of the horizontal member, for instance, flows directly into the compressive resultant of the vertical member at the interior corner of the joint (and vice versa) without further effecting the force flow in the joint.

Different from the opening knee joint, the closing knee joint, if properly detailed, can more easily realize the full flexural capacity of the adjoining members. As indicated by Fig. 3.5 the lever arms d_1 and d_2 in the joint core can often be made equal to their corresponding flexural lever arms, d_{B1} and d_{B2} in the B regions of the adjoining members. Since in a closing knee joint the flexural compressive resultant turns around the interior, concave corner and the tensile resultant around the exterior, convex corner, the corners do not tend to "pop out" as in the opening knee joint.

The effectiveness of details is primarily dependent on proper anchorage which has two aspects:

(1) the correct *location* of the anchorage plates, loops, or bends for the tensile ties, T_1 and T_2; the correct diameter of the bend if bent rebars are used,

(2) the sufficient *strength* of these anchorage details.

If anchor plates or transverse loops are used, Fig. 3.5(a) and (b), the reinforcement must interlock such that the plates or loops form a "pocket" for the diagonal compressive strut. In Fig. 3.5(b) at least the outermost loops should be welded together to prevent them from slipping off. If continuous bent bars are used, Fig.

3.5(c), the bend radius must not be larger than the depth of either member, i.e. the bend must be completely within the joint; otherwise the ratio, d_1/d_{B1} or d_2/d_{B2} becomes smaller than one.

If the bearing stresses under loops, bends, or anchorage plates are too high, such that the concrete crushes prior to development of the steel yield strength, then the flexural capacity of the members can never be realized. These bearing stresses can be minimized in three ways:

(1) increase the bend radius, if bent rebars are used, but not beyond the depth of the adjoining members,

(2) closely space the bends so as to form a "sheet" through the width, and

(3) as in the opening knee joint, provide close hoop stirrups, ideally, in two directions within the joint core, see Fig. 3.6.

Once again, the closed stirrups not only confine the concrete and give it its necessary ductility in three dimensions, but also, most importantly, "deconcentrate" the diagonal strut, thus allowing the tensile reinforcement to be developed completely or partially within the joint core. The larger the volume of these stirrups, the more the tensile forces T_1 and T_2 decrease within the joint core. Figures 3.6(a) and (b) show how the magnitude of the forces T_1 and T_2 to be anchored at the bar end and of the direct strut force can be reduced or eliminated.

While the best detailing calls for closed hoop stirrups in two directions in the joint core, such a scheme is not very practical.

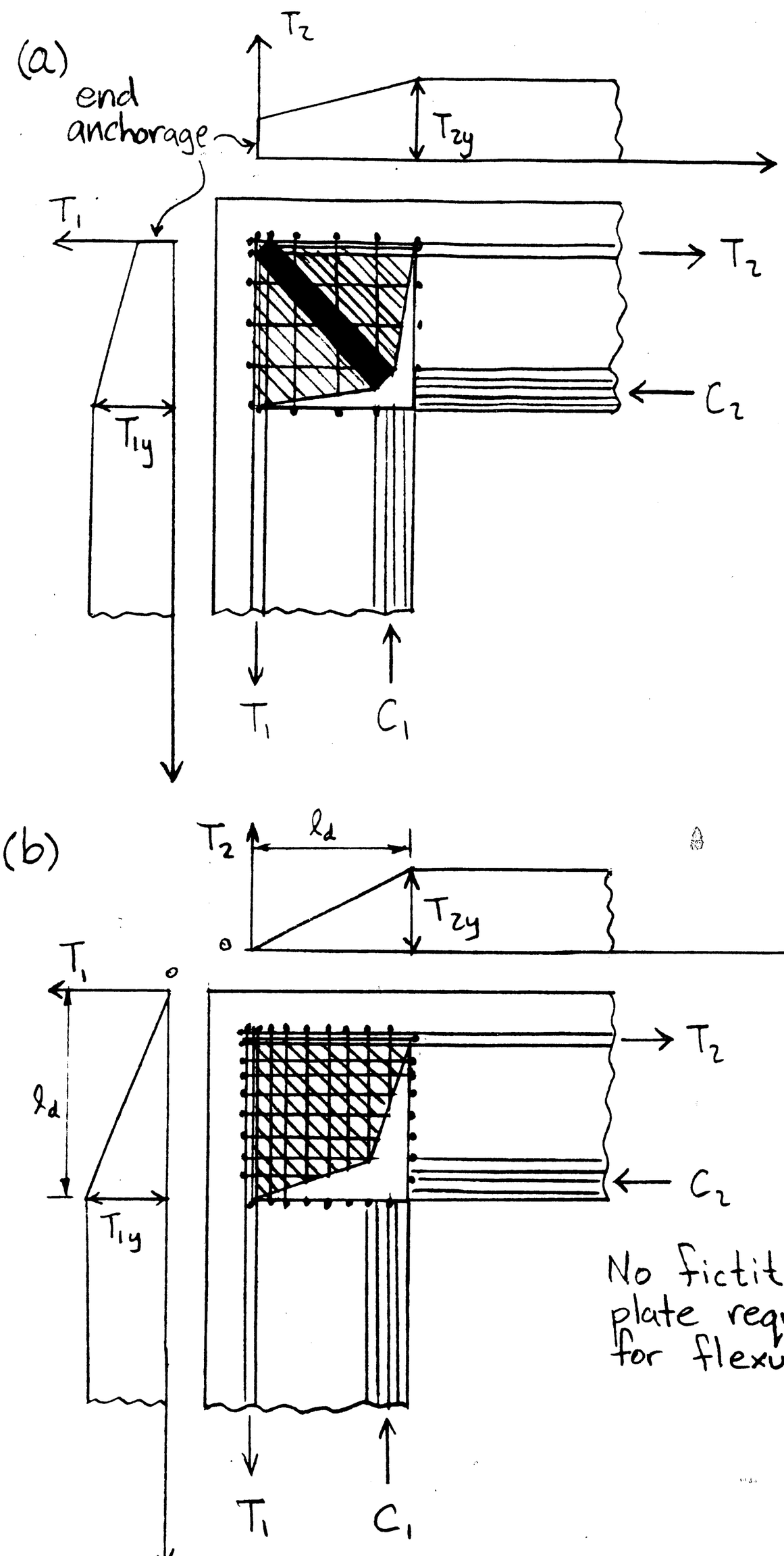

FIGURE 3.6: Closing knees with stirrups in 2 directions

Rather it is more common to provide stirrups in only one direction as shown in Fig. 3.7. For this scheme, only the tensile force, T_2, can

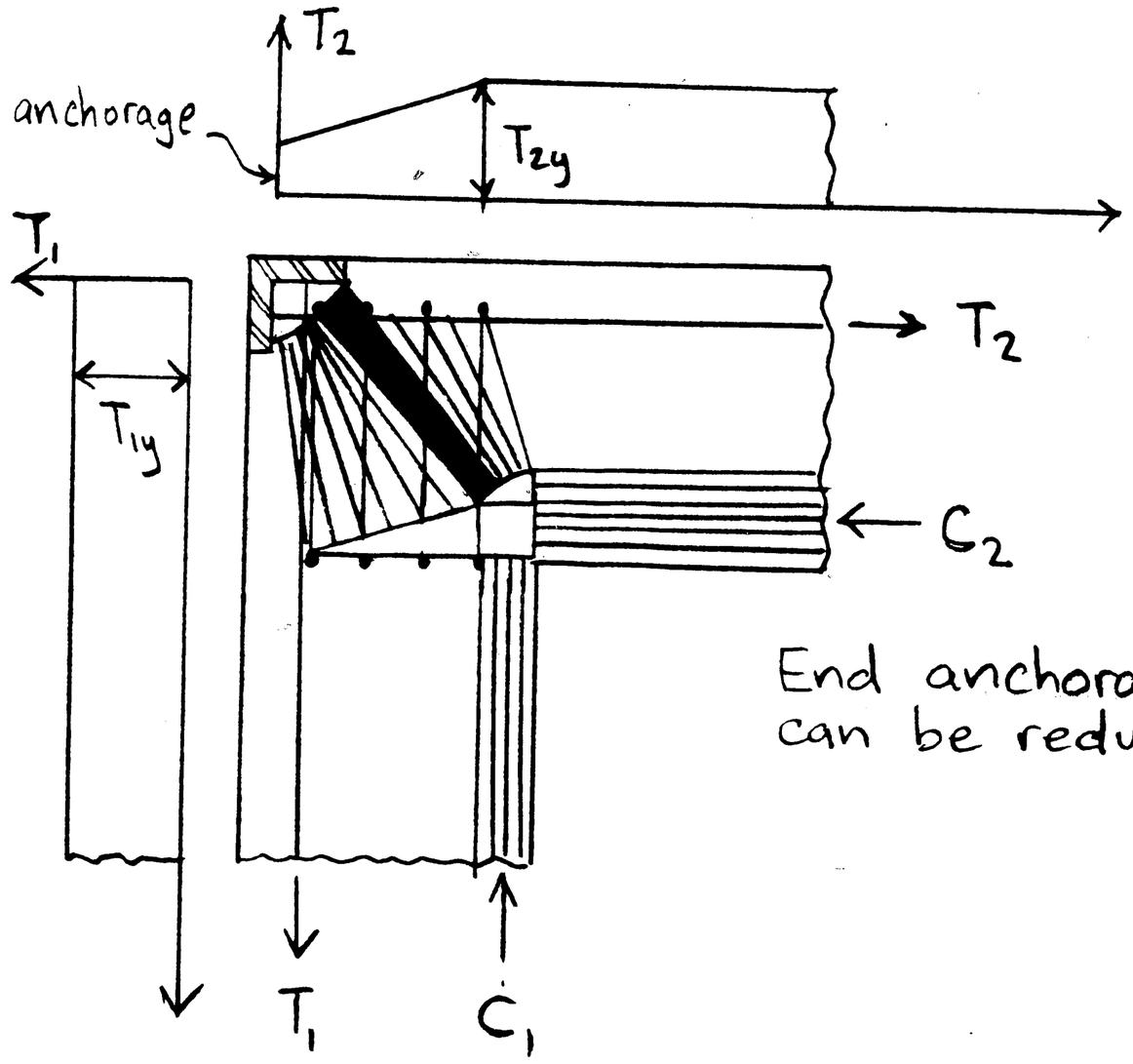

FIGURE 3.7: Closing knee with stirrups in 1 direction

be developed partially within the joint core as previously described. Since the stirrups are in only one direction, fans must originate from both the interior and the exterior corner nodes, and therefore the force T_2, which must be anchored at the bar end, can never be reduced to zero. Although the stirrups reduce the anchorage requirements at the end of tie T_2, the full capacity of tie T_1 must be anchored at the top by an anchor plate or its equivalent, as illustrated in Fig. 3.7.

If the concrete dimensions become small, bend radii and cover requirements become large relative to the depth of the adjoining members and stirrups become impractical or inefficient. Section 3.3 will investigate in more detail the closing knee joint with small concrete dimensions.

3.2.3 ANCHORAGE DEFICIENCIES OF KNEE JOINTS

Based on the truss models presented in section 3.2.1 and 3.2.2, anchorage deficiencies become immediately obvious. Figure 3.8 and 3.9 illustrate these deficiencies for the opening and closing knee joints respectively. In these figures the anchor plates indicate the point where a bar can be considered fully developed.

Consider the opening knee joint of section 3.2.1. It has been shown that the locations of the effective anchor plates directly determine the effective lever arms d_1 and d_2 for the joint core flexural capacity. If either anchor plate is located so as to reduce or eliminate either of these lever arms, then the tensile strength of the concrete is relied upon for transferring moments around the corner. Figures 3.8(a)-(d) exemplify these types of deficiencies. No truss model can be found for cases (a)-(c), while the truss model for case (d) exhibits significantly reduced joint lever arms d_1, d_2 in comparison to the flexural lever arms in the B-regions d_{1B}, d_{2B}. Therefore the joint strength is significantly lower than the flexural capacity of the adjoining members.

A rather common faulty anchorage detail is shown in Fig. 3.8(e). Although the ties are extended through the joint core, they are bent

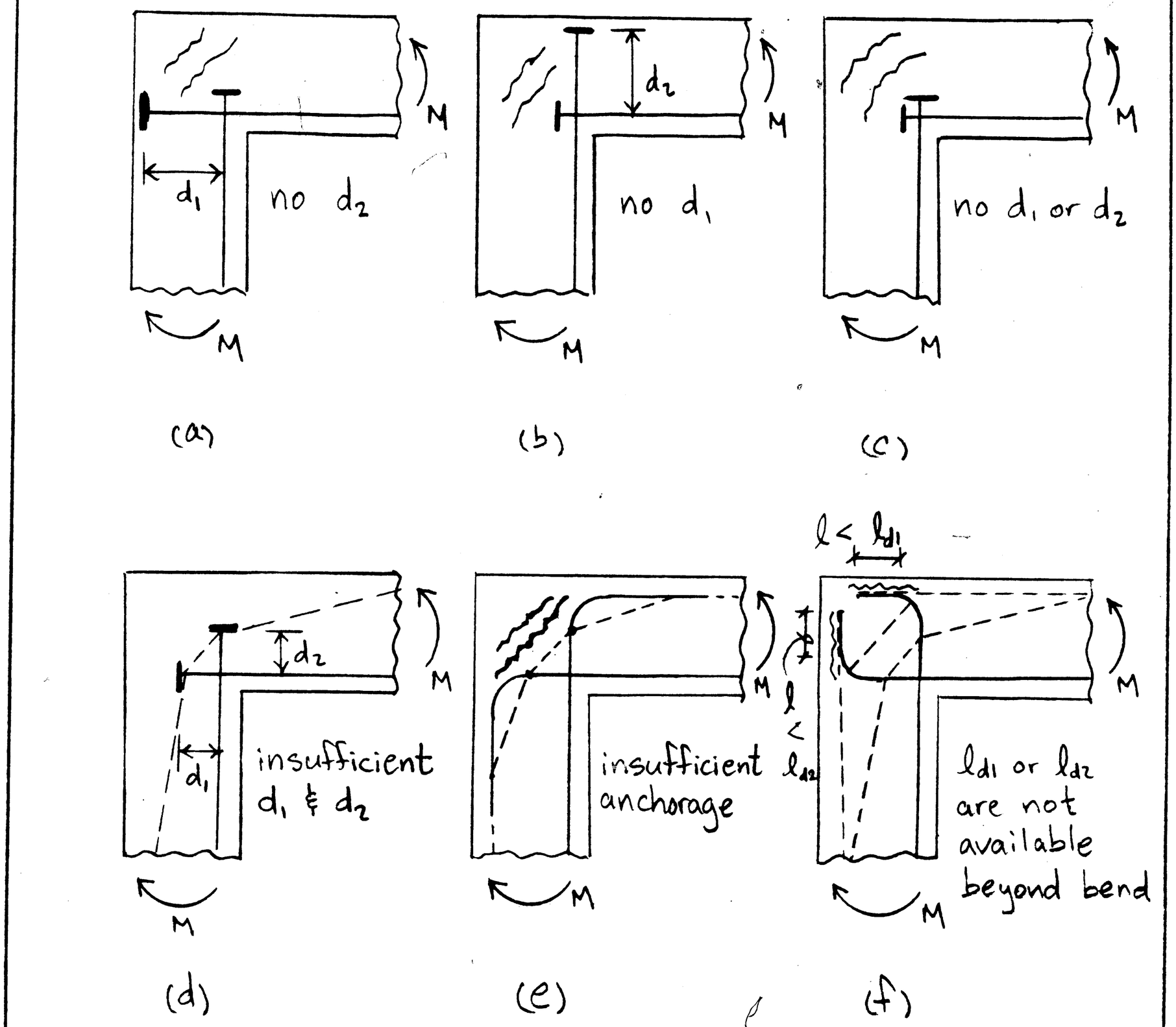

FIGURE 3.8: Opening knee joint deficiencies

in the wrong direction. The diagonal strut has no bend to bear into and simply "slips off" the outer perimeter of the bend. The bars are not anchored close enough to the exterior face and a truss of the type shown in Fig. 3.8(d) develops.

As opposed to the detail of Fig. 3.8(e), the detail in (f) bends the rebars correctly into the joint core. While the diagonal strut can now bear into the bends, the rebars are only anchored close enough to the exterior face if the extension of the rebars beyond the bends and into the joint core are long enough to fully develop its capacity. Otherwise, anchorage failure and/or insufficient lever arms as shown in Fig. 3.8(d) prevent the joint from reaching the adjoining member's capacity.

Figure 3.9 deals with the possible detailing deficiencies for closing knee joints. Closing knee joints can develop a strength close to or equal to the adjoining members capacity if the reinforcement anchorages interlock or the reinforcement is continuous around the corner. Figure 3.9(a) illustrates a detail in which the rebars and their anchor plates do not interlock. No steel whatsoever is crossing the diagonal cross-section through the joint core. Moment transfer through this joint relies solely on the concrete tensile strength. Although this error seems obvious, the deficiency of the detail shown in Fig. 1.1(a) and treated in the introduction is exactly of this type!

Figure 3.9(b) shows an insufficient lap length of the splice between the beam and column reinforcement. Although this deficiency, too, seems obvious, it is not uncommon, because the splice is not interpreted as a splice. Rather, the detail is interpreted as a hooked bar anchorage for the beam reinforcement. Furthermore the lap splice must be enclosed in stirrups to work properly near or in a joint. This is so since the bent bar tends to straighten and push

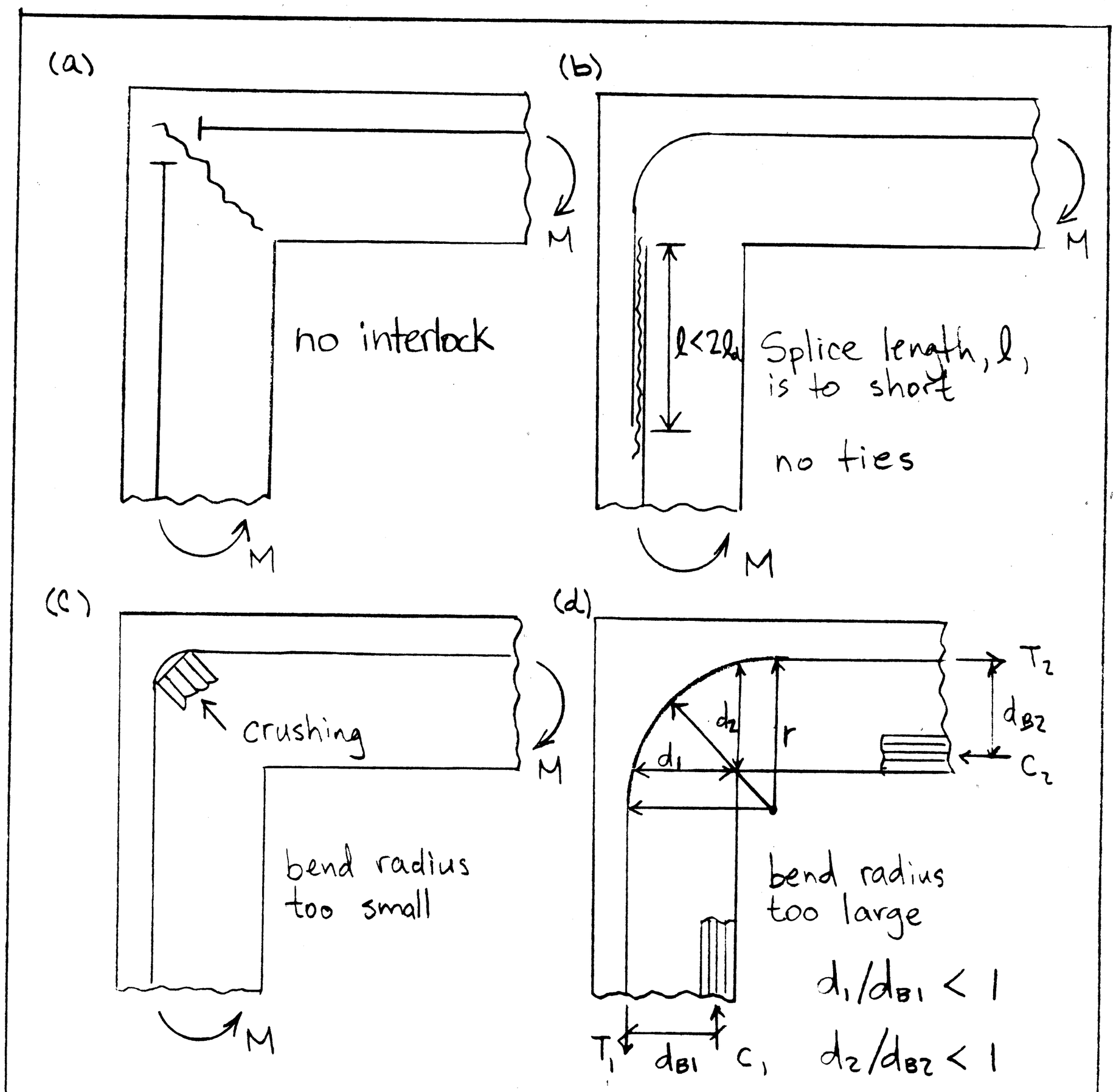

FIGURE 3.9: Closing knee joint deficiencies

off the cover. Finally, Figs. 3.9(c) and (d) illustrate incorrect radii of bent continuous bars. In the detail of Fig. 3.9(c) the bend radius is too small resulting in crushing of the concrete under the

bend before the steel yields. In the detail of Fig. 3.9(d) the bend is not completely within the joint, because its radius is larger than the depth of the adjoining members. As indicated by the figure the joint lever arms d_1, d_2 are smaller than the flexural lever arms d_{1B}, d_{2B} in the B-region and, hence, the joint cannot develop the capacity of the adjoining members. This problem could arise in joints of small dimensions.

3.3 EXPERIMENTAL STUDIES ON KNEE JOINTS

The truss models for opening and closing knee joints presented in the previous section can be used to interpret the experimentally observed behavior of such joints. In this section, various tested knee joint reinforcement details are presented and their performance is qualitatively explained using the insights of chapter 2 and sections 3.1 and 3.2. Many of the experimental results presented here are directly adapted from MacGregor[18] and Park and Paulay[24].

3.3.1 EXPERIMENTAL RESULTS ON OPENING KNEE JOINTS

Past experience with opening knee joints both in practice and in the laboratory shows that, unless they are very carefully detailed, these types of joints usually cannot develop the adjoining member's flexural capacity. Yet these types of joints are commonly found at corners of rigid frames where beams intersect with columns. They are also found at the base of retaining walls. Consequently, many experimental studies on the efficiency of a variety of reinforcing details for such joints have been conducted.

Figure 3.10 (adapted from MacGregor[18]) compares the measured efficiency of some opening knee joint details with large dimensions.

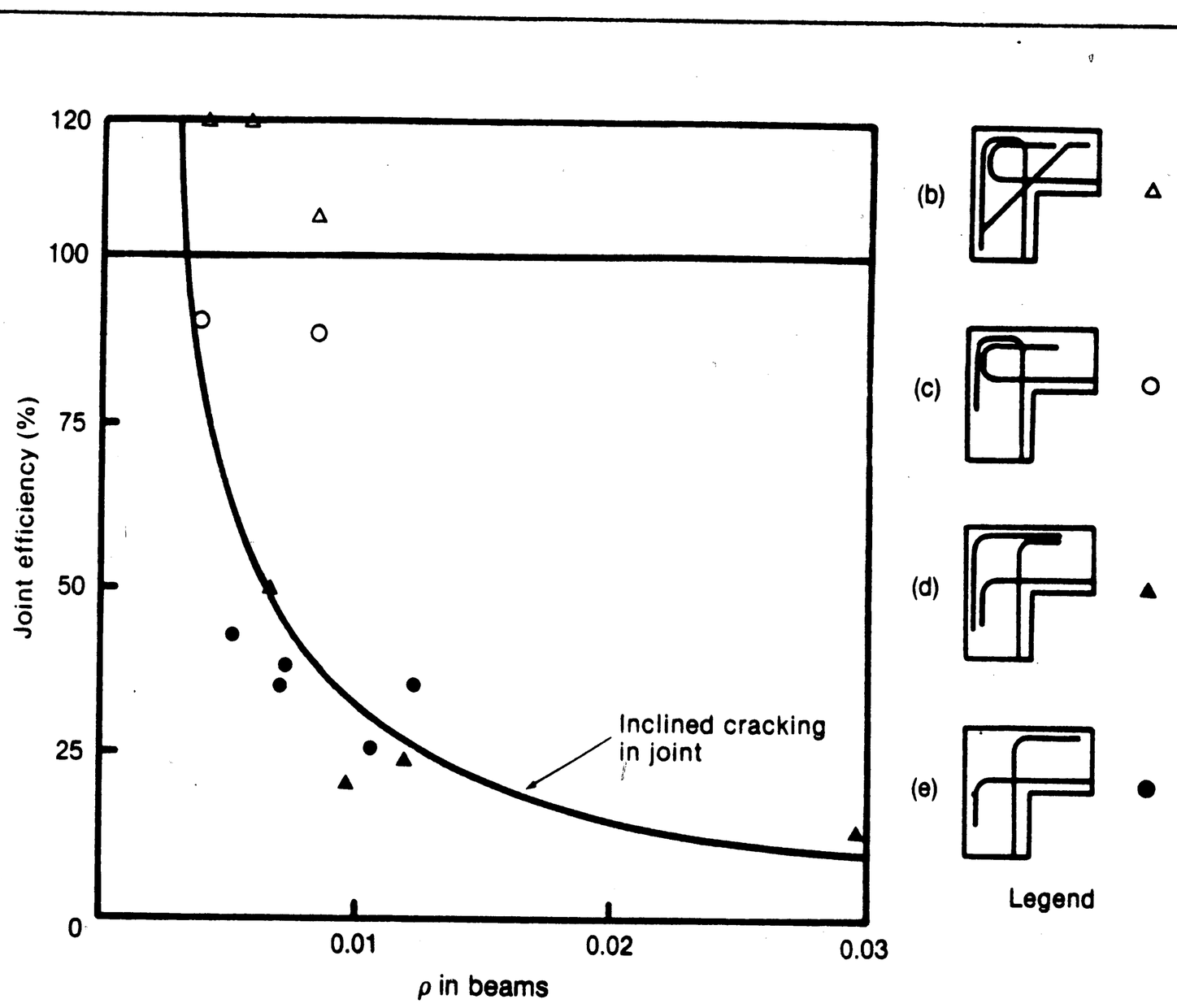

FIGURE 3.10: Experimental results for opening knee joints[18]

Efficiency is defined as the ratio, expressed in percent, of the capacity of the joint to the flexural capacity of the adjoining members. The solid horizontal line in Fig. 3.10 thus represents the flexural capacity of the adjoining members. The solid curved line represents the computed moment at which diagonal cracking is expected to occur for a range of reinforcement ratios, ρ. Most of the data points correspond to ρ between 0.5% and 1.25%.

As Figure 3.10(a) shows, the details of Fig. 3.10(b) and (c) were between 85% and 120% efficient. The high efficiency of the details shown in Fig. 3.10(b) stems from the fact that the tensile ties are bent in the correct direction, namely into the joint core, and sufficiently anchored there. In addition, the inclined bar at the inside corner limits the crack growth at the inside corner making this joint stiffer. Figure 3.11 illustrates the truss model for this detail. The resultant lines of action of the elements are shown so as

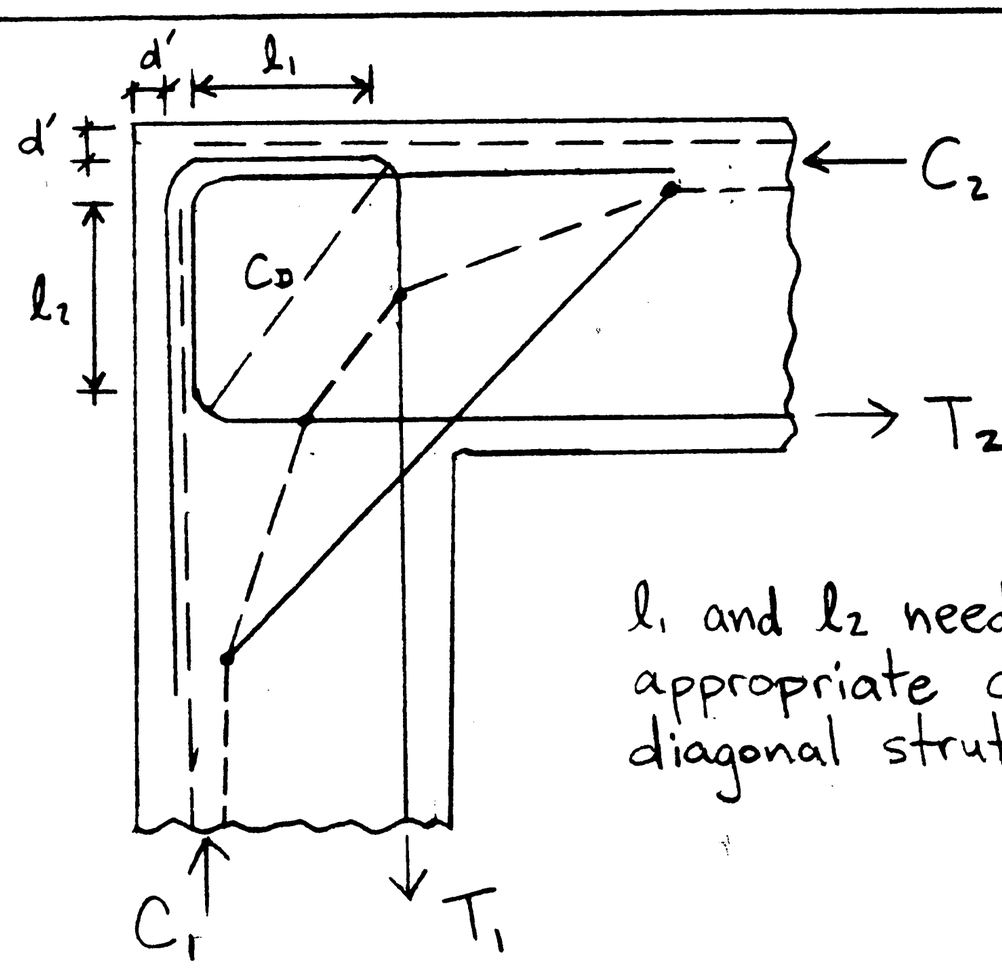

FIGURE 3.11: Opening Knee of Fig. 3.10(b)

not to clutter the load path. This truss model behaves analogously to that shown in Fig. 3.2(c) in that the flexural compression resultants of the joined members are used to develop the extensions beyond the bends. The inclined diagonal rebar enhances the moment capacity by providing, on the one hand, additional steel to resist

flexure in a diagonal section through the joint; on the other hand, its anchorage forces "pull" part of the flexural compressive resultants deeper into the joint core, thus allowing some bar development to take place in front of the first bend.

The efficiency of the detail in Fig. 3.10(c), (85%), is not as high as that of Fig. 3.10(b), (120%), since this scheme does not utilize the inclined rebar at the inside corner. The truss model for detail (c) has been given in Fig. 3.2(c). The full flexural capacity of the joint could not be achieved for this detail for either of two reasons: The full flexural lever arm of the B region, d_B, could not be realized at the joint core, because the extensions of the bars beyond the bends are located deeper than the flexural compressive resultants; this would call for additional steel across the inside corner. Or the bars could not be fully developed "behind" the bends. As explained above and evidenced by the tests, the diagonal bar helps in either case.

The efficiency of the common details of Figs. 3.10(d) and (e) is dishearteningly low (25% to 35%), since (as explained in section 3.2.3, Fig. 3.8(d) and (e)), the bends are in the wrong directions. The diagonal strut has no bend or pocket to bear into, and simply "slips off". Additionally, the bars are not anchored close enough to the compression face. At best, a truss model equivalent to that shown in Fig. 3.8(d) can develop with significantly reduced joint lever arms and, hence, reduced efficiency. Comparison of the measured joint strengths with the predicted moment at diagonal cracking shows that these details essentially failed upon diagonal

cracking. Thus, not only is their strength (efficiency) dishearteningly low, but also, it is controlled by the concrete tensile strength and, hence, their behavior is brittle. These details must be avoided.

Finding an effective but efficient reinforcing scheme for opening knee joints becomes even more of a challenge if the concrete dimensions are small, such as when walls and slabs frame into each other monolithically. The minimum bend radii of the bars and the cover requirements are large compared to the adjoining members' depth. Thus, the bars are not fully anchored close enough to the exterior face and the lever arms d_1 and d_2 of the joint core are significantly reduced in comparison to the flexural lever arms, d_{B1} and d_{B2}, in the B regions. Stirrups within the joint are usually not possible. Tests on several different details have been performed by Swann[26]. Figures 3.12(a) - (h), adapted from Park and Paulay[24], show the tested connections, and indicate the strength of each as a percentage of the moment strength of the connected members. In Fig. 3.12, cases (a) and (b) illustrate extremely poor detailing; only approximately one tenth of the member strength could be developed in the connection. Case (g) represents the strongest of the tested connections, and it could only sustain approximately 2/3 of the member capacity.

In light of the truss models presented in section 3.2 it becomes apparent why these connections behaved the way they did. Obviously, in Fig. 3.12(a) the compressive resultant could only be brought around the corner through the aid of the concrete tensile strength.

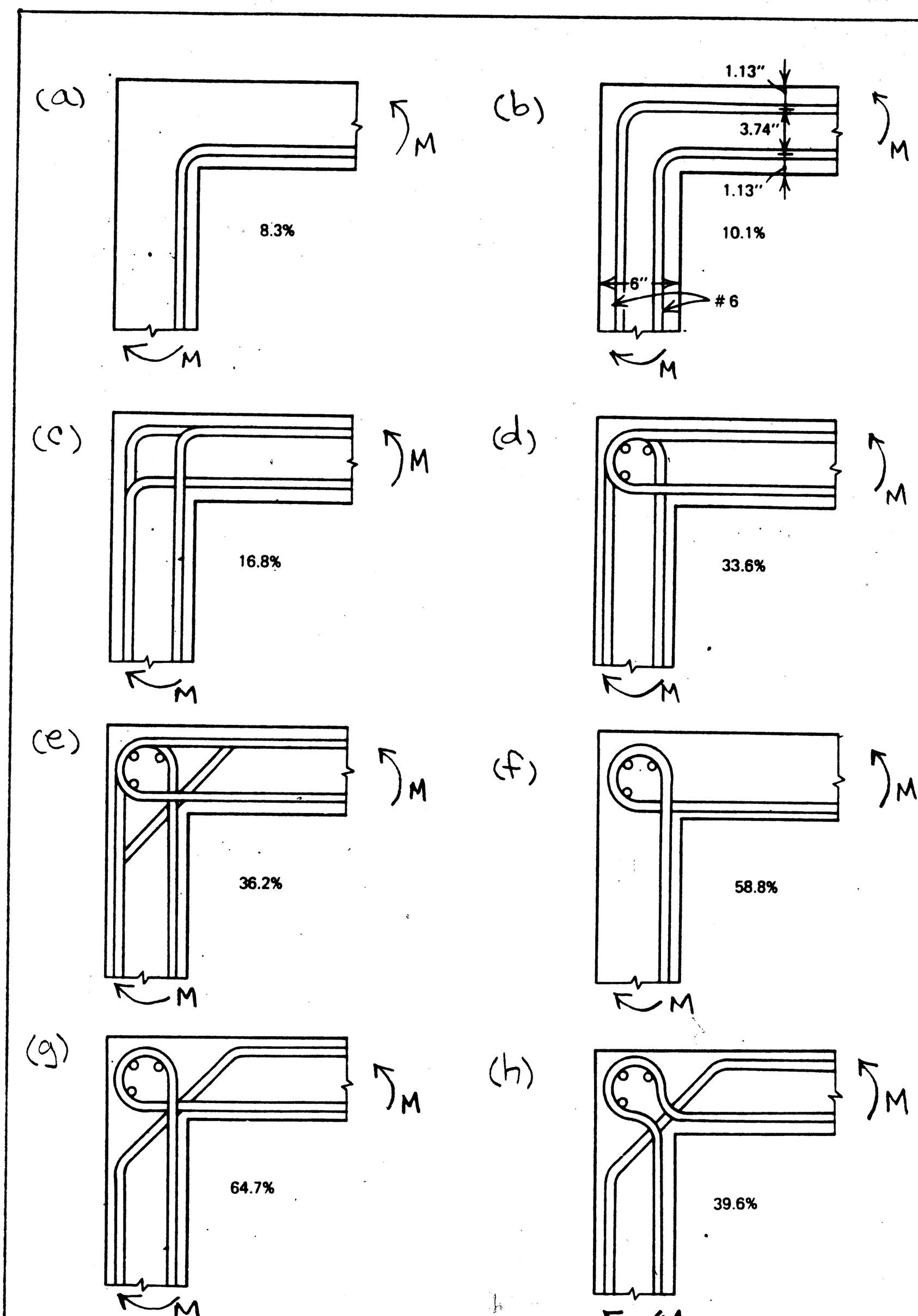

FIGURE 3.12: Opening knee joint details of small dimensions (ref. 24)

There is no diagonal tensile resistance at the inside corner equilibrating the hoop forces of the bent rebar except for the concrete tensile strength. Thus, the bent rebar simply "pops out" of the inner corner. This detail solely relies on the concrete tensile strength to turn the moment (force couple) around the corner and could only sustain 8.3% of the member capacity. The same can be said for case (b). The exterior face bent rebar serves no purpose from a truss model perspective and, hence, brings no significant increase in efficiency (10.1%).

The dishearteningly poor performance of the commonly used detailing scheme of case (c) comes as no surprise even though the interior face bent rebars are overlapped, thus eliminating the inner corner "pop-out" failure mode. The joint diagonal strut cannot bear against the inside of the bends, since they face "away" from the strut, and therefore the interior face steel is not anchored far enough out. The exterior face steel helps nothing with this problem and behavior is analogous to the truss model of Fig. 3.8(d). Thus, an efficiency of only 16.8% was achieved.

The detailing scheme of case (d) uses hooped flexural bars lapped over each other. The somewhat larger but still low efficiency (33.6%) of the detail in Fig. 3.12(d) may come as a surprise, since the bends are pointing in the correct direction and it shows some similarity with the detail in Fig. 3.10(c), which achieved ~ 85%. It must be realized, though, that the detail in Fig. 3.10(c) primarily relies on the bars being developed over the straight extension beyond the bend as indicated in Fig. 3.2(c). While this is possible for a

normal size joint, the detail for the joint with small dimensions, Fig. 3.12(d), does not provide sufficient development length within the joint. For this reason and since the looped flexural bars are not welded to each other, they will tend to rotate with respect to each other. This rotation can only be resisted by the very short splice length over which the loops are lapped. This resistance is low, and so is the strength of the joint. Case (e) is exactly analogous to case (d); the additional diagonal reinforcement obviously helped little in compensating for the basic deficiency of this detail.

Cases (f) and (g) performed the best because they allowed truss action of the type shown in Fig. 3.13(a) to develop. The loop, together with the transverse bars, effectively plays the role of the diagonal tension member and angle in Fig. 3.13(a). In its tension

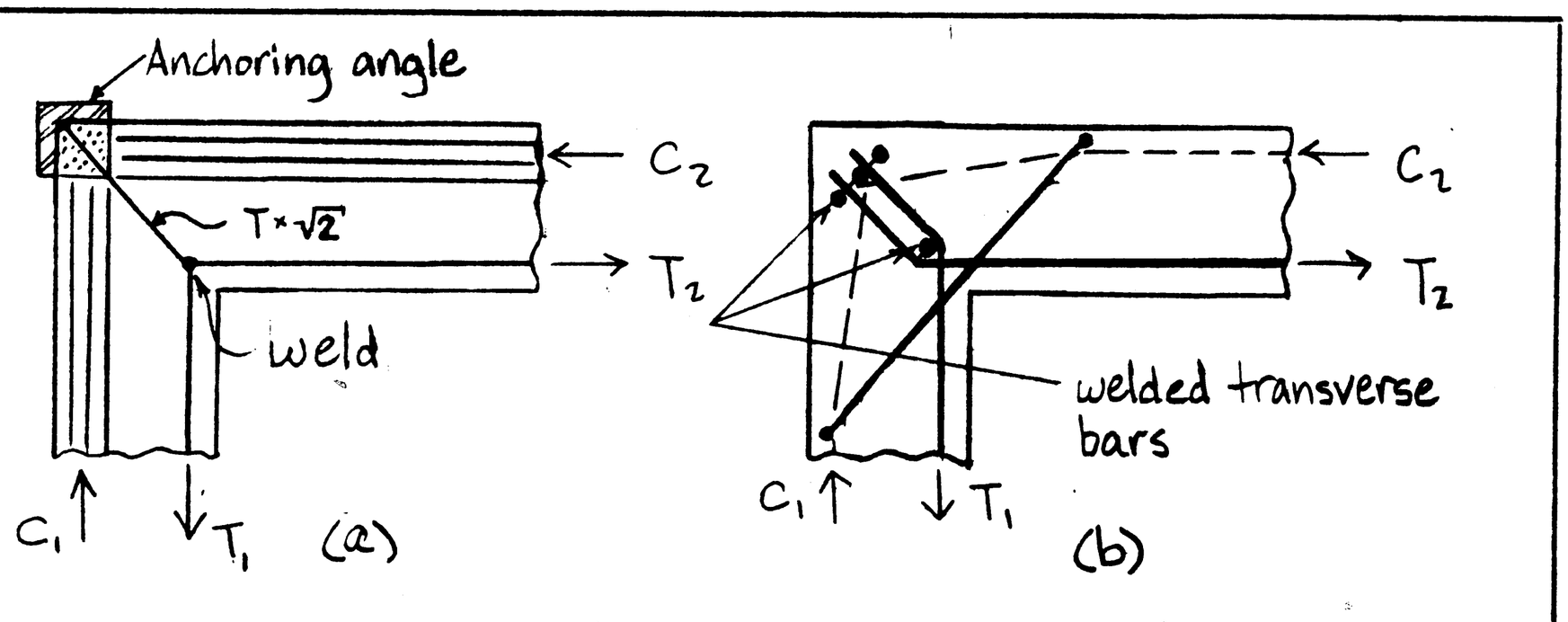

FIGURE 3.13: Alternate opening knee joint of small dimensions

member function, the loop is stiffened by a strut forming inside the loop and normal to the direction of tension. The transverse bars inside the loop help to control the bearing stresses under the bends as well as transverse splitting. The diagonal reinforcement at the inside corner of case (g) adds flexural reinforcement at that corner and its anchor forces pull the flexural compressive resultants into the joint towards the loop. However, its anchorage is not very effective and, thus, neither is the diagonal bar itself. In spite of performing best, these joints were only, at best, 2/3 as strong as the connecting members. This can be attributed to the fact that the loop, differently from the angle in the idealized truss model of Fig. 3.13(a), is located within the joint due to cover requirements. For the convex corner in compression, any concrete outside the loop is ineffective and the flexural lever arm in the joint is significantly reduced in comparison with that in the B-regions for this joint with small dimensions.

The poor performance of case (h) is analogous to case (e) in that the loop can simply open up and allow the members to rotate. On the other hand, if the detail is to function like the truss model shown in Fig. 3.13(a), the weld indicated there is necessary. The diagonal bar cannot compensate for the missing weld or other mechanical connection, because it is not effectively anchored at its ends. Note that the tension at the interior corner and the compressive resultants of the adjoining members tend to pull/push the bar in the same direction.

Utilizing the behavioral concepts learned from cases (f) though (h), the idealized truss model shown in Fig. 3.13(a) and referred to previously can be developed. The struts entering the joint core from the members can interlock with the fictitious anchor plate located at the outer corner. Equilibrium requires that the diagonal steel resists with a tensile force of $\sqrt{2}T$, the outward thrusts of the compressive struts on the anchor plate. At the inner corner, a mechanical, interlocking T-T-T node can be developed. Experimental results show that a rigid mechanical T-T-T node connection is required to permit this truss to form. For example, bending the flexural member reinforcement around the interior corner similarly to Fig. 3.12(a) and realizing the diagonal bar with hoops interlocking with the bend is not sufficient, since the flexural reinforcement "pops-out" of the corner before the diagonal stirrup develops sufficient tension. A possible reinforcing detail utilizing this truss model is shown in Fig. 3.13(b). The welded transverse bars at the outer corner act as the anchor plate. The overlapping flexural bars along the inside face must be carefully drawn on the plans indicating that the transverse bar on the inside corner fits between the bends as shown in Fig. 3.13(b). It must be welded there. If this bar is misplaced, the connection may perform extremely poorly, similarly to the detail of Fig. 3.12(h), since a crack would open up at the inside corner. An additional diagonal rebar can also be placed through the inside corner, giving the connection additional strength and crack control.

This detail will not work for closing moments without modifications.

3.3.2 EXPERIMENTAL RESULTS ON CLOSING KNEE JOINTS

Closing knee joints are considerably less critical than opening knee joints. Tests on several detailing schemes have been conducted. Details which utilized the continuous bent rebar along the outer face (as shown in Fig. 3.5(c)) are reported to have efficiencies between 80% and 100%. As mentioned in section 3.2.2, high concrete stresses on the inside of the bends create problems. Increasing the bend diameter has been shown to increase the efficiency.

For closing knee joints with small concrete dimensions, the reinforcement scheme shown in Fig. 3.14(a) worked very well, (Park and Paulay [24] Swann [26]). The truss model for this scheme, Fig. 3.14(b), shows that the steel diagonal stiffeners transfer most of the diagonal compression force completely into the exterior face tension ties through welds. Since the "steel strut" is welded to the ties, anchorage is very rigid. On the other hand, the reinforcing scheme shown in Fig. 3.14(c) performed poorly in tests. This detail, which uses looped flexural bars lapped over each other in the plane of the joint is exactly the same as case (d) in Fig. 3.12. Since the tension reinforcement around the exterior corner is not continuous, as it should be, this joint detail relies on a corner lap splice to function according to the truss model of Fig. 3.5(c). Obviously, the length of the lap splice of the looped bars (1/4 circle!) is much too short to develop their yield capacity, apart from the fact that a

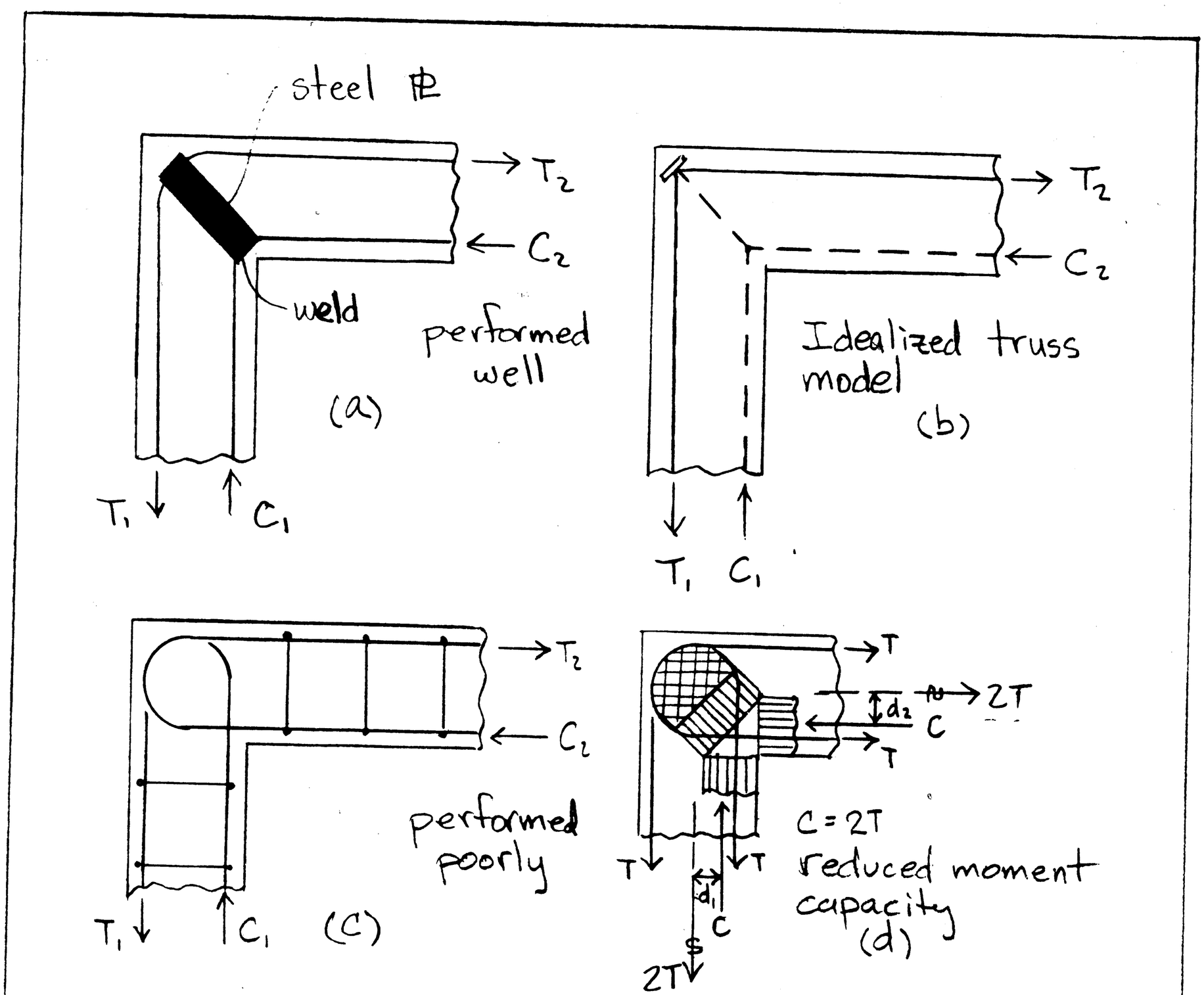

FIGURE 3.14: Details which performed well and poorly

"bent lap splice" is unlikely to work like a straight one and that it lies in an area of maximum moment. On the other hand, the joint detail cannot function according to the truss model of Fig. 3.5(a), since the bar anchorages do not interlock such that a compression node can develop. In essence, the deficiency of this detail is of the type shown in Fig. 3.9(a).

A truss model can be drawn for this detail, if it is assumed that both the tension and compression reinforcement yield in tension, Fig. 3.14(d). This significantly reduces the flexural lever arm, resulting in a low efficiency. More importantly, while the phenomenon of compression bars in tension has been experimentally observed in beam-column joints, the inelastic deformations required to achieve this "unnatural" stress state, likely exceed the capacity of this poorly confined joint.

Reinforced concrete joint design is still mostly empirical or at best, semi-rational. Joint and connection design is generally poorly treated in textbooks, if at all, and detailing manuals still contain many faulty details. This treatment shows that truss models represent a rational and simple tool to assess joint performance. All of the details that performed well, permit, with minor modifications, one of the basic, simple truss models to develop. All of the poorly performing joint details could be weeded out, because a truss cannot even form. It has become quite apparent that the basic problem in joint design is sufficient anchorage in the *correct location* and *within* the joint. Specifically in the case of opening knee joints it is worthwhile to note that any concrete lying outside straight lines connecting the bar anchorage points, is useless, since it simply spalls off.

3.4 CHARACTERISTIC BEHAVIOR OF BEAM-COLUMN JOINTS

Exterior and interior beam-column joints can be perceived as the superposition of knee joints. Such joints are usually found within

rigid frame structures. Their behavior is somewhat more complex than the knee joints', since B/D region boundary conditions must be observed at additional surfaces. But as will be shown, the primary problems arise from difficulties with anchoring the elements.

3.4.1 EXTERIOR BEAM-COLUMN JOINTS

Exterior beam-column joints are nothing more than the superposition of an opening plus a closing knee joint as shown in Fig. 3.15(a). The idealized truss model (without stirrups) for the beam-column joint is shown in Fig. 3.15(b). The beam flexural reinforcement is carried through the joint core and anchored at the opposite face with an anchor plate, such that the tension in the reinforcement is introduced as compression through the anchor plate onto the biaxially stressed node. On the orthogonal face of the node, the tension reinforcement parallel to the exterior face of the column introduces compression onto the biaxially stressed node through an anchor plate just "behind" the node. In addition, the flexural compression zone at the upper exterior column face also bears on that face of the node. Equilibrium of the node is maintained by the interlocking action of the diagonal direct strut bearing onto the hypotenuse of the node. A similar situation occurs at the node of the lower inside corner of the joint.

In practice, the longitudinal steel in the columns is usually not terminated at the boundaries of the joint core nor fixed to an anchor plate as shown in Fig. 3.15(b), but rather these rebars are continuous throughout the height of the column. The exterior face

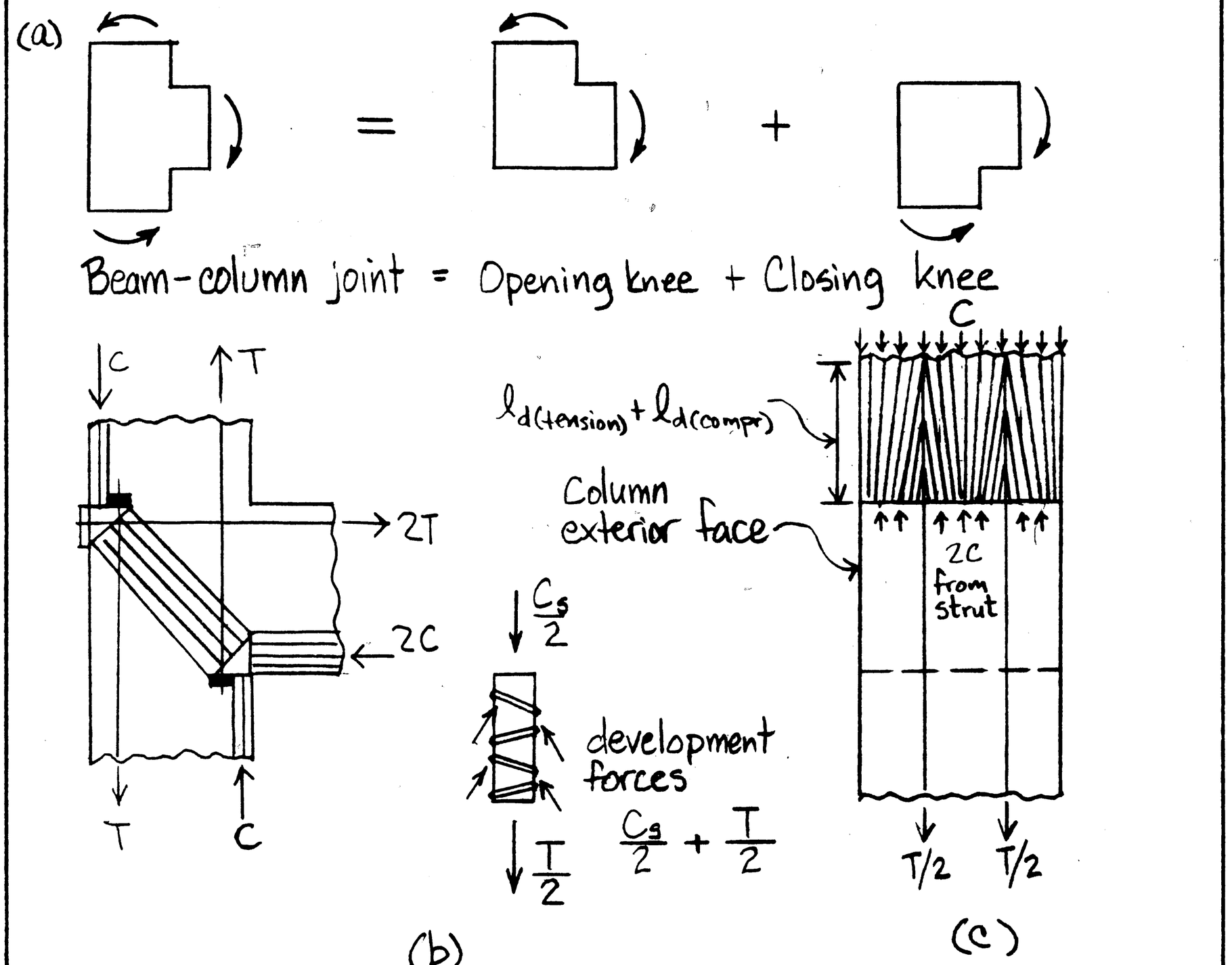

FIGURE 3.15: Exterior beam - column joint

rebars are pushed in compression above the joint core and pulled in tension below the joint core and vice versa for the interior face rebars. If the joint core is diagonally cracked and has no stirrup reinforcement, the joint shear can only be transferred in direct strut action as shown by the truss model in Fig. 3.15(b), the equilibrium of which requires that the tensile forces of the column reinforcement be introduced into the nodes from "behind." Since

joint equilibrium does not permit the column bars to be developed inside the joint, they must be developed outside the joint in the compression zone of the column behind the node. Although this at first seems contradictory, since this demands that the rebar is in tension over ℓ_d in the compression zone, it is quite possible as shown by the transverse truss model in Fig. 3.15(c). The compression zone from the loading fits in between the compression zones due to development of the bars. Indeed, in experiments on interior beam-column joints, tensile strains in the beam rebar in the compression zone just outside the joint core have been observed.

As shown by the inset of Fig. 3.15(b), the bar must be developed both in tension and compression and thus the total development length is quite long. It is important to realize that development of the column bars outside the joint means that the joint can never develop the full flexural strength of the column. Or more correctly, the joint reduces the flexural strength of the column in the zone of development. The joint D-region extends to the end of the development length. Just above and below the joint in the column, the compression reinforcement is in tension. The resultant of both the tension and compression reinforcement at the joint column interfaces is at mid-depth of the column. The compression zone depth "a" is increased and the moment arm at the interface is reduced. Thus a reduced flexural capacity results. This phenomena is identical to that shown for the closing knee joint of Fig. 3.14(d). As previously noted, without stirrups in the joint core, this bar *cannot* be developed inside the joint once it is diagonally cracked,

because joint equilibrium requires that the anchorage forces of the column rebars meet the diagonal strut at the upper left and lower right corner nodes of the joint as shown in Fig. 3.15(b). Therefore, one way to avoid the undesirable bar development outside the joint core and effectively move it completely or at least partially into the joint core, is to provide closely spaced horizontal hoops inside the joint core. This allows that part of the direct diagonal strut, which is associated with the darkened anchor plate loads in Fig. 3.15(b), to widen and distribute itself into two fans throughout the joint core over the height of the hoops as shown in Fig. 3.16(a).

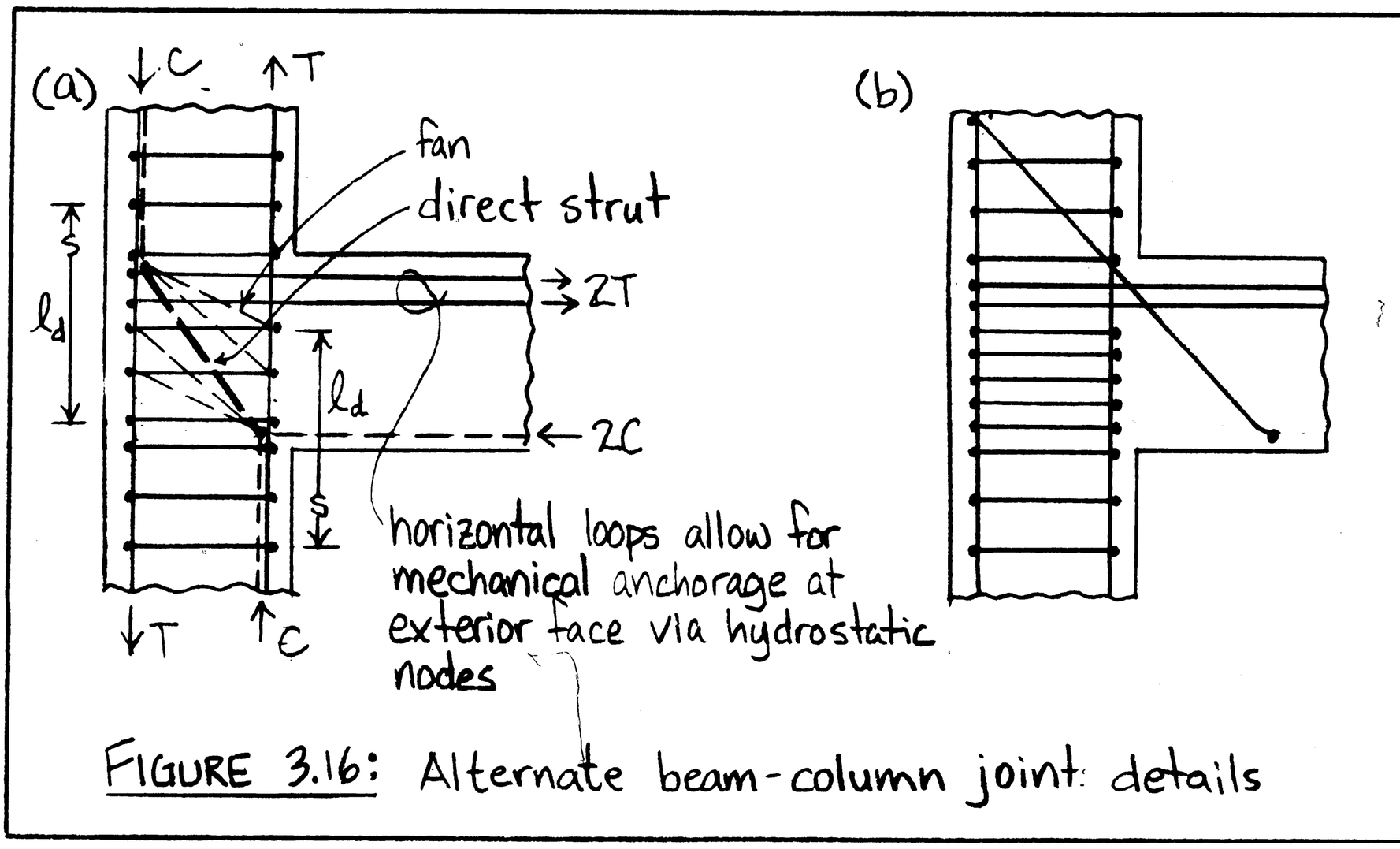

FIGURE 3.16: Alternate beam-column joint details

The hoops, which wrap around the longitudinal bars, form interlocking surfaces in which the fans can bear, thus developing the longitudinal

bar inside the core. By increasing the number of hoops the development length outside the core is reduced.

The bar force that can be developed inside the joint can be easily computed from equilibrium and strength. The hoop capacity determines the horizontal component of the fan resultants. The inclination of the fan resultants follows from the geometry of the truss model. Knowing its inclination, the vertical component of the fan resultants can be computed. This is the bar force that can be developed inside the joint, provided it does not exceed the value calculated from the embedment length of the bar inside the joint and applicable bond strength or development length. Otherwise the latter controls. This example shows that bar anchorage and development is not simply a matter of observing development lengths. Truss models allow for a check whether the forces needed to develop a bar, can actually be supplied in the correct location and magnitude by other elements of the structural component considering their strength and geometry. Again, without the hoops, the longitudinal reinforcement in the column must be developed outside the joint core after it has cracked. The horizontal hoops further provide concrete confinement as well as ductility for the joint core.

A suggested reinforcing detail for this type of joint is shown in Fig. 3.16(b). Note that this detail still leaves the problem that the full capacity of the beam's top flexural reinforcement must be anchored at the exterior face. Therefore, horizontal loops enclosing the exterior column reinforcement are shown here, which is difficult to achieve for geometrical reasons. This anchorage force could only

be reduced by providing also vertical closed hoop stirrups in the joint core. Alternatively, additional closed hoop horizontal stirrups near the beam's flexural reinforcement in the core can act as hanger bars for the tensile force of the beam's flexural reinforcement. These situations were analogously treated in section 3.2.1 for opening knee joints. But since these solutions are often impractical, the joints such as that shown in Fig. 3.17(a) are used commonly. However, exterior beam-column joints only perform well

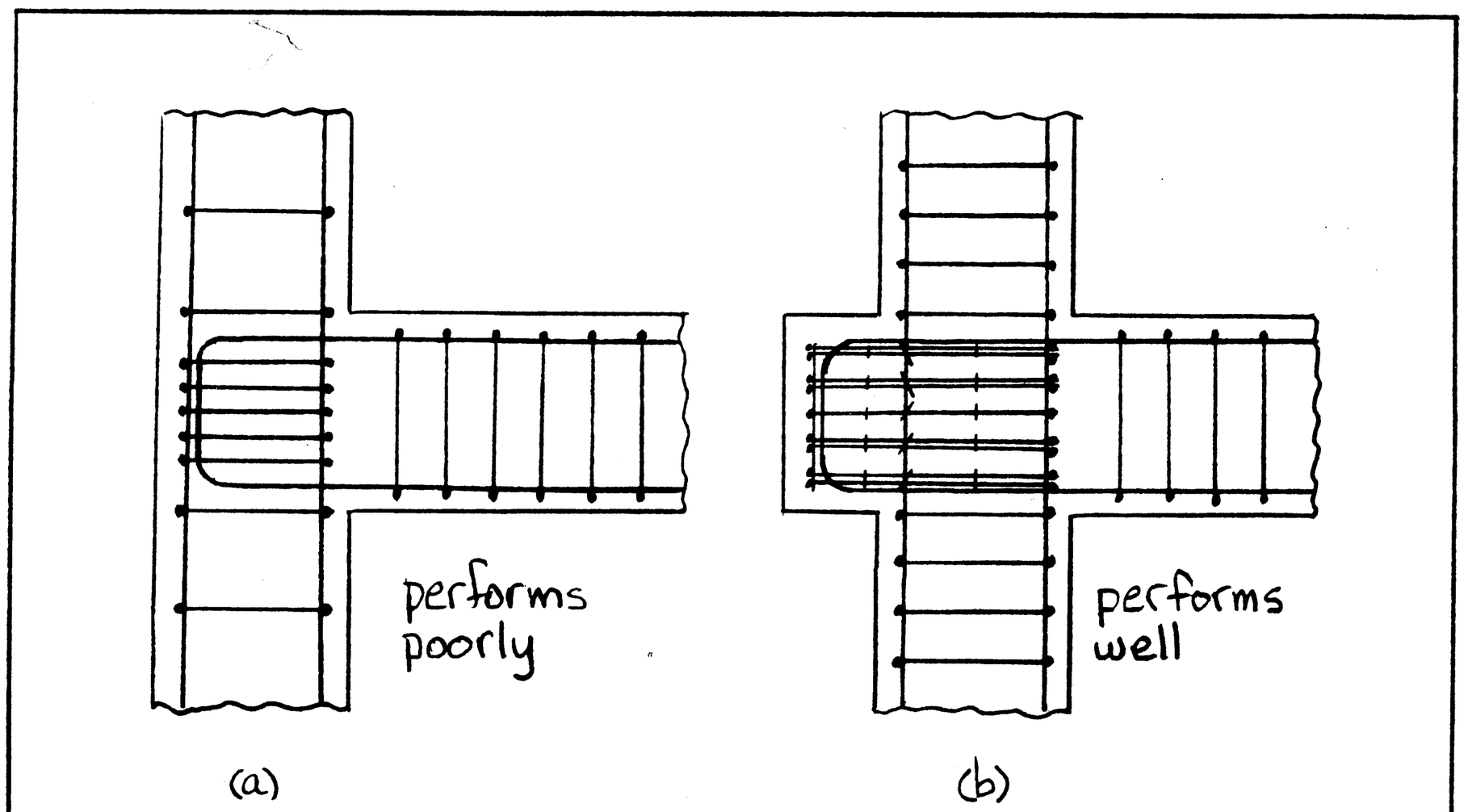

FIGURE 3.17: Tested details

under seismic loading provided the beam bars are indeed mechanically anchored by an anchor plate or are developed in a beam stub extending from the column face, (Park and Paulay[24]).

In practice, beam-column joints are usually detailed as shown in Fig.'s 3.17(a) and (b). Tests by Hanson and Connor[27], (adapted from Park and Paulay[24]), show that the reinforcement scheme of Fig. 3.17(a) exhibits unsatisfactory performance with a measured shear strength to a theoretically computed shear ratio ($V_{test}/V_{theoretical}$) ranging between .6 and .9. This ratio gives the joint's efficiency as defined previously. The low efficiency indicates that the joint could not sustain the capacity of the beam. The reinforcement scheme of Fig. 3.17(b) showed a satisfactory $V_{test}/V_{theoretical}$ ranging between 1.0 and 1.1.

The poor performance of the detail in Fig. 3.17(a) results from the fact that the flexural reinforcement in the beam does not interlock with the exterior column reinforcement or transverse hoop legs, but is vertically hooped and insufficiently "spliced" with the exterior face flexural reinforcement in the column. There is no direct load path for the beam flexural tension to turn the corner and flow into the column flexural reinforcement. This also points out that the ACI code[3] provision permitting to measure the development length from the beam-column interface is not sufficient. As pointed out in the context of Fig. 3.9(b), (section 3.2.3), this detail is not to be interpreted as a hook anchorage. A development length problem from the beam-column interface is not the issue here, but rather, a splice problem of the lap splice between the beam's bent flexural bars and the column's longitudinal bars.

The satisfactory performance of Fig. 3.17(b) is due to the additional concrete provided outside the column face for the sole

purpose of development and anchorage of the reinforcement. It acts similarly to a massive anchor plate on the column face.

3.4.2 INTERIOR BEAM-COLUMN JOINTS

Like the exterior beam-column joints, interior beam column joints can also be perceived as the superposition of opening and closing knee joints, as shown in Fig. 3.18(a) and Fig. 3.15(a).

The idealized truss model (without stirrups) for the interior beam-column joint is shown in Fig. 3.18(b). Like the exterior beam-column joint, the anchor plates are located just outside the joint core. The diagonal compression strut in the core bears onto and interlocks with these anchor plates. The diagonal strut forces are equilibrated by the tensile forces introduced into the anchor plates, (by the flexural tension reinforcement), as well as by the flexural compression zone of the adjoining members, (at diagonally opposite corners).

In practice, the longitudinal steel in the beams and columns are usually not terminated at the boundaries of the joint core and fixed to anchor plates as shown in Fig. 3.18(b), but rather, these bars are continuous through the joint to also allow for reversed moments. The rebars are then pushed on one side of the joint core, and pulled on the other. As in the exterior beam-column joint, these flexural bars must be developed completely outside the joint core after the joint has diagonally cracked, if there are no hoops or stirrups in the joint. Again, as discussed for exterior beam-column joints, the

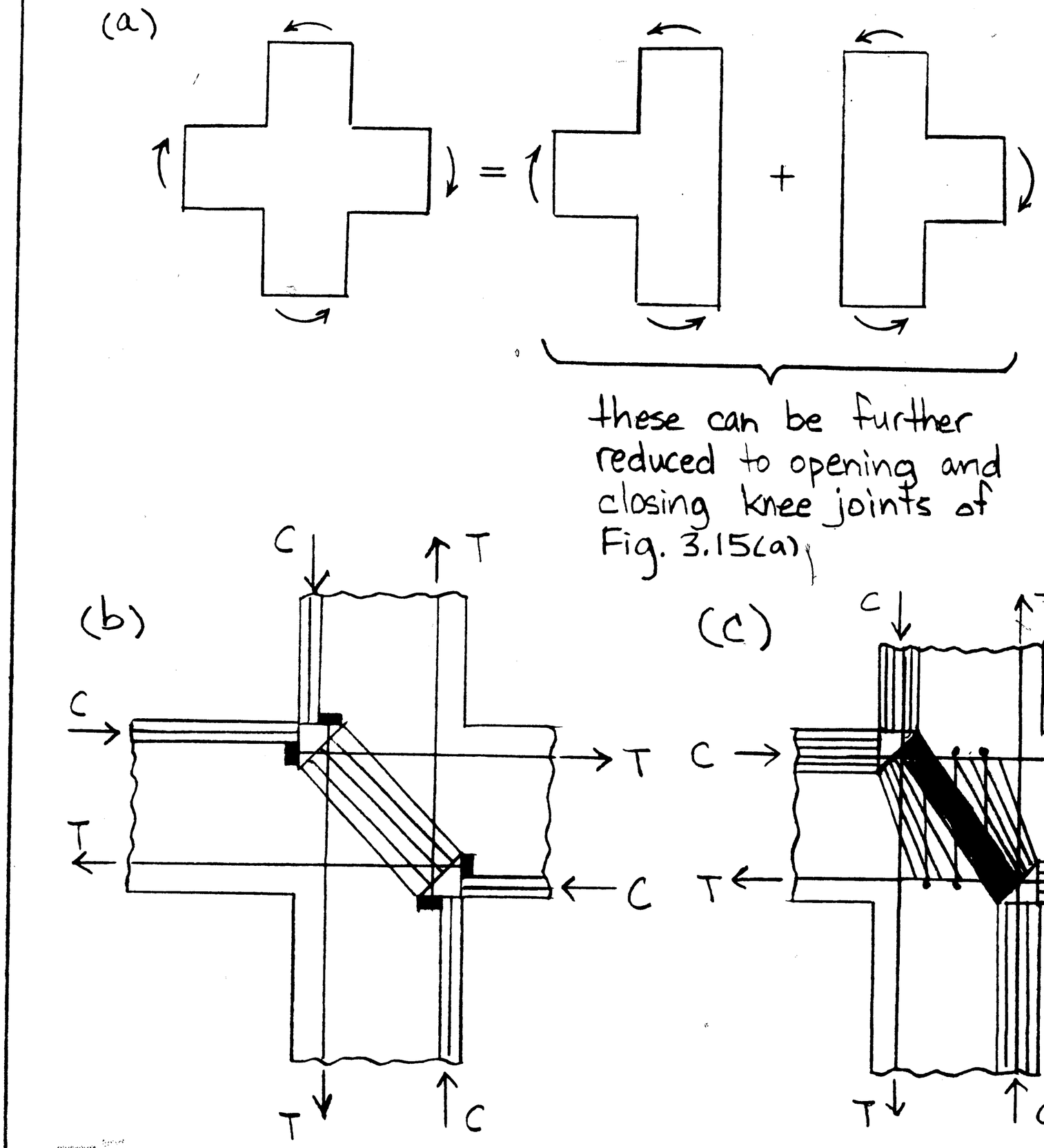

FIGURE 3.18: Interior beam column joint

addition of stirrups or hoops in at least one direction serves to move some of this bar development into the joint core for the flexural reinforcement of at least one set of adjoining members. Figure 3.18(c) illustrates the truss model for such a detail. If horizontal hoops are preferred, turn the model by 90°. The vertical

hoops not only confine the concrete and make it more ductile, but permit the longitudinal reinforcement in the beams to be developed at least partially inside the joint core. They permit part of the diagonal strut to "deconcentrate" and to shed part of its force to the fans that radiate from the upper left and lower right corners. These fans find their vertical support in the hoop bends and their horizontal thrust supplies the forces developing the bars inside the joint core.

Again, the problem with providing hoops in only one direction is that the longitudinal reinforcement in the same direction must still be fully anchored at "pinch" of the fans just outside the joint core. Indeed, in beam-column joints with horizontal hoops (the usual detail), it is the horizontal (beam) bars which tend to slip through the joint after plastic hinges develop in the beams. This may explain why precast beams connected to precast columns by splice sleeves slightly outperformed a monolithic twin specimen . In effect, the splice sleeves also serve as anchor plates for the longitudinal reinforcement. This shows that properly detailed precast concrete connections could even out-perform monolithic joints, if the connection hardware is designed to not only mechanically splice bars but also solve the inherent anchorage problems of monolithic joints.

Nevertheless, providing closed hoops in two directions is the ideal, but also impractical, solution. In beam-column joints with horizontal hoops, the longitudinal column reinforcement along the side faces is sometimes considered to play the role of vertical

hoops. However, these "hoops" or "stirrups" are themself not properly anchored! It must be realized that it is the stirrup anchorage forces which provide the support for the joint diagonal compression field which develops bars inside the joint. In this context it is also worth mentioning that the longitudinal bar bond stresses cannot flow outside into the adjoining members, since the joint equilibrium requires that they flow into the joint core. Again, it is noted that the function of hoops in joints in either direction is not simply to transfer shear, but also, just as importantly, to move development and anchorage of longitudinal reinforcement into the joint core and distribute the anchorage and development forces over the core. They are also needed to provide concrete confinement and thus the necessary ductility so that the fully cracked concrete can realize the plastic truss model. A joint can be understood as half of the span of a simple deep beam under concentrated mid-span load. As noted in section 2.5, experimental results show that such a deep beam can develop the flexural strength without stirrups, if the longitudinal bars can be anchored for their full capacity at the simple support. Stirrups then merely make the failure more ductile. If the flexural strength cannot be developed, it is usually due to an anchorage failure at the support. In section 2.5 it was therefore concluded that the amount of stirrups needed is mainly a function of how much the longitudinal bar end forces must be reduced to make the end anchorage work. The implication for joints is that if the longitudinal bars were mechanically anchored as shown in the idealized joint truss models (Figs. 3.2(a), 3.5(a), 3.15(b),

and 3.18(b)), hoops would only be needed for confinement and ductility.

3.5 ANCHORAGE AND DEVELOPMENT IN A PRETENSIONED DAP ENDED BEAM-TO-GIRDER CONNECTION: A QUANTITATIVE ANALYSIS

In simple beam-to-girder connections, the ends of beams are often dapped to save construction height. The dapped end represents a severe geometrical discontinuity or disturbance whose D-region extends far into the beam. For the purpose of a connection design methodology, this D-region is best viewed as the D-region adjacent to a connection interface.

A quantitative analysis has been performed on the D-region of a dap ended pretensioned double-tee beam for which test results are reported in a PCI report[22] describing a test program in which several specimens were tested to failure. For specimen 1B, the nib was qualitatively analyzed in section 2.9.1. As noted there, this particular nib was well detailed and permitted a truss model to form.

This section briefly demonstrates the use of and reasoning with explicit truss models for D-regions. It illustrates how truss models allow designers to extrapolate to poorly understood situations not covered by the code, such as the interaction of prestress transfer with the effect of geometric discontinuities and shear transfer over a direct strut. The truss model provides insight into the force flow path of this complex element and is compared with the test results.

As stated, the analysis of this D-region involves the transfer of prestress over the transfer length; the transfer of shear between

concentrated load and support reaction over a direct strut (actually arch); the force transfer between a strand and a rebar over a lap splice; and the existence of geometric discontinuities. While the concentration of so many complications in one location is poor practice, (and should be avoided if possible), it is not untypical of connection D-regions. Figures 3.19 through 3.22 show the test setup, the detailing arrangements, and the material properties of this beam. The following sections will simply present the results of this analysis, with a brief description of the analysis, and present the conclusions.

3.5.1 BEHAVIOR AND ANALYSIS OF SPECIMEN 1B

The beam was placed inclined in the test setup so as to simulate axial loads resulting from volumetric changes. The beam was loaded to failure. At a shear of 27^K the first major diagonal tension crack developed starting at about 13 inches from the lower corner of the sloping face. Upon formation of this crack, a stress redistribution allowed the beam to sustain a load of 26.35^K. It was possible to increase the load again to 27.93^K, when another major diagonal crack propagated up from the lower corner and the load dropped. The shear could not again be brought up to the maximum load, but the beam sustained a shear of 23^K in a stable manner.

The strategy in this analysis was to proceed in three steps: First, the isolated nib was studied and its capacity determined assuming its end to be a fixed support. Second, the analysis was extended into the region to the right of the nib and above the

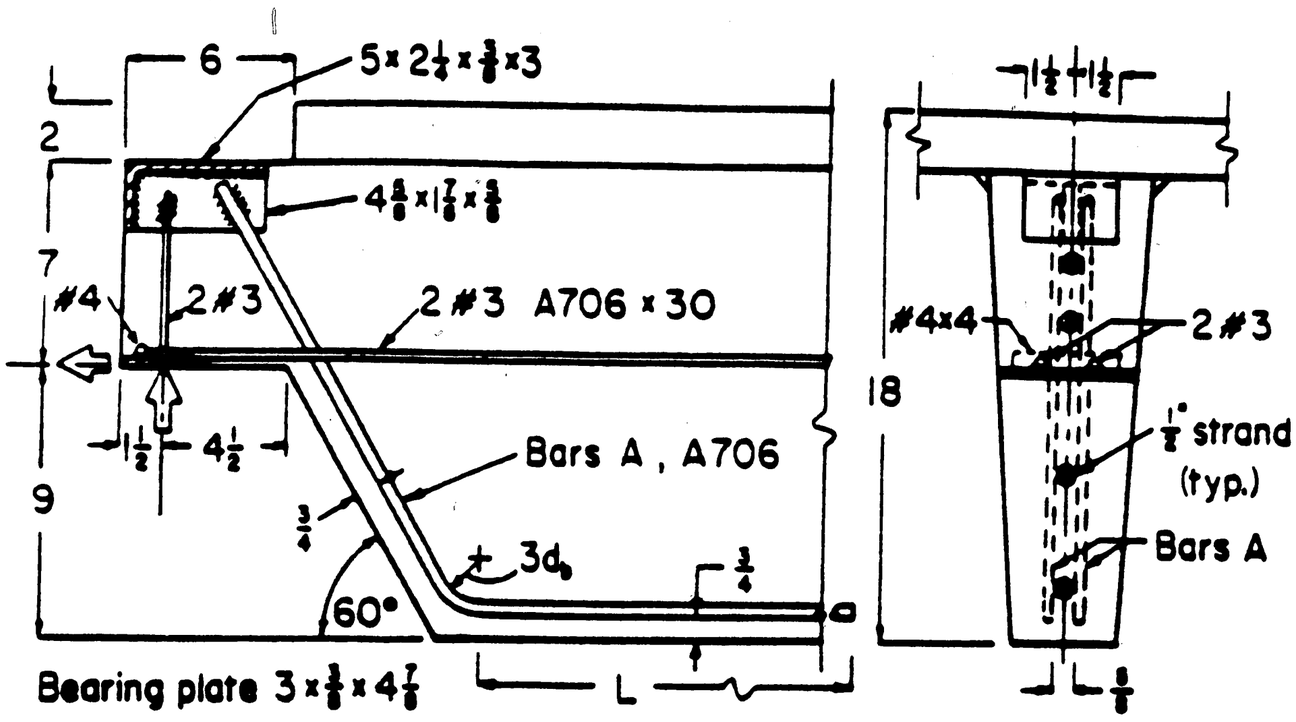

Spec. No.	Bars A	Length L
1A	2 #4	13
1B	1#4 + 1#3	22¼
1C	1#4 + 1#3	22¼

All dim. in in.

FIGURE 3.19: Dimensions of specimen 1B [22]

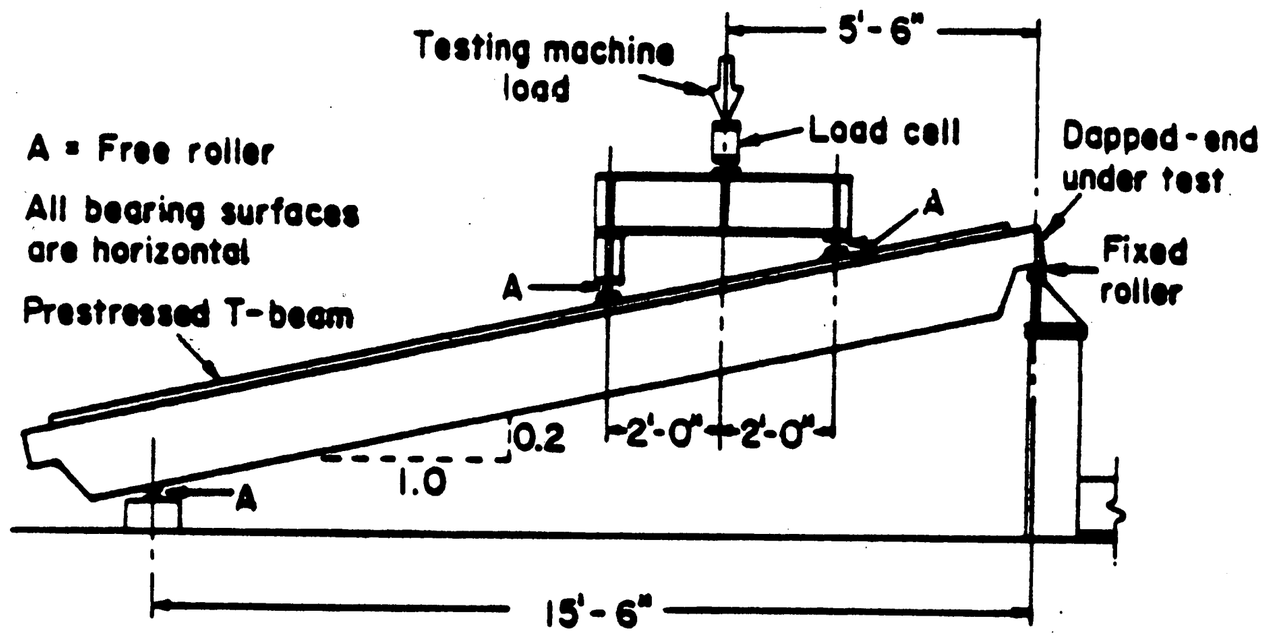

Specimen	Concrete Strength (psi)		Rebar Size	Yield Strength (ksi)
	At Transfer	At Test		
1A	4380	5345	#3	73.6
			#4	65.5
→ (1B)	5720	6820	#3	73.0
			#4	66.0

FIGURE 3.20: Test set-up and material properties of 1B [22]

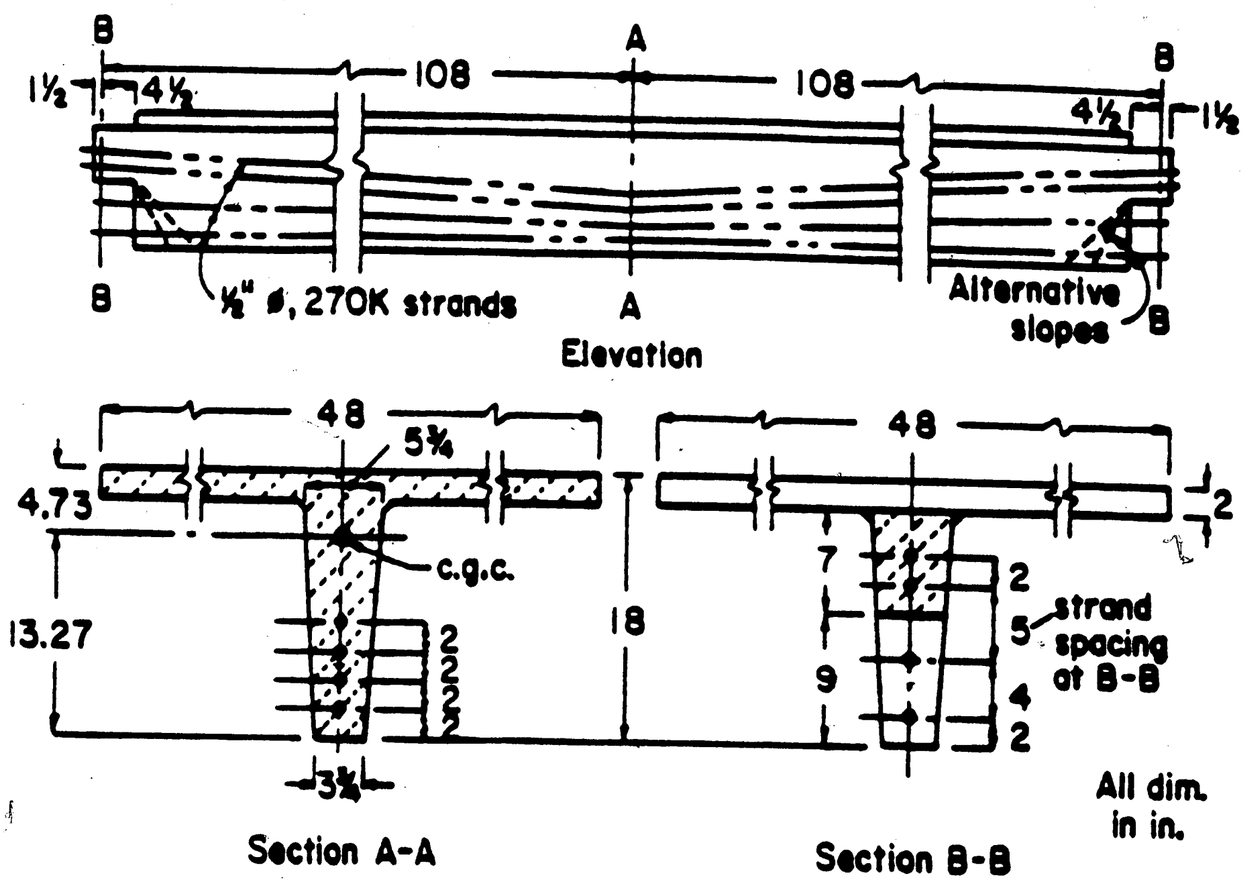

Distance of first leg of WWF web reinforcement from bottom corner of web, 1.5 in. for right-angle dap, 1 in. for sloping web end face.

FIGURE 3.21: Typical test beam 1B [22]

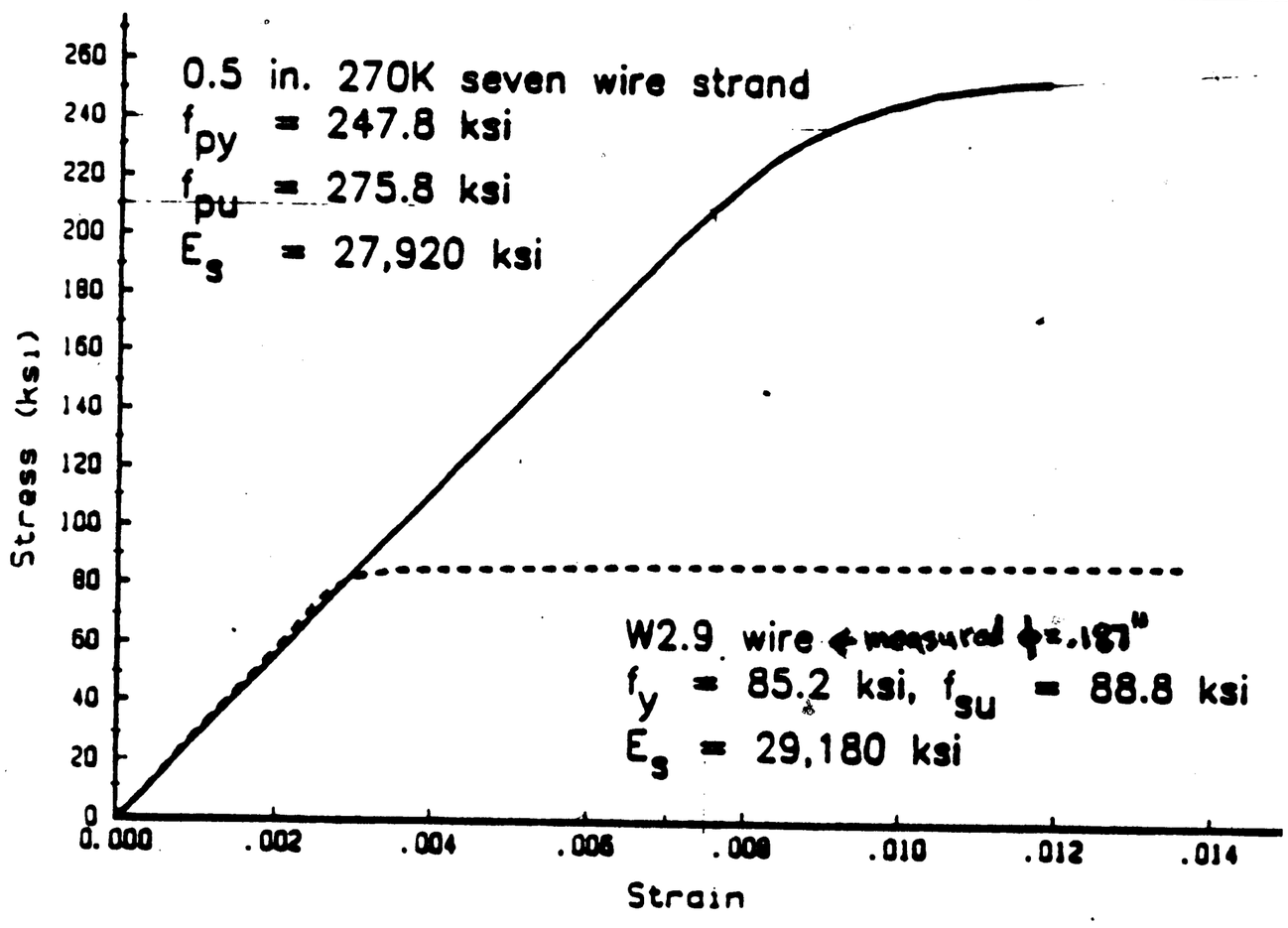

FIGURE 3.22: Stress-strain curves for prestressing strand and for welded wire used as web reinforcement. [22]

diagonal crack extending from the re-entrant corner, in order to determine whether moment, shear, and axial force from the nib at its capacity can be transferred into this region. Third, analysis and truss model were extended all the way to the right to the section of maximum moment for the maximum load that can be theoretically transferred to the beam proper. Cracked section analyses at the section of the first load and of maximum moment established boundary conditions for the strand and compression chord forces.

Because the nominal shear stresses were not high and concrete diagonal crushing did not control, only resultants of concrete stress fields such as struts, arches, and fans were dealt with in the third step. The tensile strength of the concrete was not relied upon and the effects of prestress were treated as equivalent loads as described in section 2.7.

In the analysis, three truss models were constructed. The first two were based on two different estimates for the transfer length: A conservative estimate of 36" for all four strands (the value suggested in the test report) and a more realistic liberal estimate of 20" for the top two strands and 36" for the bottom two strands. The transfer length for the top two strands which were located over the support, was computed using formulas reported in reference (21) which consider concrete strength. The bottom two strands were considered equivalent to strands sheathed over the support, and thus their transfer length was assumed to be approximately twice that for the top strands. A third truss model was constructed using the liberal estimate but double the actual number of stirrups to

demonstrate the effect of stirrups on the required longitudinal reinforcement. Figures 3.23 and 3.24 show the truss models developed in the third step for the two liberal estimates and for the observed capacity after diagonal tension cracking of 23^K.

Conceptually, the beam is divided into compression chord (flange), web, and tension chord. The latter is defined to consist of the bottom 2 in. of concrete including the bottom strand and the horizontal extension of the hanger bar, as illustrated in Figs. 3.23(b) and 3.24(b). Figures 3.23(a) and 3.24(a) show the equivalent loads of the top three strands "unloading" onto the compression struts causing them to arch.

Figures 3.23(c) and 3.24(c) plot the forces within the tension chord shown in Figs. 3.23(b) and 3.24(b). The chord tension due to the horizontal component of the arch thrusts and of the inclined hanger bar extension (stepped curve), and the prestressing force due to the bottom strand (which "unloads" onto the tension chord) are plotted separately. Where the prestress force exceeds the tension chord force (stepped curve), the chord remains precompressed (uncracked). Where the tensile force exceeds the prestress force, the chord is cracked and additional reinforcement is necessary. The required additional reinforcement capacity is indicated by the shaded area between the stepped and strand curves. Finally, the additional longitudinal reinforcement actually provided by the hanger bar extension is indicated by the cross-hatched area. Where the cross-hatched area does not fully cover the shaded area, there is insufficient longitudinal and/or stirrup reinforcement. The double

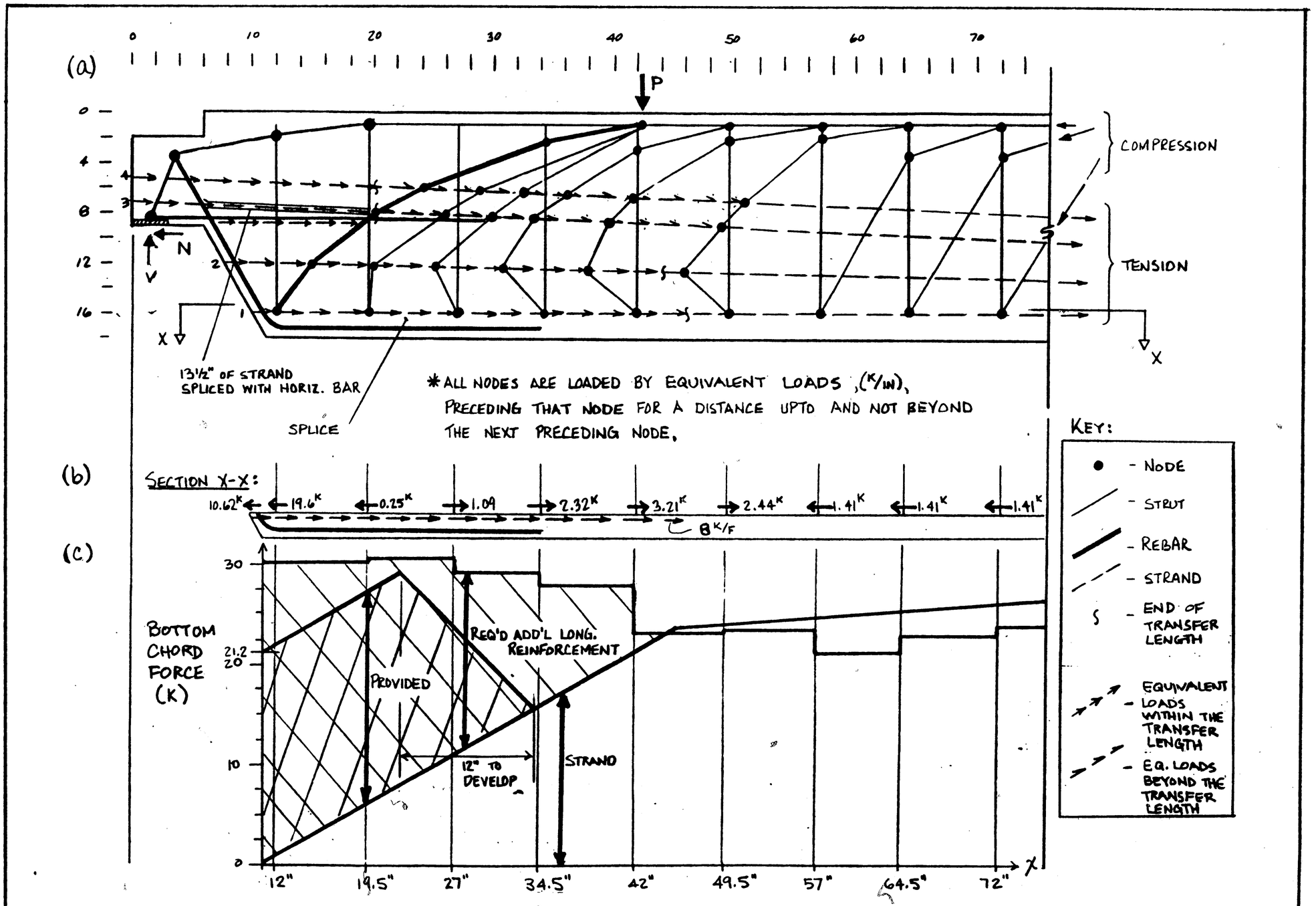

FIGURE 3.23: Truss model for dap-ended beam

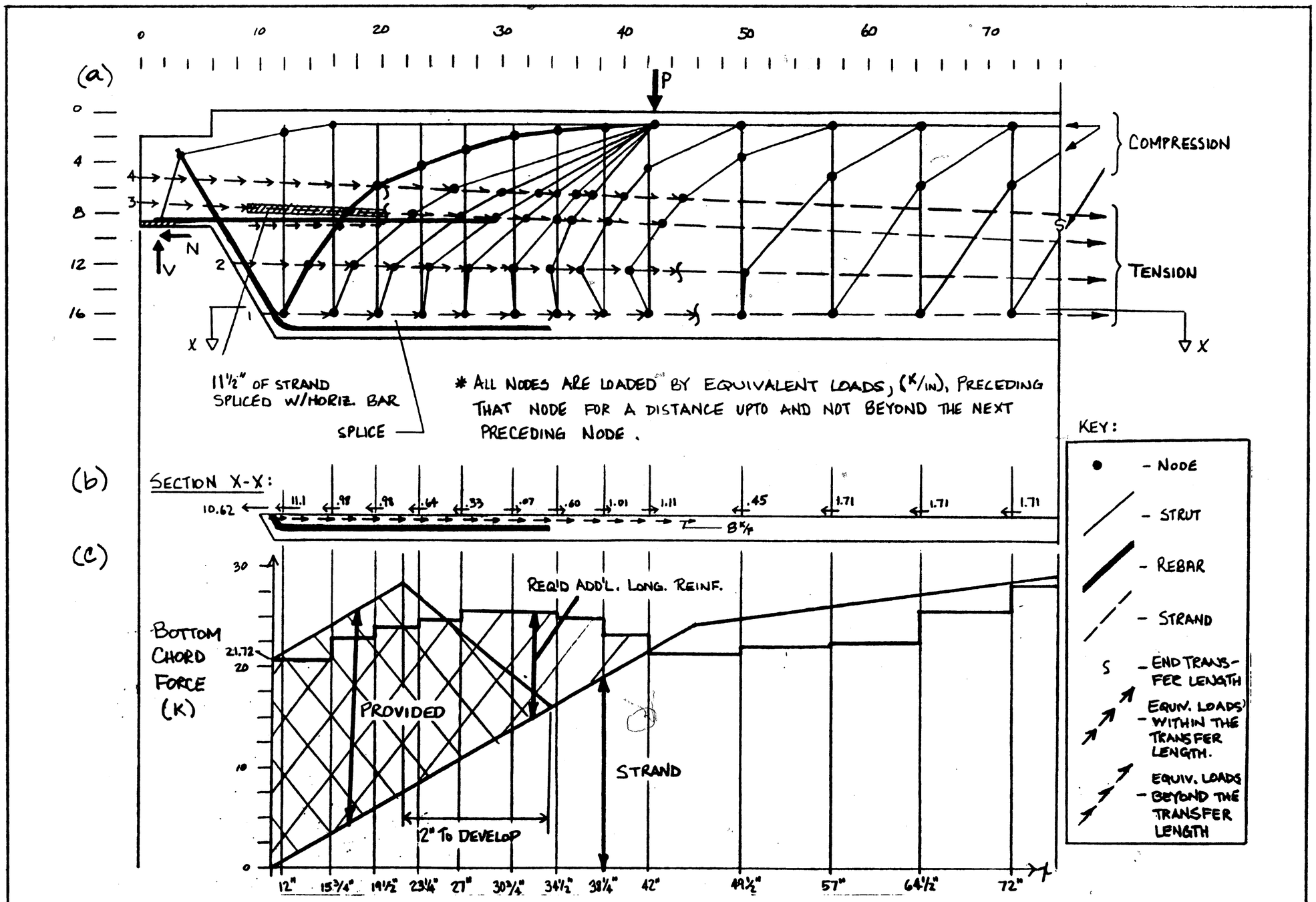

FIGURE 3.24: Truss model with doubled stirrups

stirrup model of Fig. 3.24 proves to be much less critical compared to the model of Fig. 3.23. This is to be expected since an increase in stirrups decreases the longitudinal requirements of the tensile chord as described in section 2.4.

As mentioned at the beginning, this D-region is caused by three D's: the geometric discontinuity of the dapped end, the static disturbance due to transfer of prestress over the transfer length, which extends to the first load, and the static disturbance of shear transfer over a direct arching strut from the lower left corner to the first load. Since the inclined hanger bar can transfer only 18^K of the shear force into the beam, the first two stirrups in Fig. 3.23(a) must serve the function of hanger bars transferring the "excess shear force" down to the lower left corner. This leaves only two stirrups for "shear transfer by stirrups". Therefore 18^K of the total shear force of 23^K must be transferred by the direct strut arching from the concentrated load to the lower left corner. Its large horizontal outward thrust, combined with the tension from the inclined hanger bar, results in a very high tension chord end force which should be anchored at the lower left corner. In essence, the dapped end behaves like a deep beam with virtually no stirrups and therefore nearly constant tension chord force. The prestressing force at the lower left corner is insufficient to balance the outward thrust of the arching diagonal strut, nor can the horizontal hanger bar extension anchor it, since it is itself not sufficiently anchored or spliced at its right end. The prestressing force is introduced too far to the right as indicated by the "reverse inclination" of the

diagonal struts there. It is interesting that the strut pattern agrees quite well with the observed crack pattern including this "reverse inclination".

It is found that the truss model for this specimen correctly predicts the observed controlling failure mode, but underestimates slightly the corresponding ultimate load. Specifically, it predicts that the nib is less critical than the part of the D region to the right of the nib and left of the first load. Ultimately, failure was due to a major diagonal crack extending up from the lower left corner after which the beam could sustain a shear force of 23^K in a stable manner. Indeed, the tension chord force plot in Fig. 3.23(c), clearly indicates that there is not enough or not sufficiently anchored/developed longitudinal steel and/or stirrups in the vicinity of the lower left corner to transfer more than 23^K. A bond failure of the strands and/or failure of the bottom strand/rebar splice along with insufficient capacity and length of the longitudinal hanger bar extension are the causes of this major diagonal crack.

The fact that the plot of Fig. 3.23(c) exhibits steel deficiencies, although the tested specimen was able to maintain a shear of 23^K, must be attributed to the remaining effects of concrete tensile strength, shorter actual transfer lengths, and/or higher actual prestress. It should be noted that the tensile chord forces are highly sensitive to transfer length and that the reported effective prestressing force of 24^K is only an average value for many tests. In any case, the important conclusion from a conservative designer's point of view is that the truss model yields a safe

estimate for the ultimate strength of this complex D-region after diagonal tension cracking.

The tension chord plot of Fig. 3.23(c) shows that the longitudinal and transverse reinforcement would be sufficient if only one of the two bottom strands were "mechanically" anchored by an anchor plate located beyond the location of the hanger bar. In this way, the arching diagonal compression strut can bear into the anchorage of the prestressing strand. Alternatively, if this is not possible, (because the compressive stresses become too high in the thin web), the horizontal extension of the hanger bars could be "mechanically" spliced with the strand. Considering the small web dimensions and the hybrid nature of the splice, an innovative solution is required possibly using new advanced materials. Because the horizontal extension is insufficient in capacity, it would have to be strengthened for this solution. As a third solution the end anchorage demands for the longitudinal reinforcement near the lower left corner can be reduced to the available capacity by increasing the stirrups. This is equivalent to reducing $\cot\theta$ in equations (2-7) and (2-9). However, this solution may require significantly more stirrups. The Canadian Code[16] would require about 2.6 times more stirrups. The horizontal hanger bar extension would also need to be extended further to the right to ensure a 100% splice with the bottom strand and also to ensure that longitudinal steel is present where it is needed. Figure 3.24 shows the truss model for twice the actual amount of stirrups up to the first load. Its tension chord force diagram clearly shows the reduction in tensile chord requirements.

Certainly, the results of this analysis could have been derived by a nonlinear finite element analysis in which concrete cracking, shear transfer through aggregate interlock over cracks, and inelastic bond-slip laws for strands and rebars are considered. This is clearly not a trivial task. The generation of the truss model required less time than the input preparation for such a finite element analysis. However, although the truss model approach may be quicker, it requires the analyst to understand the characteristic behavior and functions of the internal truss elements to be modeled. It must be emphasized though, that these truss models are considered analysis models which were constructed for research purposes. They can serve as reference for simpler design truss models which are under development.

3.6 SUMMARY OF ANCHORAGE AND DEVELOPMENT

The insights gained from truss modeling within D regions can be summarized as follows:

(1). Corbels, brackets, opening and closing knee joints, exterior/interior beam-column joints, nibs of dapped ends, and beam ends with short shear span and very little shear reinforcement such as the pretensioned double-tee discussed above -- they all possess similar characteristics in that they develop a direct strut in the D region which places very high demands on the end anchorages of reinforcement ties similarly as in deep beams.

(2). Poor performance usually results from poor anchorage and development of the ties and struts.

(3). The phrase "anchorage and development of reinforcement" describes only half of the problem, the other half being: Anchoring of compression struts and developing of diagonal compression fields. Compression struts must supply the forces anchoring bars and the diagonal compression fields must supply the "bond" stresses developing reinforcement. The anchor forces are in an action-reaction relationship.

(4). Anchorage and development has therefore two aspects: strength and location. An anchorage or embedment length must not only have sufficient strength (expressed as development length for the latter) but also be placed in a location, where it can intercept the compression strut, which supplies the anchorage reaction, and interlock with it in a C-C-T or C-T-T node at maximum internal flexural lever arms.

(5). Truss models make clear where the anchor reactions are coming from. They provide engineers with a tool to rationally analyze anchorage and development in joints and D-regions which, as the experimental evidence shows, is the most crucial issue controlling their performance.

(6). Equilibrium of the truss model for an opening knee joint clearly requires that the force which redirects the incoming flexural compressive resultant to turn the corner, must be supplied by the bar anchorage. This bar anchorage must therefore be located in the flexural compression zone. Thus it is not sufficient to measure development length from the beam-column interface. Rather it must be

measured from the truss node in which bar anchorage and compression struts interlock.

(7). Similarly, it is immediately evident from equilibrium whether or not a bar is bent in the correct direction in knee joints or tee joints. Since bar development is nothing else than the local truss action of "mini" diagonal compression struts bearing into the lugs of the bar, the lugs of the leg extending beyond the bend can be visualized by a fictitious anchor plate. If the incoming flexural compressive resultant acts on the correct side of this anchor plate, the bar is bent in the correct direction, otherwise not.

(8). The concentrated bar end anchorage demands in deep beams and joints can be reduced by providing stirrups, hoops, or ties. They "deconcentrate" part of the direct diagonal strut into fans (ties in one direction) or uniform diagonal compression fields (ties in two directions) and thereby spread the anchorage demands over the bar length.

(9). Since the compression fans which supply the "bond" stresses developing a bar, must be transversely supported or anchored, bar development after diagonal cracking of the concrete cannot be effective without ties. The force that can be developed over a given development length, depends therefore not only on the ultimate "bond strength" of the bar (expressed by the development length) but also on the maximum "bond stress" which can be supplied by the compression fan. The latter follows from the equilibrium of the fan and the tie capacity.

(10). Most of the important insights about anchorage and development can be gained from purely qualitative truss models and the graphic statics that they implicitly contain.

(11). These observations are equally valid for the D regions "behind" the interface of precast concrete connections, which serve exactly the same function as joints: turning moments (force couples) around corners.

4. AN UNDERSTANDING OF PRECAST CONNECTIONS

Similarly to joints in monolithically cast reinforced concrete (chapter 3), precast concrete connections disturb the flow of forces according to beam theory. The interface between connected members represents a static and/or geometric discontinuity which gives rise to D regions on either side of it as illustrated in Fig. 4.1(a). Dissimilarly to monolithic concrete joints, precast concrete connections usually have a clearly identifiable interface which joins different materials, such as steel and concrete or concretes cast at different times. Experience shows that in precast concrete it is often the D region "behind" the interface rather than the interface itself which is the cause of poor performance. It is important, therefore, to clearly define and distinguish the meaning of the terms interface, connection, connection hardware, and connection design for precast concrete.

A (connection) *interface* is defined as the surface along which two members are in contact. A *connection* is defined to include not only the interface between the connected members, but also the adjacent D regions on either side of the interface. Accordingly, *connection hardware* includes all hardware and/or reinforcement not only through the interface but also within the D regions. This definition of connection hardware specifically includes primary member reinforcement within its D-region. *Connection design* relates to the design of the interface as well as the design of the D regions adjacent to that interface. It includes the proportioning of all connection hardware and, as importantly, the detailing of the

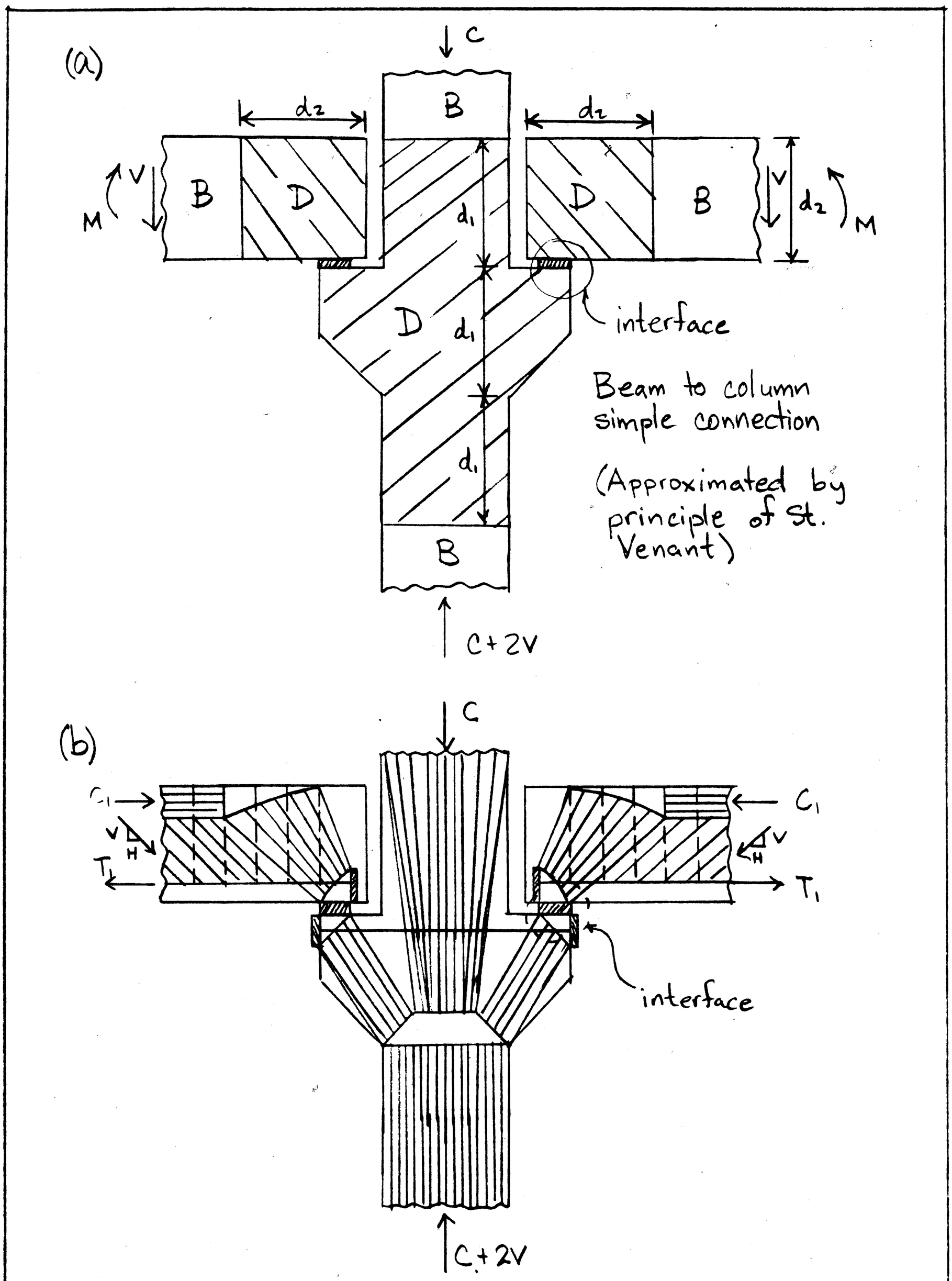

FIGURE 4.1: D Regions adjacent to interfaces

hardware. Proper design of a connection will ensure the safe transfer of the internal forces according to beam theory, from the boundary between the B and D region of one member to the boundaries between the B and D region of the other connected members, as visualized in Fig. 4.1.

The current design practice apparently is to design the interface using shear friction or other concepts, and to design the connected members using beam theory. The D regions on either side of the interface, however, are often not explicitly and rationally designed. This state-of-practice is not surprising, since neither popular textbooks nor popular design handbooks provide designers with rational models for these D regions. There is no assurance, therefore, that the stress conditions assumed for the design of the interface are compatible with those assumed for the design of the B region. Specifically, there is also no assurance that a force flow path through the D region exists which does not rely on the concrete tensile strength.

Inserts with welded headed studs, for instance, are designed using empirical data on the cone pullout strength of studs embedded in unreinforced, uncracked concrete blocks. How the tension introduced by the studs into the concrete can then be transferred to the primary reinforcement in the B region of the connected member remains an open question, particularly if the concrete tensile strength should not be relied upon. In many instances it is relied upon. In actuality, precast or non-precast concrete members crack under the primary actions due to the factored loads. Furthermore,

precast members are often precracked due to volumetric changes or frame movement. If the structural component is cracked, the concrete tensile strength on which design relied, may no longer be there. The following section shows that even in most simple connections moments (force couples) are transferred around a corner. Since the ACI Code does not allow us to rely on concrete tensile strength for moment transfer along straight or curved members, there is little reason to permit it, if a moment is transferred around a corner.

As shown in the previous chapters, truss models represent a simple tool to provide for force flow paths and reinforcement details through and beyond the D regions. They neglect the concrete tensile strength.

The following sections will study some commonly used precast concrete connections, both qualitatively and quantitatively, through truss models. The truss models will offer insight into the behavioral characteristics of these connections.

4.1 SIMPLE CONNECTIONS

Apparently, by definition, simple connections transfer only forces but no moments. However, in most simple connections, these forces are eccentric with respect to the axis of at least one member and thus both moments and forces are transferred, if not through the interface then through the D region. As an example for simple connections Fig. 4.2(a) shows angle seat bearing connections which are typically used to support or suspend cladding panels. Due to the eccentricity between the member axis and the vertical reaction or

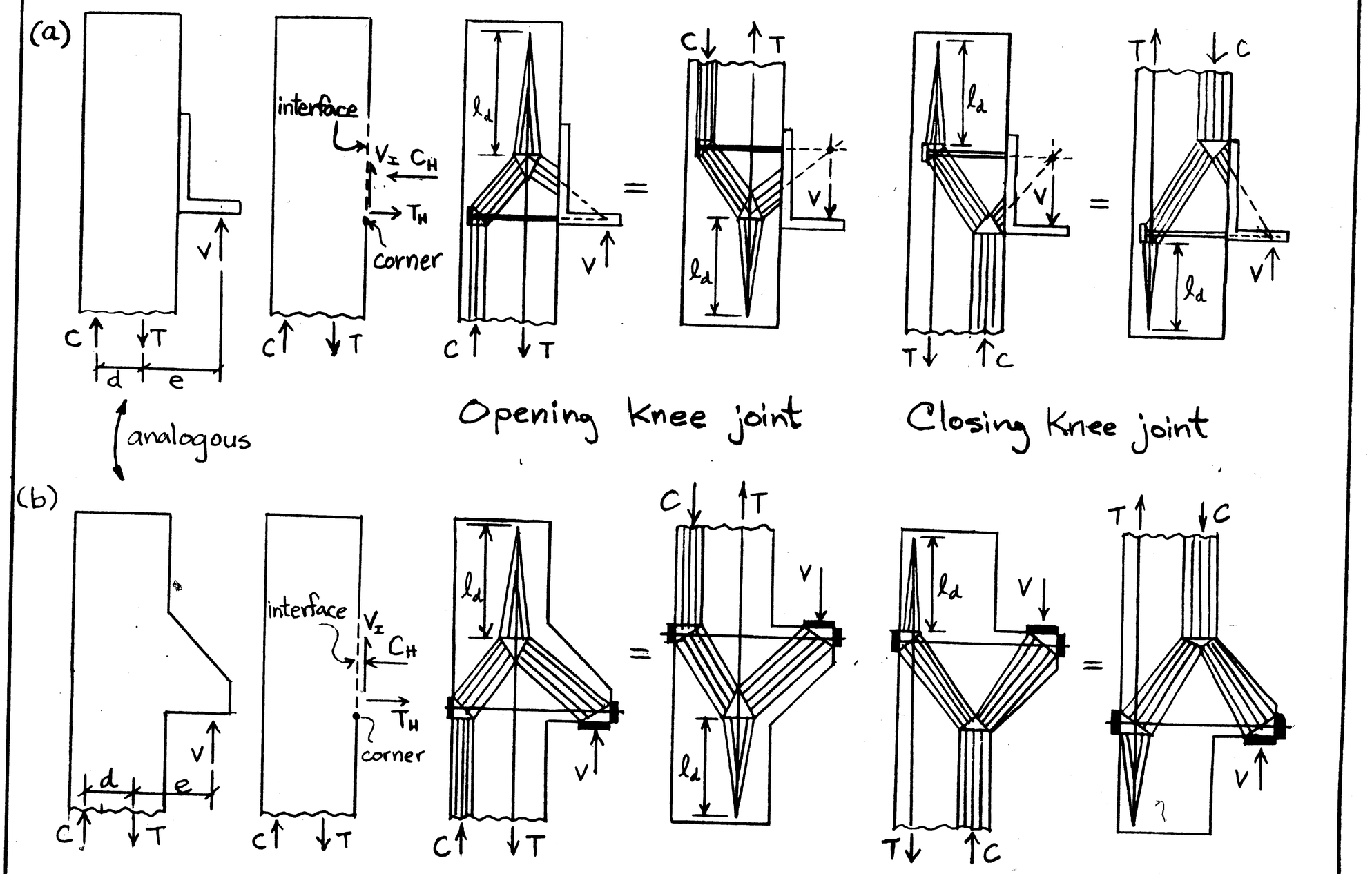

FIGURE 4.2: "Simple" connections turning moments "around a corner"

load, horizontal member sections are subjected to flexure and axial load. Due to the eccentricity between the interface and the reaction, the vertical interface is subjected to shear and a moment. Thus a moment (force couple) turns "around the corner" into the member.

Fig. 4.2(b) shows a completely analogous situation: monolithic concrete corbels. From the understanding gained in Chapter 3 it is realized, though, that it actually shows more: knee joints, where one member is a deep (cantilever) beam, i.e. a corbel. The left half shows opening knee joints, the right half closing knee joints. If the corbel was not located at the end of the member, it was a tee-joint with corbel. Truss models for this detail have been presented in section 3.1, Fig. 3.1, and also in section 1.3, Fig. 1.2, for the closing knee joint with corbel. In Fig. 4.2(b) also the truss models for the opening knee joint with corbel are shown. These truss models can be directly transferred to the analogous angle seat bearing connection in Fig. 4.2(a). The only difference is that the "corbel strut" (which is of course only fictitious outside the concrete and and represents there the thrust line for the angle) must now pass through the interface. Its inclination relative to a normal to the interface must therefore not be larger than the angle of friction.

Since the D-region "behind" the interface of this simple connection plays the role of a knee joint, this example shows that also from the viewpoint of a consistent and unified connection design methodology, the D-region is an integral part of the connection and must be included in the definition of the term connection. In view

of the critical performance characteristics of knee joints, particularly under opening moments, it seems prudent to investigate such details in more depth. In chapter 3 it has been observed that the truss models of most joints can be understood as a combination or superposition of the basic truss models for knee joints and corbels. This holds also for precast concrete connections. Indeed this force flow path is so pervasive in connections, that an understanding of it is crucial. Thus, the following several sections are entirely devoted to developing a behavioral insight into this truss system. The angle seat bearing connection is used as the vehicle to exemplify this behavior.

4.2 ANGLE SEAT BEARING CONNECTION WITH ONE STUD ROW

Angle seat bearing connections are typically found in cladding or wall panels. As shown in Fig. 4.2(a), in its simplest form this type of connection requires a single row of studs, welded to the bottom of the angle, to transfer the forces. An opening knee joint configuration is selected, since this is the most critical. Fig. 4.3(a) shows the connection hardware. It is clear from chapter 3 that the stud head must be located as close to the opposite face as possible and the distance between the stud head and the "loose" longitudinal reinforcement must be maximized. A possible configuration of the truss model for this detail is illustrated in Fig. 4.3(b).

While angle seat bearing connections typically have two rows of studs welded to the angle, a detail with only one stud row shall

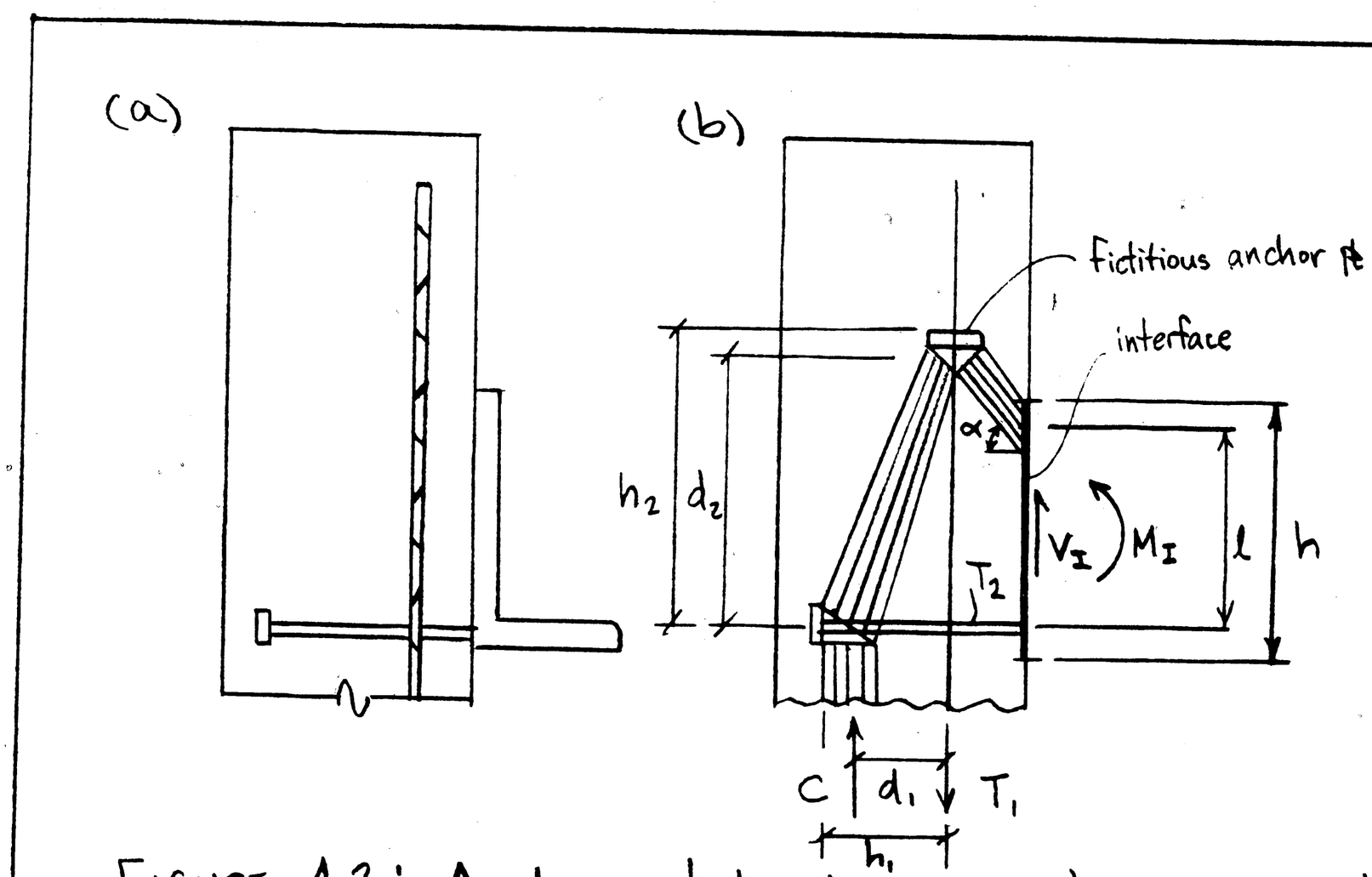

FIGURE 4.3: Angle seat bearing connection with 1 stud row

initially be treated. Without the additional complications that would be encountered if two stud rows were initially considered, the basic behavior and the structural function of each element can be better understood. Similarly, while such a connection is typically loaded not only by a vertical but also a horizontal force, this horizontal force can initially be omitted without affecting the generality of this analysis, since the formulas presented later can be easily modified to include its effect.

Treatment of this analysis will be, for several reasons, in the form of a two-dimensional (2-D) problem. Certainly, a planar understanding is first required before the more complex three-dimensional (3-D) behavior is treated. Secondly, 3-D behavior

affects the reinforcement required in the D region as determined from a 2-D analysis, only over the "effective width" of the struts in the transverse direction which, in turn, influences the depth of the struts in the plane. As long as this compression strut depth is small relative to the flexural lever arm, its influence on reinforcement proportioning is small. 3-D behavior (space truss action) should be considered at least qualitatively in the transverse layout of the "planar" reinforcement and for transverse reinforcement.

From the viewpoint of a consistent and unified connection design methodology, connection strength is best expressed in terms of the forces and moments transferred over the interface between the two members. This convention is applicable to most connections and independent of the particular members connected. Omitting initially the axial force, the interface in this case is subjected to moment and shear. Therefore connection strength is expressed in terms of a strength interaction diagram for the moment, M_I, and shear force, V_I, at the interface. This connection interaction diagram thus covers the full range of possible eccentricities between the vertical reaction or load on the angle and the interface. It must be emphasized that expressing the strength of the connection, which includes the D-regions, by the moment and shear at the interface, does not imply that it represents the interface capacity. It merely means that both the D-region capacity and the interface capacity are expressed in the coordinate system M_I-V_I. Indeed, the purpose of this analysis is to study which zones of this connection interaction

diagram are controlled by the D-region capacity and which by the interface capacity. In view of the critical role that anchorage location plays in opening knee joints, it is of particular interest how the location of anchorages affect the connection interaction diagram.

The connection interaction diagram presented below is based on the following assumptions:

(1) the steel angle is considered rigid, i.e. it does not control the connection capacity.

(2) dowel action is not considered, i.e. interface shear transfer occurs through (shear) friction.

The first assumption implies not only that the steel angle has sufficient strength, but also that the state of deformation of the angle does not significantly influence the stress distribution in the concrete. Considering this effect when it becomes significant, is beyond the scope of this analysis. The second assumption is made for several reasons. The first is simplicity and systematic separation of alternative force paths. Similarly as concrete struts supply the anchorage forces which anchor rebars, concrete struts must supply the forces which bend the dowels. Thus dowel action requires another set of struts in the D-region. The scope of this study is limited to the investigation of the force paths in the D-region associated with interface shear transfer through (shear) friction. Second, dowel action is unlikely to be large in the studs transferring the flexural tension. Experimental results on shear transfer in beams indicate that while dowel action of rebars may be significant under service

loads, it is negligible at the ultimate state. Third, the truss models including dowel action are too complicated for design. For design purposes it may be possible to include dowel action in an effective (shear) friction coefficient.

Figure 4.4 shows qualitatively the connection interaction diagram for the angle seat bearing connection of Fig. 4.3 as well as the truss models associated with various regions of the interaction diagram. Curve A-E represents the interface interaction diagram, i.e. the capacity of the interface regardless of the strength of the adjacent D region. Specifically, curve A-C represents the range of shear-moment interaction within which (shear) friction does not control while line C-E represents the region where it does and the angle can slip along and away from the interface. While curve A-E represents the interface shear-moment interaction diagram, lines F' and F represent the D region interaction diagram i.e. the flexural capacity of the D-region when the longitudinal reinforcement or the studs yield, respectively. These lines are strongly dependent on the location of the anchorages for the steel. For illustration also line G is included which represents the flexural capacity of the member itself (B region) as determined by beam theory. The interaction diagram represents the connection strength for *fixed* locations of anchor plates and reinforcement for a variety of loading combinations. By definition the *interface* interaction curves are not influenced by the D region "behind" the interface, specifically not by the anchor plate locations. However, for illustration purposes Fig. 4.4 shows truss models "behind" the interface also for the

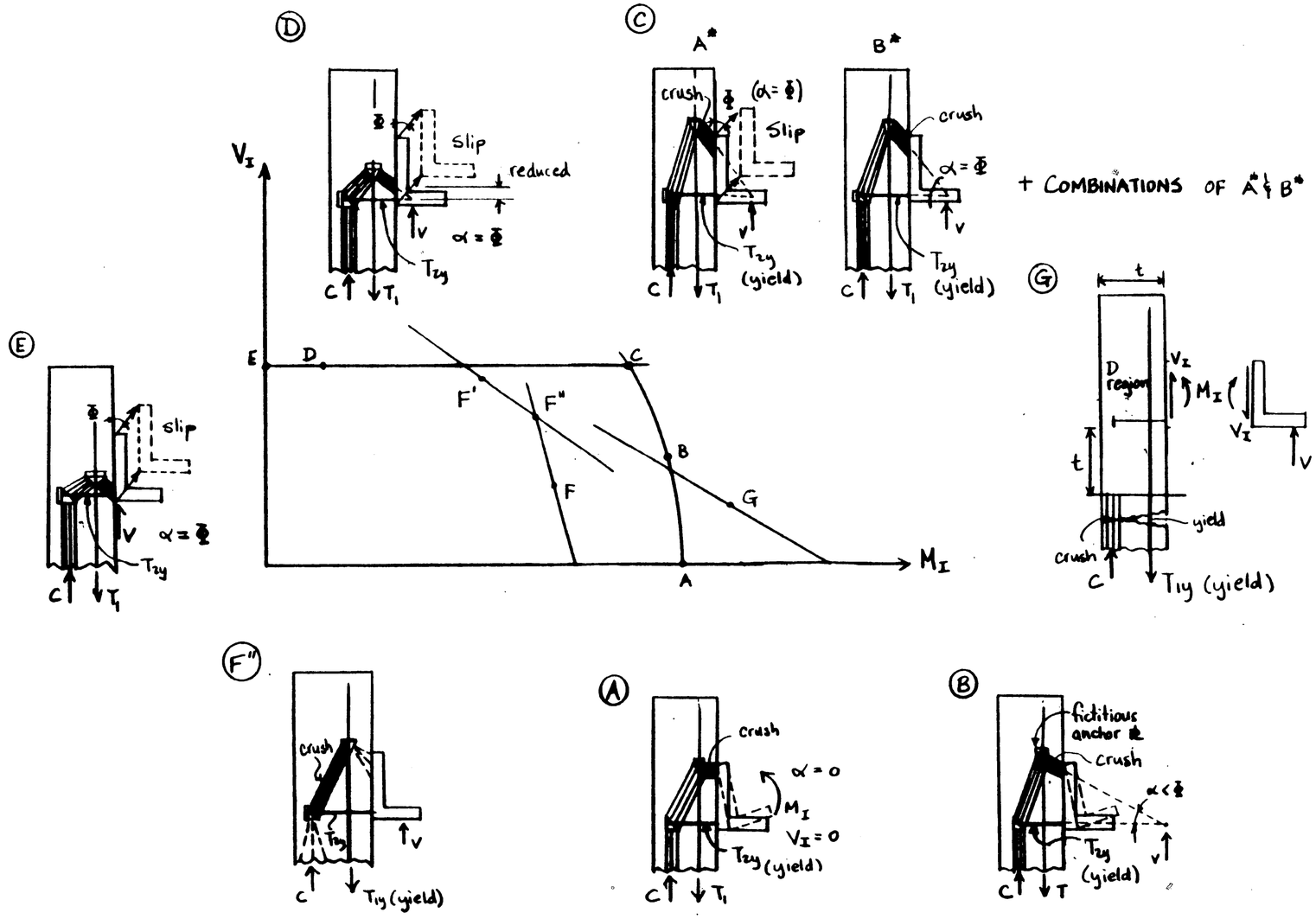

FIGURE 4.4: Connection interaction diagram in terms of shear and moment at the interface for the single stud row angle seat bearing connection

interface curve A-E. These truss models are only informative and indicate where plate and reinforcement would have to be *if the interface controls*.

While the D region concerns are irrelevant for the interface diagram A-E, the actual specified locations of anchor plates and longitudinal reinforcement become particularly important for the D region interaction diagram (lines F and F'). The truss models associated with the interaction diagram controlled by the D-region are based on these actual, specified locations of anchor plates and longitudinal reinforcement.

The remainder of this section discusses the behavior of this connection in terms of the various failure modes that control - or may control - the different regions of the interaction diagram. The stress state associated with each failure mode is visualized with inserted truss models in Fig. 4.4. Since these inserted models are rather small, the reader is referred to Fig. 4.5 for labels, where Fig. 4.5(a) and (b) label the interface including angle and the truss model in the D-region, respectively. Note that loading the angle with a load with constant eccentricity, e, as defined in Fig. 4.5(a), corresponds to a load path along a straight inclined line through the origin of the interaction diagram in Fig. 4.4.

First, the interface capacity represented by region A-E will be discussed. Point A describes pure flexure at the interface. The studs yield, while the horizontal strut A crushes under the upper tip of the angle at the interface. Maximum moment is achieved for the maximum possible lever arm, ℓ, (Fig. 4.5(a)). The failure mechanism

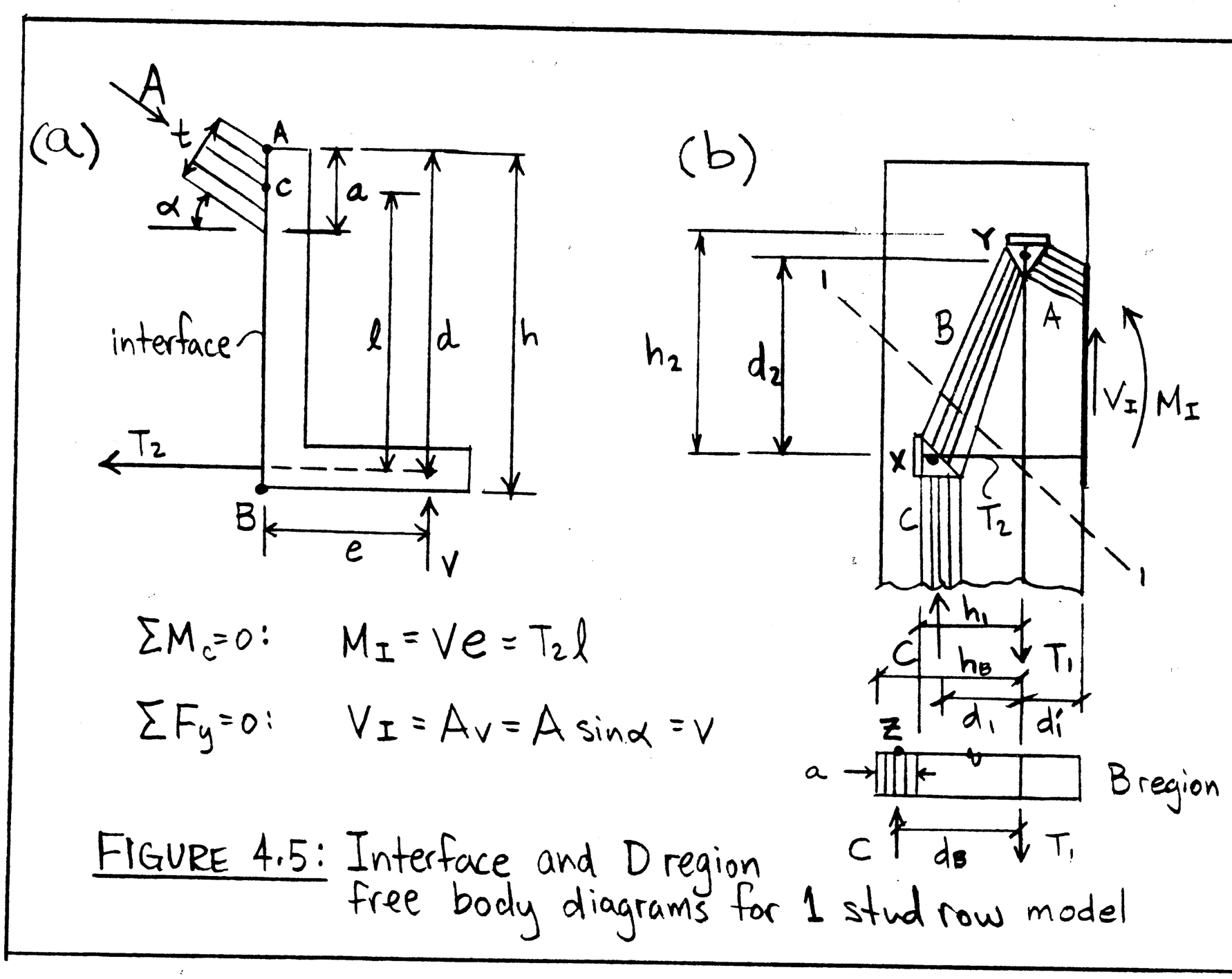

$\Sigma M_c = 0$: $M_I = Ve = T_2 \ell$

$\Sigma F_y = 0$: $V_I = A_V = A \sin\alpha = V$

FIGURE 4.5: Interface and D region free body diagrams for 1 stud row model

is pure rotation of the steel angle. As shear is transferred in addition to a moment, strut A must become inclined as illustrated by point B. The vertical component of strut A resists the interface shear, V_I, which is transferred across the interface through (shear) friction. As before, at maximum resistance the stud is yielding, while strut A crushes under the upper tip of the angle. The failure mechanism is still essentially a rotation of the steel angle relative to the concrete. The shear force at the interface may be further increased until the inclination of strut A reaches the friction angle, Φ. This condition for which the maximum possible shear force

across the interface has been reached, is represented by point C in Fig. 4.4. At point C the failure mechanism may be any combination of steel angle rotation and slip.

The slight reduction in moment capacity along curve A-C results from a reduced lever arm at the interface as described in section 2.11.1. Setting T'_s and N equal to zero in equations (2-27) and (2-28) of section 2.11.1 yields

$$M_I = T_{2y}\, d - \frac{V_I^2 + T_{2y}^2}{2\, b\, f_d'} \qquad (4\text{-}1)$$

$$\tan \alpha = V_I / T_{2y} \leq \tan\theta = \mu_s \qquad (4\text{-}2)$$

Equation (4-1) defines curve A-C, while equation (4-2) gives the inclination, α, of strut A. Its upper limit, Φ, defines the range of validity of equation (4-1). b denotes the width of the angle.

Point E in Fig. 4.4 corresponds to pure shear on the interface. According to shear friction, the maximum attainable force is given by

$$V_I = \tan \phi \;\; T_{2y} = \mu_s T_{2y} \qquad (4\text{-}3)$$

Equation (4-3) results from equation (4-2) by replacing the unequal with the equals sign. Strut A is inclined by Φ and its vertical and horizontal component equal the interface shear and the yield force in the stud, respectively. Since M_I = 0 at point E, the resultant line of action of strut A must intersect the line of action of T_2 at the interface. The failure mechanism is pure slip of the steel angle relative to the concrete. As the moment is increased at maximum shear to point D, strut A must translate upward such that its resultant intersects the interface above the stud and a flexural

lever arm develops at the interface. Strut A remains inclined at angle ϕ, while the stud yields. The failure mechanism is still pure slip of the steel angle.

Two points are worth noting in the inserts D and E in Fig. 4.4. The slip mechanism shown there also indicates movement away from the interface. Frictional failure mechanisms are always accompanied by a dilation of the material. It is this dilation which forces the steel crossing the interface to yield. Furthermore it must be stressed again that the location of the anchor plate for the longitudinal reinforcement for those truss models associated with points on the interface interaction diagram A-E represent the lowest possible position which allows for a truss model which can transfer the moment and shear associated with the point considered. If the anchor plate (point from which development length is measured) is at the location indicated in insert C, then strut B and A in insert D can spread as wide as permitted by the angle dimensions. Thus for a proper design, strut A does not crush at point D.

As the moment is further increased beyond point D, strut A, still inclined at ϕ, translates upward, thus further increasing the flexural lever arm, at the interface until it reaches the tip of the angle and contracts to its smallest possible depth: Point C is again reached. However, if the anchorage of the longitudinal reinforcement is located deeper than indicated in truss model C, point C cannot be reached and the D-region controls. This condition is discussed below.

While curve A-E describes the interface strength regardless of the conditions in the D-region "behind" it, lines F and F' define the D region capacity expressed in terms of the shear and moment at the interface. These lines essentially represent a flexural failure of the D region. Line F' represents a flexural failure of the D region in which the longitudinal reinforcement, T_1, yields as strut B crushes. Formulating moment equilibrium about the center of node X for section 1-1 in Fig. 4.5(b) and setting $T_1 = T_{1y}$, we get

$$T_{1y}\, d_1 = M_1 + V_1 (d_1' + d_1) \qquad (4\text{-}4a)$$

Node X may, for simplicity, be assumed to be fixed in a "safe" location or this location may be determined by

$$d_1 = h_1 - \frac{1}{2} \frac{T_{1y} - V_1}{b_{BX} f'_d} \qquad (4\text{-}4b)$$

where f'_d = diagonal compressive strength of strut B at node X

b_{BX} = effective width of compression strut B at node X

Similarly, line F represents the D region flexural capacity in which the stud, T_2, yields as strut B crushes. Formulating moment equilibrium about the center of node Y for section 1-1 in Fig. 4.5(b) and setting $T_2 = T_{2y}$, we get

$$T_{2y}\, d_2 = M_1 + V_1\, d_1' \qquad (4\text{-}5a)$$

Node Y may, for simplicity, be assumed to be fixed in a "safe" location or this location may be determined by

$$d_2 = h_2 - \frac{1}{2} \frac{T_{2y}}{b_{BY} f'_d} \qquad (4\text{-}5b)$$

where f'_d = diagonal compressive strength of strut B at Y

b_{BY} = effective width of compression strut B at Y

Equations (4-4b) and (4-5b) are based on the assumption that nodes X and Y are in a state of uniform biaxial compression equal to the diagonal compressive strength of strut B at the location of the node considered. This is of course not exactly true for a fixed size anchorplate such as a stud head. However, the assumption leads to simple equations which are readily recognized as the standard equations for determining the lever arm between tensile and compressive resultant for members subjected to flexure and axial load, except that the depth of the section is defined by the anchorage locations and that the (reduced) diagonal compressive strength of strut B is to be used. Once the "flexural lever arm" is known, flexural strength follows from moment equilibrium about the compressive resultant, here about the center of node X or Y, which leads to the left hand sides of equations (4-4a) and (4-5a). Thus it is seen that the truss model analysis of this D-region of type "opening knee joint" boils down to well-known flexural analysis.

However, equation (4-4) should not be misinterpreted to relate to the flexural failure of a horizontal section below node X. It relates to strut B and its (reduced) diagonal compressive strength, not to strut C. It only looks this way for reasons of equilibrium. The question arises then: How is it possible that strut B crushes while it is embedded on both sides in unstressed concrete? For the analogous plane stress problem it can be shown on the basis of the theory of plasticity that a failure mechanism exists in the D-region in which the concrete outside a straight line touching the anchor plates splits off in such a manner that strut B can crush. Thus the

concrete outside the anchor plates is useless and the anchorages determine "the depth of the section".

While the compressive strength for diagonally cracked concrete according to equations (2-1) to (2-3) indicate the correct trends -- i.e. the flatter a strut relative to the reinforcement, the lower the diagonal compressive strength -- it is unlikely that it directly applies to the present situation. Equations (2-1) to (2-3) have been experimentally determined for panels in plane stress subjected to uniform shear. The stress field shown in Fig. 4.5(b), on the other hand, is highly non-uniform and strut B must transversely reduce from the angle width at node Y to the stud head widths at node X. The diagonal compressive strength and the effective widths to be used in equations (4-4) and (4-5) remain to be determined experimentally. In the mean time conservative values should be used. However, as long as the lever arms, d_1 and d_2, are maximized and made large relative to the strut depths, the effect of the concrete strength is small.

In view of these present uncertainties too much accuracy is unwarranted. Thus equations (4-4b) and (4-5b) may be evaluated with conservative values for f'_d and b and for the worst loading condition (e.g. V_I=0). This is the meaning of the phrase "may be assumed fixed in a 'safe' location". Then equations (4-4a) and (4-5a) represent straight lines as shown in Fig. 4.4. Comparing the slopes of equation (4-4a) and (4-5a) shows that line F' is flatter than F. Hence the two lines plot as shown and intersect at a point F", which defines a flexural failure mode of the D region in which both the

stud and the longitudinal reinforcement yield as strut B crushes. The truss model for point F" is shown in Fig. 4.4.

Finally, for illustrative purposes, line G in Fig. 4.4 defines the flexural capacity of the B region as given by beam theory for the member itself. The equation for this line is obtained by formulating moment equilibrium about point Z, i.e. the center of the compression zone in the B region (Fig. 4.5(b)).

$$T_{1y}d_B = M_1 + V_1(d_1' + d_B) \tag{4-6a}$$

The location at point Z is determined by

$$d_B = h_B - \frac{a}{2} \tag{4-6b}$$

Dimension a is the flexural compression block depth given by beam theory,

$$a = \frac{T_{1y} - V_1}{b_{CB} \cdot 85f'_c} \tag{4-6c}$$

where f'_c = concrete compressive strength

b_{CB} = effective width of strut C in the B region

Inserting equation (4-6c) into (4-6b), a complete analogy between equations (4-4), (4-5), and (4-6) can be noted. Comparing the slopes of equations (4-4a) and (4-6a) shows that line G is flatter than line F' as shown in Fig. 4.4.

If the angle is loaded at a fixed eccentricity, e, (Fig. 4.5a), the loading path in Fig. 4.4 is represented by an inclined straight line through the origin. If the construction tolerances in the eccentricity e are considered, the possible loading paths lie in a cone shaped zone radiating from the origin of the interaction

diagram. The intersection of the cone with the interaction curve closest to the origin determines the connection strength and the failure mode.

In design, the lever arms d_1 and d_2 (Fig. 4.5b) as well as the steel volumes can be proportioned so as to adjust the relative positions of the different curves in the interaction diagram. For instance, if an interface failure mode is desirable, lines F and F' must plot sufficiently out so that the loading cone intersects the interface integration diagram A-E before lines F' or F. If a B region flexural failure mode is desirable, (connection develops the member strength), then line G must plot sufficiently inside both curve A-E and lines F and F' so that it is first intersected by the loading cone. In many practical cases the horizontal shear plateau, line E-D-...is large enough (due to sufficient lever arms d_1, d_2) and the eccentricity e small enough that the loading cone intersects the horizontal shear plateau first and design of the connection by shear friction at the interface alone is justified. However, if the lever arms d_1 or d_2 are small, e.g. the stud extends only to middepth of the member then flexural failure of the D region might control, and it must be checked.

Performance of this connection is dependent on two conditions, (1) the location of the anchorage points and truss elements (geometry), and (2) the steel, concrete, and anchorage capacities (strength). The anchorage and steel locations should allow the lever arms d_1 and d_2 to be maximized so that the largest possible flexural capacities of the D region can be obtained. In design, the anchor

plate location for the longitudinal rebar (T_1) may be safely defined as the point of intersection between strut A, inclined at ϕ, and located at the tip of the vertical leg of the steel angle, and the longitudinal reinforcement (T_1). The studs should be extended as far as possible to the opposite face of the panel while observing the cover requirements. Maximizing the lever arm d_1 also implies that the longitudinal reinforcement, T_1, should be placed as close to the angle as cover requirements permit. For this reason and because, as will become clear in section 4.5, this steel actually represents the suspender bars called for in section 2.4.3, the longitudinal steel shown here is in addition to panel reinforcement placed usually at the center of the panel.

If the only longitudinal reinforcement is located at the center of the connected member and the stud extends only to the center, too, then the lever arm d_1 is zero and the connection relies solely on the concrete tensile strength to turn the moment around the corner. These requirements are exactly analogous to those of the opening knee joint of section 3.2.1, and the discussion of anchorage and/or steel location deficiencies in section 3.2.3, Fig. 3.8, is equally applicable here. The reader is encouraged to review design handbooks for such deficiencies.

Since the forces anchoring the steel elements of the truss model are supplied by the compression elements of the truss, reinforcement anchorage becomes the task of designing the "truss connections" between tension and compression elements. While these "truss connections" (bar anchorages) must be in the correct location as

discussed above, they must also be strong enough. The ideal anchorage is an anchor plate. Welded headed studs almost ideally realize it; but the head must be in the correct location. Except for an anchor plate, the longitudinal reinforcement, T_1, is most efficiently and compactly anchored by looped rebars with the plane of the loop parallel to the interface plane.

Usually also a horizontal force acts on the angle. Equations (4-4) through (4-6) can be easily modified to include axial tension, N_I, at the interface: T_{2y} must be replaced by $(T_{2y}-N)$, while the moment of N_I about the stud must be included in the interface moment, M_I. The equations for the interface interaction diagram with axial force have been presented in section 2.11. Since the member is subjected to shear in the presence of axial tension at the interface, a diagonal shear compression fan enters the D-region from the member. This shear flows directly into T_2 without further affecting the D-region, if the tension on the interface is at the level of the stud. Finally it should be noted that if the applied load is or can be downward on the angle seat bearing connection (Fig. 4.2(a)), studs must be located of course at the upper tip of the angle and the closing knee joint of section 3.2.2 would serve as the corresponding analogy. Two rows of studs are treated in the next section.

4.3 ANGLE SEAT BEARING CONNECTION WITH TWO STUD ROWS

With the understanding gained from the study of the single stud row detail, it is now possible to generalize the truss model for the case of two stud rows. Figure 4.6(a) shows the connection hardware

and Fig. 4.6(b) shows a possible configuration of the truss model.

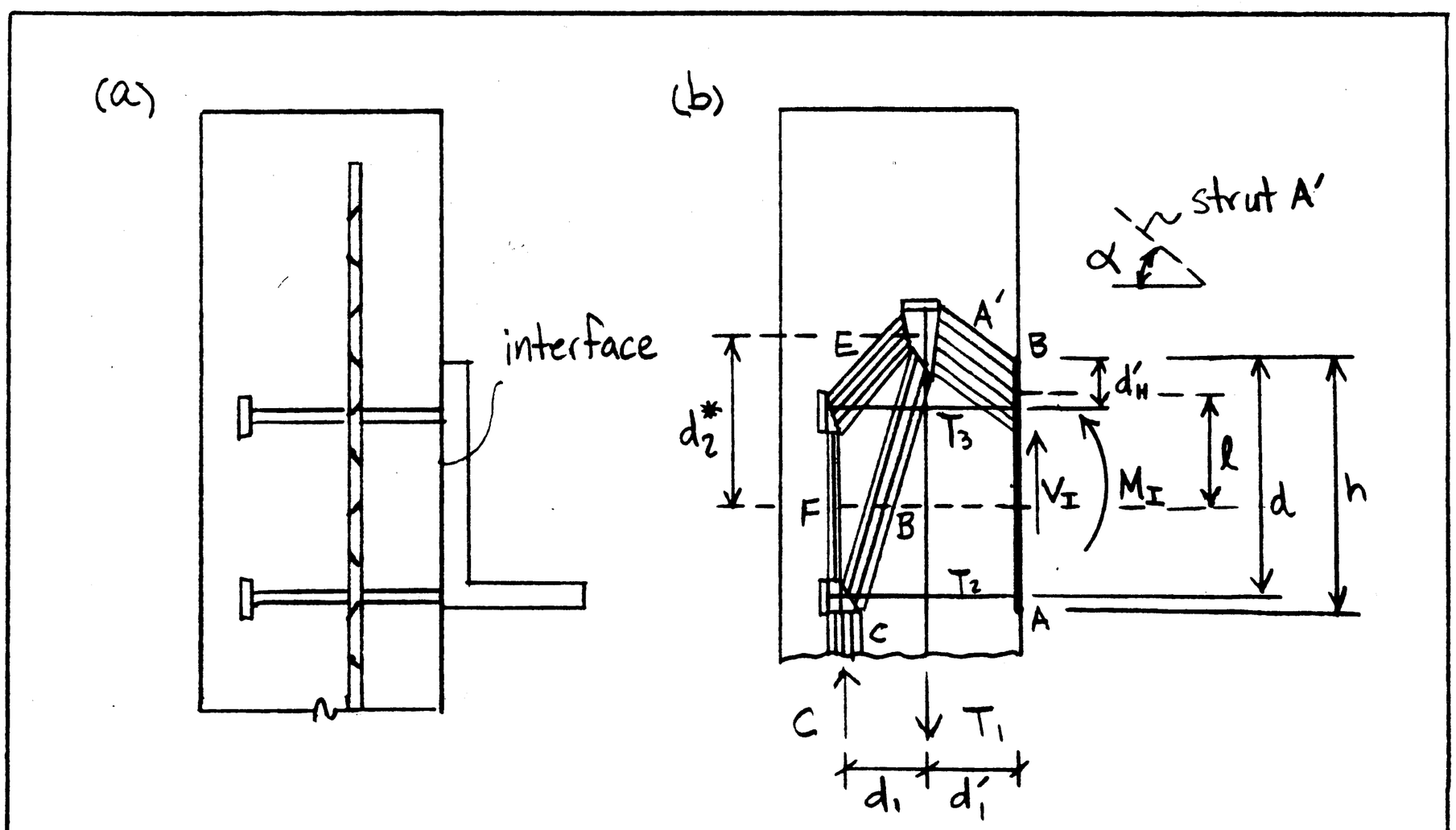

FIGURE 4.6: Angle seat bearing connection with 2 stud rows

Treatment of this truss and all of the assumptions are identical to those of the previous section. For clarity, an interface axial load is again omitted. The connection interaction diagram expressed in terms of the moment, M_I, and shear, V_I, at the interface is shown for this detail in Fig. 4.7. Curve A-F represents the capacity of the interface regardless of the strength of the adjacent D region. Lines G, G', and G" represent the flexural capacity of the D region depending on which reinforcement yields and which compression strut crushes. Line H represents the flexural capacity of the B region as determined by beam theory.

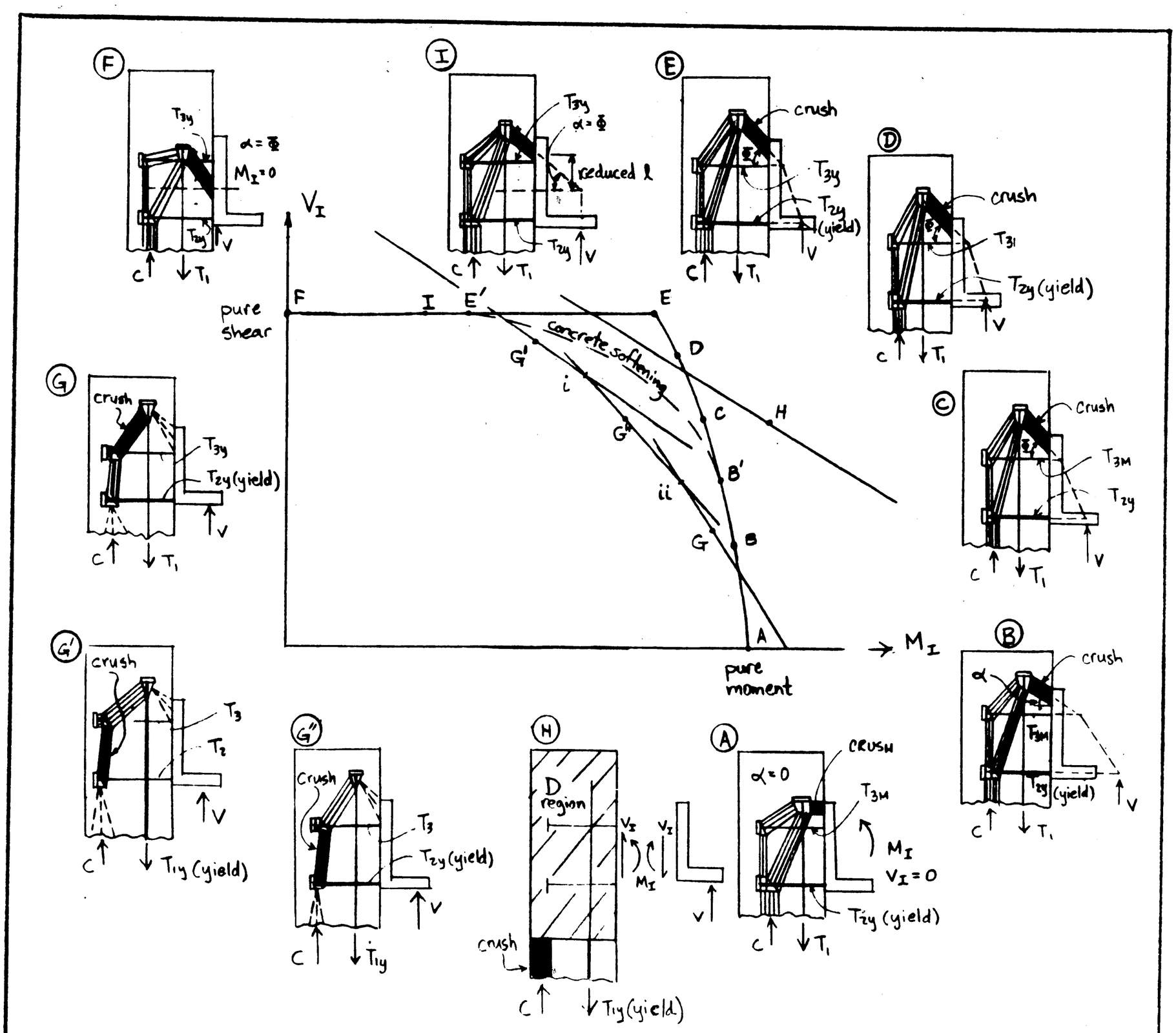

FIGURE 4.7: Connection interaction diagram in terms of shear and moment at the interface for the double stud row angle seat bearing connection

Inserted truss models again visualize the state of stress in the different failure modes associated with different regions of the connection interaction diagram. Similarly as in section 4.2, the truss models relating to the interface interaction diagram only indicate where nodes and anchorages would have to be, if the

interface controls, while the truss models for the D-region reflect the actual specified location of the anchorages.

In describing these regions and failure modes, the notation and dimensions given in Fig. 4. 8 are used. Figure 4.8(a) labels and

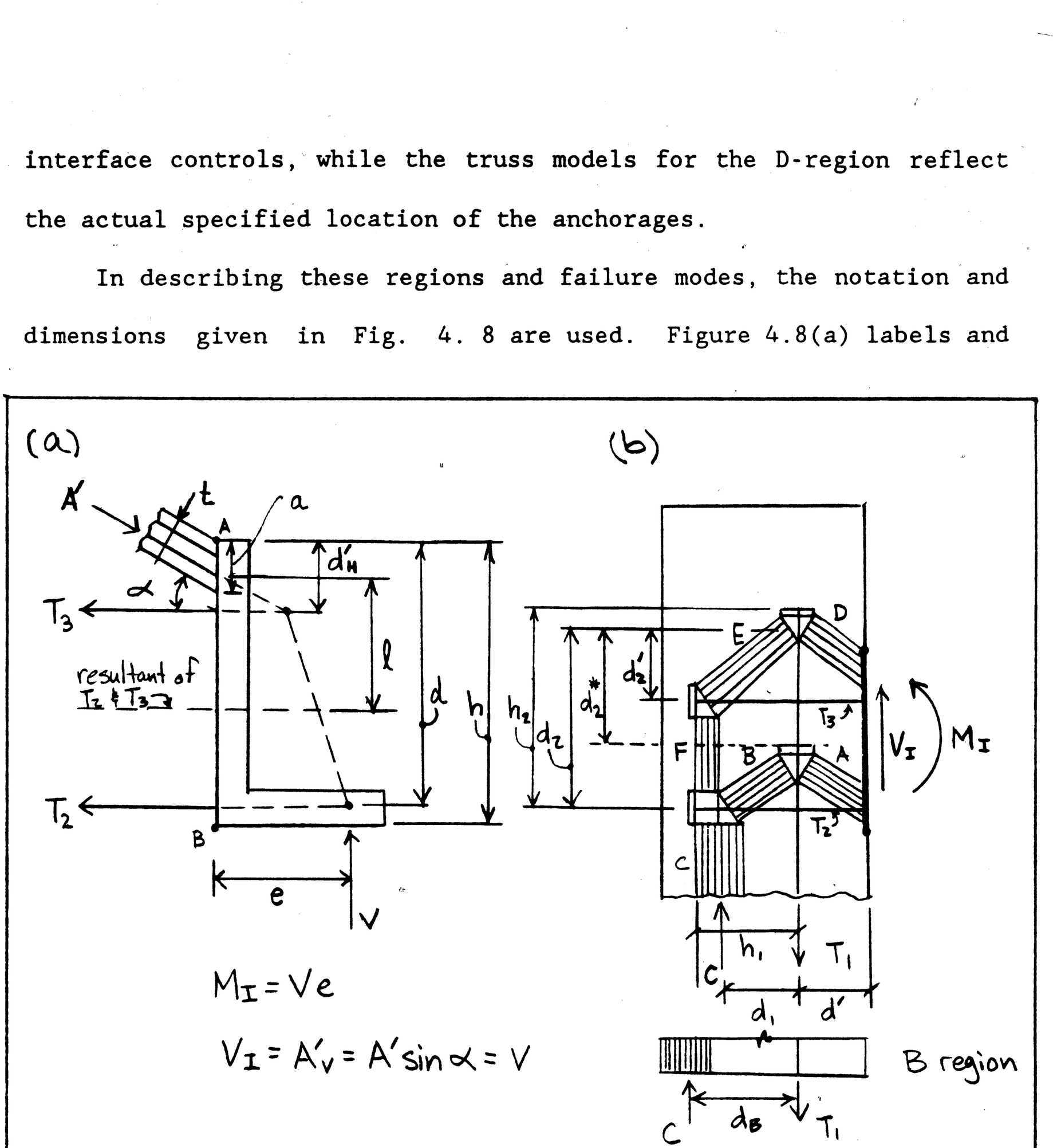

FIGURE 4.8: Interface and D region free body diagrams for 2 stud row model

dimensions the interface and the steel angle, while Fig. 4.8(b) does the same for the truss model in the D region. Note that the truss model shown in Fig. 4.8(b) is the most obvious extension of the one-stud model to the two-stud detail: It simply consists of two truss

models of the type shown in insert D of Fig. 4.4 staggered above each other.

Again, the interface interaction diagram is first discussed. The conditions of the interface shown in Fig. 4.8(a) exactly correspond to those of the interface treated in section 2.11.1, Fig. 2.36. Except for the differences in notation, the interaction diagram is therefore described by equations (2-27), (2-28), (2-31), (2-32), and (2-33).

At Point A the interface is subjected to pure flexure. The concrete crushes under the tip of the angle, while the bottom stud, T_2, yields. The top stud has an initial value, T_{3M}, which may be obtained from a strain compatibility analysis at the interface.

Since maximum moment capacity calls for the largest possible lever arm, ℓ, (Fig. 4.8(a)), not only strut D but also strut A (see Fig. 4.8(b) for labeling) must be located at the tip of the angle. Strut A and D thus combine into one strut A', which must be horizontal of course. The corresponding truss model in the D region has already been shown in Fig. 4.6(b), where $\alpha = 0$. The failure mechanism is a pure rotation of the steel angle. As shear is transferred in addition to moment, point B in Fig. 4.7, strut A' must become inclined (Figs. 4.8(a) and 4.6(b)). The vertical component of strut A resists the interface shear, V_I, through shear friction. The force in the top stud is assumed to remain at its initial value, T_{3M}, while the bottom stud yields. The failure mechanism is still essentially a rotation of the steel angle. As the shear force is increased further, the inclination of strut A' must increase, too.

However, the inclination of strut A' is limited by the angle of friction, Φ, at the interface. Strut A' reaches this limit at point C, where the failure mechanism becomes a combination of steel angle rotation and slip. The slight curvature of A-C results from a reduced lever arm at the interface as described in section 2.11.1. Curve A-C is described by equations (2-27) and (2-28) of section 2.11.1 (where $T'_s = T_{3M}$, $T_y = T_{2y}$, $M = M_I$, $V = V_I$, and $N = 0$).

A further increase of the shear force at the interface is only possible if the normal component of strut A' across the interface increases, i.e. if T_3 algebraically increases. As the top stud force increases from T_{3M} to some value T_3, the normal component of strut A' and, hence, the frictional resistance, increases. Strut A' remains concentrated at the angle tip with an inclination $\alpha = \Phi$. Its increasing depth reduces the lever arm and thus the moment further. The failure mechanism remains a rotational slip of the steel angle. Region C-E of Fig. 4.7 is described by equations (2-31) and (2-32) of section 2.11.1 (where $T'_s = T_3$, $T_y = T_{2y}$, $M = M_I$, $V = V_I$, and $N = 0$).

The limit of equations (2-31) and (2-32) is reached at point E where the top stud yields, $T_3 = T_{3y}$. The maximum attainable shear force, has been reached. The failure mechanism may now be any combination between a slip-rotational mechanism and a pure slip mechanism of the steel angle.

If the top stud is close to the upper tip of the steel angle such that compression strut A' intersects it, the question arises whether strain compatibility indeed allows the top stud, T_3, to yield in tension. It is precisely this strain compatibility condition

which is expressed by equation (2-2) of section 2.1 (where $\theta = \alpha$). It expresses that if T_3 is subjected to a tensile strain, ϵ_x, strut A' must be subjected to a transverse tensile strain, ϵ_1. This transverse tensile strain reduces the concrete compressive strength according to the concrete softening law equation (2-1). Equations (2-1) and (2-2) can iteratively be considered in equations (2-31) and (2-32) and lead to the dashed interaction curve B'-E'. As the tensile strain in T_3 increases, the depth of compression strut A' now increases not only due to the increasing magnitude of A', but also, more importantly, due to the reducing diagonal compressive strength. Thus curve B'-E' "bends over" much more sharply.

Since equations (2-1) and (2-2) have been derived from panels in uniform shear, it is not clear whether they directly apply to the interface conditions described here. If tie T_3 consists of ordinary reinforcement welded to the angle, the concrete "behind" the interface is bonded to it and torn apart as described. It is less clear what happens, if tie T_3 consists of studs which have no bond strength along the shaft. Furthermore, while at a rough crack, shearing can force the "compression stud" into tension, it is not clear whether this is possible for a relatively smooth interface. For these reasons the "compression stud" is also more likely to act in dowel action than the "tensile stud". These questions must be experimentally clarified. In the mean time it is reasonable to use a conservatively reduced diagonal compressive strength, f'_d, in the

vicinity of point E, since it leads to the intuitively expected result that point E cannot be reached.

Point F in Fig. 4.7 corresponds to pure shear at the interface. According to shear friction, the maximum attainable shear is given by equation (2-33) of section 2.11.1 (where $T'_y = T_{3y}$, $T_y = T_{2y}$, $V = V_I$, and $N = 0$). Since $M_I = 0$ at point F, the line of action of strut A' or of the resultant of struts D and A must intersect the line of action of the resultant of T_{2y} and T_{3y} at the interface. Only a pure slip mechanism of the angle is possible. As the moment is increased from zero, point I, strut A' (or D and A) must translate upward such that its line of action intersects the interface above the resultant of the studs T_{2y} and T_{3y}, and a flexural lever arm develops at the interface. Strut A' (or D and A) remains inclined at angle Φ as the studs yield; the failure mechanism is pure slip of the steel angle. As far as the interface is concerned, the diagonal compressive stress distribution is only determined by the location of its resultant (which is fixed for a given moment) and the size of the angle. Whether Strut A' in truss model F of Fig. 4.7 can spread into two struts A and D as shown in Fig. 4.8(b), depends on the anchorage locations in the D-region. As long as the D-region does not control, various truss models are possible there. The interaction diagram controlled by the D-region is discussed below.

While curve A-E-F describes the interface interaction diagram regardless of the D-region capacity, lines G, G', and G" consider the flexural failure of the D-region. Fig. 4.9(a) shows a third possible truss model for the D-region which could as well have been used

before, since it is statically equivalent to that in Fig. 4.6(b). As

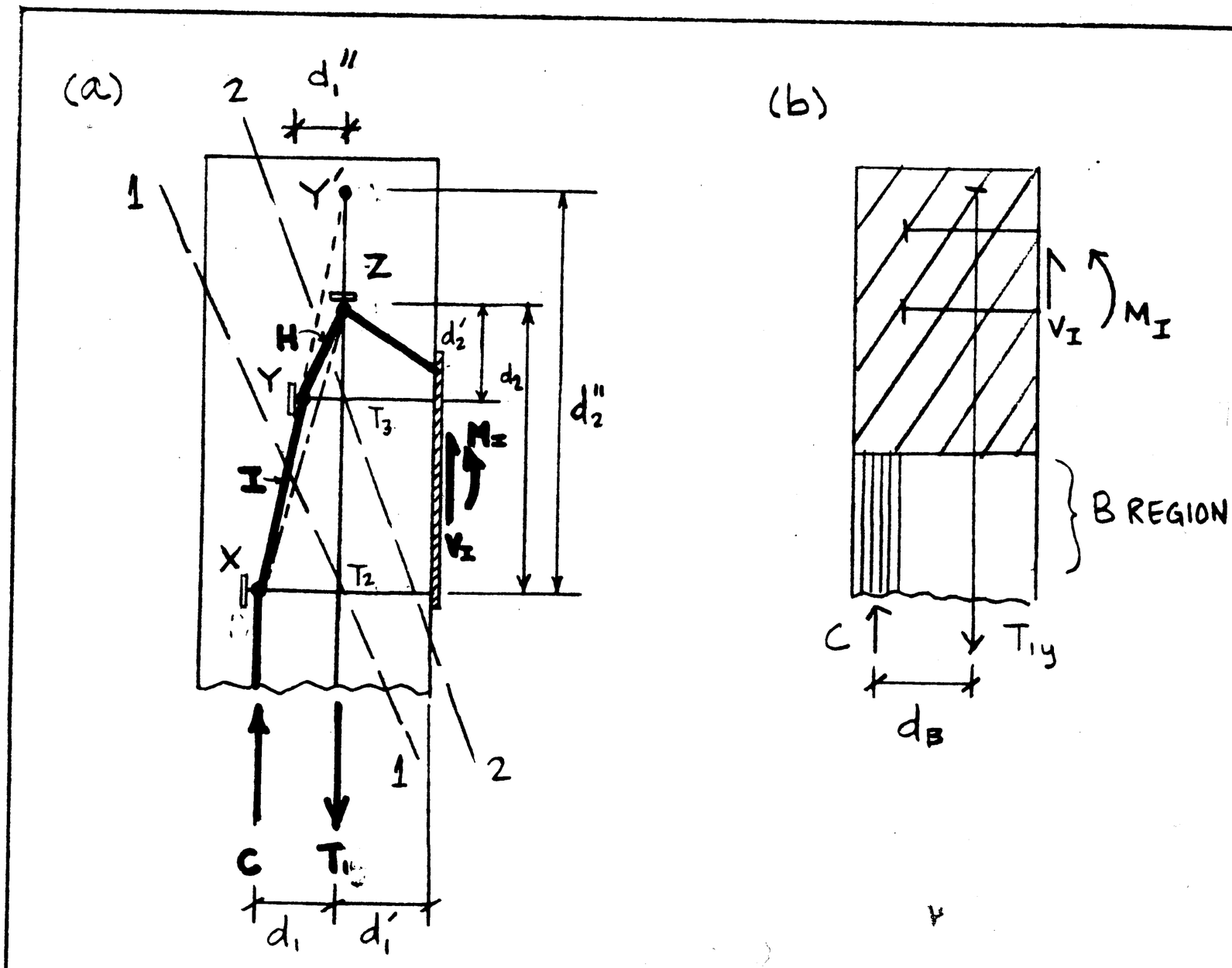

FIGURE 4.9 : D and B region flexural capacities

noted in section 2.3, Fig. 2.5, fans (including compression zone) and arches can equivalently replace each other and require the same amount of reinforcement. Here the "fanning struts" B, E, and the "compression zone strut" F of Fig. 4.6(b) are combined into the "arching struts" H and I of Fig. 4.9(a). For clarity only the discrete truss of the resultants is shown. The line of action of the resultant of struts B and E coincides with that of strut H and intersects the line of action of strut F at the line of action of the resultant of ties T_2 and T_3. Similarly, the line of action of the resultant of struts B and F coincides with that of strut I. Note in

passing, how much of the reasoning with truss models is graphic statics!

While the forces, T_1, T_2, and T_3 are exactly the same in the truss models of Figs. 4.6(b) and 4.9(a) for analogous geometry, the anchorage requirements are different. The "arching" truss model of Fig. 4.9(a) permits the anchorage of T_3 to be located closer to the interface than the "fanning" truss model of Fig. 4.6(b). Thus if the capacity of the D-region is to be assessed not only from the viewpoint of the strength of the concrete, reinforcement, and anchorages, but also -- since it has been shown to be so critical in chapter 3 -- from the view point of the anchorage locations, the "arching" truss model of Fig. 4.9(a) is optimal. It is assumed, though, that the anchorage of T_3 is not located inside the dash-dotted line X-Z in Fig. 4.9(a). For this case other truss models have to be considered.

Using the notation of Fig. 4.9(a) the D-region capacity can again be computed by formulating moment equilibrium about the point of intersection of the lines of action of two elements crossing the selected section and considering the yield conditions for the element(s) remaining in the equilibrium equation. Considering section 1-1, formulating moment equilibrium about the center of node X, and setting $T_1 = T_{1y}$ gives

$$T_{1y}d_1 = M_1 + V_1(d_1 + d_1') \qquad (4\text{-}7)$$

Equation (4-7), shown as line G' in Fig. 4.7, represents a flexural failure of the D-region in which the longitudinal reinforcement, T_1,

yields as strut I crushes near node X. The geometry of the truss model is optimal with respect to T_1, if the lever arm, d_1, is maximal, i.e. if point X is located as far out as equilibrium, anchorage, and concrete strength permit. This location is again given by equation (4-4b) (where strut B is now strut I) and may be assumed fixed at a "safe" value as discussed in section 4.2. Equation (4-7) represent then a straight line.

Formulating moment equilibrium about point Y' for section 1-1 and setting $T_2 = T_{2y}$ gives $T_{2y}\, d''_2 = M_I + V_I d'_1$. The geometry of the truss model is optimal with regard to T_2 if the lever arm d''_2 is maximal, i.e. of d''_1 is maximum and d_1 is minimum. Since d_1 can only be reduced until the longitudinal reinforcement, T_1, yields, its minimum value can be found from equation (4-7). Solving equation (4-7) for d_1 expressing d''_2 by d_1 and d''_1, and inserting d''_2 in the equilibrium equation above gives equation (4-8). This equation can also be found by formulating moment equilibrium about the center of node Y for section 1-1 and setting $T_1 = T_{1y}$ and $T_2 = T_{2y}$, that is

$$T_{2y}(d_2 - d'_2) + T_{1y}d''_1 = M_I + V_I(d''_1 + d'_1) \qquad (4\text{-}8)$$

Equation (4-8), shown as line G" in Fig. 4.7, represents a flexural failure mode of the D-region in which the ties T_1 and T_2 yield as strut I crushes near node Y. The optimum geometry of the truss model leading to maximum resistance is achieved, if d''_1 is maximum as observed above, i.e. if point Y is located as far out as equilibrium, anchorage location, and concrete strength permit. This location can be calculated analogously as in section 4.2.

Considering section 2-2, formulating moment equilibrium about the center of node Z, and setting $T_2 = T_{2y}$ and $T_3 = T_{3y}$ based on similar reasoning as above gives

$$T_{3y}d'_2 + T_{2y}d_2 = M_1 + V_1 d'_1 \qquad (4\text{-}9)$$

Equation (4-9), shown as line G in Fig. 4.7, represents a flexural failure mode of the D-region in which ties T_2 and T_3 yield as strut H crushes near node Z. The optimum geometry of the truss model leading to maximum resistance is achieved, if the lever arms d_2 and d'_2 are maximum, i.e. if point Z is located as high as equilibrium, anchorage location, and concrete strength permit. This location is again given by equation (4-5b) (where strut B is now strut H, node Y is node Z, and T_{2y} is replaced by $T_{2y} + T_{3y}$). Finally, formulating moment equilibrium about the compressive resultant of the B region and setting $T_1 = T_{1y}$ gives the flexural capacity of the B region (Fig. 4.9(b)).

$$T_{1y}d_B = M_1 + V_1(d_B + d'_1) \qquad (4\text{-}10)$$

where d_B is again given by equations (4-6b) and (4-6c). Equation (4-10) is also shown in Fig. 4.7 as line H. Comparing the slopes of equations (4-10), (4-7), (4-8), and (4-9) shows that lines H, G', G", and G, respectively, become steeper in this order. An axial force at the interface can be readily included in equations (4-7) through (4-10) by including the moment of the axial force about the point considered for each equation or as described in section 4.2.

In design, the location of the reinforcement anchorage points and internal truss elements, as well as the relative steel and

concrete capacities can be chosen so as to adjust the relative position of the various failure mode curves in Fig. 4.7 and achieve the desired failure mode for the loading considered. The discussion presented in section 4.2 on the single stud row model is equally applicable here and shall not be repeated except to emphasize that the lever arm ratios, d_1/d_B and $d"_1/d_B$, as well as the lever arms d_1, $d_1"$, and d_2 themselves must be made as large as possible. Once again, this detail is analogous to the opening knee joint treated in section 3.2.1; thus the discussion of anchorage deficiencies in section 3.2.3, and Fig. 3.8 also applies here. The reader is encouraged to review design handbooks for such deficiencies.

Comparing the D-region truss models for the angle seat bearing connection and the monolithic knee joint with corbel shows that tie T_2 (Fig. 4.6(b)) plays the role of the primary flexural corbel reinforcement, while tie T_3 plays the role of the closed stirrups or hoops, although it is in an inefficient location for this purpose. It has been assumed so far (Fig. 4.6) that ties T_2 and T_3 are realized with welded headed studs, since they are frequently used and efficiently anchored, (if the heads are in the correct location). If ties T_2 and T_3 are realized with ordinary reinforcement welded to the angle, it is clear from the treatment of opening knee joints in chapter 3 that both bars must be bent upward and anchored by a development length beyond the bend. In this way struts B and E (Fig. 4.6(b)) can bear into the bends and struts C and F supply the forces developing the vertical legs. If both bars are bent away from the angle (i.e. bar T_2 is bent downward), then bar T_2 is anchored

precisely like the opening knee joint details which performed so poorly (Fig. 3.10(e) and 3.12(c)).

Bending bar T_3 in the "wrong" direction might be less detrimental, since the arching truss model of Fig. 4.9(a) shows that its anchorage may be located somewhat further away from the opposite face. The best bar anchorage is of course achieved with horizontal loops (provided that the center of the bend is close enough to the opposite face).

4.4 ANGLE SEAT BEARING CONNECTION WITH ONE STUD ROW AND WELDED LONGITUDINAL REINFORCEMENT

Differently from the angle seat bearing connections treated in the last two sections, in this connection the longitudinal reinforcement is welded to an embedded steel angle as illustrated in Fig. 4.10(a). The simplest form of this type of connection with a single row of studs welded to the bottom of the angle is again treated first. The truss model for the D region of this detail is shown in Fig. 4.10((b). Treatment and assumptions are similar as in section 4.2. The interaction diagram for this connection, expressed in terms of the interface shear and moment, is shown in Fig. 4.11 along with inserted truss models visualizing the state of stress for the various failure modes. Lines F-G-H-I in Fig. 4.11 represent the angle-panel interface capacity, while lines A-C-E represents the D region capacity. Line K defines the flexural capacity of the B region outside the connection. Fig. 4.12 shows notation, labeling, and dimensions (a) for the interface and angle, and (b) for the truss

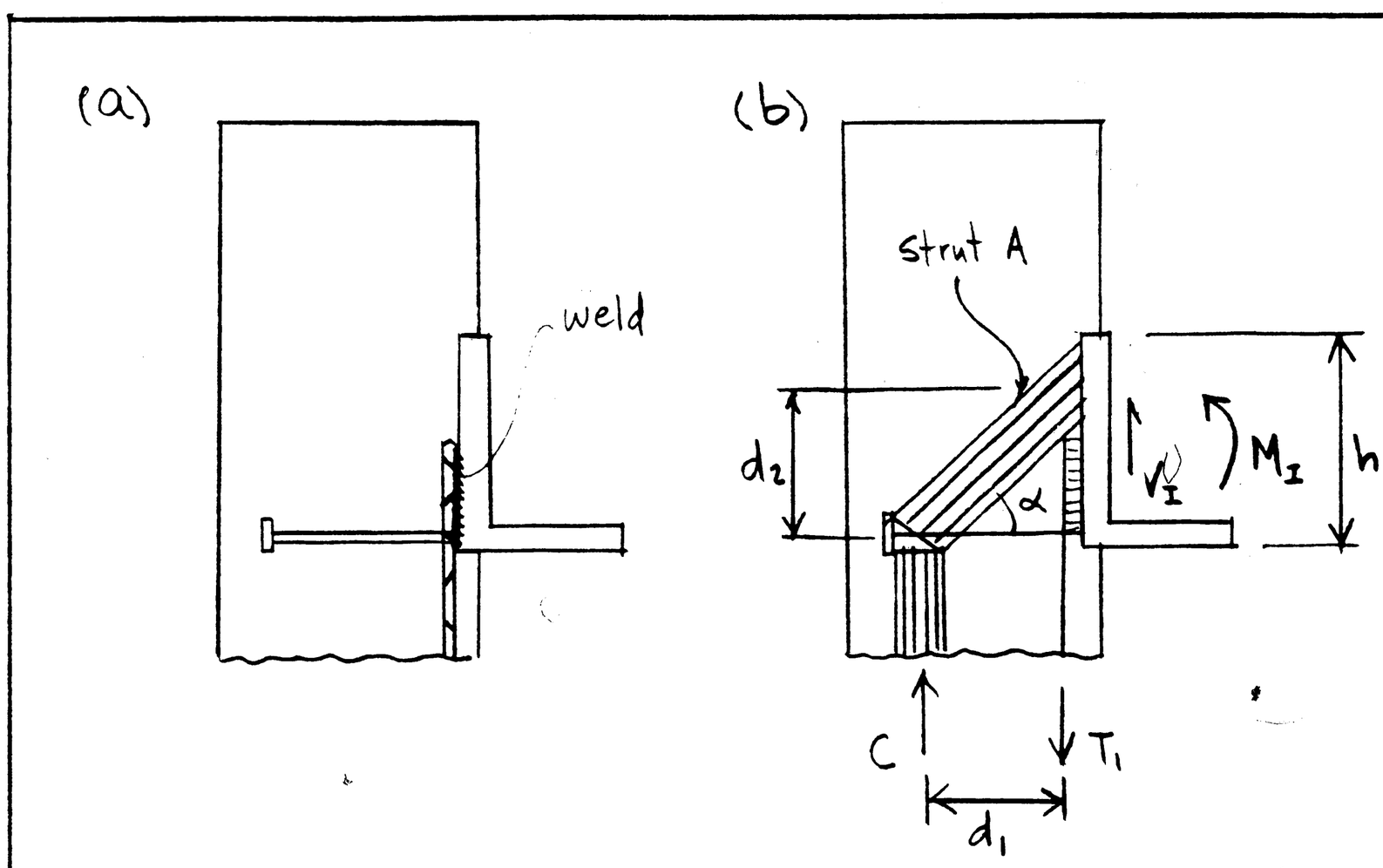

FIGURE 4.10: Angle seat bearing connection with welded longitudinal reinforcement

model in the D region and is referred to in the following discussion of the connection interaction diagram in Fig. 4.11.

As in previous sections, the interface interaction diagram F-G-H-I regardless of the D region detailing is first described (Fig. 4.11). Point F corresponds to a pure moment at the interface. Strut A in Fig. 4.12(a) is horizontal, $\alpha = 0$, and is located at the upper tip of the angle. Accordingly the maximum moment is given by

$$M_1 = T_{2y}\left(\ell - \frac{1}{2}\frac{T_{2y}}{.85f'_c b}\right) \qquad (4\text{-}11)$$

where b is the width of the angle. As the shear force at the interface is increased from zero to $V_I = T_{1y}$ at point G, it can be

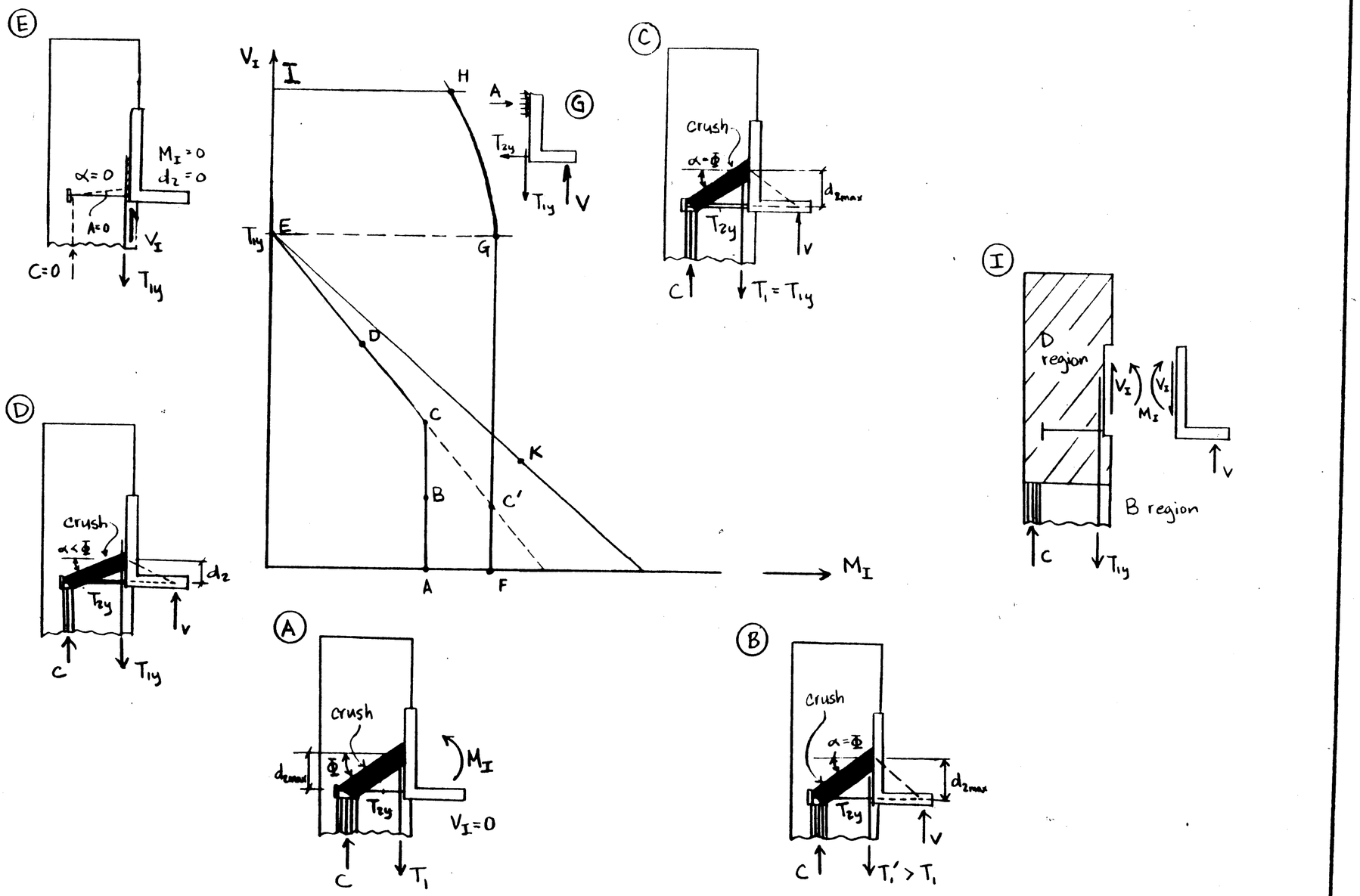

FIGURE 4.11: Connection interaction diagram in terms of shear and moment at the interface for the single stud row with welded longitudinal reinforcement angle seat bearing connection

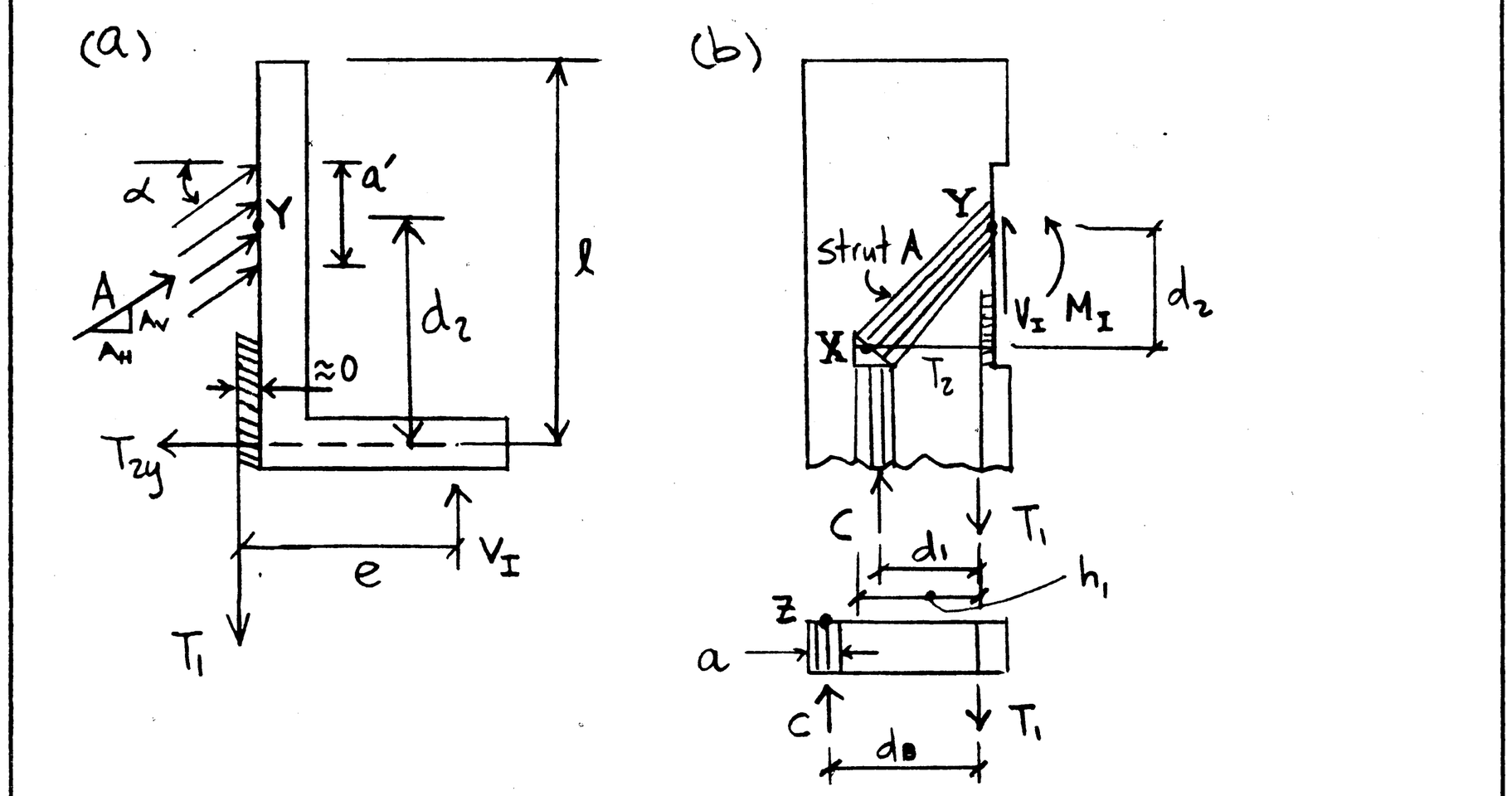

FIGURE 4.12: Interface and D region free body diagrams for welded longitudinal reinforcement model

directly resisted by the vertical reinforcement, T_1, welded to the angle, and strut A remains horizontal and located at the tip of the angle. Thus the moment capacity is not affected and given by equation (4-11).

If the shear force is increased above the yield strength of the vertical reinforcement, T_{1y}, the additional shear force must be resisted by (shear) friction and strut A in Fig. 4.12(a) must become inclined at a negative angle, $\alpha < 0$, while remaining at the upper tip of the angle. When its inclination reaches the friction angle, $\alpha = \phi$ the maximum possible shear force is reached

$$V_I = T_{1y} + T_{2y}\tan\phi \quad ; \quad \tan\phi = \mu_s \tag{4-12}$$

Equation (4-12) describes line I-H in Fig. 4.11. The portion of the interface interaction diagram above line E-G, namely lines G-H-I, is identical to lines A-C-E in Fig. 4.4 and given by equations (4-1) to (4-3).

No truss models for the D region "behind" the interface are shown in Fig. 4.11 for points on the interface interaction diagram F-G-H-I, since none exist. Strut A in Fig. 4.12 can neither be horizontal nor point upward from the tip of the angle, since there is no reinforcement there to anchor its other end. As shown by the truss model for the D region, Fig. 4.12(b), strut A must point downward from the angle to the anchorage of tie T_2, where it supplies at node X the force anchoring this tie. The connection interaction diagram controlled by the D region is described below.

Point A describes the D region capacity if only a pure moment is transferred at the interface. For the maximum possible pure moment resistance, the lever arm d_2 must be maximized as the tie, T_2, yields. But the length of lever arm, d_2, is controlled *either* by the steel angle's vertical height, *or* the point where the line of action of strut A through node X intersects the interface when strut A is maximally inclined at the friction angle, Φ, (measured with respect to the normal of the interface

$$d_{2(max)} = \ell - \frac{a'}{2} \tag{4-13a}$$

or

$$= d_1 \tan \phi \qquad (4\text{-}13b)$$

The smaller controls. Moment equilibrium about the center of node Y and setting $T_2 = T_{2y}$ gives the maximum possible moment capacity

$$M_1 = T_{2y}\, d_{2(max)} \qquad (4\text{-}14)$$

where $d_{2(max)}$ is given by equation (4-13). Equation (4-14) shown as line A-C in Fig. 4.11 represents a D-region failure mode in which tie T_2 yields as strut A slips along the angle (equation (4-13b), or crushes (equation (4-13a).

Formulating moment equilibrium about the center of node X in Fig. 4.12(b) and setting $T_1 = T_{1y}$ gives

$$M_1 = (T_{1y} - V_1)d_1 \qquad (4\text{-}15)$$

Equation (4-15), shown as line C-E in Fig. 4.11, represents a flexural D-region failure in which the longitudinal reinforcement, T_1, yields as strut A crushes. As in section 4.2, node X is assumed to be fixed in a "safe" location given by the minimum of equation (4-4b).

In the following, the behavior of the connection along the D-region interaction diagram A-C-E is discussed in more detail and from a slightly different point of view. Let us begin at point A which, as described earlier, represents pure moment and for which $\alpha = \phi$, $d_2 = d_{2(max)}$, and $T_2 = T_{2y}$. Vertical equilibrium of the angle (Fig. 4.12(a)) clearly shows that the force T_1 equals the vertical component of strut A, i.e. A_v if the angle is subjected to a moment only and the vertical force is zero. If a shear force, V_I, is

introduced in addition to the maximum moment at the interface, this shear force can be directly transferred into T_1, thus increasing T_1 to $T_1 = A_v + V_I$ (point B). The shear force can be further increased without affecting the moment capacity until $T_1 = T_{1y}$ at point C. At this point, vertical equilibrium of the steel angle gives

$$V_I = T_{1y} - A_v \tag{4-16}$$

As can be seen from equation (4-16), a further increase in interface shear, V_I, beyond point C is only possible, if the vertical component of strut A decreases. However, since horizontal equilibrium of node X demands

$$A_v = T_2 \tan \alpha \tag{4-17}$$

a decrease in A_v requires that either the inclination of strut A, α, or the tie force, T_2, must decrease from their maximum values Φ and T_{2y}. Since moment equilibrium of the angle requires

$$M_I = T_2 d_2 = T_2 d_1 \tan \alpha \tag{4-18}$$

both a reduction in α and, hence, lever arm, $d_2 = d_1 \tan\alpha$, and a reduction in T_2 result in a reduced moment capacity, M_I. In a nutshell, an increase in shear capacity beyond point C must be accompanied by a reduction in moment capacity. Indeed, inserting equation (4-17) into equation (4-16), solving equation (4-16) for $T_2 \tan\alpha$, and inserting the result in equation (4-18) yields again equation (4-15). The maximum attainable shear force at the

interface, $V_I = T_{1y}$, is reached at point E and can only be transferred by the D-region if the interface moment is zero.

Finally, Fig. 4.11 shows also line K which represents the B region's flexural capacity. Its equation (4-6a), where $d_1' = 0$, is obtained by formulating moment equilibrium about the compressive resultant in the B region in Fig. 4.12(b) and setting $T_1 = T_{1y}$.

The longitudinal steel, T_1, yields as compression strut C crushes along the extreme fibers of the member. The location of the compressive resultant is given by equations (4-6b) and (4-6c).

As observed in the previous sections, in design the relative locations of these lines can be adjusted by proportioning and locating the reinforcement wisely. As the equations show, moment resistance can be maximized by maximizing the lever arms d_1 and d_2. The shear resistance can be increased by increasing the longitudinal reinforcement, T_1 and/or the lever arm d_1.

To eliminate the (shear) friction problem of strut A at the interface, a cross bar can be welded to the steel angle tip, which prevents strut A from slipping up, Fig. 4.13(a). Providing an additional stud row welded to the tip of the angle, Fig. 4.13(b), is useless from a truss modeling point of view, and it can only serve in reverse dowel action in preventing strut A from slipping up. Rather, it is much better to weld the second stud row nearer to the mid-depth of the angle leg, Fig. 4.13(c). This stud row now serves the exact same function as a stirrup in a beam. Rather than increase the shear capacity of this connection (which is limited by equation (4-15)) as one might expect, the addition of both the cross bar and the second

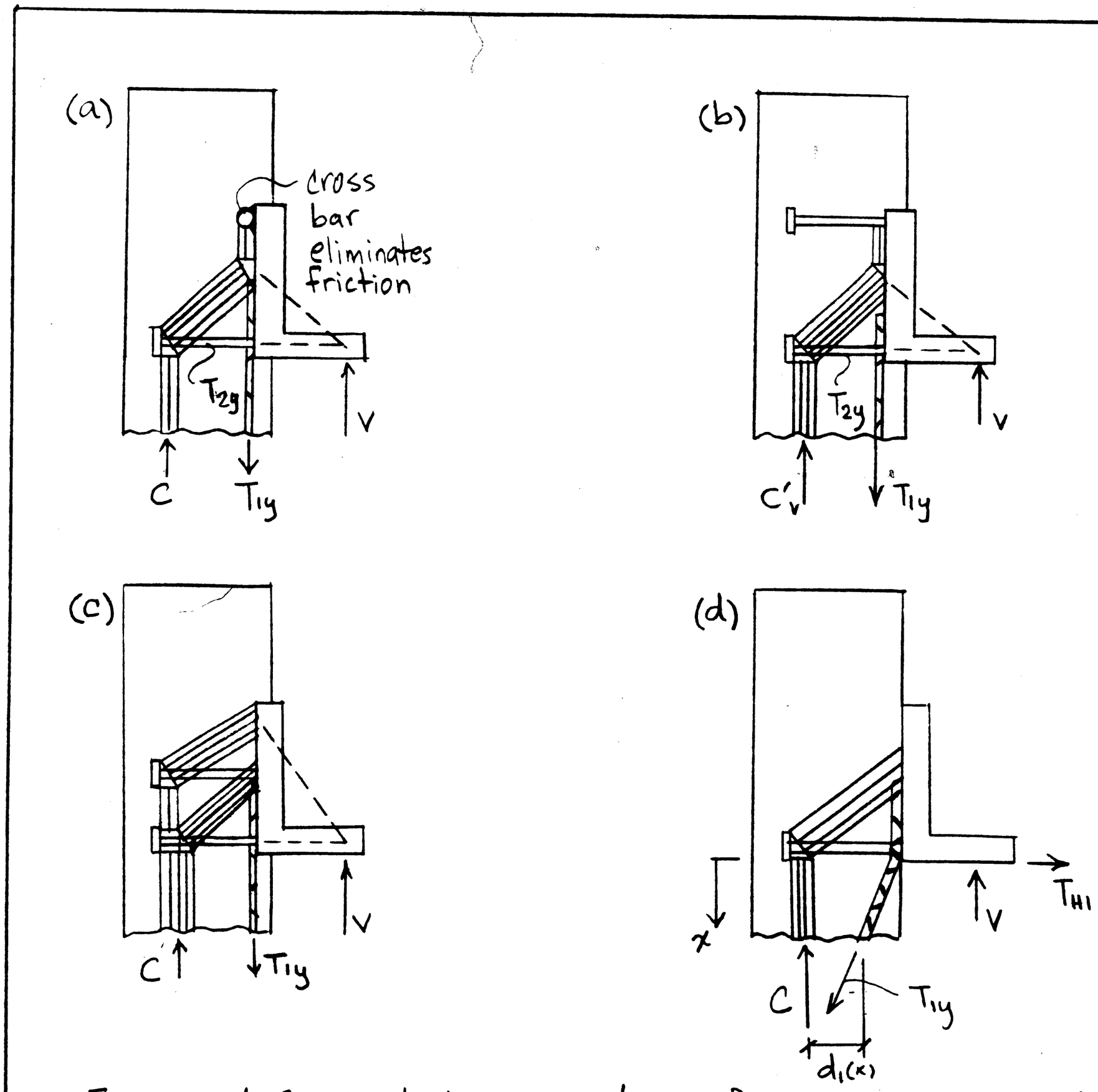

FIGURE 4.13: Detailing variations for welded rebar model

stud row near mid-depth increases the lever arm d_2, and thus the moment capacity.

The purpose and function of longitudinal reinforcement bent into the member as shown in Fig. 4.13(d) should be carefully studied before it is being used for several reasons,

(1) the tension bar T_1 is not parallel to the tension face where it is most effective,

(2) bars welded to the angle and bent inward are usually discontinued some distance below the connection; however, it will become clear in the next section that the longitudinal reinforcement T_1 serves the function of suspender bars which must extend below the bottom longitudinal reinforcement of the suspended member; and

(3) if the welded bar bent inward is spliced with primary longitudinal reinforcement serving the role of suspender bars, the "kinked" splice may need stirrups to be effective.

In sections 4.2, 4.3, and 4.4 deliberately the most simple reinforcement details leading to clean, simple, and understandable truss models have been studied. While clean and simple solutions are often the best, details can of course be combined. For instance, if bars are welded to an embedded angle with a double row of studs and "loose" longitudinal reinforcement (Fig. 4.6), and the bar is bent diagonally inward, the detail is analogous to the best performing opening knee joint details (Fig. 3.10(b)) provided the bent bar is fully anchored in the compression zone at the opposite face so that it can "pull in" part of the compressive resultant (Fig. 3.11). If furthermore the "top" row of studs is located closer to mid depth of the angle, they could more effectively serve the role of stirrups in an opening knee joint.

For clarity none of the details of sections 4.2 to 4.4 show reinforcement for reversed moment which requires "closing knee joint

details". If the top row of studs serves this purpose, they must of course be located at the top. Longitudinal reinforcement should then be located close to the tension face of the member but inside the stud heads.

From a more general viewpoint the connection detail treated in this section, Fig. 4.11, illustrates particularly well the consequences of designing only the interface and the B region explicitly: there is no assurance that the ultimate stress state assumed for the design of the interface is compatible with a "safe" internal force path through the D region to the B region. The (shear) friction contribution, G-H-I, to the interface interaction diagram in Fig. 4.11 calls for a concrete compression strut pointing upward from the tip of the angle. However, there is no reinforcement in the D region which can intercept this strut, anchor it, and transfer its force down to the B region. While interface design must be integrated with D region design, connection design must be integrated with the overall member design. This is the subject of the next section.

4.5 CHARACTERISTIC BEHAVIOR OF WALL PANELS WITH ANGLE SEAT BEARING CONNECTIONS

In the previous sections the behavior of angle seat bearing connections was studied independently of the member they support. But in good connection design, it is just as important to properly design the member so that it does indeed allow the connection to behave as modeled. In this section, the behavior of wall panels with

angle seat bearing connections shall be studied. This study will demonstrate

(1) how the angle seat bearing connections just described interact with the connected member (in this case a wall panel).

(2) the wall panel behavior itself, and how to design it utilizing the concepts of section 2.4.3 (suspended loads and indirect supports), and

(3) the importance of considering truss systems in three dimensions.

At first glance, rational design seems complex: Since the panel is suspended from angle seat bearing connections it is indirectly supported. Since its distributed load is not a compressive load applied to the top, but rather the self weight arising over the depth of the panel, it must be considered as a suspended load (Fig. 4.14(a)). But the design of this panel is rather simple if it is broken down to three basic design problems already treated in chapter 2: (1) a simply supported deep beam with distributed compressive loads along the top flange and compression supports at the bottom (section 2.5); (2) suspended loads (section 2.4.3); and (3) indirect supports (section 2.4.3). Thus, the design of the panel itself proceeds in three steps. A fourth step, finally, integrates the panel design with the connection design.

(1) Assume all loads and supports as compressive and use normal procedures in choosing the required shear and flexural reinforcement.

(a)

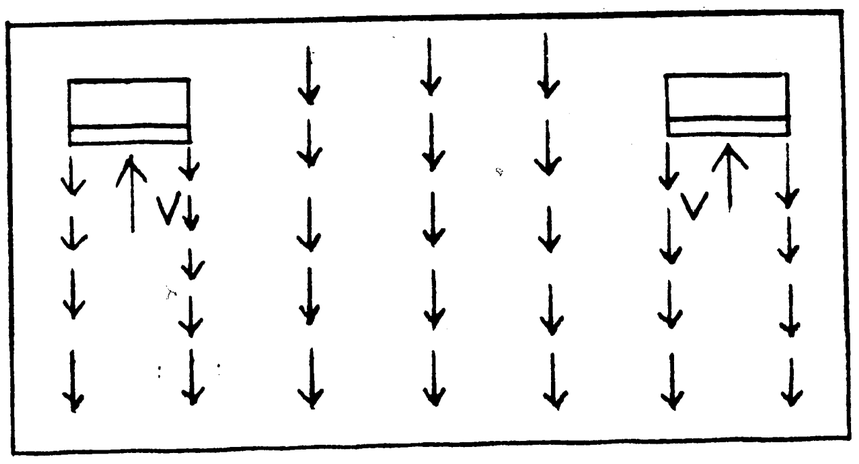

(b)

treat self weight as acting over depth of the panel

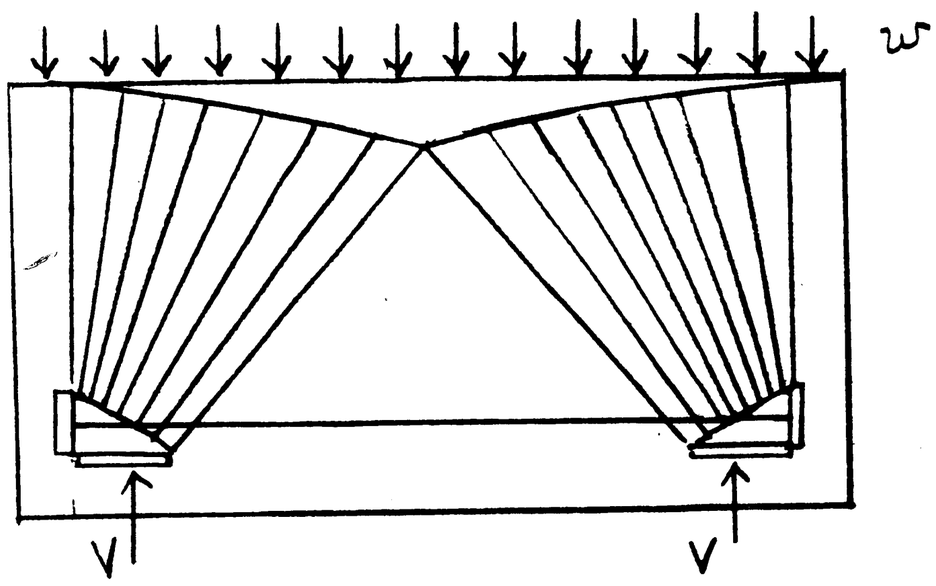

(c)

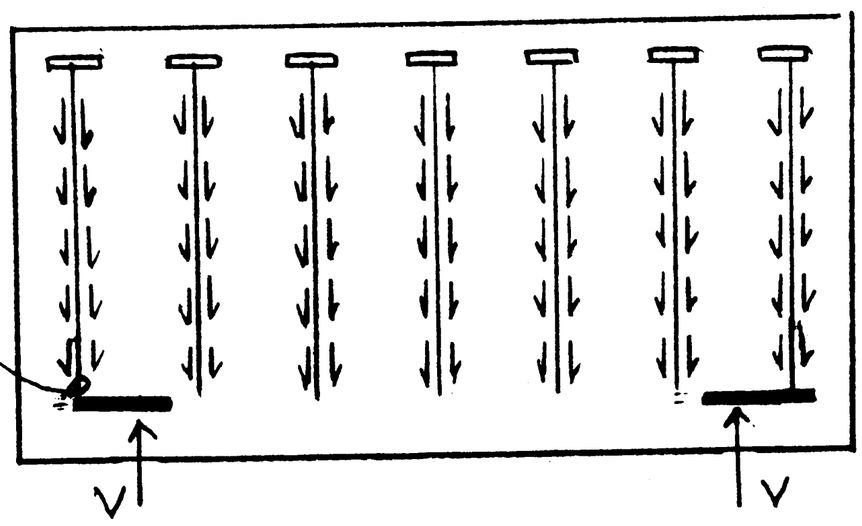

(d)

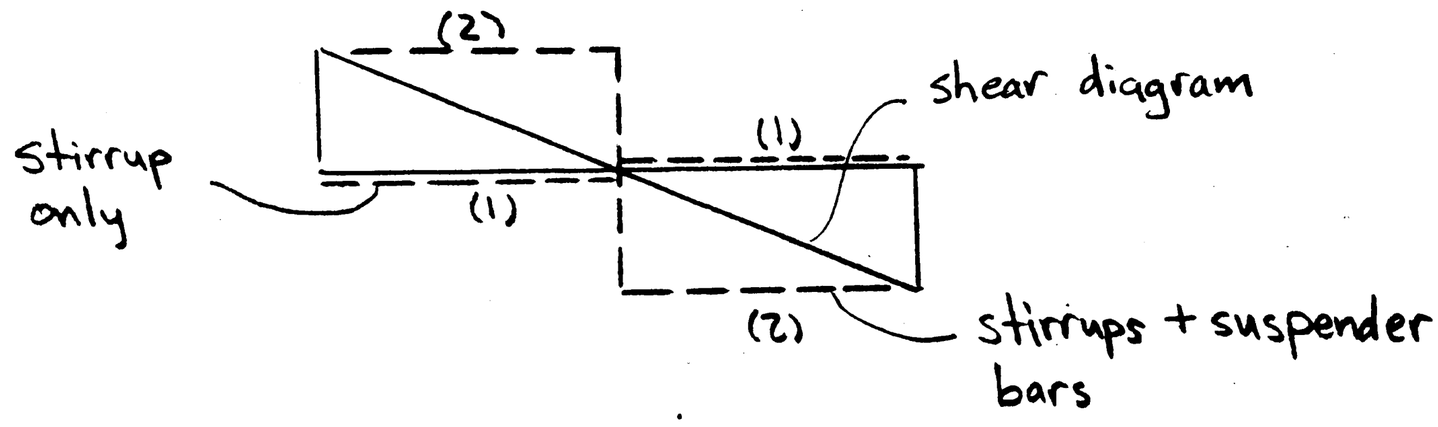

FIGURE 4.14: Wall panel design

(2) Since the self weight is actually hung from the depth of the panel rather than applied to the top, provide suspender bars to transfer the full self weight to the top of the beam.

(3) Since the supports are not actually compressive at the bottom (direct) but rather indirect at the top, provide hanger bars that transfer the full support reactions from the bottom to the indirect support at the top.

(4) Finally, integrate the panel design and the connection design and ensure that the models used are compatible.

In the first step, the panel is modeled as a deep beam with a uniformly distributed compression load on top of the beam. The support reactions are assumed to act as compression supports *near* the bottom of the panel. The truss model for this step is shown in Fig. 4.14(b). For this beam, flexural and shear reinforcement may be located and proportioned using the truss modeling concepts described in chapter 2. For demonstrative purposes, the panel length shown is very short, thus steep diagonal compressive fans can develop which can transfer the loads directly to the supports without any stirrups. The panel is a deep beam consisting only of D regions (section 2.5).

The flexural reinforcement must extend longitudinally near the bottom of the beam, but above the assumed compression support locations and anchored there for its full capacity. This steel is proportioned for the outward thrusts (horizontal components) of the fans.

Since the vertical components of the fans (for this example only) exactly equilibrate the uniformly distributed compression loads along the top, no stirrups are needed for this beam at this step by analysis, provided the full capacity of the longitudinal reinforcement can be anchored at the support. If not, stirrups must be added until the bar end force decreases to a value that can be anchored. In any case, the final design will be checked for minimum horizontal and vertical distributed reinforcement.

In the second step hanger ties, in addition to any stirrups possibly supplied in step (1), must be placed so as to hang the self weight of the panel (which accumulates over the depth of the beam), up to the top (Fig. 4.14(c)). These suspender bars must be fully anchored at the top within the compression zone similarly to stirrups in beams. The suspender bars are uniformly spaced across the entire length of the panel, and must be proportioned for the full self weight (remember this is the only vertical reinforcement up to this step). A complete discussion on suspender bars and the consequences of omitting them or not anchoring them at the top may be found in section 2.4.3. Note that although the stirrup diagram staggers below the shear diagram, (dashed line (1) in Fig. 4.14(d)), staggering occurs above the shear diagram (dashed line (2) in Fig. 4.14(d)), if suspender bars are added.

In the third step, the vertical reaction supplied at the level of the angle seat bearing connection is connected with the fictitious support through hanger bars, (Fig. 4.15(a)). These bars must be fully anchored at the level where the compression supports are

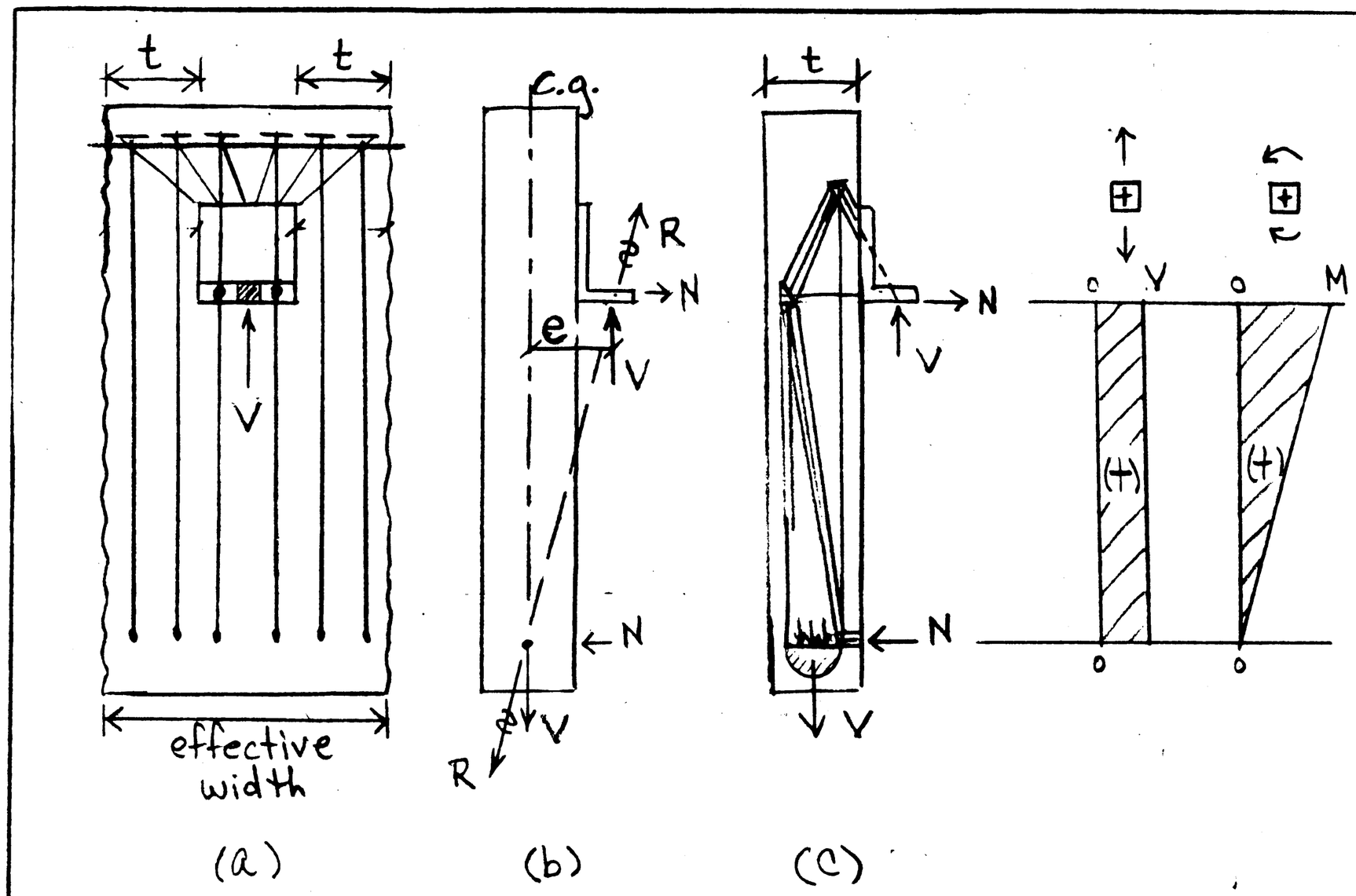

FIGURE 4.15: Effective indirect support strip

assumed to act. More specifically, the hanger bars must interlock with the flexural tension steel. If the hanger bars are loosely placed behind the angle, they must be closely spaced over an effective width which allows a compression fan to transfer the vertical reaction from the steel angle (through shear friction) to the hanger bars, as shown in Fig. 4.15(a). By the principle of St. Venant, this effective width might be estimated at this stage of the design as the width of the steel angle plus a wall thickness on either side of the angle (however see below).

Up to this point treatment of this panel is identical to the (planar) design of a deep beam with indirect support reactions and suspended loads acting in the center plane of the deep beam. However, while the self weight does act in the center plane, the reactions are eccentric to the member axis as illustrated in Fig. 4.15(b). Thus the panel is subjected to out of plane flexure. However, since the moment due to the eccentric reaction is only locally applied at the angle seat bearing support and only locally resisted at the horizontal support beneath it, this flexure must remain contained in a vertical effective strip including the two supports as shown in Fig. 4.15(a). A freebody diagram of the isolated effective strip shows then that it is also subjected to a axial tensile force applied at the level of the assumed fictitious support, namely the vertical component of the diagonal compression fan entering that fictitious support. Thus, the effective strip is subjected to flexure and axial tension as shown in Figs. 4.15(b) and 4.15(c). Note that the panel outside the effective strip is subjected only to in plane flexure and shear, but not to torsion. The diagonal compression fan loading the effective strip, Fig. 4.16(b), "unloads" therefore, its vertical component at the level of the fictitious support at the centroid of the effective strip member as shown in Figs. 4.15(a), (b), and 4.16(a).

At this point, it becomes clear that from the point of view of member design (i.e. of the panel) the D region disturbed by the presence of the connections is the effective strip containing the hanger bars, the seat angle bearing connection at the top, the

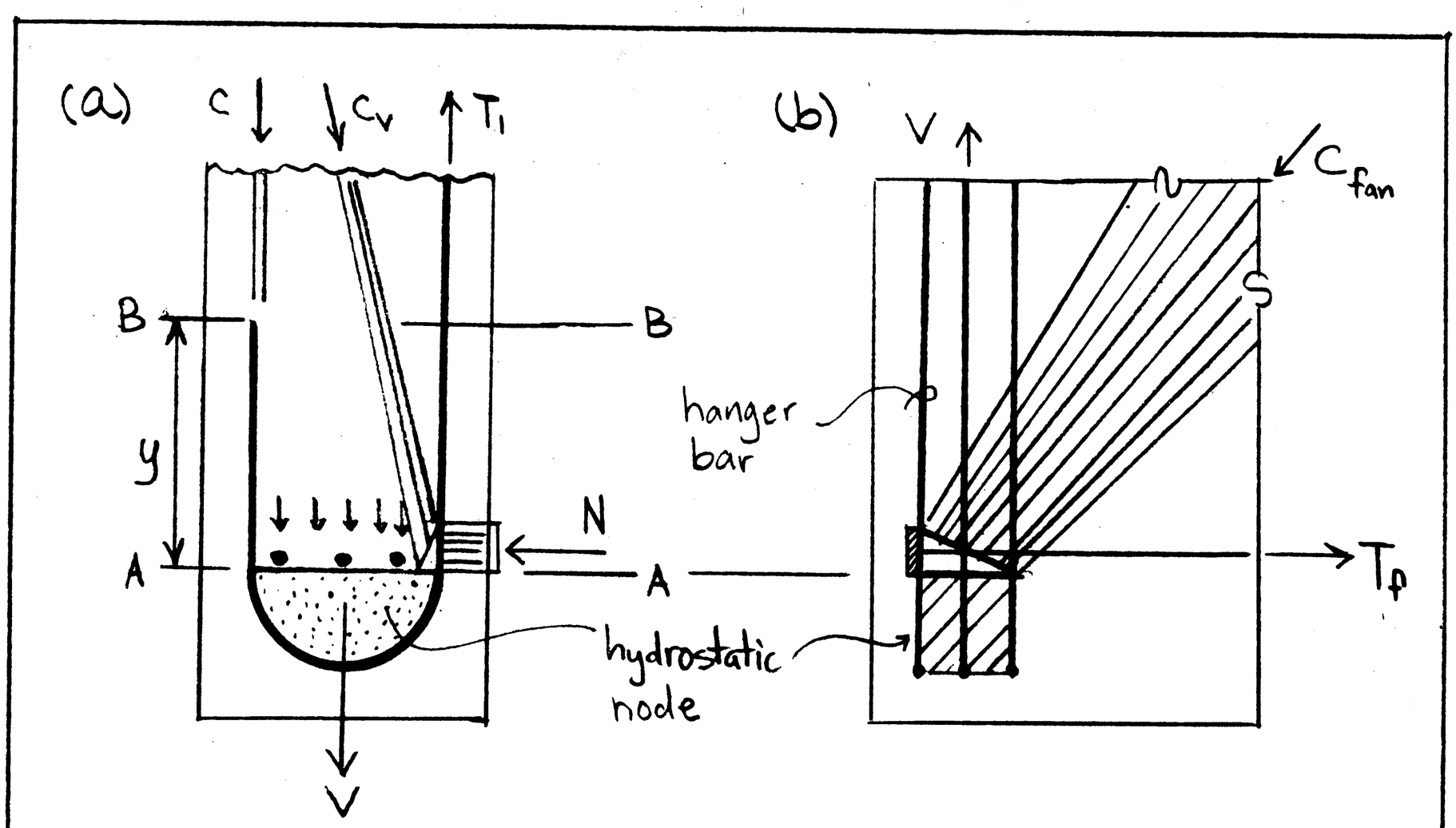

FIGURE 4.16: Hanger bar anchorage for wall panel

horizontal support or connection at the bottom, and the fictitious support. Step (4), integrating connection and member (panel) design, thus amounts to designing and detailing the effective strip beam. This effective strip beam has its own B and D regions. Its upper end D-region comprises the vicinity of the seat angle bearing connection as treated in sections 4.2 to 4.4, while its lower end D-region comprises the vicinity of the horizontal support and of the fictitious support introduced in step (1).

The fact that from the viewpoint of the equilibrium of the panel the disturbances of the connections must be contained within an effective strip beam, is the major justification for treating the connections as planar problems in sections 4.2 to 4.4. While a

fraction of the moment applied by the angle might be resisted by torsion along the top edge of the panel, particularly in the elastic uncracked range, this torsion would have to "circle back" into the effective strip beam. Furthermore, the panel edge is seldomly, if ever, designed for torsion (closed hoops, two layers of longitudinal reinforcement). Even if it were, the drop in torsional stiffness upon cracking is drastically lower than that in flexural stiffness. For these reasons, this effect is judged minor at the ultimate state when the panel or the connection are cracked, particularly if the seat angle bearing connection is located in a flexural tension zone of the panel as it often is. Concrete seeks the shortest, most direct, stiffest, and strongest internal force path and this is flexure of the effective strip beam. Of course, the concept of an effective strip beam is analogous to the strip method of slab design.

The effective strip beam, subjected to flexure and axial tension, can now again be treated with the methods presented in chapters 2 to 4. Either an explicit truss model is constructed for the entire strip beam by extending the "local" connection truss model as shown in Fig. 4.15(c). Or the B region of the strip beam between the connection D-regions of the top and bottom connection is treated with normal beam theory according to chapter 2 or ACI code. As illustrated by the "effective strip truss model" of Fig. 4.15(c), the hanger bars have actually two functions, (1) to transfer the vertical reaction from the steel angle down to the bottom of the panel, and (2) to resist flexure within the effective strip. In other words, the hanger bars from the point of view of planar panel design are the

longitudinal reinforcement for flexure and axial tension from the viewpoint of effective strip beam design, and the latter is, in turn, the longitudinal reinforcement labeled T_1 in the connection truss models presented in sections 4.2 to 4.4.

Thus, the estimation of effective width from the viewpoint of planar panel design (Fig. 4.15(a)) can be refined: the hanger bars should be distributed over a width which allows the hanger bars to intercept strut A and B (Fig. 4.5(b) or A' and E (Fig. 4.6(b)). For this purpose it may be assumed that struts A and B in Fig. 4.5(b) can fan out transversely (out of the figure plane) by 45^o from the tip of the angle or the stud heads. The smaller of their width at node Y controls the width over which the hanger bars should be placed. Of course, equilibrium requires that longitudinal panel reinforcement be placed at node Y which can resist the outward thrusts of the fanning struts A and B.

If the effective strip beam is treated with normal beam theory in its B region, it may be treated as a T beam. The web width of this T beam is the width over which its flexural reinforcement, i.e. the hanger bars, are placed (as defined above). Its "compression flange" in the exterior face of the panel may be assumed to spread by 45^o from a width equal to the angle width at the top connection to an effective width as defined by the ACI code at midspan (where web width has been defined above and span is the distance between top and bottom connection).

If the effective strip is treated as a slender beam, then shear reinforcement in the B region of this beam can be designed using the ACI code[3],

$$V_{strip} = N \leq \frac{V_c}{2} \qquad \text{(no stirrups are needed)} \tag{4-19a}$$

$$V_{strip} = N > \frac{V_c}{2} \qquad \text{(stirrups are needed)} \tag{4-19b}$$

where

N = the horizontal reaction (Fig.4.15(b))

= normal force on angle interface

V_c = shear carried by concrete (ACI[3])

and where the axial tensile force in the effective strip beam is to be considered in the calculation of V_c.

Step (4), integrating member and connection design or design of the effective strip beam, also includes design of its D regions. Design of its upper D-region, the seat angle bearing connection, has been treated extensively in sections 4.2 to 4.4, and the discussion above was devoted to ensuring compatible models for connection design, effective strip beam design, and panel design. Thus, there remains the task of designing the lower D region of the effective strip beam, which contains not only the horizontal support or connection, but more importantly, the fictitious support for the direct fans in the panel transferring the loads to the effective strip beam. Also here compatibility of the truss models or of the assumed internal force paths must be ensured: the hanger bars at the bottom of the panel must be detailed so as to allow the fans of Fig. 4.14(b) to indeed develop in the plane of the wall. Since the

effective strip beam is subjected to axial tension (and shear) but no flexure at the bottom, as shown in Fig. 4.15(c), reinforcement should be placed at each face of the effective strip beam. The detail shown in Fig. 4.16(a) uses therefore looped hanger bars whose center of the bend is located exactly at the level where the fictitious compression support was assumed to act (section A-A). The loops not only supply the required reinforcement for axial tension at each face of the effective strip beam, but also, equally importantly, provide for a "pocket" to intercept the diagonal compression fan entering the strip from the panel as shown in Fig 4.16(b). A hydrostatic node can form in the loops, as shown in Fig. 4.16(a), providing a "bearing surface" for the diagonal in-plane fans to bear against, Fig. 4.16(b). The left leg of the hanger bar loops may be cut off at section B-B, Fig. 4.16(a), where the compressive resultant for flexure and shear, equation (2-8), cancels the tributary axial tensile force V/2 (i.e. where the "compressive" resultant for flexure, shear, and axial tension changes from tension to compression). The diameter of the looped bars must of course be chosen small enough that the bars can develop a force V/2 over the distance y between the bend and cut-off point.

Since section A-A locates the level at which the fictitious compression support acts, the longitudinal flexural reinforcement for the panel must be located just above section A-A such that the hanger bar loops interlock with the longitudinal reinforcement. As shown in Fig. 4.16(b), the longitudinal reinforcement must be fully anchored at the left most hanger bar. If

anchor plates or loops are not desirable, and the development length, measured from the anchor plate shown in Fig. 4.16(b), is not available, then stirrups must be added in the span of the panel, in addition to the suspender bars provided for the self weight in step (2), until the horizontal outward thrust of the panel fans, 1/2 Vcote , is reduced to a value that can be anchored or developed at the location of the anchor plate. The available anchorage capacity determines the value of cote above, and shear design is carried out for the panel with this cote as described in chapter 2.

Similarly, as the longitudinal reinforcement must be pulled through the node and anchored "behind" the node, the support hanger bars must be pulled through the node and fully anchored below the node (see sections 2.8 and 2.9). The concept of the fictitious compression support is simply another way of defining the lower face of a C-T-T node (Figs. 2.6(c) and 2.28). If the longitudinal reinforcement is to be placed close to the tension face of the panel proper anchorage of the hanger bars is only possible through anchor plates or loops as shown in Figs. 4.16(b) and 4.17(a). If the hanger bars extend only to mid-depth of the panel or if they are only fully developed at mid-depth, Fig. 4.17(b), then the fictitious support or C-T-T node is located at mid-depth, too, and the longitudinal reinforcement would have to be placed at this level, as shown in Fig. 4.17(b), to permit a truss to form. Apart from being uneconomical, this is of course also highly undesirable, since the cracking moment likely exceeds the flexural strength, resulting in brittle failure.

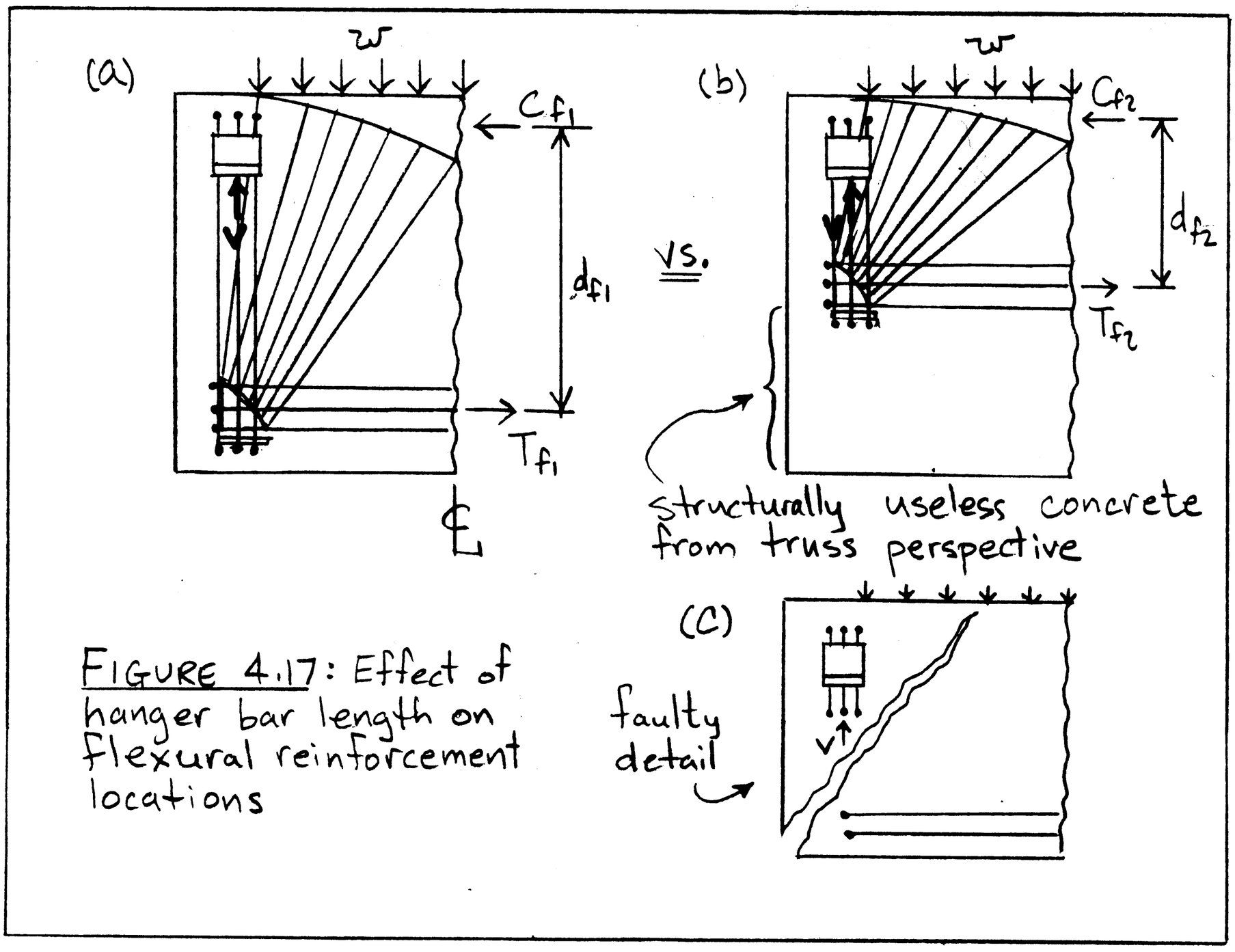

FIGURE 4.17: Effect of hanger bar length on flexural reinforcement locations

However, if the "hanger bars" welded to the angle or "loose" rebars placed behind the angle are discontinued above the flexural reinforcement placed at the bottom of the panel, a diagonal tension failure crack can open up, as shown in Fig. 4.17(c), which is intercepted by little more than minimum distributed reinforcement. It doesn't mater whether the panel is suspended at the top or supported at the bottom by an angle seat bearing connection. As long as the studs of the angle are located above the primary flexural panel reinforcement, this failure crack can open up, unless hanger

bars extend *below* the primary flexural reinforcement and are fully anchored there.

This failure crack may form not only due to diagonal cracking under factored load, but even more importantly under service loads due to volumetric changes and/or movement of the building frame. In at least one case the support connections of practically all precast concrete cladding panels of a multistory building were ripped off in this manner. The panel detailed according to Fig. 4.17(c) will loose its load bearing capacity upon formation of this crack. The panel detailed for the truss model shown in Fig. 4.17(a), on the other hand, will safely maintain its strength after being cracked. In the case cited above, only luck prevented the cladding panels from falling: they were cantilevering in an unintended way from the other end.

Since, from the point of view of the panel, the D region is the entire effective strip, connection design not only includes the interface and the D region adjacent to the interface, but also design of the entire effective strip. This shows that connection design must really start with the global truss of the entire structural member. The loads must be provided with a path to the reactions. In this example, the self weight of the panel is developed onto the suspender bars. The tensile forces in the suspender bars are transferred to the top of the panel and fully anchored there. Compression fans develop and equilibrate the suspender bar anchorage forces at the spread of the fan. At the pinch of the fan, the self weight (vertical component of fans) is equilibrated by the hanger

bars within the effective strip, while the horizontal components of the fans are equilibrated by the flexural reinforcement. The hanger bars transfer the self weight up to the D region of the angle seat bearing connection. The forces "turn the corner," transfer through the rigid steel angle, and finally equilibrate the reactions. The final step is to provide everywhere minimum distributed reinforcement in both directions, where it is not already required by analysis, to provide the concrete with the ductility to indeed develop the design truss model. Fig. 4.18 shows the final reinforcement layout.

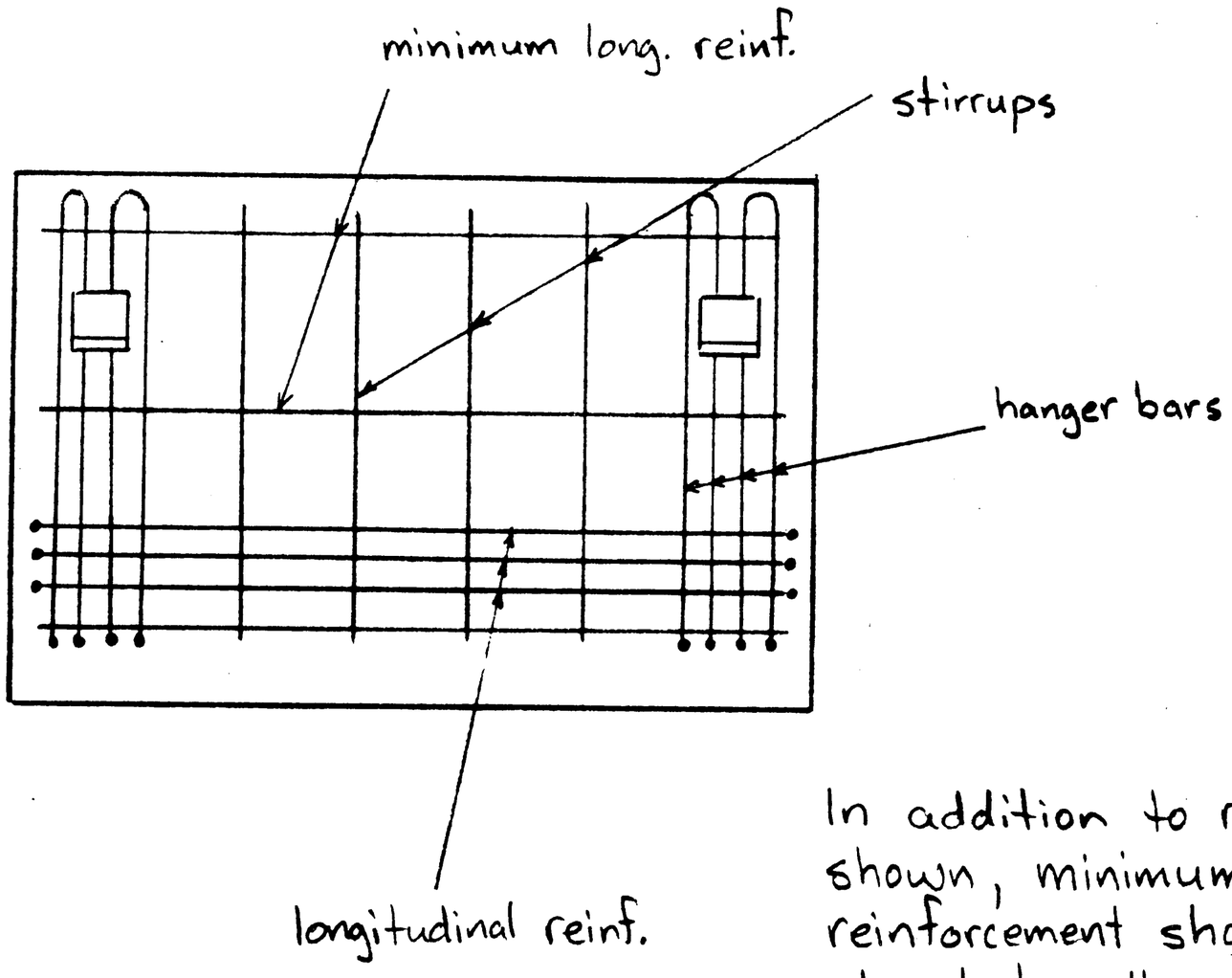

FIGURE 4.18: Reinforcement scheme for hanging wall panel

4.6 MOMENT CONNECTIONS

Moment connections are typically used in building frames and transfer both forces and large moments from one structural member to the next. Moment connection behavior and simple connection behavior relate to each other similarly as a knee joint with beam to a knee joint with corbel. The truss models described in chapter 3 apply to moment connections of both monolithic and precast concrete elements. For instance, the truss models for the monolithic knee and beam-column joints of chapter 3 can also be used for the design of the D-regions and interface of precast beam to precast column connections.

In principle, there are two ways to proceed:

(1) Design first the corresponding monolithic joint using directly the truss models of chapter 3; second, cut the adjoining members along the desired interface; and, third, design the resulting interface and connection hardware to accommodate the selected internal force path.

Or, if the resulting interface characteristics or connection hardware are not desirable from a construction or erection point of view:

(2) Select first desirable interface characteristics; second, distort the corresponding characteristic truss model of chapter 3 by translating nodes with "rubber-banded" truss elements, until the truss model does no longer interfere with the interface; and, third, design the D regions and proportion the connection hardware for the resulting truss model.

In either case, the truss models ensure that both the D regions of the connected members and the interface are designed with compatible models. Since the truss models presented in chapter 3 represent the internal force paths selected by the concrete "if left alone," method (1) usually results in the more direct, simpler internal force paths, i.e. to the better structural solution. However, since precast concrete gains its advantage through ease of erection and construction, structural and erection/construction requirements must be carefully balanced. Truss models do not prevent this balancing. On the contrary, they provide the engineer with a tool, to rationally adapt monolithic details to the needs of precast concrete without compromising the general structural integrity and ductility of monolithic concrete.

As an example, consider the moment connection of Fig. 4.19(a), (adapted from the PCI Design Handbook[1]). Since no loads or boundary forces are shown, it is assumed that this connection serves to resist a closing moment. As a simplification, it is also assumed to be a corner or knee connection. Thus, proceeding with method (1), if the detail of Fig. 4.19(a) is to behave as a monolithic closing knee joint, the truss of Fig. 4.19(b) must develop. The L-shaped interface can be detailed so that these internal force paths can indeed be realized as illustrated in Fig. 4.19(c). The space between the beam and column is filled with grout so that the diagonal compressive strut can pass from the beam to the column. The grout should have a compressive strength not less than that of the

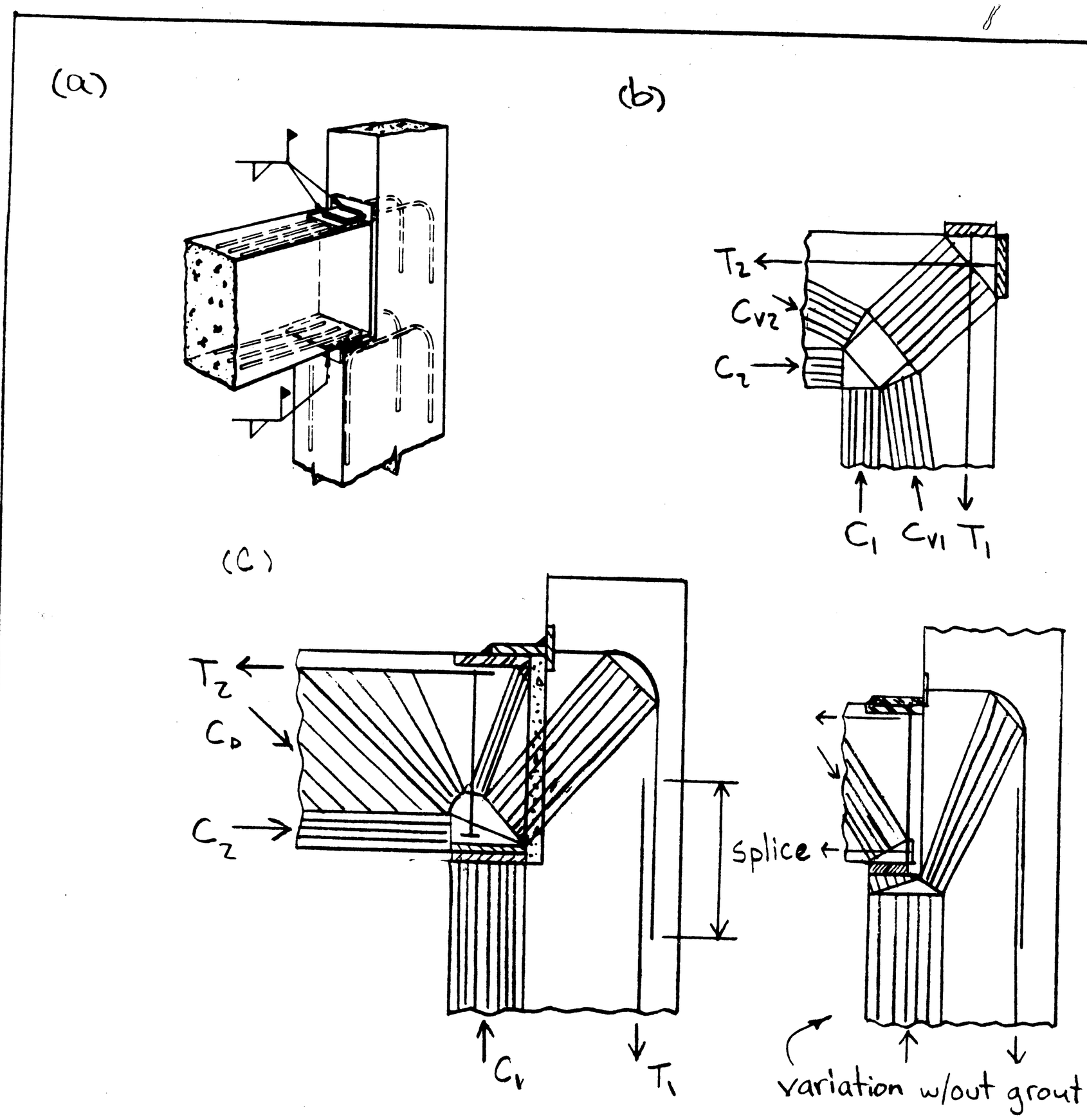

FIGURE 4.19: Moment connections

connected elements. Furthermore, the friction angle between the diagonal strut and the beam-grout interface must not be exceeded.

If it is desired that the vertical leg of the interface remains ungrouted, then (method 2) the truss node in the lower right corner of the beam is translated down to the right into the column, until

its upper tip is located at the corner of the L-shaped interface and the stress free triangle above the node (disregard the strut and tie connecting to the top insert plate) contains the interface and does not need to be grouted.

Careful attention must be given to the top embedded and loose plate detail of the beam (Fig. 4.19(c)). Its primary function is to transfer the top rebars' tensile forces from the beam to the column. But due to the nature of the assembly, unattended eccentricities exist as shown in Fig. 4.20(a). As a result, the embedded plate may rotate as shown in Fig. 4.20(b). This rotation can lead to premature failure of the connection, if reinforcement is not placed to resist the resulting moment. Indeed, this very same embedded plate detail was used in a beam-column moment connection test (PCI report 1/4[23], connection BC15). Failure of the connection was due to rotation of the embedded plate, which led to rupture of the top longitudinal reinforcement in the heat affected zone of the weld. Figure 4.21 shows this plate.

If reinforcement, such as a stud, is welded to the end of the embedded plate furthest from the beam end, the embedded plate will not rotate, since a resisting force couple can develop as illustrated in Fig. 4.22(a). In the tested specimen, although a welded stud was present, it was located in the compression rather than tension zone and therefore, pretty useless.

Not only must the stud be correctly placed, but it must also be anchored. The simplest solution is to extend the stud to the bottom into the beam's compression zone. An inclined strut between the stud

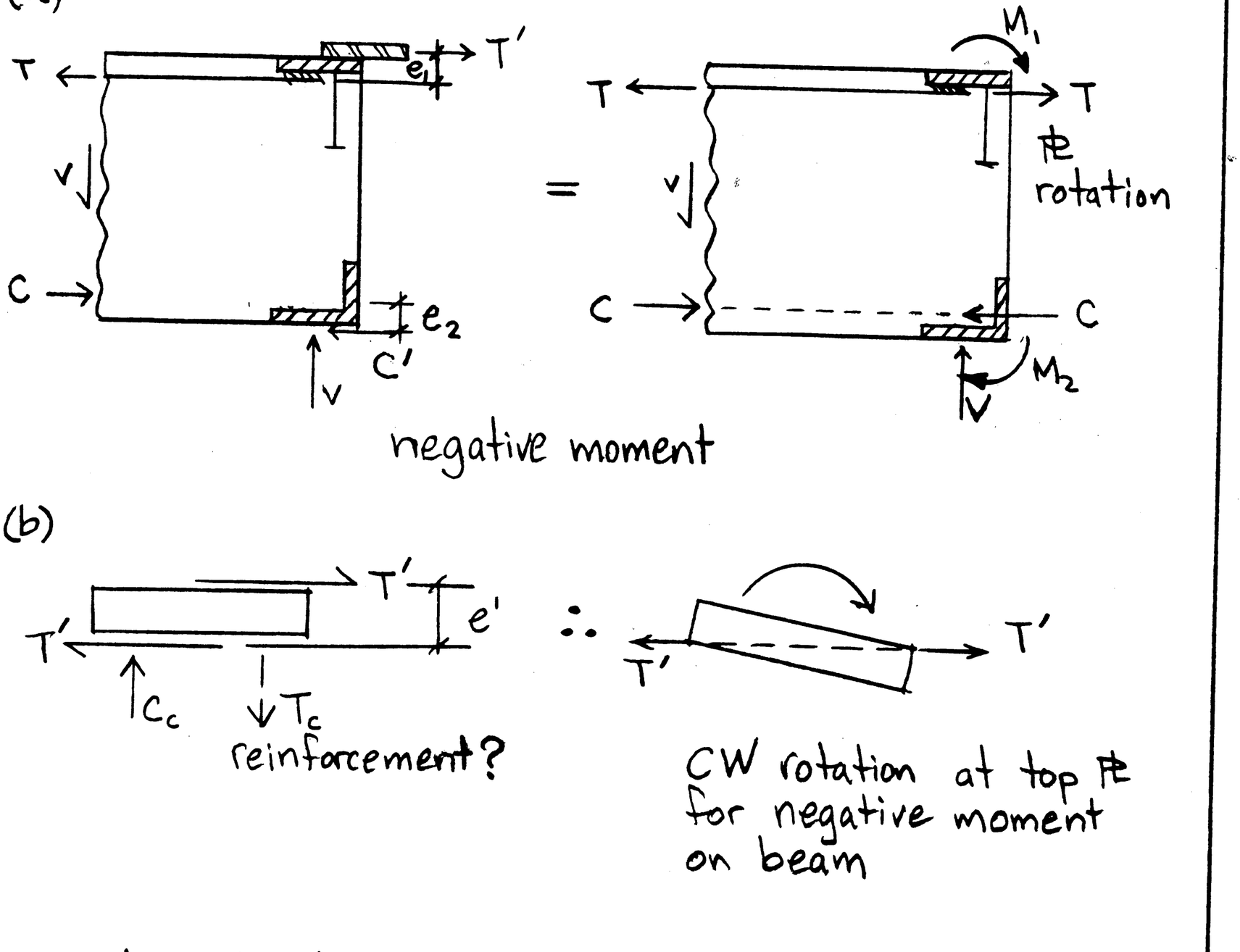

FIGURE 4.20: Unattended eccentricities

head and the embedded plate can then form, which supplies the resisting compressing resultant, C_s in Fig. 4.22(a), to the embedded plate and the vertical anchor force to the stud head. Its horizontal component is resisted by the difference between T and T' (Fig. 4.20(a)) at the top and between C and C' at the bottom. Note that attending to the moment M_1 in Fig. 4.20(a) amounts to turning the vertical force couple, M_1, around the corner into a horizontal force couple at the level of T and C. This is an opening knee joint

problem and, indeed, the truss model in Fig. 4.19(c) combines a "local" opening knee joint truss model with a "global" closing knee joint truss model.

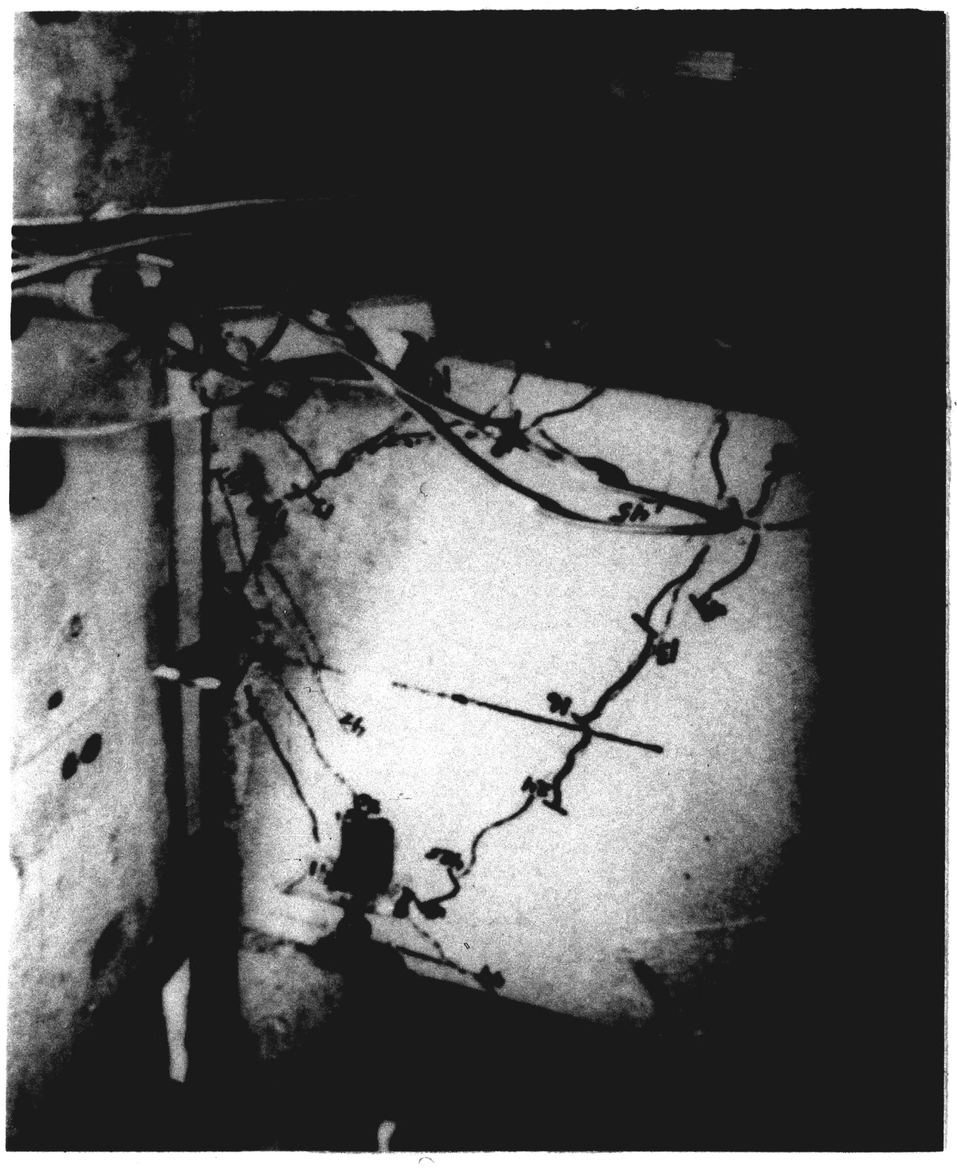

FIGURE 4.21: Failed specimen BC15 (23)

If the stud is too short Fig. 4.22(b) the efficiency of the stud may be reduced, since the inclination of the strut is limited by the friction angle, ϕ. This limits the lever arm d' in Fig. 4.22(a) to stud length times tanϕ, unless a crossbar is welded to the outer edge of the embedded plate. Furthermore, the horizontal component of the strut at the stud head must now be resisted by a "kinked shear strut."

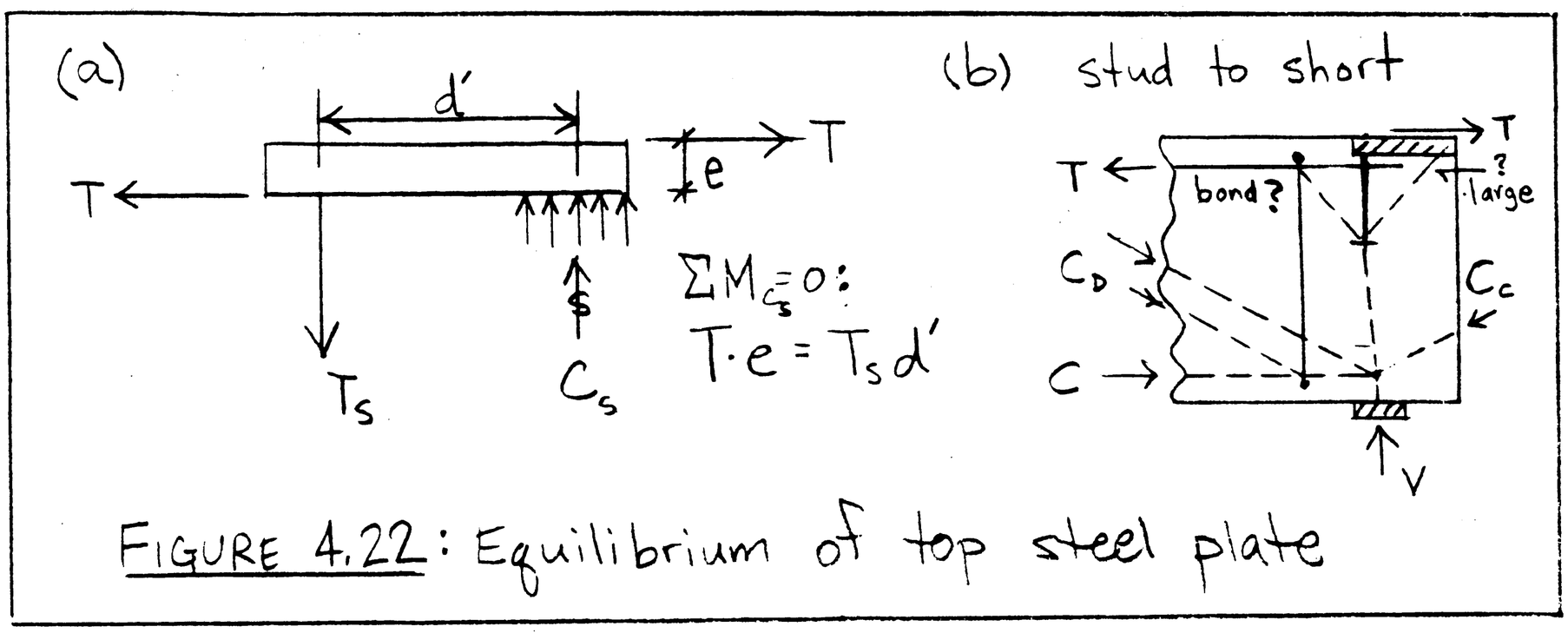

FIGURE 4.22: Equilibrium of top steel plate

Similar unattended eccentricities may exist at other locations and/or interfaces of the connection. The engineer must either detail the connection so as to eliminate them, or provide reinforcement to "intercept" them.

Not only does the detail of Fig. 4.19(a) show no additional reinforcement to attend to the eccentricities, but also the top bent rebars in the column are too short. As the truss model of Fig. 4.19(c) shows and as should be clear from section 3.2, the problem at hand is not to anchor the top rebar in the column concrete through development length and hook, but rather to turn the tensile resultant of a moment around the corner into the column and splice it there with the longitudinal column reinforcement. The deficiency of this detail is of the type shown in Fig. 3.9(b).

If the detail of Fig. 4.19(a) were to serve for an opening moment, the lower bent bar in the column would be bent in the wrong direction and the detail would be identical to the extremely poorly

performing detail in Fig. 3.10(e). In view of the drastic performance differences between opening and closing knee joints and the crucial importance of the relative position of reinforcement and anchorage points, the practice of cataloguing connection details without showing the primary reinforcement nor the forces and moments for which they are intended, is questionable.

4.7 QUANTITATIVE ANALYSIS OF CORNER CONNECTIONS

In this section, both opening and closing precast beam to column corner connections are quantitatively studied using truss models. This analysis may be particularly instructive to practicing engineers since it provides some guidance on the reasoning with and use of truss models in a practical situation.

In particular, two test specimens described in a PCI report[23] are studied -- namely, specimens BC28 (opening knee joint) and BC29 (closing knee joint). The analysis of these specimens serves two purposes; (1) the engineer can "get a feel" for truss modeling in general, and (2) a comparison can be made between the computed truss model predictions and the actual test results.

Specimens BC28 and BC29 are specifically chosen because their analysis illustrates the truss models presented in section 3.2 (opening and closing monolithic knee joints), and shows how those truss models apply to precast concrete corner joints. Equally importantly, this analysis demonstrates how truss models can be used to identify both the function of and the anchorage requirements for the various reinforcements.

Section 4.7.1 describes the test setup and test results, while section 4.7.2 generally outlines the analyses. Sections 4.7.3 and 4.7.4 describe more specifically the analyses of the D regions, and section 4.7.5 presents the conclusions.

4.7.1 TEST SETUP AND TEST RESULTS

The analysis of specimens BC 28 and BC 29 is based on tests results and data reported in a PCI report[23]. Figures 4.23(a) and (b) show the test setup and the test specimens. Two dowels extend from a rigid support simulating a column and are grouted into corrugated steel tubes cast into the precast beams. The material properties are shown in Fig. 4.23(c). Figures 4.23(a) and (b), show the reinforcement layout and Figs. 4.24 and 4.25 show the D-region reinforcement details. For specimen BC28, an upward concentrated load is applied to the beam, while for specimen BC29 a downward concentrated load is applied. For both specimens, an axial force of $N = 7.8^{K}$ is applied at the ends of the beams. The axial load serves to simulate the axial forces that result from volumetric changes such as creep and shrinkage in practice.

Both were tested to their ultimate capacities. For specimen BC28, the inside corner front dowel yielded at an applied load of $V = 10.6^{K}$. At a load of $V = 11.07^{K}$ a 45^{o} crack in the joint core propagated from the tip of an earlier vertical crack near the exterior dowel. The interior dowel then entered the strain hardening range ($f_s = 96^{ksi}$) as the exterior dowel yielded, too. At a vertical

(a)

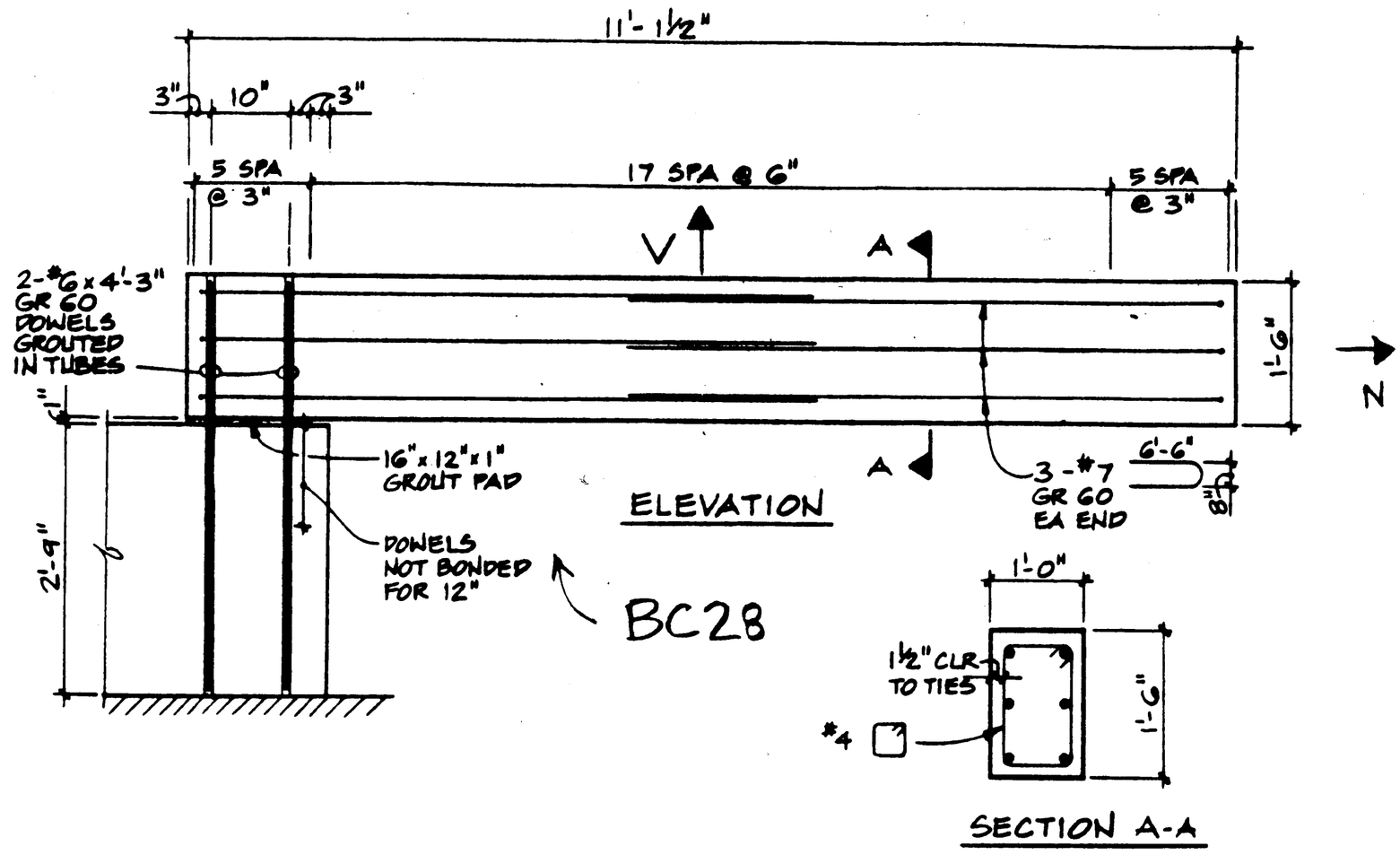

(b)

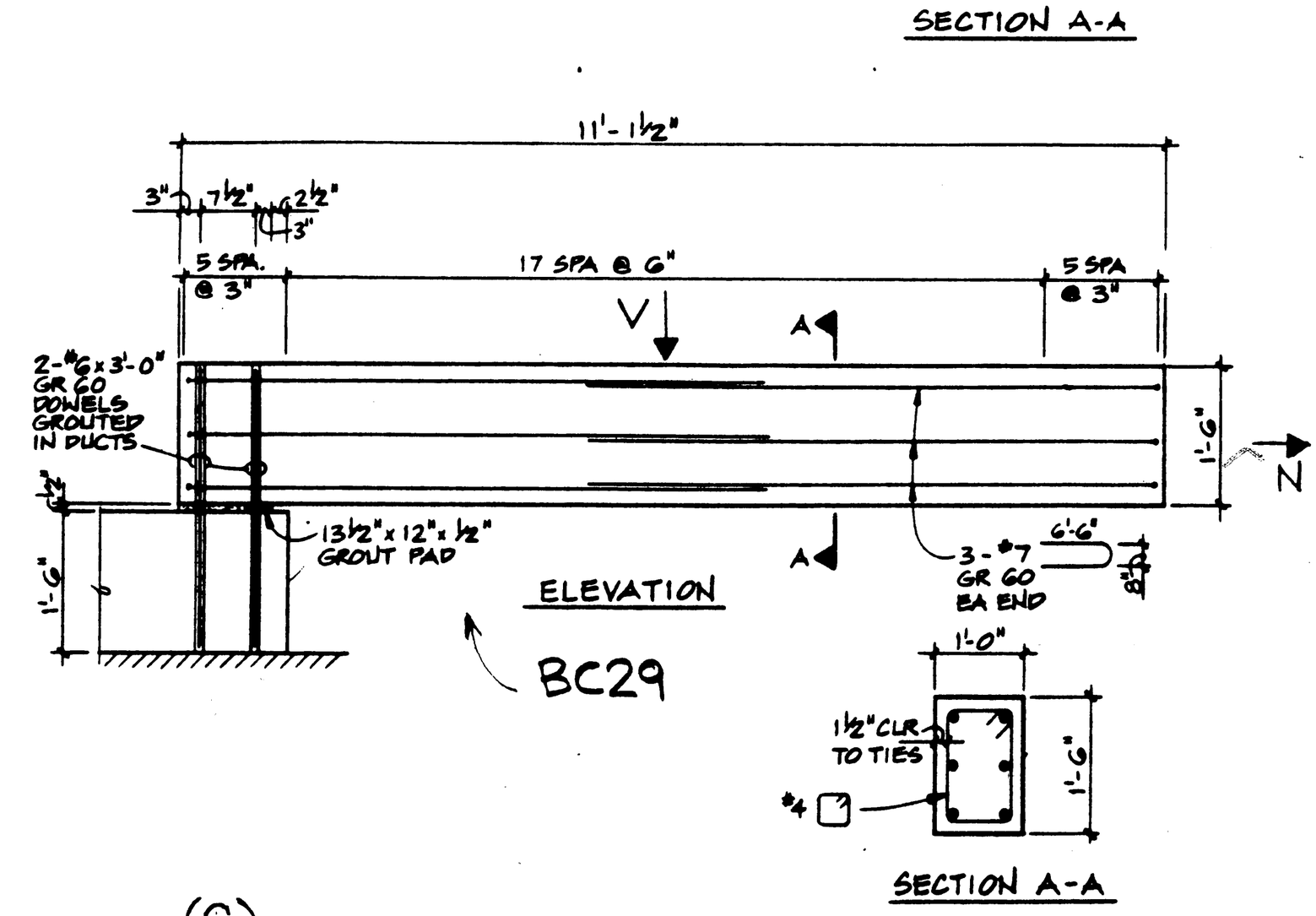

(C)

material \ property	f'_c (ksi)	f_y (ksi)	l_d (in) (ACI)
Concrete	7.02	—	—
grout	4.79	—	—
#4 tie	—	60	—
#6 dowel	—	68.9	14
#7 reinf.	—	63.7	23¾

(Ref. 23)

FIGURE 4.23: Test setup and material properties (BC28 & BC29)

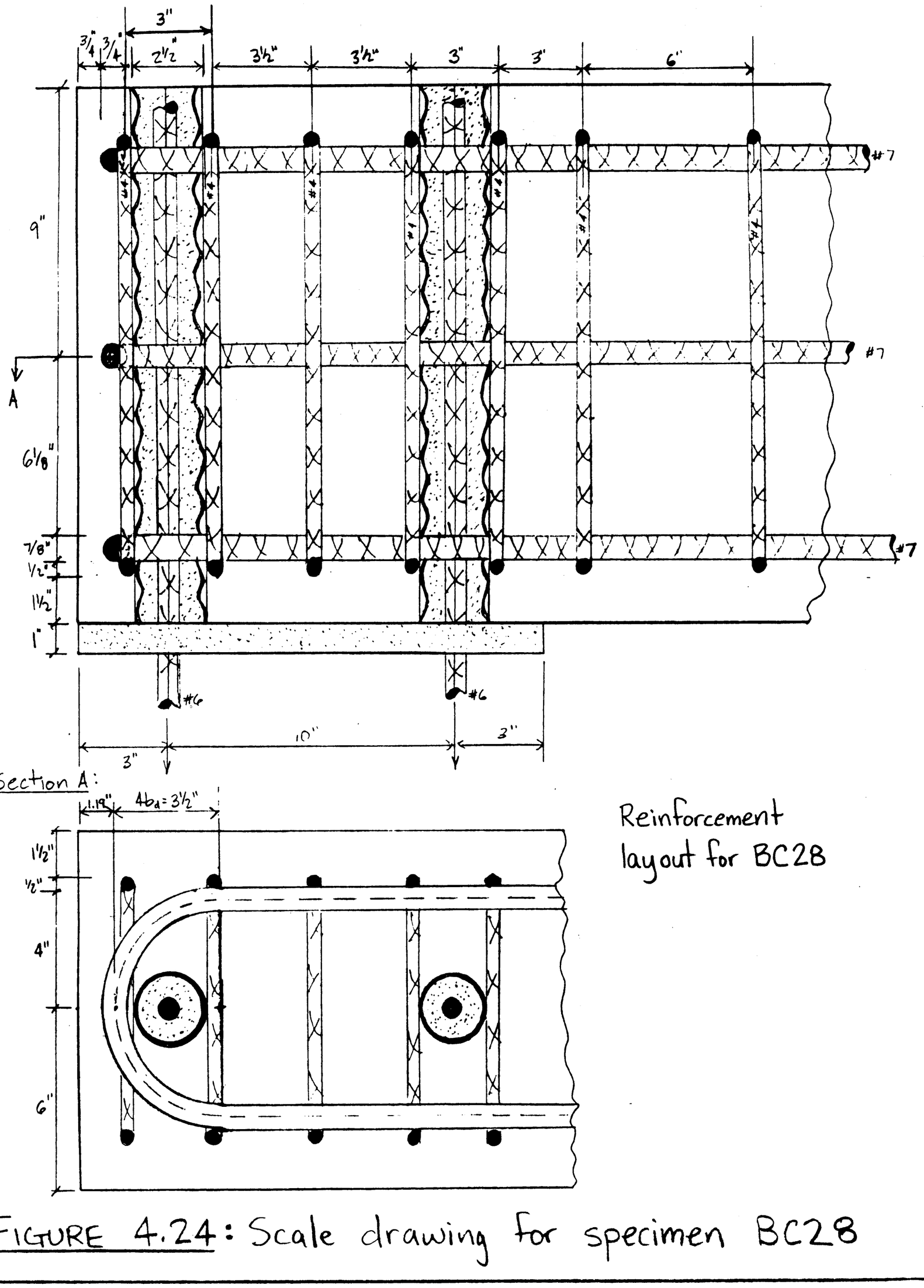

Reinforcement layout for BC28

FIGURE 4.24: Scale drawing for specimen BC28

(a)

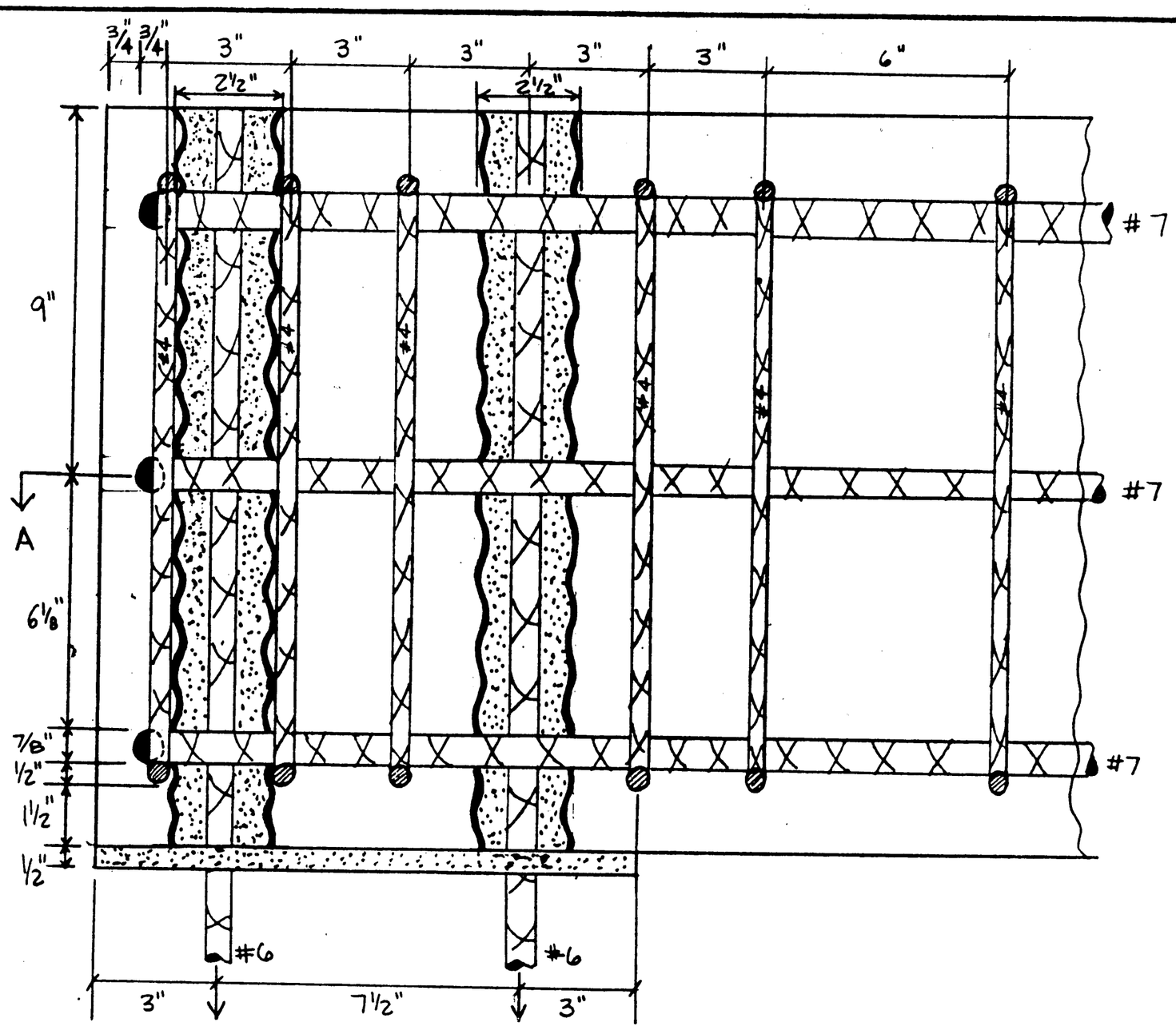

(b)

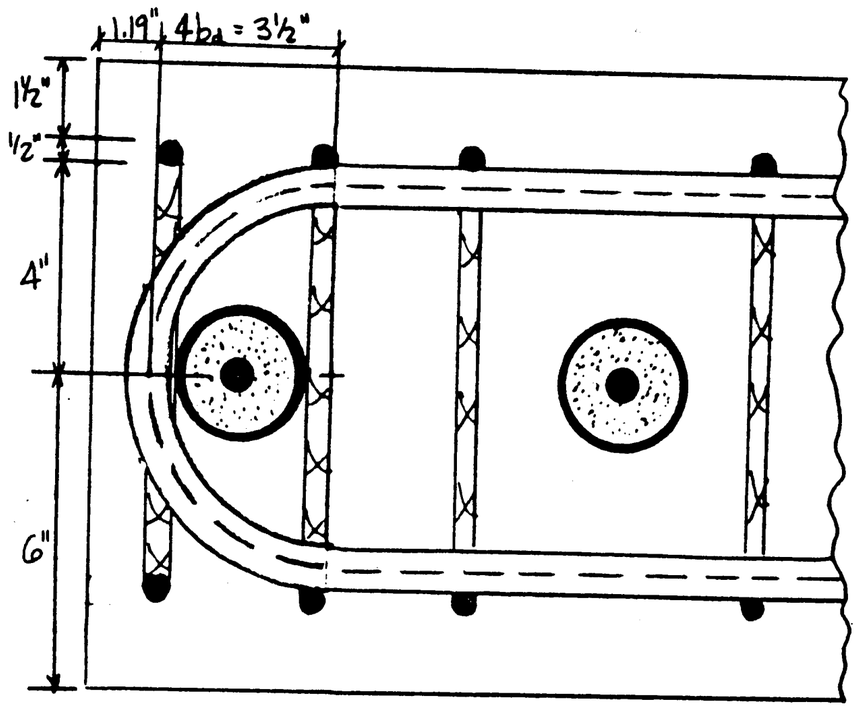

Reinforcement layout for BC29

FIGURE 4.25: Scale drawing for specimen BC29

load of V = 11.82^{K}, the axial load was released and the vertical load dropped to 8.7^{K}. The vertical load could then again be brought up to and sustained at V = 10.48^{K} (for which both dowels have long since yielded).

For specimen BC29, a progressive loading history with its associated beam behavior was not completely outlined.

4.7.2 OUTLINE OF ANALYSES

In view of the observed test results, the strategy used in these analyses is as follows. Since it has been observed that the dowels have yielded at the ultimate state, it is suspected that the beam-column interface controls the capacity of the connection. Therefore, analysis is separated into two parts: (1) investigation of the interface capacity, and (2) investigation of the D region capacity. In the first part the interface is indeed assumed to control and to be at its ultimate state. This means that for specimens BC28 and BC29, the dowels attain their yield or ultimate capacity, while the interface compression strut, as defined in section 2.11, crushes. Since the interface is also subjected to a shear force (which resists the axial force in the beam), the interface compression strut must be inclined. The normal and shear components of the inclined strut on the interface may be determined from vertical, horizontal, and moment equilibrium for the interface with the assumed condition that the dowels yield.

Indeed, for specimen BC28, the computed ultimate interface forces and the corresponding ultimate load agree with the measured

test date; i.e., a computed load capacity of 11.25^K compares quite well with a measured load capacity of 11.82^K. Similarly the interface also controls for specimen BC29, since the dowels through the interface yield at the ultimate state; since the measured capacity for BC29 is not reported a comparison with test data is not possible. While the agreement between computed and measured ultimate load for BC28 supports the assumption that the interface controls, it remains to be shown that the truss model within the D-region develops stresses which are less than or equal to the ultimate capacities of the internal elements. Particularly, it also remains to be shown that the ultimate anchorage and development capacities are not exceeded in the D-region.

The second step, the analysis of the D region, begins with the determination of the location of the B/D region boundaries. By the principle of St. Venant (section 2.2), a B/D region boundary is located approximately at a distance equal to the depth of the beam away from the inside corner of the interface. The connection D region for the beam is thus enclosed between this B/D region boundary and the interface.

Next, the boundary forces and their locations need to be determined. The interface force magnitudes are at least approximately (see below) known from the interface analysis. The compression strut on the interface must be inclined and this inclination is determined by the struts vertical and horizontal components. As previously described, these components may be

computed from moment and force equilibrium of the entire specimen about the interface. It is important to realize, though, for specimen BC28, that the horizontal component of interface compression strut must be anchored by the loop of the bottom flexural reinforcement of the beam. Thus the location of the interface compressive resultant is not only controlled by the geometrical constraints of the interface (grout pad) and the grout strength, but also by the geometrical constraint of the loop anchorage location in the D-region. If the latter controls, as it does for BC28, the location of the inclined compressive resultant in the interface is given by the point of intersection of its line of action through the loop anchorage with the interface. If this geometrical constraint from the D region which slightly reduces the flexural lever arm, was not considered in the interface analysis, the computed ultimate load might have to be adjusted. The conclusion that the D-region constraint controls, is supported by the crack pattern which shows that the lower end corner of the beam outside the loop split off and was therefore useless.

In this respect a difference between specimens BC28 and BC29 should be noted. While the location of the interface compression strut for specimen BC28 is related to the location of the loop anchorage of the bottom flexural reinforcement into which it bears, anchorage for the inclined interface strut of specimen BC29 is not dependent on the location of the bottom steel, since BC29 is a closing knee joint and the strut points into the joint. Thus depth and location of the strut are only controlled by the geometric

constraints of the interface (grout pad) and the grout strength.

The resultant forces and their locations along the B/D region boundary (located d away from the joint core) can also be determined through vertical, horizontal, and moment equilibrium about the B/D region boundary. The resultant of the compression chord is assumed to be located approximately at the level of the top reinforcement. The axial force in the beam is assumed to be transferred directly by the longitudinal steel located at mid-depth. A cracked section analysis may be performed to determine the force distribution of this section, if more accuracy is needed. While this was done for the pretensioned dapped end beam of Fig. 3.23, where the longitudinal and vertical distribution of the strand forces is crucial, it was not judged necessary in the present case.

Once the magnitude and location of all forces acting on the interface and B/D region boundary are known, a truss model can be fit into the D region in between. If this truss can transfer the boundary forces without exceeding the strength of its elements and "connections" (anchorages), the D-region does not control. If it cannot, the D-region controls, and the analysis has to be repeated starting from the controlling element(s) of the D region truss model.

4.7.3 ANALYSIS OF D REGION BC28

The D region truss model for specimen BC28 is shown in Fig. 4.26. For clarity, only the discrete truss model of resultants is shown at this stage. The physical dimensions of struts or fans are

(a)

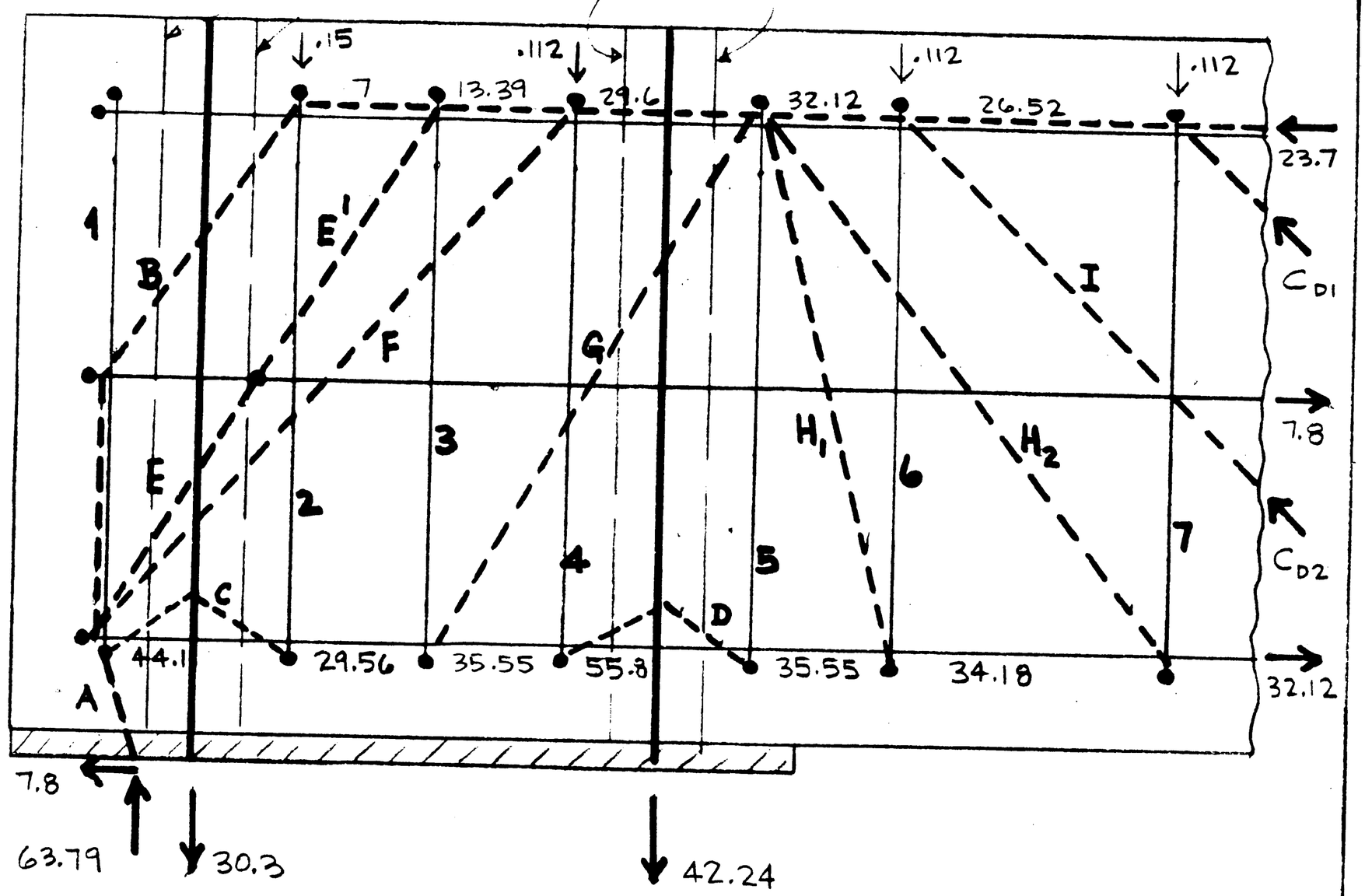

(b)

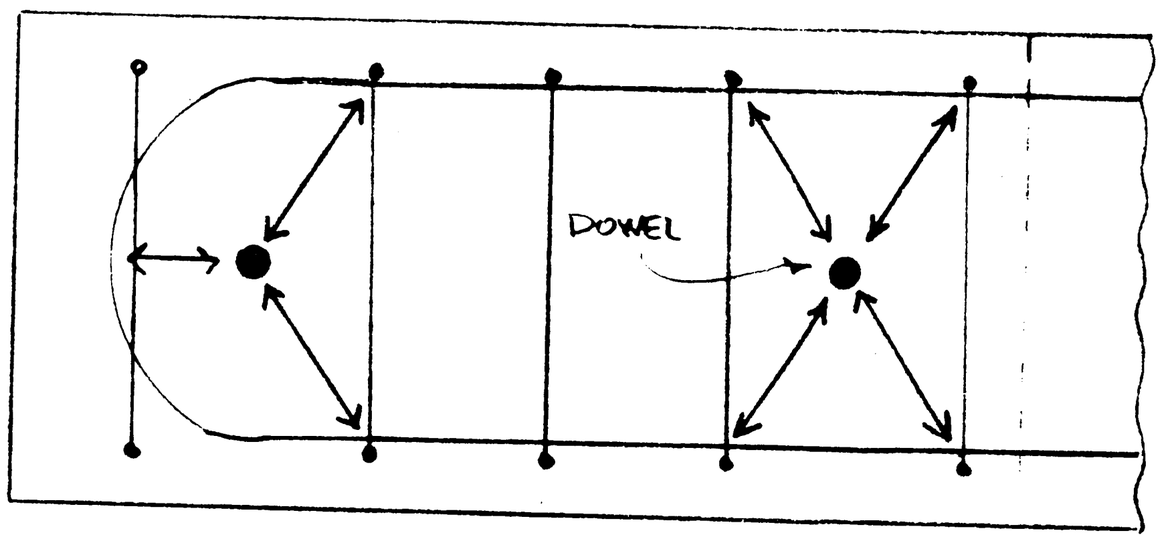

Transverse action

Elemental and boundary forces not shown in (a) : kips

A : 64.27	F : 26.69	1 : 0	7 : 3.00
B : 16.83	G : 13.51	2 : 15.15	C_{D1} : 4.22
C : 21.00	H_1 : 6.16	3 : 12.11	C_{D2} : 8.29
D : 29.28	H_2 : 3.64	4 : 21.12	
E : 13.34		5 : 21.12	
E' : 13.69		6 : 6.01	

FIGURE 4.26 : D region truss for BC28

considered at a later stage. The truss model was constructed for the computed ultimate load of 11.25^K. The corresponding truss element forces are also indicated in Fig. 4.26.

To understand the truss model in Fig. 4.26, the "characteristic model" for this situation must be considered. The truss model for an opening knee joint with vertical ties is shown in Fig. 3.4. Note in Fig. 3.4(a) that part of the flexural compressive resultant C_2 "turns the corner" into C_1 in the form of a direct strut. The other part fans out down to the stirrups which transfer it up to the top, and from here it is finally transferred through another fan to the "support" provided by compressive resultant C_1. Note also that the vertical bar, T_1, must be mechanically anchored through an anchor plate, transverse loops, or equivalent above compressive resultant C_2, since it is this anchorage force which redirects C_2 into the direct strut and lower fan. If, on the other hand, bar T_1 is developed over the depth of the joint core as shown in Fig. 3.4(b), the bar force must be transferred through hanger ties again to the top so that it can redirect C_2 around the corner.

Thus it becomes clear that the first and crucial step in constructing the truss model of Fig. 4.26 is an analysis of the anchorage conditions for the dowel bars so that the available stirrups or ties can be assigned to the shear transfer (Fig. 3.4(a)) and hanger bar (Fig. 3.4(b)) functions.

Obviously (Fig. 4.24) the dowel bars ar not anchored at the top but transfer their forces over their development lengths within the joint core. A development length of 14 in. (using the ACI code[3]

equations) is computed for the dowel bars at yield capacity (30.3^K). If the fictitious anchor plate of the yielding exterior dowel is conservatively considered to be located 14 in. from the top of the beam, then struts C, Fig. 4.26, can interlock with this fictitious anchor plate and the adjacent stirrup. Its mirrored companion can transfer its force directly to the "support" provided by the interface compression strut and the loop anchorage. Since the interior dowel bar is at strain hardening (42.24^K), its development length per the ACI code[3] equations is 17 in. While this length exceeds the depth of the truss it is still within the corrugated tube. Since the ACI development lengths already include a capacity reduction factor of 0.8 (i.e. the actual development length is shorter) and because, if a small force is developed below the truss, the corrugated tube could transfer this small force up, the fictitious anchor plate is also for the interior dowel considered to be located 14 in. from the top. This permits struts D to transfer the dowel force to the adjacent stirrups. The dowel forces hang onto hanger stirrups 2, 4, and 5 through struts C and D respectively. The hanger stirrups then transfer the dowel forces to the top of the beam (truss).

At this point the question arises whether it is not possible to treat the corrugated tubes as hanger reinforcement, since the dowel development forces can bear into the corrugations of the tube. The tube itself would then hang the dowel forces to the top of the beam in tension. However, this would require that the tubes are

structurally designed to not only hang the dowel forces, but also anchor them at the top of the beam. Since it is unlikely that the top two corrugations can act as anchor plates and since no data is given for the tubes, they are conservatively assumed to have insufficient tensile strength and end anchorage capacity. The corrugated tubes thus serve no primary structural purpose (except to serve as spiral reinforcement for the dowel bar development length) and the adjacent vertical ties (ties 2, 4, and 5 of Fig. 4.26), must therefore act as hanger reinforcement. This merely leaves tie 3 for the function of a shear stirrup in the joint core. Thus the ties in the joint core are assigned their function.

The tensile forces in the hanger bars must be equilibrated at the top of the beam with diagonal compression struts. As illustrated in Fig. 4.26, the vertical component of strut B balances the second hanger bar. Similarly, strut F balances hanger bar 4, and struts G, H_1, and H_2 balance hanger bar 5. Strut E balances the shear stirrup labeled as 3 which itself provides the vertical "support" for the bottom end of strut G. The horizontal components of these struts are equilibrated by the compression chord force differentials at the top of the beam, and by the tension chord force differentials (i.e. bond forces of the longitudinal reinforcement) at the bottom of the beam. Finally, strut A in Fig. 4.26 represents the inclined compression resultant at the interface as previously discussed which provides the vertical support for the incoming struts B, E, F, and the strut from the fictitious anchor plate of the exterior dowel bar. The horizontal components of these incoming struts supply the reaction to

the loop anchorage which mechanically anchors the bottom longitudinal steel. Note from the high forces in the longitudinal steel at the beam end that the loop anchorage is crucial to the performance of this joint. Similarly, the outward thrust of the kinked strut B supplies the reaction to the loop anchorage of the longitudinal reinforcement at mid-depth. Since this outward thrust is not sufficient to resist the full beam axial load which has been assigned to this reinforcement, strut E-E' must also be slightly kinked. The outward thrust due to this kink develops the remaining bar force within the joint core.

Comparing the truss of Fig. 4.26 to its "model" in Fig. 3.4 shows that strut E-E' represents the fan spreading from the column compression resultant, while F represents the direct strut between the column and beam compression resultants. The fan spreading from the beam's compression resultant is represented by strut G.

Thus part of the joint shear is transferred by direct strut F and the other part is transferred through fan G to stirrup 3 and fan E. Stirrup 2, 4, 5 play the role of the hanger reinforcement in Fig. 3.4(b). Stirrup 1 is useless as hanger tie, since it does not properly interlock with the top loop (Fig. 4.26(b)) and not needed, because "its share" can be directly transferred to strut A. Since stirrup 1 is not located within the span of the D region truss, it is also useless as shear reinforcement. Strut B has no equivalent in the truss model of Fig. 3.4(a), since there is no longitudinal column reinforcement close to the compression zone. Finally, struts H_1 and

H_2 play the role of the shear fan in beams near supports. The basic truss model of the resultants for an opening knee joint including shear and axial forces is shown in Fig. 3.2(d) where the fan is only represented by its resultant.

Since the diagonal struts unload their horizontal components onto the compression and tension chords, the chord forces vary across the joint. Note how the tension chord force essentially varies as indicated for reinforcement T_2 in Fig. 3.4(a) except for the local disturbances due to the extremely flat "local trusses" transferring the dowel bar forces out to the hanger stirrups.

While the function or role of each truss element has now been clearly identified, there may remain the question of how the geometry of the diagonal struts is found when the paper is blank. It has already been observed that practically all connections and joints can be understood as a combination or modification of opening or closing knee joints and corbels. Thus the basic truss models presented in chapters 2 and 3 provide guidance. From here the task is a rather simple one. One usually looks at either transverse or longitudinal equilibrium. Since usually the stirrups yield over most of the span and thus their forces are known, while the longitudinal reinforcement forces are not known except at the section of maximum moment, transverse equilibrium is usually considered first.

Here transverse or vertical equilibrium is considered. It takes 2 stirrups, close to yield (i.e. the two hanger stirrups), to transfer the interior dowel force of 42^K. Since the beam shear force resists only 20% of that, 80% must be transferred over the joint.

Since only one shear stirrup is available, capable of transferring only 50%, a direct strut must form. Here the force of hanger stirrup 5, which is not resisted by the beam shear force is assigned to shear transfer by stirrup(s), while the force of hanger bar 4 is assigned to shear transfer by direct strut. Hence direct strut F must connect the bottom loop anchorage with the top of hanger bar 4. Fan strut G must connect the top of hanger bar 5 with the bottom of shear stirrup 3. Fan strut E-E' must connect the top of shear stirrup 3 with the bottom loop anchorage. A direct strut B must connect the top of hanger bar 2 with the bottom loop anchorage. The beam shear force is selected to be transferred by two stirrups. Finally strut B is kinked to the mid-depth loop anchorage and the necessary kink in strut E-E' is calculated. Thus the geometry of the truss is established.

Since the vertical components of all element forces are known, their horizontal components follow immediately from the geometry. The horizontal components of the diagonal struts, in turn, determine the forces in the top and bottom chord as well as in the mid-depth bar. Since the boundary forces are (must be!) in equilibrium an equilibrium check is available at the end. In principle this is all graphic statics!

If the tensile strength or the end anchorage capacity at the longitudinal reinforcement is exceeded, the truss is adjusted. For instance, shear stirrup 3 is only loaded to half its capacity. By introducing an additional strut between the top of hanger bar 4 and

the bottom of shear stirrup 3, shear transfer by stirrup(s) can be increased. This reduces the force in direct strut F and, hence, the end anchorage requirements at the loop anchorage. Here this is not needed and not done because, whenever freedom exists in the assignment of forces, the selection is done so that diagonal struts result which do not deviate too much from 45^{o}. At 45^{o} degrees the diagonal compressive strength according to equations (2-1) to (2-3) is maximum. Figure 4.27 illustrates the truss model for the entire specimen. Construction of the truss model for the entire specimen is not really needed, though, since the boundary forces can be calculated by the beam theory equations (2-5) through (2-9) provided the B/D region boundary is placed a distance $d\cot\theta$ away from the dowel bar.

Figure 4.26(a) illustrates particularly nicely, that this joint or D-region in essence represents the left shear span of a deep beam as shown in Fig. 2.17(a) which is loaded by a suspended load, namely the interface tensile resultant, while the interface compressive resultant represents its support reaction. As shown in Fig. 2.17(b) test results agree well with the truss model analysis. Unfortunately, no reinforcement strains were reported or measured for BC28 which would allow a similar comparison.

The final step in this analysis is to check whether the D region capacity is adequate. The steel stresses need to be checked as well as the concrete compressive stresses, development/bond stresses within the joint, and the end anchorage of the bottom reinforcement. The largest tensile force in the tensile chord is 55.83^{K} which is

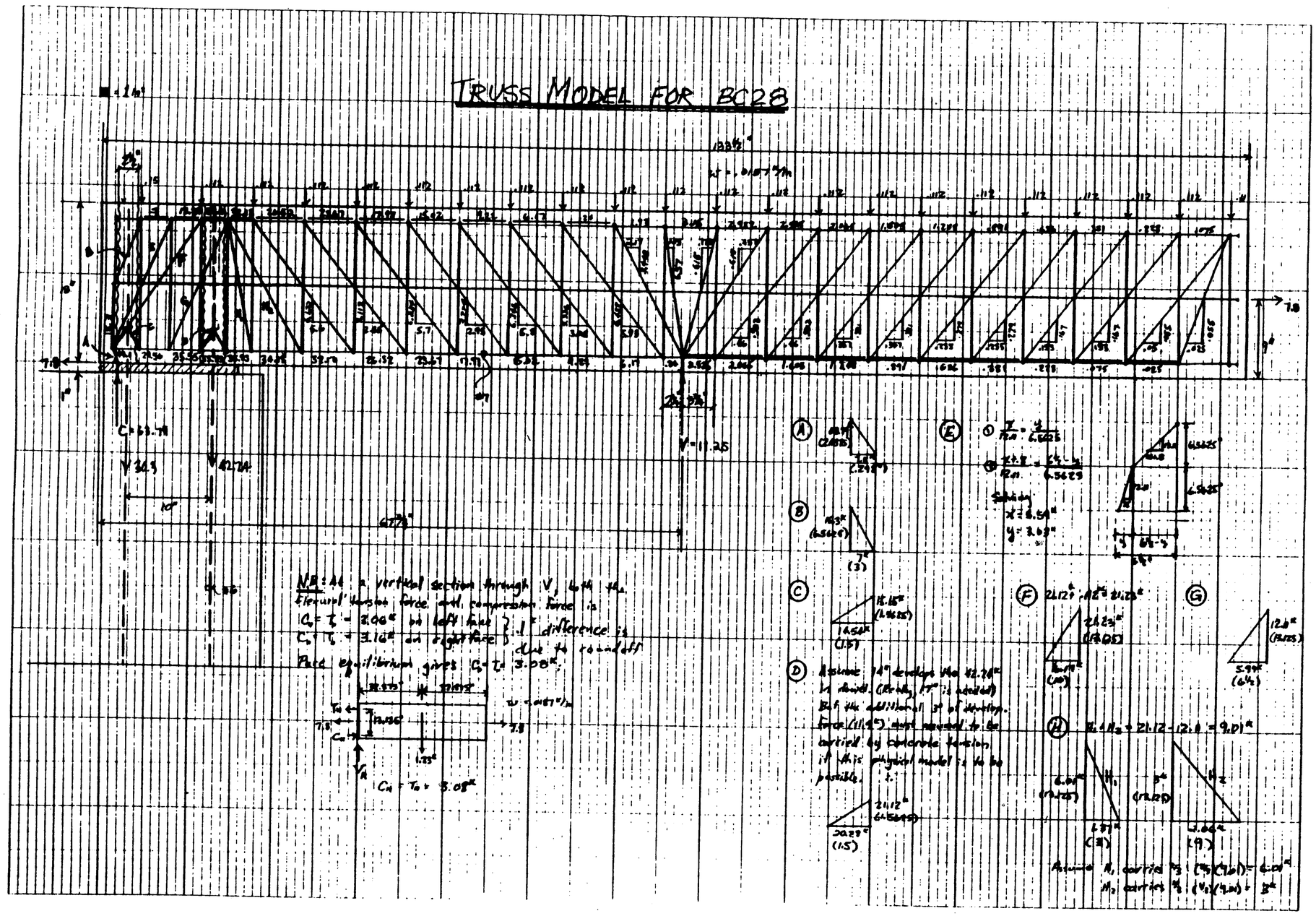

FIGURE 4.27: Truss model for specimen BC28

less than the yield capacity (76.4^K). The stirrup strength has already been considered in the construction of the truss model. The steel strength is thus adequate. The compressive strength of the concrete may be checked by computing the required thickness, a, for some of the largest compression element forces, and checking whether it does not violate the geometric constraints. For this specimen, the largest compression force in the chord at the top of stirrup 5 is 35.6^K. The computed compression block depth at the ultimate state is a = .50 in., which does not violate the geometric boundaries of the beam.

Next the diagonal compressive stresses are checked. In normal beam design the stress concentration at the center of the compression fans above support reactions and below concentrated loads do not usually need to be checked, since the concrete is in biaxial compression. For the same reason the diagonal compressive stresses are checked here only in the "shear span of the deep beam" i.e. between the tubes. The tangent of the angle between direct strut F and stirrup 3 is 10/14. Equation (3) gives therefore $f'_d/f'_c = 0.5 \cdot 10/14 = 0.36$. Hence, $f'_d = 0.36 \times 7020 = 2570$ psi. The required strut thickness is therefore a = 26.69/(2.57.8) = 1.3 in., where conservatively only an effective strut width of 8 in. lying within the stirrups is considered (i.e. the side cover is neglected). Thus strut F requires a/2 = 0.65 in. of "clear" concrete on either side which is clearly available between struts F and E. Similarly struts E and G are checked. Thus the compressive stresses are adequate and

the concrete is not crushing.

Since the struts' horizontal components unload onto the flexural rebar, the development/bond stresses acting over the horizontal width of the intersecting strut must transfer the horizontal components without violating the bond force requirements. More specifically,

$$\frac{A_s f_y}{\ell_d} = \frac{C_H}{a'} \qquad (4\text{-}20)$$

where A_{sfy} = capacity of rebar

ℓ_d = development length of rebar

C_H = horizontal component of the intersecting strut

a' = horizontal width of the intersecting strut

For specimen BC28 the diagonal compression strut with the largest horizontal component is strut D ($C_H = 20.28^K$). Its minimum horizontal extension a', (as given by equation (4-20)), is 6.3 in. Since a/2 is equal to the stirrup spacing strut D appears to interfere with strut G. Strut G and D together transfer a total horizontal component of 26.2^K. Hence, they need together a' = 8.2 in. Since this includes already a capacity reduction factor of 0.8 the actual minimum length is 6.5 in. Since the clear space between the tubes provides 7 in., bond and development is adequate and the bond stresses close to strut D are considered a local problem.

Finally, the compressive stress at the end anchorage loop must be checked. The computed compressive stress in the loop is, f_d = 8.06 ksi. Thus the computed compressive stress is only 15% higher than the uniaxial compressive strength of the concrete which is 7

ksi. Since the loop itself creates biaxial compression in its plan and is subjected to transverse compression, the stress state is triaxial compression. Because the concrete strength in triaxial compression can be several times larger than the uniaxial cylinder strength the loop anchorage is considered adequate.

Checks such as the preceding examples verify that the D region did not control the strength of the beam.

4.7.4 ANALYSIS OF D REGION BC29

Since the analysis procedure for this specimen is exactly the same as for specimen BC28 (section 4.7.3), only the characteristic difference in the D region truss model will be discussed.

Specimen BC29 is a closing knee joint which is discussed in detail in sections 3.2 and 3.3 For this specimen, with vertical ties in the joint, the characteristic truss model is shown in Fig. 3.7. Vertical, horizontal, and moment equilibrium of this beam about the interface at ultimate, (i.e. both dowels yield), predicts a maximum vertical load of $V = 3.21^{K}$. The large difference in capacity between the two specimens is due to the beneficial (BC28) or adverse (BC29) effect of the applied axial load.

The actual observed capacity was not reported. Figure 4.28 shows the discrete truss model of the resultants for the D-region and Fig. 4.29 for the entire beam. The truss element forces shown correspond to the computed maximum load $V = 3.21^{K}$.

Similarly as for specimen BC28, the dowel forces must be considered as "suspended loads". They are transferred from the

fictitious anchor plates of the dowels through compressive struts A' and A" to the lower bends of the adjacent hanger ties 1, 2 and 3, 4 respectively. The hanger ties then transfer these forces to the top of the beam (truss). For this specimen, all ties are "used up" as hanger ties so that no shear stirrups are available within the joint core. Rather all of the shear is transferred through direct strut action. Thus the characteristic truss model is really that of Fig. 3.5(b) rather than Fig. 3.7. However, since the hanger ties spread the dowel anchorage forces along the top of the beam, the direct strut of Fig. 3.5(b) becomes a "direct fan".

The tensile forces in the hanger bars are equilibrated at the top of the beam with diagonal compression struts. The vertical components of struts B, C and D, E balance hanger bars 1, 2 and 3, 4 respectively. Struts F and G balance beam shear stirrups 5 and 6 respectively. The horizontal components of struts B, C, D, E, F and G are balanced by the bond stresses along tensile reinforcement at the top of the beam. At the bottom, strut A, which is the interface compression resultant, equilibrates both the vertical and horizontal components of struts B, C, D, E, F, G together with the compression resultant of the beam.

Since no shear stirrups in the joint core are present, struts B, C and D, E essentially represent two direct fans. Struts F and G represent the beam end fan introducing the beam shear into the column compressive resultant as illustrated in Fig. 3.5(d). Note how the spreading of the direct strut into a fan significantly helps reduce the end anchorage requirements for the flexural reinforcement at the

(a)

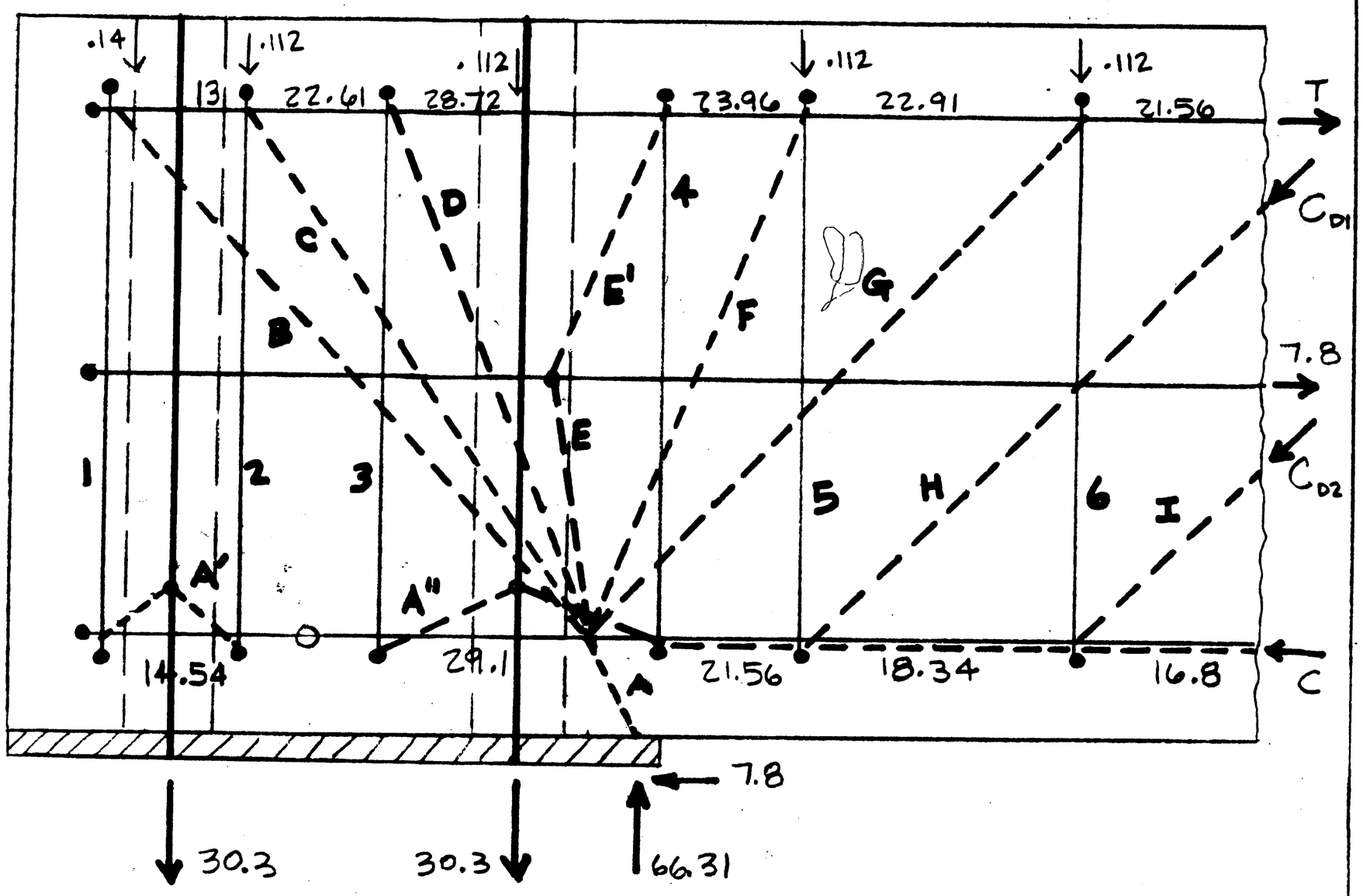

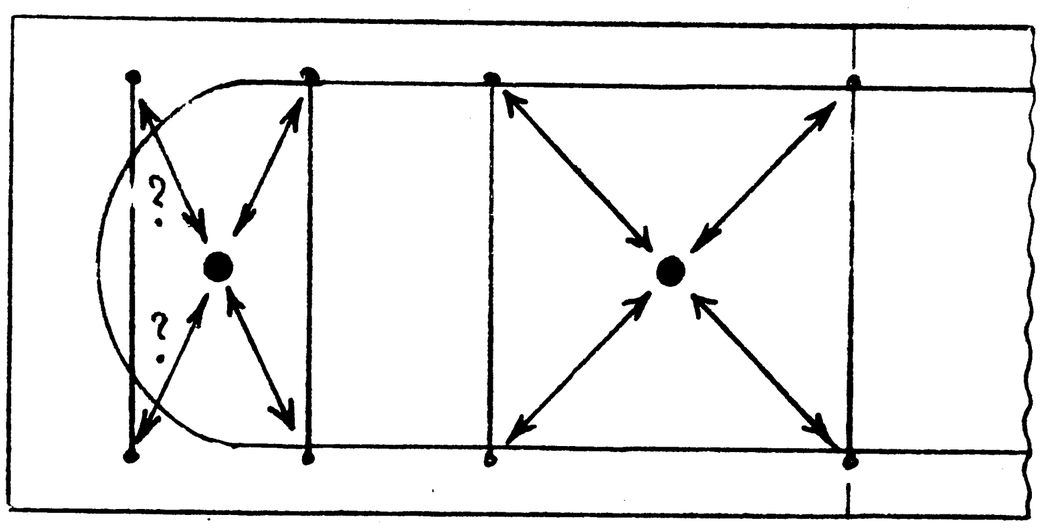

(b)

Transverse action

Elemental and boundary forces not shown in (a): kips

A :	66.77	D :	3.79	1 :	15.15	6 :	1.71
A′ :	21.00	E :	15.51	2 :	15.15	C_{D1} :	4.78
A″ :	32.81	E′ :	15.94	3 :	15.21	C_{D2} :	2.31
B :	19.96	F :	3.79	4 :	15.21		
C :	18.06	G :	2.27	5 :	3.53		

FIGURE 4.28: D region truss for BC29

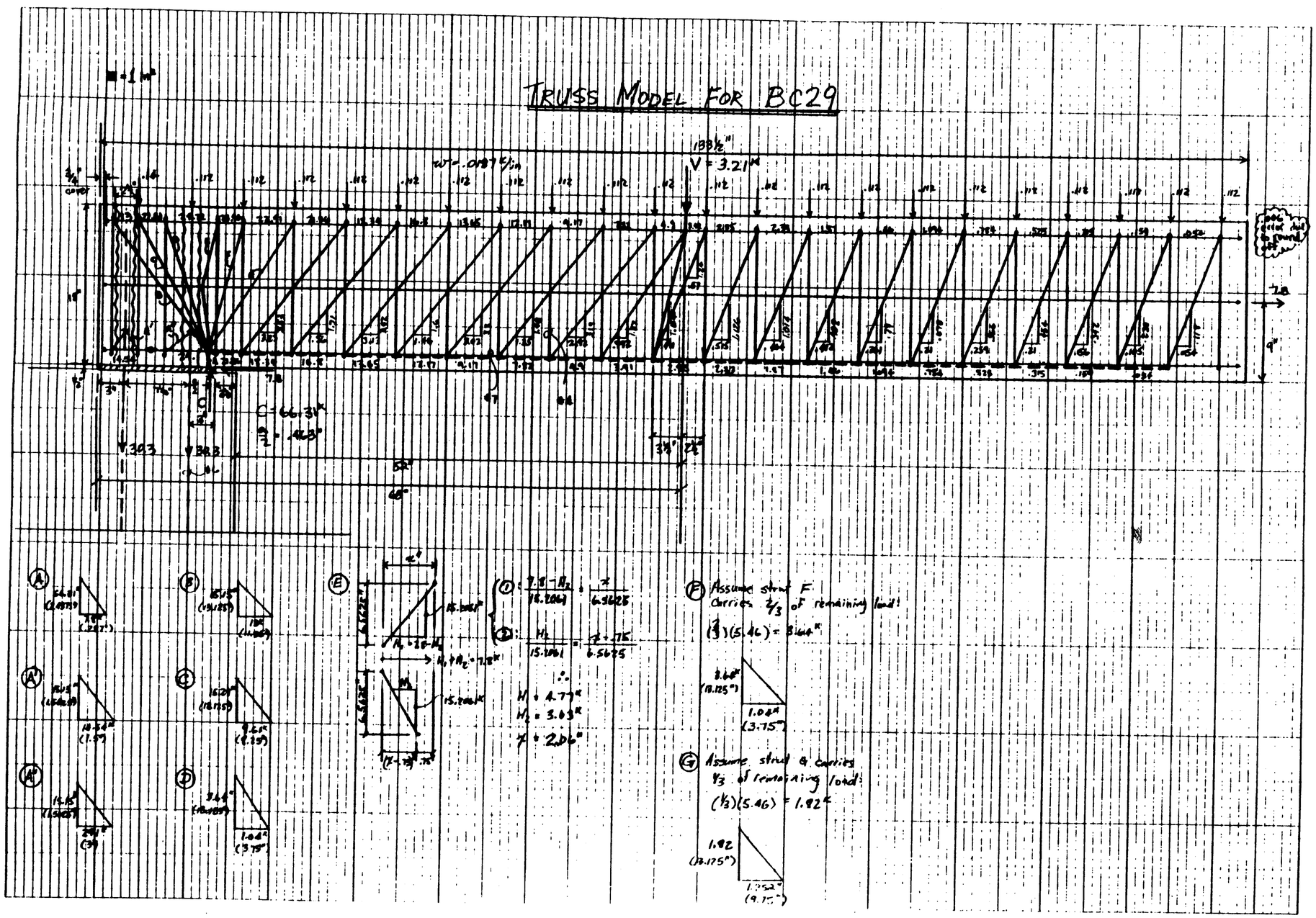

FIGURE 4.29: Truss model for specimen BC29

top of the beam. While the maximum tensile force of 28.7^K would be constant out to the loop anchorage for a concentrated direct strut, it reduces to 13^K at the loop anchorage for the direct fan. It should also be noted that at the bottom (compression) chord of the beam high tensile forces exist in the bottom reinforcement within the joint core, between struts A' and also between struts A". These are due to the "local trusses" which in "transfer girder" manner transfer the dowel forces out to the hanger ties.

As in specimen BC28, the last step in the analysis is to ensure that the steel strengths, concrete compressive stresses, development/bond stresses, and end anchorage conditions within the joint core are satisfactory. If so, the D region does not control and the assumption that the interface controls is valid and verified.

Since the truss element forces are rather smaller than in BC28 these checks are not repeated here. Rather, the basic deficiency of this detail and truss model shall be discussed. The crucial detail in a closing knee joint is proper interlocking anchorage of the bars in the upper exterior corner, if the tensile reinforcement is not continuous around the corner. However hanger tie 1 is not properly interlocked with the loop of the longitudinal reinforcement as evidenced by Fig. 4.28(b). When a diagonal tension crack propagates from the exterior upper corner along strut B, the tie simply "slips off" the loop. Thus strut B and A' (left) cannot form.

According to the truss model of Fig. 4.28, though, tie 2 is not

loaded to its capacity of 24^K. When tie 1 slips off, the force in tie 2 and accordingly the vertical component of strut C can increase to 24^K while the force in tie 1 and strut B drops to zero. Since dowel bar and hanger tie 2 are eccentric, a moment develops tending to rotate the tube. However, since the grout tube is firmly enclosed in the loop anchorages and the loop forces are small, this moment can easily be resisted by the top and bottom chords. Thus a safe prediction of the ultimate load would have to be based on the dowel forces that can be anchored, namely 24^K. To make the hanger tie 1 effective and permit it to transfer the yield strength of the dowel bar, hanger bar and loop anchorage must be welded together or otherwise mechanically connected top and bottom.

4.7.5 CONCLUSIONS OF ANALYSIS

Creating the truss models for these specimens is a relatively quick and simple task. Minimal effort has been used, yet quite a bit has been learned with respect to the function of the internal elements. Equipped with such understanding, an engineer may rationally and intelligently design the internal elements to meet both strength and anchorage requirements. The truss models of Figs. 4.26 through 4.29 show that the function of the connections themselves is to bring moments (force couples) "around the corner" as described in chapters 2, 3, and 4. The monolithic knee joint truss models of chapter 3 can be used for these precast corner joints, since the D region in the beam above the beam-column interface plays of course exactly the same role.

Since the truss models allow distinguishing between different functions of the reinforcement such as between "hanger reinforcement" and "shear stirrups", a designer can appropriately detail the connections so that specific reinforcements are optimally located and anchored for specific uses. For instance, designing the corrugated dowel tubes as hanger reinforcement relieves the stirrups from the "hanging task". Thus those stirrups can then be used to transfer joint shear which reduces the end anchorage requirements for the longitudinal flexural reinforcement, as described in chapter 3.

However, designing the corrugated tubes for the hanger bar function requires not only that they have sufficient tensile strength to transfer the dowel forces, but also that they themselves are fully anchored above the top beam reinforcement. The truss further indicates where reinforcement is not needed. For example, in the D region truss of specimen BC28, the stirrup closest to the beam end over the column support is useless since, for this loading it is not needed as hanger tie nor can it serve as shear stirrup. On the other hand for the closing knee joint BC29 this same stirrup is the most critical element, along with its companion, to turn the flexural tensile resultant around the corner. Yet it cannot interlock with the loop and the compression strut. Since it cannot be physically engaged, it does not contribute any resistance to the loads. Thus truss models can draw attention to such critical details because they show which those critical details are.

The details shown in Figs. 4.24 and (as qualified) 4.25 indeed allow a plastic truss model to develop. The preceding analyses show

though that the D region did not control the behavior of the specimens, rather the interface controls. However, if the dowel forces are doubled by providing more realistically a dowel in each corner of the column, the capacity of the existing stirrups would be insufficient. If the capacity of the dowels is doubled without increasing the capacity of the stirrups, the D region would not be able to transfer the boundary forces and would therefore control the behavior and strength of the specimen.

Once again, rational design requires that the function of the internal elements be identified. The truss models just described allow for this identification. However, it must be realized that the geometry and strength of the truss models which form the basis of the analysis and the design, strongly depend on the anchorage details. In principle, therefore, detailing must be done by the engineer while he develops his analysis model, namely the truss model. In truss modeling, analysis, design, and detailing represents one integrated process.

The purpose of this analysis was to analyze a test specimen. Thus actually measured material properties and loads were used along with capacity reduction factors of unity. In design one proceeds exactly the same way except that the boundary forces are evaluated with the factored loads and the truss member capacities are multiplied with a capacity reduction factor, ϕ, of 0.9 for steel tension elements and 0.7 for concrete compression elements.

Finally, a need for well documented experiments with well

instrumented specimens is noted for verification of these truss models for precast concrete connections. Of particular importance are tests on anchorage details which can answer questions such as: When does a tie "slip off" a loop? Is the anchorage capacity dependent in the inclination of the strut that bears into it?

5. CONCLUSIONS

The preceding chapters show that truss models represent a rational and unifying analysis or design tool through which structural behavior can be understood. It is demonstrated that truss models offer both a quantitative and qualitative insight into the characteristic behavior of a structural component and the functions of its details. The engineer becomes aware of the internal force paths which indicate the correct locations of reinforcement and anchorage points. Since truss models are based on the fundamental principles of structural mechanics, including theory of plasticity and compression field theory, reinforcement proportions as well as anchorage and development locations follow from geometry, equilibrium, and material strengths rather than from empirical rules of thumb. If the concrete is given some ductility by providing "caging type" minimum distributed reinforcement, design by truss modeling guarantees at least one internal force path through which the loads can safely be transferred to the reactions. In other words, truss models ensure local equilibrium throughout a component. This contrasts with typical current design methods which check only one or two failure planes, such as an interface and a beam or column section, which doesn't assure a safe force path between these failure planes.

The preceding chapters suggest that truss models are a unifying design tool in that they apply to beams, deep beams, corbels, and slabs; to flexure, shear, axial load, and torsion; to prestressed and non-prestressed concrete; to precast and cast-in-place concrete; to

monolithic concrete joints and to precast concrete connections; and most importantly chapter 4 suggests that they can also be applied to a wide variety of different precast concrete connection types. This unifying nature, while appealing, is of course not the primary reason for using truss models. Rather, the primary reason is that truss models provide for consistent transitions between different member types, such as beams and deep beams or beams and slabs, and consistent treatment of combined actions, such as combined flexure, shear and torsion.

It is shown, particularly in section 4.5, that not only do truss models unify design for different types of components, load actions, and materials but also truss models - when used at different levels: "global" truss models for member design, "local" truss models for connection D regions - allow connection design to be integrated into member design in a consistent, methodical, and simple manner.

Using truss models results in a design methodology which is distinct not only in its consistency of treatment of different types of members and connections, but also in its emphasis on design as synthesis. Today's engineer often seems to be relegated to the role of an analyst. He tries to find out with powerful computational tools in a black box, how a component actually behaves which has been proportioned with crude empirical rules. While truss models can also be used for analysis, they reveal their power and simplicity only in design: The engineer quite literally constructs the internal force paths into the member or connection which it needs to perform its intended function.

At a very general level, this methodology may be outlined in the following five steps:

1. identify the general purpose and function of the structural component to be designed;

2. determine the location and magnitude of all loads and reactions;

3.(a) locate all B and D regions; note that connections include both the connection interface and the D regions on either side;

(b) design the B regions with ordinary beam theory or truss models and determine the boundary forces at the boundaries between B and D regions;

(c) construct a truss model that geometrically fits into the D region and does not violate equilibrium and strength conditions; the truss is modeling the internal force paths between the ends of B regions or between loads and supports at the ultimate state;

4. provide a reinforcement layout that realizes the truss model of step 3 in steel and concrete, and proportion the steel and concrete elements;

5. make sure that the selected truss can indeed develop by (a) ensuring that all the reinforcement and compression elements are fully anchored or developed at the locations indicated by the truss' geometry and by (b) providing "caging type" minimum distributed reinforcement for ductility.

Since at least one load path is ensured at the ultimate state, these five steps guarantee a structurally sound design. The following sections elaborate on these five steps.

5.1 IDENTIFICATION OF THE STRUCTURAL COMPONENT

As obvious as it is, the design process must begin with the determination of the purpose and intended function of the structural component. Only then can all loads and reactions be estimated and properly located. This step is necessary since the loads and reactions define the boundary conditions of the structural component for which a truss is to be realized.

Handbooks catalogue many suggested precast concrete connection details merely in the form of labeled sketches. It is recommended that these details are also fully described with respect to their intended purpose and function, and that the boundary forces and moments be shown directly on the sketches. Thus, there is no question as to the scope of the suggested detail and its range of applicability. Furthermore, the suggested details must also show all of the primary reinforcement of the connected elements and their locations. Chapter 3 and 4 clearly show that the exact location of the anchorages of primary reinforcement and the exact location of connection hardware anchor points with respect to the primary reinforcement can play a crucial role. The location of a stud head or other mechanical anchorage may be satisfactory for a closing moment, but lead to extremely poor performance for opening type moments. For this reason, the definition of connection hardware in

the introduction of chapter 4 includes all reinforcement not only at the interface, but also in the adjacent D regions.

5.2 MODELING: TRUSS MODELS

If the location and magnitude of all loads and reactions are known, design begins with the identification of all the B and D regions of the structural component. The D regions are characterized by disturbances in the internal force paths according to beam theory, which result from geometric discontinuities, concentrated loads and reactions, transfer of prestress and, of course, connections. The extension of a D region can be estimated by the principle of St. Venant as a distance equal to the member depth measured from the disturbance (for the present purposes this estimate has been refined to mean a distance dcotθ). B regions are located between the D regions. If the B regions are designed with standard methods, the boundary forces at the B/D region boundaries must be determined. Engineers familiar with truss models usually prefer to model also the B-regions with truss models, at least qualitatively. Thus the internal force paths between the supports and the loads are modeled with concrete compression fields and steel tension fields. While the stress trajectories of these fields are uniformly distributed within B regions, they fan or radiate out from the center of disturbance in D regions. A discrete truss model can now be drawn by replacing compression and tension fields with the lines of action of their resultant. The intersection of compression and tension lines mark off the center of the truss nodes.

In the design of connections, the truss must be explicitly drawn for the D regions on either side of the interface. The truss which models the internal force paths must be statically and geometrically stable and satisfy equilibrium at all the nodes, boundaries and interfaces. The struts and nodes must fit within the geometric constraints of the D-region and must not overlap. Truss model and stress distributions used to design B regions or interfaces must be locally in equilibrium and geometrically compatible at B/D region boundaries and interfaces.

Once a discrete design truss is chosen, layout and proportioning can begin.

5.3 LAYOUT AND PROPORTIONING: REALIZING THE TRUSS IN STEEL AND CONCRETE

In design, layout requires that the appropriate materials be placed so that all the elements of the truss can be realized. Tensile members in the discrete truss indicate where tensile reinforcement is necessary. Except for shear in slabs, the tensile strength of concrete is not relied upon. Compression members in the truss define where compression elements such as struts, fans, and/or arches are to be placed. Static analysis of the discrete truss gives the forces in these elements which are then used to proportion the reinforcement and compression elements.

For design, the static analysis is carried out at ultimate state, as defined by the ACI code[3], i.e. at factored loads, while the elements are proportioned using the appropriate capacity

reduction factors, ϕ, for tension and compression elements. The reinforcement should yield prior to concrete crushing. For flexure and axial load (i.e. for the tension and compression chords of the truss model) the ACI code specifies for this purpose, limits on the reinforcement ratio or index, which follow from the strain distribution in the desired failure mode. For diagonal compressive elements, equations (2-1) to (2-3) similarly make the diagonal compressive strength dependent on the strains in the desired failure mode. For the compression chord, the familiar effective compression block strength of $0.85f'_c$ is used. Using the appropriate concrete compressive strength and capacity reduction factor, the required dimensions of the compression elements and of the nodal zones can be computed and checked against the physical geometric limits of the structural component. If the struts or nodal zones exceed these limits or overlap, the geometry of the truss or of the structural component itself must be adjusted. Working only with the discrete truss of the resultants may therefore be dangerous.

The B regions may also be designed using beam theory as specified by the ACI code[3]; some care is needed in this case, though, in evaluating the boundary forces at the B/D region boundaries. To ensure compatibility between the different models, equations (2-5) to (2-9) must be used where cotθ is calculated with equation (2-7) using the stirrups actually provided in the B region. No special problems arise if the section-by-section approach of section 2.4.1 is used or the provisions for combined shear and torsion in the PCI Design Handbook[1].

All restrictions and provisions of the draft for a new chapter 11 of the ACI code, which codifies truss models, shall be satisfied.

5.4 DETAILING THE TRUSS CONNECTIONS: ANCHORAGE AND DEVELOPMENT

Poor performance of structures, particularly of precast concrete structures, can more often than not be traced to connections. However, as the preceding chapters show, poor performance of the connections themselves can again equally likely be traced to the "local connections" of the truss that tries to form within the D regions of connections after the concrete has been cracked; i.e. to poor anchorage and development of the primary reinforcement and connection hardware. If the truss elements are not properly connected, i.e. not properly anchored and developed, the truss "dismembers" and disappears. A major cause of cracking of the D regions of precast concrete connections are the restraining forces due to imposed deformations such as movement of the building frame and volumetric changes resulting from creep, shrinkage, and temperature changes. These restraining forces are difficult to predict and are not distributed as in monolithic concrete, but concentrated at a few connections. They tend to grow until the material limits are exceeded somewhere and they are released through concrete cracking in the D region or steel yielding at the interface. Anchorage and development of the steel in accordance with the D region truss model ensures that these imposed movements do not jeopardize the connection load capacity for the primary design loads.

Realization of the design truss model requires that the truss

nodes be detailed so as to fully anchor and develop the truss elements for the forces entering the node. Not only must the reinforcement be anchored, but so do the compression elements. In essence, the compression elements supply the forces which anchor and develop the tension reinforcement, while the tension reinforcement supplies the forces which support and anchor the compression elements. Thus, the concrete compression struts and steel tension ties are in an action-reaction relationship. Consequently, mechanical anchorages and development lengths must be placed in a location where compression struts can supply the reaction, i.e. "behind" the truss node. In other words, anchorage of tension ties with compression struts requires that the tension tie be extended far enough out that it can introduce its tensile force as compression behind the node. Thus proper anchorage and development has two aspects: Sufficient strength of the anchorage or embedment length and correct location.

The ACI code[3] specifies that development length be measured from the "critical section". For connections and joints this is usually interpreted to mean the interface between the joined members. Chapters 3 and 4 clearly show, though, that this does not generally ensure that the truss nodes can form in a location which permits the connection D region or joint to develop the flexural strength of the adjoining structural components. Rather equilibrium and bond strength may force the truss nodes to form in locations which imply a reduced internal flexural lever arm in comparison to that of the connected members. For D regions and joints the "critical section"

must therefore be specified to lie behind the nodes of the design truss model.

Realization of the design truss model requires not only that the truss elements be properly anchored at the correct location, but also that the concrete be given minimum ductility so that it can form the compression struts. The final step in the design process is therefore to ensure that the concrete is "caged" by a minimum amount of distributed reinforcement.

The next section presents a preliminary version of design guidelines for connections. Proper anchorage and development of truss elements play of course a prominent role in these guidelines.

5.5 PRELIMINARY DESIGN GUIDELINES FOR CONNECTIONS

The insights gained through the qualitative and quantitative analyses presented in the preceding four chapters allow us to make a first step toward a consistent unified design methodology for connections based on rational models. The insights and conclusions drawn are formulated in the form of "code provisions and commentary" and may be viewed as a first rough draft for provisions on connections design

(a) Field experience and the experimental and analytical evidence presented in the preceding chapters show that the performance of connections and joints is often controlled by the D regions on either side of the interface between the connected components. Design and detailing of these D regions must therefore be an integral part of connection design. Similarly, in connection experiments the test

specimen must include realistically modeled D-regions, and the possibility must be considered that these D regions are precracked due to imposed deformations. Chapters 3 and 4 demonstrate that truss models represent a simple yet rational and powerful tool to understand and design these D regions and to integrate connection design into member design.

1. Each connection creates a locally disturbed region (called D region) adjacent to the interface between the connected members, the extension of which can be estimated using the principle of St. Venant. The regions within which, according to the principle of St. Venant, the stress flow determined by beam/plate/slab/shell theory is no longer disturbed, are called B regions.

2. Connection design shall include both the design of the interface and the design of the D region(s).

   2.1 Design of the interface between dissimilar materials such as steel against concrete and concrete cast against hardened concrete shall be based on the applicable provisions for interface shear transfer of the ACI code.

   2.2 Design of the D region(s) shall be based on a truss model which geometrically fits within the D region and satisfies the static boundary conditions (forces, stresses) at the interface and at the transition to the B region(s).

   2.3 Alternatively, design may be based on tests or empirical rules derived from tests provided that these tests include the D region(s) and simulate the actual conditions of service, including effects of imposed deformations such as building frame movement or volumetric changes due to phenomena such as creep, shrinkage, temperature changes, and temperature gradients.

(b) ACI Committee 318(E) has prepared in collaboration with ACI/ASCE Committee 445 a draft for a revised chapter 11 for the ACI code. The provisions introduce explicit truss models, define the elements of truss models, specify the concrete compressive strengths to be used

for compression chord, diagonal struts, and nodal zones as well as the applicable capacity reduction factors, and refer to or modify chapter 12 for anchorage and development as needed. Connection design provisions can therefore simply refer to chapter 11 of the ACI code, when the revision is enacted, and need only deal with issues of connection design which are not sufficiently covered there.

3. Truss models shall satisfy chapter 11 AC1318-92 as well as all provisions of this chapter.

4. Design of B regions shall be based on the applicable provisions of the ACI code.

(c) The performance of the moment connection BC15 with top embedded plate[23], discussed in section 4.6, Fig. 4.20, demonstrates the danger of unattended eccentricities. The behavior of the connection was ultimately governed by rotation of this plate which led in turn to rupture of the rebar welded to it in the heat affected zone. The review of the 24 other tests described in the same reference[23] reveals a very high percentage of connection details for which performance problems can be traced to unattended eccentricities. Particularly in simple connections eccentricities often seem to be neglected.

5. In a truss node, the lines of action of the stress resultants of concrete compression struts (including fans and arches) and reinforcement ties shall intersect in one point. Eccentric joints are not permitted unless this eccentricity is explicitly considered in the truss model.

(d) As described in sections 2.8 to 2.10, chapters 3 and 4, and section 5.4, anchorage and development of the truss elements in the correct location is crucial if the design truss model is to be realized. The experimental evidence presented suggests that

connection and joint details perform satisfactorily, if rebars are anchored or developed in accordance with a truss model which can develop the flexural strength of the connected components. The truss models for the nib details (section 2.9), for the opening and closing knee joints (sections 3.2 and 3.3) and for the precast corner connections (sections 4.6 and 4.7) - they all demonstrate the same principle: For reasons of equilibrium the forces which redirect compressive resultants (struts) to turn the corner, must come from the bar anchorages, while the forces which redirect tensile resultants to turn the corner, must come from the compression strut anchorages. Struts and ties anchor each other, their anchor forces are in a action-reaction relationship, or simply,

6. At truss nodes both anchorage of rebars and anchorage of concrete compression struts shall be ensured.

The truss models for the nibs, knee joints, and precast simple and moment connections all demonstrate that the rebars must be extended through the truss node and anchored "beyond" the node through anchor plates or its equivalent. This mechanical interlocking allows a biaxially compressed nodal zone to form against which the compression struts can bear. Only through such interlocking can a tension tie intercept a flexural compressive resultant in a C-C-T node and redirect it to turn the corner, or can a compression strut intercept a flexural tensile resultant in a C-T-T node and redirect it to turn the corner. Hence,

6.1 Anchor plates, closed loops, fictitious anchor plates, or bent continuous bars shall interlock with the concrete struts at a node such that a biaxially compressed nodal zone can form in-between.

6.2 Compression struts shall be anchored by bearing against biaxially compressed nodal zones or anchor plates.

6.3 Rebars shall extend through the nodal zone and be anchored beyond the nodal zone through anchor plates, closely spaced loops, bends, or by extending them by a development length into a block of concrete which is *not* used by other compression struts. This block of concrete may be considered as a fictitious anchor plate located a development length from the bar end.

Welding a rebar to a steel plate that is parallel to the bar, is clearly not an effective anchorage since the steel plate may simply "knife" through the concrete. Since such details are being used (nib 2C, section 2.9.2);

6.4 If a rebar is anchored by welding it to a plate that is oriented parallel rather than normal to the bar, this plate shall in turn be anchored according to these provisions.

(e) According to the ACI code[3], development length is to be measured from the "critical section." For connections and joints this is usually interpreted to mean the interface between connected members. The experimental evidence presented in chapter 3, particularly the poor performance of many opening knee joint details (section 3.3), suggests, though, that this is not generally sufficient and that the development length should be measured from the applicable truss node as discussed above. Therefore, the concept of a "fictitious anchor plate" is introduced in provision 6.1 and used to define the location of the "critical section."

6.5 The critical section from which development length is to be measured shall coincide with the location of the fictitious anchor plate in accordance with 6.1. The final width of struts and nodal zones shall be considered in determining this location. This provision shall supersede any provisions of chapter 12 of the ACI code.

(f) In general, it is preferable not to rely on friction for anchorage of struts. This can be achieved, for instance, by welding a crossbar to the plate as discussed in section 2.9.1. If friction is relied upon, it must be checked.

6.6 If compression struts are anchored by inclined bearing against a surface without a biaxially compressed nodal zone in-between, interface shear transfer between surface and strut shall be limited by the shear friction provisions of chapter 11 ACI318.

(g) Because the detailing for anchorage and development determines the geometry of the very truss model on which design is based, and also, since detailing influences the function of the internal elements (such as the function of the corrugated steel tube and of the ties in specimens BC28 and BC29 treated in section 4.7) it is concluded,

7. Detailing of D regions for anchorage and development is the responsibility of the structural engineer.

(h) Since the tests underlying the empirical formulas for development, transfer, and splice lengths in the ACI code[3] may have satisfied boundary conditions which are quite different from those "behind" a truss node of a D region, these formulas must be used with caution. Clearly, the splice provisions of the ACI code[3] cannot apply, for instance, to a splice bent around the corner of a closing knee joint. Until anchorage and development provisions are formulated specifically for use with truss models, the engineer must be aware of this situation and carefully check the applicability of these formulas.

8. Anchorage details which cannot or are not resolved by

truss models into elementary conditions of bearing and bond strength covered by ACI318, shall be validated by tests.

Clearly, these guidelines or provisions represent only a first rough draft and obviously do not cover all the ground. They do demonstrate though, and that is their primary purpose, that truss models allow connection design to be codified at a similar level as design for flexure and axial load: Only general principles of modeling, analysis, design, and detailing need to be specified, which are common to all types of connections. Thus codification of connection design becomes possible without imposing on the industry the standardization of details which would be necessary, if empirical rules are codified for each detail.

5.6 FUTURE RESEARCH NEEDS

Generally, a scarcity of well-documented experiments with well-instrumented specimens is noted in the precast concrete connection area. An experimental program with carefully and well instrumented connection specimens which include the D regions, is needed. These specimens should allow the internal force paths to be measured for comparison with the truss model predictions, as has been done for monolithic concrete D regions.

Considerable uncertainty exists regarding the use of the anchorage and development formulas of the ACI code, Chapter 12, in the context of truss models for D regions. The range of applicability of these formulas is limited to the test conditions from which they were derived. Thus the test data underlying Chapter

12, ACI318, should be reviewed with the objective to specify the (boundary) conditions for which these provisions hold, in a form suitable for truss modeling. An experimental program should be started on anchorage details which frequently occur in many different types of connections. The test results should be presented in a form that is independent of a specific connection type and in terms of parameters that are useful for truss models.

The formula for the compressive strength of diagonally cracked concrete, equation (2-1), has been derived from test specimens subjected to uniform diagonal compression fields. Further experimental research on its applicability to concentrated struts is needed. Closely related to this problem is the question of which effective strut width should be used in the truss models for simple connections.

Since a high percentage of the failures of the 25 tests reported in references[23] is due to weld ruptures in the heat affected zone, newer, more advanced materials need to be developed. Perhaps some advanced adhesives can replace welding all together. The effectiveness of a connection designed with truss models is limited by the effectiveness of the anchorage and development of its elements. Thus if the quality of welds in anchorage details cannot be sufficiently controlled, new adhesives may offer a solution.

Chapter 3 shows that monolithic concrete joints have many inherent anchorage and development problems. This clearly represents an opportunity for precast concrete. If connection hardware such as splice sleeves, is innovatively designed to not only join reinforcing

bars, but also solve at the same time some of the inherent anchorage problems of monolithic joints, precast concrete moment connections might even outperform monolithic joints. At least the reinforcement congestion could be reduced resulting in better constructability.

REFERENCES

1. PCI,
   PCI DESIGN HANDBOOK, PRECAST AND PRESTRESSED CONCRETE, 3rd Ed., 1985, Prestressed Concrete Institute, Chicago, Illinois.

2. PCI,
   MANUAL ON DESIGN AND TYPICAL DETAILS OF CONNECTIONS FOR PRECAST AND PRESTRESSED CONCRETE, 2nd Ed., 1988, Prestressed Concrete Institute, Chicago, Illinois.

3. ACI,
   BUILDING CODE REQUIREMENTS FOR REINFORCED CONCRETE, (ACI 318-86), American Concrete Institute, Detroit, Michigan.

4. Hawkins, N. M., Mitchell, D., and Roeder, C. W., "Moment Resisting Connections for Mixed Construction", American Institute of Steel Construction Engineering Journal, first quarter, 1980, pp. 1-10.

5. Roeder, C. W. and Hawkins, N. M., "Connections Between Steel Frames and Concrete Walls", American Institute of Steel Construction Engineering Journal, first quarter, 1981, pp. 22-29.

6. Schlaich, J., Schafer, K., and Jennewein, M., "Toward A Consistent Design of Structural Concrete", PCI Journal, Vol. 32, No. 3, May-June, 1987, pp. 74-149.

7. Rogowsky, D. M. and MacGregor, J. G., "Design of Reinforced Concrete Deep Beams", Concrete International: Design and Construction, Vol. 8, No. 8, August 1986, pp. 49-58.

8. Grob, J. and Thurlimann, B., "Ultimate Strength and Design of Reinforced Concrete Beams under Bending and Shear", Publications, International Association for Bridge and Structural Engineering, Zurich, Vol. 36-II, 1976, pp. 107-120.

9. Collins, M. P. and Mitchell, D., "Design Proposals for Shear and Torsion", Journal of the Prestressed Concrete Institute, Vol. 25, No. 5, September-October 180, 70 pp.

10. Cook, W. D. and Mitchell, D., "Studies of Disturbed Regions Near Discontinuities in Reinforced Concrete Members", ACI Structural Journal, Vol. 85, No. S23, March-April, 1988.

11. Mueller, P., "Plastic Analysis of Torsion and Shear in Reinforced Concrete", Final Report, IABSE Colloquium of Plasticity in Reinforced Concrete, Kopenhagen, Denmark, May 1979.

12. Marti, P., "Basic Tools of Reinforced Concrete Beam Design", ACI Journal, Vol. 82, No. 1, January-February, 1985, pp. 46-56.

13. Marti, P., "Truss Models in Detailing", Concrete International, Vol. 7, No. 12, December, 1985, pp. 66-73.

14. Marti, P., "Applications of Plastic Analysis to Shear Design of Reinforced Concrete Members", Lecture note for a visit to Japan sponsored by the Building Research Institute, Ministry of Construction, Japan, February, 1987.

15. Bruchwiderstand und Bemessung von Stahlbeton-und Spannbetontragwerken (Ultimate Limit States and Design of Reinforced Concrete and Prestressed Concrete Structures), Schweizerischer Ingenieur-und Architekten Verein (SIA), Zurich, 1976

16. CSA Technical Committee on Reinforced Concrete Design, Design of Concrete Structures for Buildings, CAN3-A23.3-M84, Canadian Standards Association, Rexdale, Ontario, December 1984, 281 pp.

17. CEB-FIP Model Code for Concrete Structures, Bulletin d'Information 124/125E Comite Euro-International du Beton, Paris, 1978, 348 pp.

18. MacGregor, J. G., REINFORCED CONCRETE MECHANICS AND DESIGN, Prentice Hall, New Jersey, 1988.

19. Vecchoi, F. and Collins, M. P., "The Response of Reinforced Concrete to In-Plane Shear and Normal Stresses", Publication No. 82-03, Dept. of Civil Engineering, Univeresity of Toronto, March 1982.

20. Mattock, A. H., Private Communication.

21. Nilson, A. H., DESIGN OF PRESTRESSED CONCRETE, Second Edition, Wiley, New York, 1987.

22. Mattock, A. H. and Thergo, T., "Strength of Members with Dapped Ends", PCI Research Project No. 6, University of Washington, 1986.

23. Stanton, J. F., Dolan, C. W., Anderson, R. G., and McCleary, D. E., "Moment Resistant Connections and Simple Connections", PCI Research Project 1/4, 1986.

24. Park, R. and Paulay, T., REINFORCED CONCRETE STRUCTURES, Wiley-Interscience, New York, 1975, Chapter 13.

25. Franz, G. and Niedenhoff, H., "The Reinforcement of Brackets and Short Deep Beams", Cement and Concrete Association, Library Translation No. 114, London, 1963.

26. Swann, R. A., "Flexural Strength of Corners of Reinforced Concrete Portal Frames", Technical Report, TRA 434, Cement and Concrete Assoc., London, November, 1969.

27. Hanson, N. W. and Connor, H. W., "Seismic Resistance of Reinforced Concrete Beam-Column Joints", Journal of Structural Division ASCE, Vol. 93, ST5, October, 1967, pp. 533-560.

28. Pensiero, J. P. and Mueller, J. P., "Analysis of a Pretensioned Dap Ended Beam Using Truss Models", Lehigh University, Dept. of Civil Engineering, 1988.

29. Taylor, H. P. J. and Clarke, J. L., "Some Detailing Problems in Concrete Frame Structures", The Structural Engineer, Vol. 54, No. 1, Janaury, 1976, pp. 19-32.

30. Mattock, A. H. and Chow, J. L., "Shear Transfer in Reinforced Concrete With Moment or Tension Acting Across the Shear Plane", PCI Journal, July-August, 1975, pp. 76-92.

31. Mueller, P., Lecture notes for course CE 365 Prestressed Concrete, Lehigh University, Bethlehem, PA.

Vita

The author was born in the Bronx, New York City on November 15, 1964. He is the youngest son of Italian immigrants, Mario and Maria Pensiero.

The author received his early education at Cardinal Spellman High School located in the Bronx, and graduated in 1983. In August of 1983 he enrolled in Manhattan College, located in Riverdale of the Bronx, to pursue an education in structural engineering through the Department of Civil Engineering. He was inducted into Chi Epsilon Civil Engineering Honor Society, Tau Beta Pi Engineering Honor Society, and Epsilon Sigma Pi Honor Society at Manhattan College. The author also received an award from the New York State Society of Professional Engineers in his junior year. He is a member of the American Society of Civil Engineers. In June of 1987, the author was awarded the Bachelor of Science Degree with Highest Honors in Civil Engineering and graduated at the top of the Civil Engineering class.

The author was employed in the summer of 1987 at M. G. McLaren and Associates consulting firm in Valley Cottage, New York, where he predominantly was involved in the design of a pretensioned, precast concrete parking garage structure.

For the following August, the author was awarded a fellowship and worked as a Research Assistant for the Center of Advanced Technology for Large Structural Systems, at Lehigh University. He was involved in research concerning precast and prestressed concrete connection analysis and design by truss modeling under the auspices of Dr. Peter Mueller, principle investigator in the ATLSS program. It is this research which has formed the basis for the author's publications and thesis work.